EFFECT OF IMPLANT MATERIAL AND SURFACE CHARACTERISTICS ON THE SURFACE AND MECHANICAL PROPERTIES OF DENTAL IMPLANTS

A thesis submitted to The University of Manchester for the degree of
Doctor of Philosophy
in the Faculty of Biology, Medicine and Health

2019

Eman Abuhajar

SCHOOL OF MEDICAL SCIENCES

Division of Dentistry

List of Contents

Word Count

44,478

List of Tables

List of Figures

List of Abbreviations

&	and
§	Section
°C	Centigrade
µm	Micrometre
µN	Micronewton
2D	Two dimensions
3D	Three dimensions
AES	Auger spectroscopy
AFM	Atomic force microscopy
Al	Aluminium
Al_2O_3	Aluminium oxide
ALP	Alkaline phosphatase
BIC	Bone implant contact
BMPs	Bone morphogenetic proteins
BSD	Backscattered detector
BSE	Backscattered electron
C	Control
Ca	Calcium
CAD	Computer-aided design
CaO	Calcium oxide
CaP	Calcium phosphate
CLA	Chromatic length aberration
CO^+	Carbon oxide ion

CO_2	Carbon dioxide
Cp	Commercially pure
CpTi	Commercially pure titanium
Cr	Chromium
ECM	Extracellular matrix proteins
EDM	Electro discharge machining
EDS	Energy dispersive x-ray spectroscopy
Er:YAG	Erbium-doped yttrium aluminium garnet
ev	Electron volts
Fe	Iron
FGF	Fibroblast growth factor
FGF-FN	Fibroblast growth factor-fibronectin
g	Gram
GBR	guided bone generation
GFs	Growth factors
GPa	Gigpascal
H_2SO_4	Sulphuric acid
H_3PO_4	Phosphoric acid
HA	Hydroxyapatite
HCl	Hydrochloric acid
HF	Hydrofluoric acid
HNO_3	Nitric acid
IGF	Insulin-like growth factor
In	Indium
Kv	Kilovolt

Mg	Magnesium
MgO	Magnesium oxide
mm	Millimetre
mN	Millinewton
Mo	Molybdenum
MPa	Megapascal
N	Nitrogen
N_2	Nitrogen molecule
NaCl	Sodium chloride
NaOH	Sodium hydroxide
Nb	Niobium
Ncm	Newton centimetre
NDIs	Narrow diameter implants
nm	Nanometre
O	Oxygen
P	Phosphate
PDGF	Platelet-derived growth factor
PGE_2	Prostaglandin E_2
PO_4^3	Phosphorus
PSHA	Plasma sprayed hydroxyapatite
R	Roxolid®
RGD	Arginine-glycine-aspartic acid
rhBMP-2	Recombinant human bone morphogenetic protein-2
rhVEGF	Recombinant human vascular endothelial growth factor
SB	Sandblasted

SBE	Sandblasted acid etched
SBF	Simulated body fluid
Se	Secondary electron
SEM	Scanning electron microscopy
Si	Silicon
SiC	Silicon carbide
Sn	Tin
Ta	Tantalum
TGFs	Transforming growth factors
TGF-β1	Transforming growth factor beta 1
Ti	Titanium
TiO_2	Titanium dioxide
TiZr	Titanium Zirconia
TPS	Titanium plasma spray
V	Vanadium
VEGF	Vascular endothelial growth factor
XPS	X-ray photoelectron spectroscopy
XRD	X-ray diffraction analysis
Y_2O_3	Yttrium oxide
Zr	Zirconia
ZrO_2	Zirconium dioxide
α	Alpha
β	Be

Abstract

Implant material and surface properties are critical factors that determine implant success. Commercially pure titanium and its alloys are considered the gold standard. However, they still have some limitations. Different approaches have been used to improve and accelerate healing through modifying the implant surfaces. Surface modifications will render the implant with different surface topographies and chemical composition compared to the underlying material, and bioceramic treatments are known to enhance the bioactivity of implant surfaces.

The aim of this study was to investigate the effect of the implant material and surface modifications on selected surface and mechanical properties. The surface roughness of commercially pure titanium (CpTi) and titanium-zirconia (TiZr) alloy with different surfaces were investigated. The results revealed that implant material and surface modification had a significant effect on the mean roughness parameters S_a and R_a (p = 0.002 and 0.002, respectively).

Nanoindentation and micro–nanoindentation testing was used to assess the effect of manufacturing processes on the bulk material sub-surface hardness and elastic modulus. It was found that the manufacturing process had a significant effect on material sub-surface elastic modulus at both nano and micro-nano levels (p= 0.006, and 0.001, respectively), and nano and micro-nano hardness (p= 0.002, and 0.010, respectively). In the TiZr alloy group there was a general tendency for increased hardness and decreased elastic modulus compared to CpTi.

Air abrasion treatment of the CpTi and TiZr surfaces with calcium phosphate abrasives resulted in a non-uniform distributed coating. Surface analysis using optical profilometry, (SEM-EDS) confirmed the incorporation of CaP powders and the change of surface properties. Surface characterisation revealed no significant differences in Ca/P weight percentages, S_a and R_a parameters between different implant materials, or surfaces using different powder compositions. Dissolution of the deposited CaP powders from different implant materials and surfaces in deionised water were examined. The calcium and phosphorous ions continued to release for 3 weeks. More investigations of different alloys and treatments are needed before considering the optimum implant material and surface.

Declaration

No portion of the work referred to in the thesis has been submitted in support of an application for another degree or qualification of this or any other university or other institute of learning.

Copyright Statement

Dedication

First and foremost, I would like to dedicate my work to my beloved parents for their love and support. They have taught me to believe in myself and work hard to achieve my dreams. All I have accomplished is due to their endless love and encouragement.

This thesis is also dedicated to my dear husband Ibrahim for his continuous love, patience and support. It is also dedicated to my children Ahmed, Lojain, and Noor.

Acknowledgement

I would like to express my gratitude to my supervisors, Prof. Nick Silikas and Prof. Julian Satterthwaite for their support and guidance during my study. I would also like to thank my advisor Prof. Craig Barclay for his support.

I would like to extend my thanks to Dr Riaz Akhtar and Miss Abby Peters from University of Liverpool for their help with my work on the nanoindenter. Thanks are also extended to Dr Xiaohui Chen and Mr Michael Faulkner for their assistance with SEM imaging. I would also like to thank Mr Paul Lythgoe from the School of Earth and Environmental Sciences for his help with ICP-OES. Special thanks are also conveyed to Mr Brain Daber for his assistance throughout my study.

Chapter 1

Review of the Literature

1.1 Introduction

The prevalence of oral diseases is increasing around the world due to an increase in life expectancy and an aging population (Kassebaum *et al.*, 2017). Dental caries and periodontal disease are the most common causes of tooth loss (Kassebaum *et al.*, 2015). The increasing demand for replacing missing teeth has given rise to various options for oral rehabilitation. These options can be either fixed or removable depending on several factors such as the clinical demands, patient expectations and cost. A dental implant is one of the options for replacing missing teeth, and is a device usually made from titanium and installed into the oral tissues to support a dental prosthesis.

The history of early dental implants goes back to the ancient Egyptians and South American civilisations, where ivory or animal teeth were used to replace missing teeth (Block, 2018). A variety of implant methods were developed in the following centuries in Europe, using either teeth donated from humans or those taken from animals, with other implants being made from materials such as gold and lead (Sullivan, 2001).

The development of modern dental implants stems from the work of Branemark in the 1960s: when studying the healing process in a rabbit fibula, he noted that the experimental titanium implant being used was fixed to the underlying bone after healing. This formed the concept of osseointegration and the basis of contemporary dental implants (Branemark, 1983; Buser *et al.*, 2017). Following various animal studies, Branemark and co-workers studied the human biological response to

titanium implants, and it was confirmed that implant to bone contact can be achieved and maintained in humans (Albrektsson *et al.*, 1981). Furthermore, such implants were proven to be successfully osseointegrated after 15 years of follow up (Adell *et al.*, 1981). The success of dental implants depends on the integration between the implant and surrounding bone, with this interaction largely dependent on the implant material and surface characteristics, as well as the quality and quantity of bone (Albrektsson *et al.*, 1986). Over 2,000 dental implant systems are now available in the market, all with different materials, designs and surface characteristics (Gaviria *et al.*, 2014; Jemat *et al.*, 2015).

1.2 Osseointegration

Osseointegration was defined histologically by Albrektsson *et al*. (1981) as "a direct – on the light microscopic level – contact between living bone and implant". Clinically, it was defined by Albrektsson and Zarb (1993) as "a process in which a clinically asymptomatic rigid fixation of an alloplastic material is achieved and maintained in bone during functional loading". Recent published work by Albrektsson *et al*. (2017a) on the biological response initiated at the bone-implant interface after implantation defined osseointegration as "a foreign body reaction where interfacial bone is formed as a defense reaction to shield off the implant from the tissues". It will result either in new bone formation, or connective tissue encapsulation. The former indicates a successful integration, while the latter indicates unsuccessful integration that will eventually lead to implant failure (Albrektsson *et al.*, 2017b). Therefore, the bone-implant interface has been the

main area studied by many researchers using different techniques such as light microscopy, electron microscopy, and radiography (Albrektsson *et al.*, 1994).

Berglundh *et al.* (2003) designed a model to closely observe the healing mechanism after implant placement from 2 hours up to 12 weeks. This *in-vivo* study suggested that osseointegration undergoes two phases:

1- Establishment phase

This phase starts from the first 2 hours to 4 weeks after fixture implantation. It involves the formation of coagulum shortly after the bone has been drilled, which soon becomes occupied by inflammatory cells. Osteoclast cells evident on the fourth day demineralise the bone close to the implant surface. However, it was suggested that *de-novo* bone formation had taken place to maintain implant stability after bone loss during the first week post-implantation. Osteoblast and osteocyte cell activities were noted in week 1, which in turn resulted in woven bone formation. Then, osteoblast cells continued to lay new bone up to week 4 after implantation.

2- Maintenance phase:-

This involves the biological reaction that takes place 4–12 weeks' post-implantation. This phase is characterised by bone remodelling and includes evidence of woven bone formation that is replaced by lamellar bone both at the bone–implant interface and in remote areas.

Terhaeyden *et al.* (2012) studied the peri-implant tissue response after implant insertion and up to the establishment of osseointegration. Their study implies the same sequence of soft-to-hard tissue healing, dividing it into four phases: the haemostasis, inflammatory, proliferative and remodelling phases.

Osseointegration is achieved when all factors involved in the osteconductive, osteogenesis, and osteoinduction process are controlled (Albrektsson and Johansson, 2001). Some of these factors are related to the implant itself in terms of the material, design, and surface characteristics (Ogle, 2015), while other factors are related to the type of bone in terms of the quality and quantity, surgical technique, and biomechanical loading (Albrektsson *et al.*, 1981; Davies, 2003; Turkyilmaz and McGlumphy, 2008).

Esposito *et al.* (1998) classified implant failure in relation to osseointegration into: biological, mechanical, iatrogenic failures, and failures related to patient satisfaction. Their work focused on biological failure and was subdivided according to the time of occurrence into early or late failure. Anything that jeopardised the biological host response to form and establish a rigid fixation with bone was considered as a failure.

Osseointegration is crucial for implant success and researchers are continuing to introduce implants with varying compositions, sizes, surface characteristics and treatments to enhance osseointegration.

1.3 Implant material

1.3.1 Titanium

Titanium and its alloys have been suggested as the gold standard material for dental implants due to proven biocompatibility and superior corrosion resistance properties in comparison to stainless steel and cobalt chrome alloys (Niinomi, 2008; Chaturvedi, 2009). Titanium's higher strength and low modulus of elasticity in comparison to other metals enables it to withstand forces applied to it (Niinomi, 2008; Ananth *et al.*, 2015). However, some adverse host tissue reactions have been reported with titanium implants both clinically and histologically (Siddiqi *et al.*, 2011; Chandar *et al.*, 2017; Noronha Oliveira *et al.*, 2017).

1.3.1.1 Titanium structure and alloys

Titanium exists in two crystalline forms: a hexagonal close-packed crystal structure, which is known as the alpha phase (α), and a body-centered cubic structure beta phase (β) (McCracken, 1999; Liu *et al.*, 2004), with the former being the stable phase that undergoes transformation to the metastable beta phase at 883 °C (Imam and Fraker, 1996). These structures have different compositions and characteristics in terms of strength, corrosion, and elastic modules (Gonzalez and Mirza-Rosca, 1999). Each phase can be stabilised by specific elements, which affects its properties. The alpha phase is stabilised by oxygen (O), aluminium (Al), carbon, nitrogen (N), tin (Sn), and zirconium (Zr). The beta phase is stabilised by magnesium

(Mg), iron (Fe), chromium (Cr), vanadium (V), molybdenum (Mo), and niobium (Nb) (Imam and Fraker, 1996; McCracken, 1999).

Alloys containing V and Al metals have been reported to have a toxicological effect and an ability to reduce osteoblast cell proliferation and bone matrix formation; therefore, they have been avoided and replaced by alloys with other metals such as niobium (Nb), zirconium (Zr), or tantalum (Ta) (Hallab *et al.*, 2002; Niinomi, 2008). Titanium alloys containing the aforementioned metals showed a slower metal release of the alloy material including Ti when immersed in different solutions when compared to other alloys with V and Al (Okazaki and Gotoh, 2005).

Commercially pure titanium (CpTi) α, Ti–6Al–4V α+β alloys are the preferred alloys used for dental implant fabrication. Commercially pure titanium has four grades depending on the oxygen percentage that determines its degree of purity: grade 1 is the purest type of CpTi and grade 4 is the least pure (Shrestha and Joshi, 2014). In addition to oxygen, other trace elements of carbon, nitrogen, and iron are also present in CpTi. Higher percentages of these elements are found in the grade 4 CpTi, which is known to affect its mechanical properties (Osman and Swain, 2015). Beta-type titanium alloys with lower elastic modulus are gaining interest due to their non-toxic and non-allergic properties, as well as their increased strength and biocompatibility (Niinomi *et al.*, 2002; Niinomi, 2008; Edamatsu *et al.*, 2015; Cordeiro and Barão, 2017).

1.3.1.2 Titanium oxide layer

The biocompatibility of titanium is related to a thin passive surface oxide layer (TiO_2) that is formed when titanium is exposed to air or tissue fluids (Sul *et al.*, 2005). This oxide layer formed on the titanium surface prevents ionic exchange with the external environment, thus acting as a dense protective layer, which may explain its biocompatibility and corrosion resistance (Chaturvedi, 2009). It has been suggested that this layer is responsible for initiating and enhancing osseointegration. Therefore, research has been directed towards modifying this layer either chemically or physically (Yang and Huang, 2010; Kubies *et al.*, 2011).

The titanium oxide layer in nature may occur in several phases: as well as TiO_2 (B), rutile, anatase, and brookite may be found, with different structures, densities and properties (Figure 1.1). The rutile phase will be formed at higher temperatures, while at low temperatures anatase and brookite will be formed (Chen and Mao, 2007; Yang *et al.*, 2009). On the other hand, TiO_2 (B) can be found naturally or synthesised (Zukalova *et al.*, 2005).

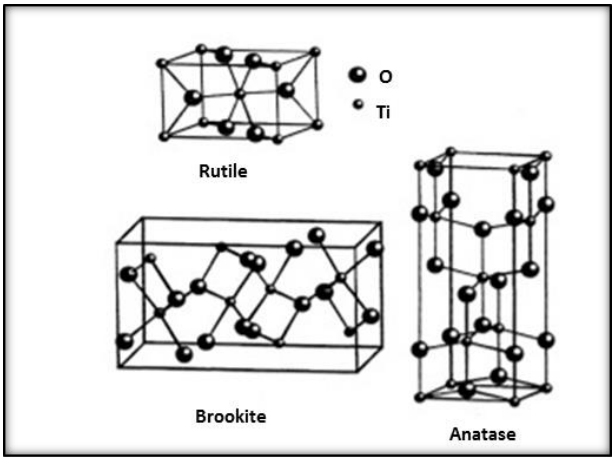

Figure 1.1 Phases of titanium dioxide (Mo and Ching, 1995)

1.3.2 Zirconia

Zirconia (ZrO_2) is a ceramic that was introduced as an alternative bio-inert material to be used in dentistry due to its superior aesthetic, biocompatibility and osteconductive properties, as well as its enhanced corrosion resistance (Hisbergues *et al.*, 2009; Al-Amleh *et al.*, 2010). Zirconia exists as a crystalline structure in one of three forms at different temperatures: monoclinic, cubic, and tetragonal (Figure 1.2). At room temperature the monoclinic structure is predominant, while the cubic structure exists at 2,680 °C and the tetragonal structure below 2,370 °C (Kohal and Klaus, 2004; Conrad *et al.*, 2007), all forms are stabilised with different oxides. These oxides are MgO, CaO, and Y_2O_3, with the latter (yttrium-stabilised tetragonal polycrystal) being the most commonly used in dentistry (Manicone *et al.*, 2007).

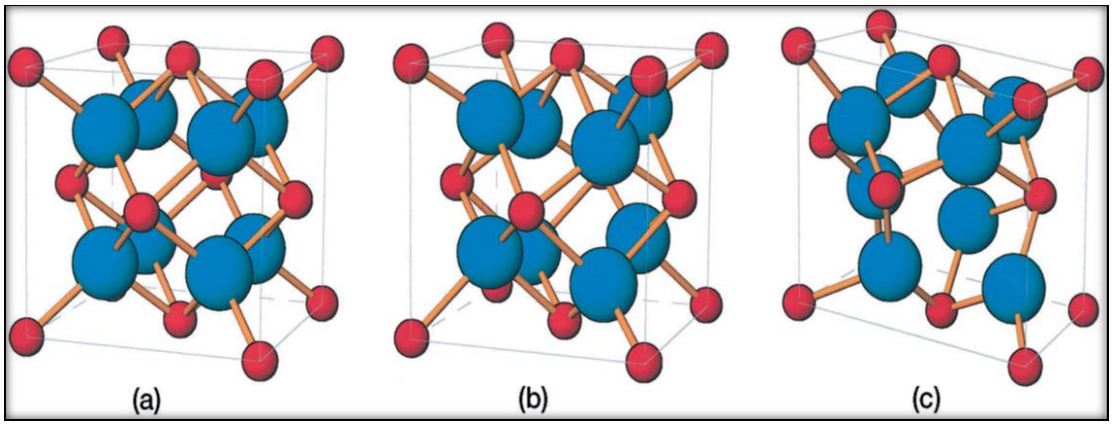

Figure 1.2 Crystalline structures of zirconia: (a) cubic, (b) tetragonal, (c) monoclinic (Hannink *et al.*, 2000)

1.3.2.1 Osseointegration of zirconia implants

Zirconia implants osseointegrate similarly to titanium implants in animal studies (Manzano *et al.*, 2014). A recent systematic review concluded that zirconia implants do not show any significant difference in osseointegration from titanium implants *in-vivo* (Pieralli *et al.*, 2017). Furthermore, a study conducted by Stadlinger *et al.* (2010) reported bone implant contact (BIC) percentages of 53 % for both Ti and submerged ZrO_2 implants (Stadlinger *et al.*, 2010). Also, Depprich *et al.* (2008) found that BIC increased from 35.3 % to 71.0 % for ZrO_2 between week 1 and week 12, compared to 47.7 % at week 1 and 82.9 % at week 12 for Ti implants. This result suggests that sandblasted ZrO_2 implants are able to osseointegrate similarly to blasted Ti implants *in-vivo*. In contrast, another study comparing acid-etched and sandblasted zirconia implants with the same geometry as other titanium implants with various surface treatments (placed in the iliac bone of sheep) demonstrated the superiority of Ti implants over ZrO_2 ones assessed by removal torque testing after 8 weeks healing (Ferguson *et al.*, 2008).

Möller *et al.* (2012) investigated the difference between titanium and zirconia implants in terms of biocompatibility and osseointegration *in-vivo* and *in-vitro*. The biocompatibility results using human osteoblast cells did not reveal any significant difference between the implants. Regarding osseointegration, both implants formed firm contact with the bone, with the titanium implant revealing slightly better results in comparison to the zirconia implants. However, the statistical analysis did not conclude any significant difference.

Microscopic analysis reveals that zirconia implants showed a BIC of 68.4 % when implanted in rabbits, and did not appear to introduce any adverse effect on the osteoblastic cells' ability to form new bone, nor was any inflammatory response observed (Scarano *et al.*, 2003).

Langhoff *et al.* (2008) did not report any statistical difference in BIC values between sandblasted ZrO_2 implants and other titanium implants, that were plasma anodised or coated with Ca, bisphosphonate, or collagen type 1. Surface-treated ZrO_2 implants also showed enhanced osseointegration in comparison to untreated ZrO_2 implants (Gredes *et al.*, 2014; Saulacic *et al.*, 2014; AlFarraj *et al.*, 2018). However, there are insufficient studies about the long-term survival and success of zirconia implants (Hashim *et al.*, 2016; Cionca *et al.*, 2017).

1.3.3 Titanium-zirconia alloy

To enhance the mechanical properties of the dental implant, as well as the biocompatibility, corrosion resistance, and wear, several elements other than Al and V have been added to titanium alloys (Khan *et al.*, 1999; Okazaki and Gotoh, 2005). These elements are niobium (Nb), zirconia (Zr), tantalum (Ta), palladium (Pd), and indium (In) (Khan *et al.*, 1999; Niinomi, 2003; Grandin *et al.*, 2012).

A binary alloy composed of a mixture of titanium and zirconium (TiZr) has been introduced as an alternative material for dental implants. Different percentages of Zr and Ti have been investigated. A mixture of 60 % Zr and 40 % Ti with different particle sizes to create a porous surface, revealed biocompatibility and the ability of

the alloy to form a strong contact with bone when implanted in a rabbit femur (Shibata and Okuno, 1987).

Alloys containing zirconia were reported to have increased tensile strength (Okazaki *et al.*, 1993). In addition, it was reported that Ti alloys containing 50 % zirconia have showed better hardness and tensile strength values when compared to Ti-6Al-4V (Kobayashi *et al.*, 1995), besides a superior biocompatibility (Ikarashi *et al.*, 2005). Ho *et al.* (2008) examined the mechanical properties of Ti alloys with different concentrations of zirconium from 10 % up to 40 %. It was concluded that alloys with higher Zr content had better mechanical properties in terms of hardness, elasticity, and strength. Furthermore, titanium-zirconia alloys were claimed to be superior to titanium implants and its alloys in terms of tensile and fatigue strength, and biocompatibility (Kobayashi *et al.*, 1995; Ikarashi *et al.*, 2005).

In 2012, Steineman suggested the use of TiZr alloy in both surgical and dental fields. This alloy contained zirconium (10–19 %), oxygen (0.1–0.3 %) and less than 1 % other additives. When mechanically tested, it was concluded that this alloy was equal to alpha and beta alloys in toughness measurements, with higher tensile strength and yield points than grade IV titanium (Steinemann, 2012). The TiZr alloy with 13–17 % Zr is one of the alloys that has been extensively studied for dental implants and is now commercially available under the name Roxolid® (Institut Straumann AG, Basel, Switzerland). The tensile strength reported with Roxolid® implants is 953 MPa in comparison to 310 MPa for CpTi, and Young's modulus in the 102–104 GPa range when measured using ultrasound methods (Brizuela-Velasco *et al.*, 2017).

1.3.3.1 Performance of TiZr implants

Grandin *et al.* (2012) reported that TiZr narrow diameter implants (NDIs) behaved similarly to Ti implants, with no adverse biological effect noted both *in-vivo* and *in-vitro*. Several clinical studies investigated the performance of TiZr implants over a period of time. A clinical randomised control study conducted by Al-Nawas *et al.* (2012) compared TiZr implants to CpTi grade 4 implants over 1 year, where the study demonstrated survival rates of 98.8 % and 97.8 % for TiZr and Ti, respectively. Success rates were 96.6 % and 94.4 %, respectively, with no statistical difference noted between both implant materials radiographically. Furthermore, the success and survival of the TiZr implants in this study continued to be high when followed up for another year (Al-Nawas *et al.*, 2015).

Similarly, a pilot study by Barter *et al*. (2012) using Ti and TiZr implants with SLActive surfaces supporting a fixed prosthesis and followed for 2 years revealed 95.2 % success and survival rates for all implants included in the study. Furthermore, early and immediately loaded TiZr implants showed comparable survival and success rates when compared to conventionally loaded implants, even in cases of reduced bone quality and quantity (Ganeles *et al.*, 2008).

1.3.3.2 Osseointegration of TiZr and CpTi implants

Several studies investigated the osseointegration of TiZr implants in comparison to Ti implants (Jimbo *et al.*, 2015; Wen *et al.*, 2016; Galli *et al.*, 2017). Galli *et al.* (2017) assessed how the TiZr implants behaved in comparison to CpTi implants after implantation by studying the healing process and the gene expression of the bone

surrounding the TiZr implants. Their results indicated that the bone surrounding the TiZr implants showed significantly higher levels of genes associated with osteogenesis in the first 2–4 weeks of healing compared to the CpTi implants.

TiZr implants with SLActive surfaces have higher BIC percentages when compared to CpTi implants with the same treatment *in-vivo* in the first few weeks after implantation (Saulacic *et al.*, 2012), it was also noted that these percentages continued to increase for both the TiZr and CpTi implants. Similar histological, histomorphometric, and radiological results have been obtained in other animal studies to compare CpTi and TiZr implants with SLActive surfaces (Thoma *et al.*, 2011; Kämmerer *et al.*, 2013). Jimbo *et al.* (2015) reported higher BIC with TiZr SLActive implants at 4 weeks in comparison to Ti SLActive implants.

In line with the previous studies Gottlow *et al.* (2012) showed no difference in the percentages of BIC between CpTi and TiZr implants *in-vivo*, however, significant difference was noted in the removal torque values of 230.9 Ncm and 204.7 Ncm for TiZr and CpTi, respectively. Moreover, a significantly higher amount of bone was deposited around the TiZr implants than around the CpTi implants. All the studies mentioned above concluded that TiZr implants did show superiority over Ti implants at 2 weeks following placement, but as the healing time elapsed they showed similar osseointegration ability to Ti implants.

1.4 Surface characterisation

Surface analysis was defined by Briggs as the ‘’analysis of the element composition of the outermost atom layer of a solid’’ (Briggs, 1990). When studying any material, characterisation of its surface can determine the chemical composition, homogeneity, and different atomic structures (Briggs, 1990).

Several methods to study the effect of dental implant surfaces have been proposed, some of which are descriptive studies of the osseointegration zone, and the type and amount of bone formed at this zone. These studies are either histological or histomorphometric. Others are biomechanical, which assesses the force required to remove the implant from the bone, to determine how fixed the implant is to the underlying hard tissue. These techniques are the removal torque, push-out/pull-out, and resonance frequency tests.

Research has also been directed towards studying the surface topography and detailed analysis of the chemical and atomic composition of dental implant surface layers using scanning electron microscopy (SEM), profilometry, x-ray photoelectron spectroscopy (XPS), auger electron spectroscopy (AES), energy dispersive X-ray spectroscopy (EDS), and atomic force microscopy (AFM).

1.5 Surface roughness

Surface topography is divided into form, waviness, and roughness. Surface roughness is one of the important parameters that effects osseointegration (Albrektsson *et al.*, 1981). All surface treatments will result in a level of surface roughness (i.e. micro, macro, nano) as well as a change in both the chemical composition and morphology of an implant surface, which will enhance or reduce osseointegration and primary stability (Cooper, 2000; Rasmusson *et al.*, 2001; Le Guéhennec *et al.*, 2007). Research has revealed that rough surfaces enhance bone formation directly on their surfaces (Piattelli *et al.*, 1996; Cochran *et al.*, 1998; Piattelli *et al.*, 2002). Furthermore, long-term survival rates of moderately rough implants are better than minimally rough implants, especially in the maxilla (Jimbo and Albrektsson, 2015). Various opinions have been suggested regarding the optimum surface roughness for osseointegration, however, most of the studies agreed on the role of surface roughness in establishing a strong contact with bone (Wennerberg and Albrektsson, 2009; Del Fabbro *et al.*, 2017; Giannasi *et al.*, 2018)

Increased surface roughness also plays a role in increasing the surface area and improving cellular adhesion and in turn increases the biomechanical interlocking of implants with bone (Cooper, 2000). Clinical studies performing histomorphometric and histological analysis revealed that rough blasted implants are superior to turned implants in terms of osseointegration (Ivanoff *et al.*, 2001). Moreover, some *in-vivo* experimental studies noted the effect of roughness on enhancing bone formation around implants was only comparable to turned surfaces in unloaded conditions. The surface topography did not seem to have a significant effect under specific

loading conditions (Vandamme *et al.*, 2007). In contrast, another study performed on dogs to investigate the osseointegration ability of rough titanium surfaces under excessive occlusal conditions compared to unloaded conditions for 8 months revealed that rough implants can withstand excessive loading without loss of osseointegration (Heitz-Mayfield *et al.*, 2004). Published work comparing different surface treatments *in-vivo* for 8 weeks suggested that all surface treatments tested for both Ti and Zr implants showed better biomechanical test results for sandblasted and acid-etched Ti surfaces along with bisphosphonate and calcium coatings, over Zr and Ti anodic plasma treatments (Ferguson *et al.*, 2008).

1.5.1 Measurement of surface roughness

Surface topography can be assessed either qualitatively or quantitatively, with the latter being the most recommended. The quantitative measurement of surface roughness is done by using several devices that are categorised as mechanical contact instruments, or optical instruments (Wennerberg and Albrektsson, 1999). Among the different devices used to assess surface roughness, the ones primarily used in conjunction with dental implants are profilometry (Rupp *et al.*, 2004) and AFM (Löberg *et al.*, 2010). For dental implant surfaces, profilometers are preferable to AFM when measuring rough surfaces due to the inability of the AFM instrument to measure textured surfaces, especially implant bodies (Wennerberg *et al.*, 2015).

A wide range of profilometers are available in the market, and they are categorised according to their relationship with the surface examined, either as contact or non-contact profilometers. Contact profilometers rely on moving a stylus tip over the

surface to obtain the measurement. This contact with the surface could damage the surface or the stylus tip, and due to this contact, the stylus may not be able to give accurate measurements of the surface irregularities. With non-contact optical profilometers a reflecting beam is used to scan the surface to make the measurement. The reflecting beam is able to access the irregularities on the surface and give a more accurate measurement with higher resolutions (Wennerberg *et al.*, 2015).

1.5.1.1 Optical profilometer

The optical profilometer was defined by Whitefield (1975) as "a measuring instrument that utilizes a laser beam reflected from a surface to generate a profile of the reflecting surface". An example is the 3D optical profiling system (Talysurf CLI1000, Taylor Hobson Precision, UK) (see chapter 3).

1.5.2 Surface roughness parameters

Quantitative measuring devices calculate the surface roughness and give different roughness parameters. These parameters are obtained from either 2D profiles or 3D surfaces, depending on the device used for measurement (Santos and Júlio, 2013). The difference between the 2D and 3D roughness parameter is that the 2D parameters are calculated based on a single line on the surface, while the 3D parameters are calculated based on an area of the surface (Gadelmawla *et al.*, 2002). In addition, other parameters such as spatial and hybrid parameters are considered essential to fully characterise a surface (Wennerberg and Albrektsson, 2010).

The commonly used 3D parameters described by Wennerberg *et al*. (1996b) are:

- **S_a:** The arithmetic mean of the absolute values of the surface departures from the mean plane within the sampling area or profile for R_a.
- **S_q:** The root mean square value of the surface departures within the sampling area (or profile for R_q).
- **S_z:** The average value of the absolute heights of the five highest peaks and the absolute value of the five deepest valleys within the sampling area (or profile for R_z).
- **S_{sk}** (skewness): The measurement of the symmetry of surface deviation (or profile for R_{sk}) about the mean plane.
- **S_{ku}** (kurtosis): The measure of the sharpness of the surface (or profile for R_{ku}) height distribution.

Other 3D parameters that describe the surface roughness are:

- **S_p**: Representing the distance from the mean to highest peak of the surface or profile for R_p.
- **S_v**: Representing the distance from the mean to the lowest valleys of the surface or profile for R_v.

The use of 2D parameters is still widely accepted to quantify surface roughness which are R_a, R_q, R_z, R_{sk}, and R_{ku} (Gadelmawla *et al.*, 2002). However, with the advances in 3D technology, the use of 3D parameters is recommended as they are considered more realistic and representative of the surface than 2D parameters (Stout and Blunt, 2000). Guidelines published by Wennerberg and Albrektsson suggested using the 3D parameters S_a, S_q, S_{cx}, S_{tr}, S_{dr}, and $S_{\Delta q}$ to characterise the surface topography of dental implants, however, it was documented that different measuring devices can give different results, partly due to the use of different filters that separate the roughness from the waviness and form (Wennerberg *et al.*, 1996b).

Dental implant surface roughness is often described in the literature using the R_a and S_a parameters, and according to the value of these parameters they are categorised into different groups. Minimally rough implants have an S_a value of 0.5–1.0 µm; moderately rough implants have an S_a value range of 1.0–2.0 µm; and rough implants have an S_a value that exceeds 2.0 µm. Systematic reviews have concluded that moderately rough surfaces with an S_a value ranging from 1.0–2.0 µm demonstrated the best bone anchorage in comparison to the minimally rough or rough surfaces (Wennerberg *et al.*, 1996a; Wennerberg and Albrektsson, 2009).

Recent research on osteoblast cell proliferation confirmed that R_a values of 1.0–2.0 µm showed the most favourable results (Andrukhov *et al.*, 2016).

1.6 Scanning electron microscopy and energy dispersive spectroscopy

The SEM is one of the main instruments used for detecting the surface morphology and chemical composition of different materials. The principle of SEM imaging depends on hitting the specimen with an electron beam generated from an electron gun. The electron beam will travel through an anode, alignment coil, multiple condensing lenses, and a scanning coil until it hits the specimen (Figure 1.3). When the specimen is hit by the primary electron beam the interaction between the beam and the atoms on the surface of the specimen will result in the emission of several signals: electrons, X-rays, auger electrons, cathodoluminescence and transmitted electrons. Each signal is utilised to give different information (Reichelt, 2007).

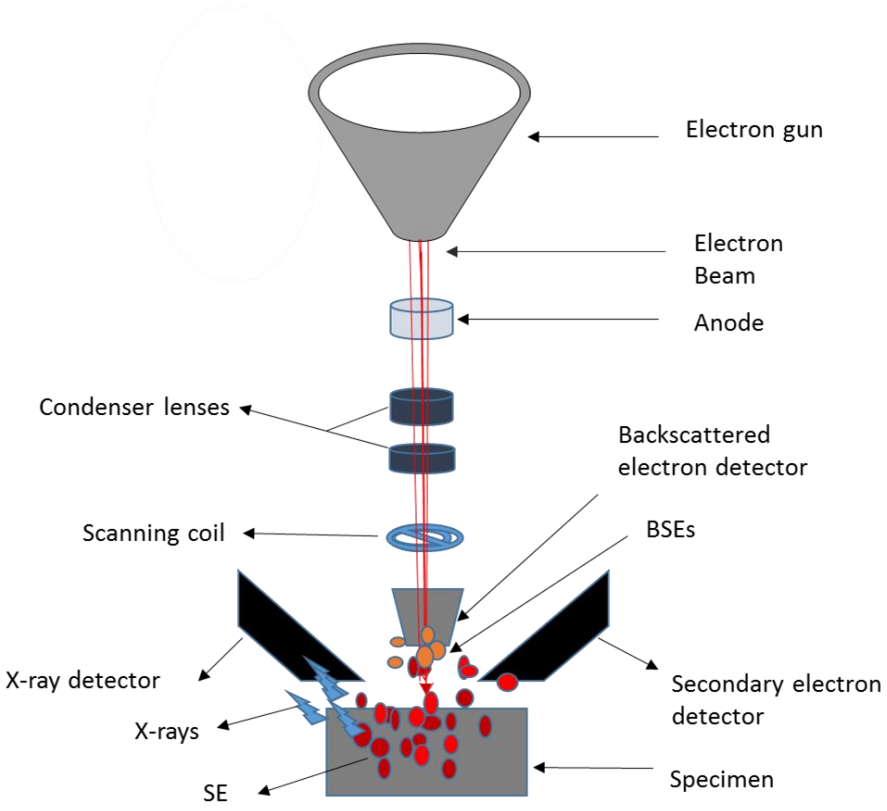

Figure 1.3 Schematic drawing of the scanning electron microscopy

The SEM image is formed by two types of electrons. First, the electrons with low energy of 3–5 eV known as secondary electrons (SEs) will emit from the surface of the material and will be collected by the secondary electron detector. These electrons will represent the topographical information of the surface. Secondly, the electrons with higher energy (more than 50 eV) known as backscattered electrons (BSEs) emitted from the deeper part of the specimen will spring back to the main source and be collected via the backscattered detector (BSD). These electrons will give both topographical and general compositional information about the specimens (Zhou *et al.*, 2006).

When the primary beam strikes the specimen, along with the emitted electrons some X-rays are emitted as well. These X-rays result from the transition of the

electrons between the inner and outer orbital shells of the constituent atoms, and the difference in the energy resulting from this transmission will determine the elemental composition. These X-rays can be collected by another detector which will give the information needed for the compositional analysis of the sample with energy dispersive X-ray spectroscopy (EDS).

1.6.1 Test parameters

The quality of the SEM image and the statistical validity of the EDS analysis are dependent on the test parameters selected for imaging, such as the working distance (WD), accelerated voltage (Kv), and the number of counts (i.e. the number of X-rays hitting the detector). Variation in these parameters could result in inaccurate concentration measurements of the EDS analysis (Zhou *et al.*, 2006).

1.6.2 Sample preparation

The sample preparation is crucial to ensure a good quality SEM image and accurate EDS analysis. The specimens need to have a clean electro-conductive surface. Specimens with low atomic numbers will emit low energy electrons when exposed to the electron beam, resulting in a poor-quality image. Therefore, it is necessary to coat these types of samples with conductive coatings. The coating materials commonly used are gold, silver, and carbon (Goldstein *et al.*, 2017). However, the low vacuum mode is a less sensitive mode where rough surfaces can be viewed without any prior preparation (Reichelt, 2007).

1.7 Mechanical properties

The successful application of titanium as an implant material has been proven through many human and animal studies (Niinomi *et al.*, 2002). Increasing attention has been directed towards producing small implants with enhanced strength to fit certain clinical situations where implants will be subjected to heavy occlusal forces (Sierra-Sánchez *et al.*, 2014; Tolentino *et al.*, 2014). Therefore, the implant material should have enhanced mechanical properties such as hardness, elastic modulus, tensile and fatigue strength to be able to withstand such forces (Saini *et al.*, 2015).

Implant materials with a higher elastic modulus than bone will result in bone atrophy, followed by localised bone resorption due to the stress-shielding effect (Geetha *et al.*, 2009; Niinomi and Nakai, 2011). The elastic modulus of dental implants was highlighted as one of the factors that could affect the load adaptation and allow better subsequent stress distribution in bone (Geng *et al.*, 2001; Muddugangadhar *et al.*, 2011). Research found that implant materials with higher strength and similar elastic modulus to bone contribute to favourable stress distribution, which enhances the bone density (Niinomi and Nakai, 2011; Shi *et al.*, 2013). Brizuela *et al.* (2019), reported that dental implants with lower elastic modulus demonstrated significantly higher BIC compared to implants with higher elastic modulus *in-vivo*. Generally, titanium has a lower elastic modulus than other metals such as steel and chrome. The commercially pure titanium elastic modulus is in the range of 102–104 GPa (Niinomi, 1998). However, its elastic modulus is still higher than bone, which is 10–30 GPa (Niinomi, 2008).

Furthermore, research has shown that in addition to implant composition the implant surface treatment might affect the mechanical properties of dental implants such as fatigue strength (Ayllón *et al.*, 2014; Medvedev *et al.*, 2016a; Medvedev *et al.*, 2016b), hardness and elastic modulus (Fomin *et al.*, 2016; Grubova *et al.*, 2016). Among these mechanical properties, two of the most important properties related to dental implant materials are hardness and elastic modulus.

Hardness

Hardness measures the resistance of the material to permanent deformation when subjected to load (Welsch *et al.*, 1993).

Elastic modulus

The elastic modulus is the measure of the ability of the material to resist non-permanent deformation when it is exposed to load (Ilie *et al.*, 2017).

1.7.1 Measurement of hardness

Hardness is measured using two methods: the scratch test and indentation tests (Ilie *et al.*, 2017). The indentation method is the most common method used to measure hardness, which involves applying a load on an indenter to make a depression in the material. Following indentation, the hardness data will be generated from the load, and depth or size of the indent. According to the amount of force applied, the hardness measurement is categorised as macro, micro, or nano hardness (Herrmann, 2011).

The indentation tests commonly used for biomaterials are Vickers hardness, Knoop hardness, Rockwell hardness, or Brinell hardness. These tests use different indenter size and shape to make the indents, the hardness measurement will be calculated from the load and size of the indents using only the plastic deformation part of the indentation process (Ilie *et al.*, 2017).

Another indentation test known as the depth sensation hardness test is used to assess the plastic deformation of materials. This test applies the same principle of using an indenter to make a depression, however, it calculates the hardness in relation to the load and depth of penetration (Oliver and Pharr, 2004).

Most of the studies assessing the hardness of dental implants are gained from indentation hardness testing using Vickers and Knoop indenters (Pazos *et al.*, 2010). These studies use higher forces and calculate the mechanical properties in relation to the size of the indent (Lee *et al.*, 2016).

1.7.2 Measurement of elastic modulus

Elastic modulus is measured from the stress-strain curves that result when a load is applied to a tested material. Such curves result from different testing methods, namely the tensile test, flexural test, and indentation tests (Ilie *et al.*, 2017). Indentation testing is the most widely used method with dental implants (Elias *et al.*, 2015). The principle of indentation testing as described by Fischer-Cripps is “a simple method that consists essentially of touching the material of interest whose mechanical properties such as elastic modulus and hardness are unknown with another material whose properties are known” (Fischer-Cripps, 2011). Indentation

testing can be performed using a static approach (as per hardness testing using Vickers, Berkovich, and Knoop testing), or by using a depth sensing method (nanoindentation) (Ilie *et al.*, 2017). The nanoindentation method is recognised as an accurate method for measuring the elastic modulus (International Organization for Standardization, 2015).

The indentation head of a nanoindenter is typically composed of a column that has the indenter tip at its end, and a magnet and coil at the top to control the applied force and springs and a displacement gauge to control its movement in both vertical and lateral directions (Oliver and Pharr, 2010) (Figure 1.4).

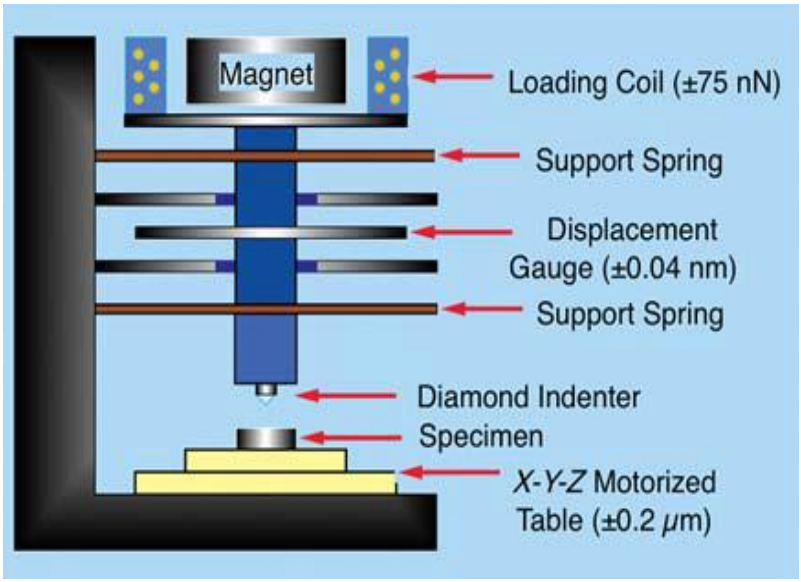

Figure 1.4 Schematic drawing of the nanoindenter head (Oliver and Pharr, 2010)

Nanoindentation theory relies on knowing the mechanical characteristics and geometry of the indenter tip to calculate the mechanical properties of a specimen (Oliver and Pharr, 2010). Indenter tips used for nanoindentation are made from diamond with an elastic modulus of 1,000 GPa and Poisson's ratio of 0.07. These tips come in different geometries to suit the material and mechanical property

being investigated (Fischer-Cripps, 2011). The indenters used in nanoindentation studies are Berkovich, Vickers, Knoop, and Cube Corner. The one that is most commonly used is the Berkovich indenter, with its characteristics presented in Table 1.1.

Table 1.1 Representing the specifications of the Berkovich indenter (Fischer-Cripps, 2011)

Specifications	Value
Geometry	Three sided
Face angle θ	65.27˚
Tip radius	50–100 nm
Geometry correction factor β	1.034
Strain within specimen	8%
Cone angle α	70.3˚
Project area of contact A	24.5 h

1.7.2.1 Calculation of elastic modulus and hardness

Nanoindentation testing applies a given load through the loading column to a pyramidal indenter that is in contact with the test material. When a load is applied, the indenter makes a depression into the tested material that will result in a load-displacement curve. Data obtained from the curves are used to determine the hardness and elastic modulus of the tested material (Doerner and Nix, 1986; Panich and Yong, 2005).

Data obtained from the loading and unloading curves has been interpreted using several methods; the most widely accepted one is the Oliver and Pharr method

proposed in 1992. This technique depends on three measurements: load (*P)*, maximum displacement (*H*), and unloading stiffness (*S*) (Doerner and Nix, 1986; Oliver and Pharr, 1992).

From these three parameters, the contact depth and function area are used to calculate the contact area (*A*), which is divided by load (*P*) to determine the hardness using the following formula:

$$H = P/A$$ (Gouldstone *et al.*, 2007)

The elastic modulus is computed from the stiffness that represents the curve of the load-displacement *P-H* curve using the equation below:

$$S = 2E_r a = \frac{2}{\sqrt{\pi}} E_r \sqrt{A}$$ (Oliver and Pharr, 2010)

Where *S* is the stiffness, *a* is the contact radius, *A* the contact area, and E_r the elastic moduli.

1.8 Narrow diameter implants

Recently, the growing interest in dental implants and change in patient needs demands different treatment modalities. Commercially pure titanium and titanium alloys have been used for many decades as the material of choice for dental implants. However, different clinical situations require different implant properties (Saini *et al.*, 2015). When the residual ridge dimensions are insufficient to place a regular size implant, this necessitates the use of implants with smaller diameters (Davarpanah *et al.*, 2000). One of the main drawbacks of narrow diameter implants is reduced fatigue strength (Allum *et al.*, 2008).

Clinical reports have shown similar success and survival rates of NDIs when compared to standard diameter implants. The results from the clinical studies by Vigolo *et al*. (2004), and Romeo *et al.* (2006) after a 7 year placement in both maxilla and/or mandibles revealed a high survival rate for NDIs. The study by Vigolo *et al*. (2004) evaluated implant diameters of 2.9 mm or 3.25 mm compared to standard implants, whereas Romeo *et al*. (2006) investigated 3.3 mm implants in comparison to standard 4.1 mm implants. Both studies emphasised that bone quality could be one of the factors influencing implant survival. However, Olate *et al.* (2010) reported no significant relationship between the use of NDIs and bone quality on early implant failure. Nevertheless, this study indicated that early implant loss was associated with the implant length and implantation site.

Retrospective data obtained by Degidi *et al.* (2008) reported overall survival rates of 99.4 %, where 510 implants were studied with diameters ranging from 3.0 mm to

3.5 mm over 8 years. The implants evaluated were placed in anterior and posterior regions of maxilla and mandible. The results showed no significant differences in the survival rates between the maxilla and mandible at different locations and bone densities. Similarly, another retrospective study by Arisan and co-workers (2010) assessed the success and survival rates of 316 implants with 3.3 mm and 3.4 mm diameters over 10 years. The success and survival rates reported were 91.4 % and 92.3 %, respectively, with no significant difference between implants placed in the maxilla or mandible. They also noted that the peak of marginal bone loss occurred in the first 2 years of loading in both the maxilla and mandible. Furthermore, when comparing implants placed in the posterior and anterior sites, it was noted that the marginal bone loss was significantly higher around the posterior implants.

A 12 year retrospective study on NDIs reported cumulative survival and success rates of 98.1 % and 91.8 %, respectively (Lee *et al.*, 2013b). The results were based on 541 implants with the diameters of 3.3 mm, 3.4 mm, and 3.5 mm placed in the maxilla and mandible at posterior and anterior regions. The study by Lee *et al*. (2013b) concluded that the bone quality and implant location had no significant effect on survival and success rates. However, when analysing the failed implants it was noted that implant failures were more frequent in the implants inserted in the maxilla and in the anterior regions. Zinsli *et al*. (2004) demonstrated a 96.6 % cumulative survival rate after 6 years of placement of 3.3 mm diameter implants over a 10 year observational period. The implants studied were inserted in the maxilla and mandibles at different locations. In another study assessing 22 NDIs placed in the maxilla and mandible at different anterior and posterior locations with

insufficient alveolar bone width, a 96 % success rate was reported following 5 years of placement (Comfort *et al.*, 2005).

In contrast to the above studies, some studies reported significant early failure rates associated with the use of NDIs (Baqain *et al.*, 2012; Grisar *et al.*, 2017). Baqain *et al.* (2012) evaluated 399 implants and reported higher numbers of failures with implants measuring < 3.5 mm and 3.5–4.5 mm, compared to implants with wider diameters greater than 4.5 mm. Moreover, this latter study did not report any association between early implant losses and implant location. However, Grisar *et al.* (2017) investigated 1,390 implants placed in the maxilla and mandible at different locations and reported that implant failures were associated with implant diameters 3.5–4.4 mm and > 4.4 mm, with no failures in the implants narrower than 3.5 mm. Although in both studies the implant length did not show any significant effect on implant failure, both studies related the effect of implant diameter to be attributed to the insufficient bone quality and volume or lack of space. One possible explanation for the different outcomes demonstrated in the latter two studies is that the studies included cases with bone augmentation and sinus lift procedures, whereas the long-term studies above did not include studies with bone augmentation or sinus lift procedures.

A systematic review reported the success and survival rate of NDIs 3.3–3.5 mm in diameter to be 91.4–97.6 % and 88.9–100 %, respectively. Survival rates were reported for 3.0–3.25 mm implants in the 93.8–100 % range (Klein *et al.*, 2014). The study by Klein *et al.* (2014) included NDIs placed in both maxilla and mandible due to reduced bone width and/or limited mesiodistal space. The authors highlighted

that their systematic review may have a high risk of bias due to the unavailability of prospective randomised control studies and the lack of a control (standard-sized implants) to compare with in some studies. However, the risk of bias was considered to be low for the 3.3–3.5 mm implants. Therefore, a meta-analysis was conducted and did not indicate any significant difference in survival rates between the 3.3–3.5 mm implants and standard implants. A recent review paper indicated that a higher risk of failure is associated with the use of NDIs (Griggs, 2017). This review was based on failure rates reported from different clinical studies and meta-analyses, and concluded that the rate of failure is greater with implant diameters less than 3.7 mm.

A review by Grandin *et al*. (2012) concluded that narrow implants made from TiZr alloy showed 40 % higher strength than conventional commercially pure titanium implants. Furthermore, a recent systematic review by Legami *et al.* (2017) reported similar success rates of narrow diameter implants made from TiZr compared to CpTi. Short-term studies indicated high survival and success rates associated with TiZr (Roxolid®) NDIs (Chiapasco *et al.*, 2012; Tolentino *et al.*, 2014). A clinical pilot study on 3.3 mm implants placed for 24 months reported 95.2 % survival rates with a mean bone loss of less than 1 mm (Barter *et al.*, 2012). Another prospective study on Roxolid® 3.3 mm implants with SLActive surface reported 98.9 % survival rates. The study did not show any significant difference between the Roxolid® and grade 4 Ti implants after 12 months following placement, while the success rates reported were 96.6 % and 94.4 %, respectively (Al-Nawas *et al.*, 2012). Furthermore, no

significant difference was noted between the Roxolid® and the Ti implants when the same study was followed up 3 years latter (Quirynen *et al.*, 2015).

Nevertheless, finite elemental analysis studies concluded that the ability of NDIs to withstand occlusal forces and stress is reduced when compared to wider implants (Himmlova *et al*., 2004; Anitua *et al*., 2010), although the risk of fracture under loading in fatigue testing showed favourable results (Allum *et al*., 2008; Hirata *et al*., 2016). However, the risk of fatigue fracture of NDIs in the long term may take place (Zinsli *et al.*, 2004).

In summary, NDIs demonstrated a high survival and success rate, with implants measuring 3.0–3.5 mm showing the most favourable prognosis. However, the bone quality and implant location (anterior or posterior) could be a factor that might influence the long-term failure rates of NDI implants.

1.9 Implant surface modifications

The bone-implant interface is the area where the primary tissue response occurs after implant placement. At this interface, the implant surface plays a crucial role in initiating this tissue response from clot formation until osseointegration is established (Huang *et al.*, 2012). Therefore, different approaches have been used to improve implant surfaces by using different surface modifications (Wirth *et al.*, 2017). The most important surface characteristics that are altered by surface modification that affect osseointegration are surface topography, surface energy, and chemical composition (Barbosa *et al.*, 2017).

Implant surfaces can be machined (turned), soft, polished, and textured. Each surface has its own characteristics and ability to bond to underlying bone (Wennerberg, 1998; Wennerberg and Albrektsson, 1999; Puleo and Thomas, 2006; Dohan Ehrenfest *et al.*, 2010). Surface treatments modify the surface topography at both the micrometre and nanometre scales (Mendonça *et al.*, 2008; Dohan Ehrenfest *et al.*, 2010). Wennerberg and Albrektsson (2009) divided the techniques that produce changes in surface tomography into additive or subtractive methods. The first technique implies adding material to the implant surface, such as hydroxyapatite (HA) and calcium phosphate coatings, titanium plasma spray (TPS), or ion deposition. In contrast, the subtractive method will involve removing some of the implant surface by blasting and/or etching, oxidation, and polishing (Wennerberg and Albrektsson, 2009).

1.9.1 Physical modifications

1.9.1.1 Mechanical modification

The surface topography of an implant may be modified using mechanical treatment during its manufacture. Depending on the techniques used by the manufacturer, different surface roughness parameters (R_a/S_a values) will result (Wennerberg and Albrektsson, 2009). These techniques are described as follows:

a- Cutting and turning

This is a technique employed in the early days of implant production, which involves using turning machines that have a stainless steel cutting element that results in a surface with a directional pattern. This surface will have an R_a value ranging from 0.3 µm to 0.6 µm, which is considered as a minimally rough surface (Bagno and Di Bello, 2004).

b- Surface smoothing or polishing

In order to obtain a smooth finished implant surface it undergoes a smoothing procedure using grit paper and/or diamond cloths with an abrasive element such as corundum (Bagno and Di Bello, 2004). The particle size of the abrasive element will determine the surface characteristics. Fine particles produce smooth surfaces, while larger particles produce rough surfaces. Simka *et al.* (2012) used an electrochemical technique to polish titanium alloys with ammonium fluoride and sulphuric acid. The R_a values measured by a profilometer were 0.27 µm, while AFM measurements

revealed an R_a value of 39.35 nm. Moreover, better corrosion resistance was also noted.

Reddy *et al.* (2007) compared the surface roughness of Ti samples finished and polished using different materials. The Ti samples were polished with different agents. The results obtained from the perthometer (instruments used for measuring surface roughness) and SEM demonstrated that implants polished with silicon carbide cones and orange polishing cake, had the lowest R_a values of 0.27 µm.

Electro discharge machining (EDM) was used for finishing the CpTi surfaces. It was concluded that this finishing technique produced a rougher titanium surface when compared to conventional finishing with burs. Moreover, SEM, XPS and EDS analyses confirmed the significant effect of EDM on inducing chemical and topographical changes, as well the hardness of CpTi surfaces (Zinelis *et al.*, 2014).

c- Grit blasting

Grit blasting is a subtractive technique used to increase the surface topography. Blasting of titanium surfaces is done by spraying the surface with a combination of air and abrasive particles such as aluminium oxide (Al_2O_3) and/or titanium dioxide (TiO_2) (Marinho *et al.*, 2003). Silicon carbide has also been used for sandblasting (Aparicio *et al.*, 2003).

It was noted in an animal study that implants made from CpTi and blasted with Al_2O_3 particles sized 25 µm and 250 µm showed mean BICs of 26.1 % and 20.2 %, respectively. This difference in the bone response was explained due to the

variation in the size of particles producing different levels of roughness that might lead to increased ionic exchange, leaving the material in close contact to the surrounding tissue (Wennerberg *et al.*, 1996a).

Mustafa *et al.* (2001) found that a larger TiO_2 particle size of 180–300 µm produced a higher level of roughness (S_a= 1.38 µm) in comparison to other surfaces blasted with particle size of 63–90 µm, 160–180 µm and non-blasted machined implants, which had an S_a value of 0.72 µm, 1.30 µm, and 0.20 µm, respectively. They also reported a significant increase in osteoblastic-like cell differentiation with increased surface roughness. However, no differences in osteoblast-like cell response were reported with increased particle size. Similarly, Gotfredsen *et al.* (2000) reported higher removal torque test values with larger TiO_2 particle sizes at 6, 9, and 12 weeks. The particle grain sizes examined were 10–53 µm, 63–90 µm, 90–125 µm, while the S_a values were 1.05 µm, 1.16 µm, and 1.45 µm, respectively.

Rønold *et al.* (2003) pre-treated TiO_2 blasted implants with two concentrations of hot hydrochloric acid (0.01 M, 1 M), and compared them to non-treated TiO_2 blasted implants. Tensile test analysis was undertaken 8 weeks after implantation in a rabbit tibia, to assess the attachment capacity of implants to bone. The test discovered better mechanical retention was associated with the non-treated TiO_2 blasted implants. Aparicio *et al.* (2003) assessed the corrosion behaviour of different particle sizes and materials used for sandblasting. They found that large particles increased the R_a values and particles made from Al_2O_3 showed higher R_a values than ones made from SiC. They also concluded that both materials and particles sizes tested had acceptable corrosion behaviours.

1.9.2 Chemical modification

1.9.2.1 Acid etching

Acid etching is a subtractive chemical method used to increased surface topography. This method involves using a variety of acids such as hydrofluoric (HF), nitric (HNO_3), or sulphuric acid (H_2SO_4) in different concentrations. These acids can be used alone or combined together to form an acidic solution (Dohan Ehrenfest *et al.*, 2010).

Bone-to-implant contact was evaluated by Trisi *et al.* (2003) on dual acid-etched surfaces and machined untreated surfaces. Histomorphometric and histological analysis 2 months after implant placement in the posterior maxilla revealed that the implant surfaces treated by acid etching produced an enhanced BIC of 47.81 % in comparison to the machined surfaces' 19.00 %, thus proving clinically that osseointegration can be improved by acid etching in areas with poor bone quality. Guo *et al.* (2007) also reported improved osteoinductive reaction of the cells in close contact to surfaces that were grit-blasted and treated with 0.2 % HF acid than other grit blasted surfaces.

Lamolle *et al.* (2009) also demonstrated better biocompatibility and higher surface roughness values for surfaces treated with HF acids. They also found a correlation between the amount of surface roughness produced and the time of exposure to HF acids, where discs that were left for more than 90 seconds in HF acids showed greater S_a values. Cooper *et al.* (2006) also noted improvement in osteoblastic cells' differentiation and interfacial bone formation associated with HF acid treatments of

titanium grit-blasted surfaces. Iwaya *et al.* (2008) reported an increase in the roughness parameter R_a for titanium discs etched with concentrated H_2SO_4. Moreover, this did not seem to cause any adverse biological effect when osteoblasts-like cells were cultured on their surfaces.

Synthesised phosphoric acid treatment was used as a chemical treatment to increase the bioactivity of implant surfaces (Viornery *et al.*, 2002). Three phosphoric acids were tested: methylenediphosphonic acid (MDP), propane-1, 1, 3, 3-tetraphosphonic acid (PTP), and ethane-1, 1, 2-triphoshopnic acid (ETP). The XPS and time-of-flight secondary ion mass spectrometry (ToF-SIMS) results demonstrated a chemical reaction between titanium and phosphoric molecules. Bioactivity testing by incubating the modified titanium samples in Hank's solution suggested an ability to grow calcium phosphate after 14 days.

A study by Marino *et al.* (2012) used SEM and AFM to investigate the microstructure and topography of four different treatments, with the sandblasted and acid etched in HF/HNO_3 being the control. Their study did not report any difference between the control group and tested groups, which were a) acetone, acid etched; b) acetone, acid etched nitric acid; and c) acetone, acid etched, sulphuric acid. All acid etching was carried out using the combination of HF/HNO_3. The R_a values were 0.72 µm for the control and 0.74 µm, 0.70 µm, and 0.71 µm for groups a, b, and c, respectively.

1.9.2.2 SLA and SLActive surfaces

The increasing demand for early loading led to the development of new surfaces such as SLA and SLActive surfaces from Straumann. These surfaces are produced by sandblasting the surface with large grit size particles followed by acid treatment with a combination of acids: HCl/H_2SO_4 or HF/HNO_3 (Ferguson *et al.*, 2006; Miron *et al.*, 2010) (Figures 1.5 & 1.6). SLA surfaces revealed a high success rate in prospective human studies (Roccuzzo *et al.*, 2001; Bornstein *et al.*, 2005).

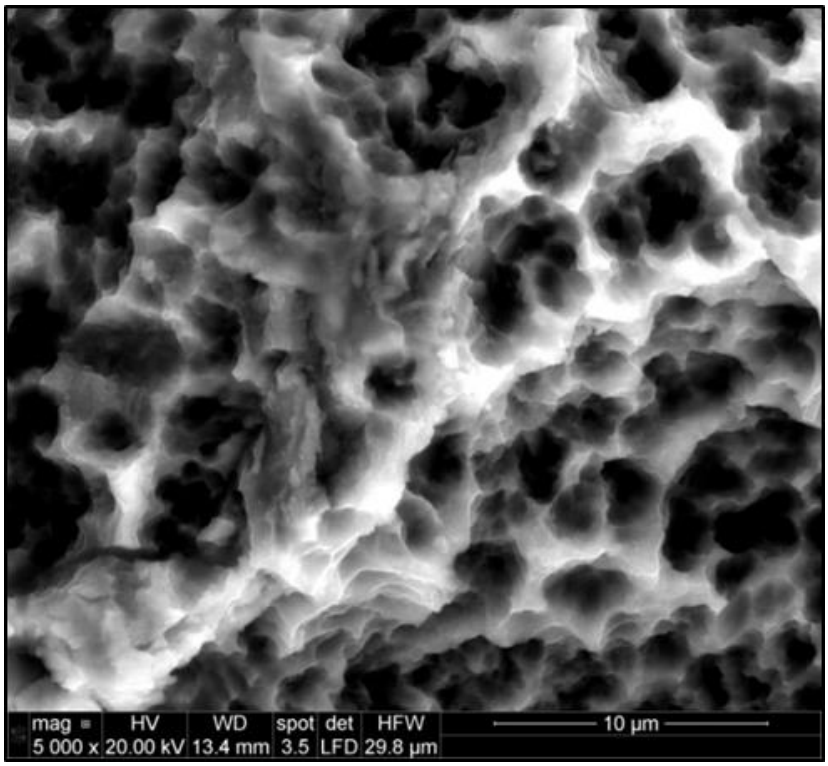

Figure 1.5 SEM image of a titanium sample with SLActive surface at 5000x magnification

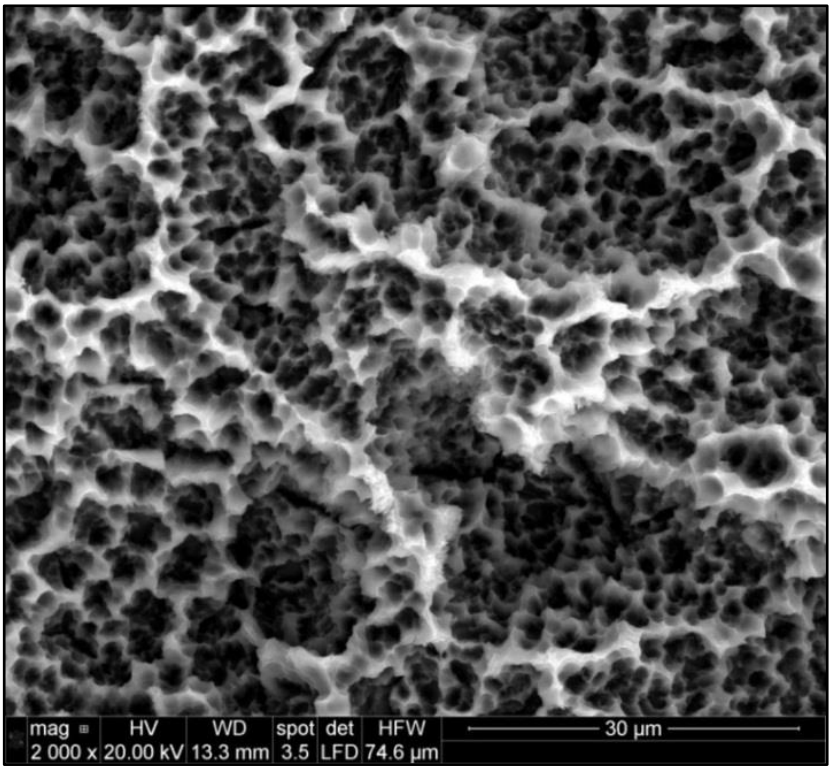

Figure 1.6 SEM image of (Roxolid®) sample with SLActive surface at 2000x magnification

Abrahamson *et al.* (2004) assessed the osseointegration ability of both SLA surfaces and turned implants in their early phases of healing, using experimental chambers imbedded in dogs. They found that SLA surface implants promoted more bone apposition in close contact to surfaces than turned surfaces during the first week. The BIC values continued to increase significantly for the SLA surface from 24.8 % in the first week, until it reached 65 % at 12 weeks. Whereas, for the turned surfaces, the BIC was 13.9 % at the first week, which then increased to 36.8 % at 12 weeks. Another study on rats was in agreement with these results. However, the significant difference between the SLA surfaces and turned ones was only evident after 30–60 days (Marinho *et al.*, 2003).

SLA surfaces which are sandblasted and acid etched with a combination of HCl/H_2SO_4 showed the highest removal torque values after 52 weeks in pigs. These values were 6.9 Nm at 24 weeks in comparison to 5.3 Nm for the TPS implants (Buser *et al.*, 2004). Busser *et al.* (1991) reported an enhanced BIC of 60 % when sandblasted surfaces were etched with HCl/H_2SO_4 in comparison to other non-acid treated sandblasted surfaces with the same grit size. This was explained by the ability of the latter acid combination to produce a secondary level of roughness.

Ferguson *et al.* (2006) modified the SLA surface by chemically enhancing the SLA surface through rinsing in NaCl under N_2 protection after they had been acid etched, and then storing in NaCl solution to produce the SLActive surface. They suggested that these modified surfaces performed better in the biomechanical testing than the SLA surface. Moreover, Rupp *et al.* (2006) reported the effect of these surfaces on increasing wettability and hydrophilicity along with the surface energy of the TiO_2 implant surface.

Busser *et al.* (2004) confirmed the hydrophilicity of SLActive surfaces in comparison to SLA surfaces. Differences in the chemical composition were also reported by XPS. Their *in-vivo* results concluded better BIC with the SLActive surface in the early weeks. However, the difference between the SLActive and SLA surfaces was not significant after 8 weeks. Bornstein *et al.* (2008b) noted increased bone apposition around the SLActive surfaces after 2 weeks of implantation in animal mandibles. However, in the study this effect disappeared after 4 weeks. The above studies suggest that SLActive surfaces have the ability to reduce healing times and accelerate early healing. Recent research comparing SLA and SLActive surfaces

suggested that the enhanced osseoconductivity of SLActive surfaces could be attributed to the nano-protrusions detected on its surface (Murphy *et al.*, 2017).

Several treatments have been introduced to SLA surfaces to increase their ability to osseointegrate. Some research was directed towards increasing the bioactivity of the SLA surface first with acid etching, and then immersing it in an alkaline solution (NaOH), followed by thermal treatment. It was noted that this type of treatment resulted in a nano-structure topography, with the ability to produce HA layers when implanted *in-vivo*. Moreover, the pull out results confirmed their ability to anchor to bone (Aparicio *et al.*, 2011).

1.9.2.3 Alkaline treatment

Kim *et al.* (1997) proposed a novel method to improve implant bioactivity by immersing CpTi plates in 5 M of NaOH solution at 60 °C for 24 hours. The Ti plates were then washed and dried at 40 °C for 24 hours, followed by heat treatment at 400–800 °C for 1 hour. The SEM results showed that the aforementioned treatment resulted in a strong porous sodium titanate coating on the titanium surface. Furthermore, they had the ability to grow bone-like apatite on their surfaces when immersed in simulated body fluid (SBF).

Nishiguchi *et al.* (2003) used the pull-out test and SEM to evaluate the effect of alkaline and heat treatment *in-vivo*. Titanium rods were first immersed in sodium hydroxide solution and subsequently heat treated following the same previously described method. The control group was polished implants. The pull-out test revealed stronger bone implant anchorage related to alkali and heat-treated rods

than polished rods. However, profilometry did not show any difference in the surface roughness between the control and studied groups, thus suggesting an enhanced chemical bond between the alkaline and heat-treated surfaces with the underlying bone.

In-vivo studies have noted the formation of apatite on Zr, CpTi, and binary TiZr surfaces following alkaline and heat treatment (Chen *et al.*, 2008). The X-ray diffraction (XRD) analysis and XPS results concluded that all surfaces with the aforementioned treatment had the ability to grow apatite on their surface following their immersion in SBF.

1.9.2.4 Electrochemical treatment

Electrochemical modification, combines chemical and physical modifications, to improve bone fixation due to the resultant biochemical bonding (Sul *et al.*, 2009). Electrochemical treatments used in dentistry can be either anodic or cathodic treatments. These techniques are anodic oxidation, electrophoretic HA deposition, and cathodic depositions (Kim and Ramaswamy, 2009).

Sul (2010) investigated the influence of nanotubes on Ti implant surfaces, which were created using the anodisation technique. Nanotubes were fabricated using grit-blasted Ti implants, which were anodised by potentiostatic anodisation using H_3PO_4 and HF acids for 3 hours. Sul compared these implants with blasted implants as controls *in-vivo*. Chemical composition and morphology of the nanotubes were analysed using SEM, XPS, optical profilometry, and light microscopy (LM). Six weeks after implantation in rabbits, the surface analysis results revealed the formation of a

porous nanostructure on modified Ti surfaces with a uniform spacing of 40 nm between them, and a wall thickness of 15 nm, 700 nm long. Nanotube implants revealed more bone apposition and moreover, demonstrated higher values in removal torque test than the controls. The outcomes were explained by the formation of fluorinated titanium oxide on the nanotubes' surfaces, which had the ability to form a chemical bond with bone.

Sul *et al.* (2006) showed that osseointegration can be improved and accelerated with the use of magnesium ion (Mg) oxidised implants (in comparison to machined implants at 3 weeks). Moreover, implant failure occurred inside the amorphous layer itself in the Mg implants rather than between the implant and amorphous layer, which happened in the controls. The same results were noted when blasted and Mg incorporated implants were compared to machined, blasted implants (Sul *et al.*, 2009).

Kuromoto *et al.* (2007) assessed the effect of using different voltages in anodic oxidation. 1.4 M H_3PO_4 was used for oxidation the 50, 100, 150, 200, and 250 voltages were tested, respectively. The SEM and atomic force microscope (AFM) results showed a positive correlation between TiO_2 film thickness and increased oxidation voltage. Yamagami *et al.* (2004) tested cylindrical titanium implants placed in rabbits. The implants were treated first by anodic oxidation with phosphoric acid 0.1 % at 150–200 voltage, and thereafter sandblasted. Shear loading test and histological examination results showed that this type of treatment demonstrated increased surface roughness and better interfacial bonding strength.

Giavaresi *et al.* (2003) studied four different surface treatments for CpTi implants placed in sheep. Their study showed that surfaces anodised and hydrothermally treated had higher surface roughness when compared to machined surfaces and surfaces treated with HF acids, or hydroxyapatite. Moreover, they behaved similarly *in-vivo* to HA coatings after being placed for 12 weeks.

A study using XPS, SEM, and AES by Kang *et al.* (2009) evaluated the effects of different surface treatments on implant topography and chemical composition. The study included three implants treated with different blasting and acid-etching techniques from three companies: OsseoSpeed® (Astra Tech AB, Mölndal, Sweden), Osseotite® (3i Implant Innovations Inc., FL, USA), and SLA® (Institut Straumann AG, Basel, Switzerland) surfaces and one electrochemical oxidised implant TiUnite® (Nobel Biocare, Göteborg, Sweden). They noted that the electrochemical oxidised surface had the ability to combine both microstructural and chemical alterations to TiO_2 surfaces with the detection of phosphate ions in porous oxide coatings.

Surface analysis studies by Schüpbach *et al.* (2005) observed the bone-oxidised implant zone of clinically retrieved implants that had oxidised surfaces. The SEM, backscattered electron (BSE) imaging, and EDS analysis demonstrated the presence of a mixed-surface structure containing micro and nano pores. They also indicated the existence of bone growing inside these pores. Anodised surfaces were also shown to be highly hydrophilic with low contact angle measurement when compared to machined, sandblasted, and acid etched surfaces. Moreover, a higher removal torque of 83.15 Ncm with the highest surface roughness of R_a = 0.87 µm was demonstrated by Elias *et al.* (2008).

1.9.3 Other surface modifications

1.9.3.1 Ion implantation

De Maeztu *et al.* (2003) assessed the carbon, carbon oxide, nitrogen, and neon ion implantation on Ti and Ti alloys *in-vivo*. Surface analysis of the surface-modified implants using SEM, EDS, and XPS indicated superiority of the ion implanted surfaces in terms of BIC values over machined implants, with significant BIC results for surfaces treated with carbon and carbon oxide at 69.50 % and 84.65 %, respectively. Moreover, the quality of bone integration was also enhanced with ion implantation. The same group of researchers assessed the implantation of carbon oxide ion (CO^+) on 22 mini implants in humans. The implants treated with (CO^+) were placed in an ion implanter, subjected to temperature of 170 °C, and then sterilised with dry heat at 120 °C for a period of 4 hours. The control group were machined implants; both implants were placed in upper and lower jaws. Both the SEM and histological analysis results revealed higher BIC values for the CO ion implants in comparison to the machined implants. The authors did not report any harmful effect accompanied with (CO^+) treated mini implants during the prospective period of 3 years (De Maeztu *et al.*, 2013).

1.9.3.2 Titanium plasma spraying

Plasma spraying was one of the early additive techniques used to increase surface roughness. It is a widely accepted thermal spraying technique used to deposit coatings such as Ti, Al_2O_3, and ZrO_2 on dental implant surfaces using different gases at high temperature (Sutter *et al.*, 1988; Liu *et al.*, 2004). The plasma spraying

techniques used are: vacuum plasma spraying (VPS) and atmospheric plasma spraying (APS) (Liu *et al.*, 2004).

In 1970, the plasma spraying of titanium surfaces was first introduced by Hahn and Palich *et al.* (1970) through spraying unalloyed titanium pins with a titanium hydride powder using nitrogen gas at high temperature, which resulted in a porous rough coating 0.35 inches thick. The level of roughness of this porous coating was believed to be in the range of moderate to high, and it increased the surface area approximately by a factor of 6 (Sutter *et al.*, 1988; Braem *et al.*, 2014). Sutter *et al.* (1988) described the technique used for the plasma spraying of ITI implants, which was undertaken by exposing the titanium powder to a flame with an argon gas stream at a temperature in the 15,000–20,000 °C range and a gas velocity of more than 3,000 m/s. This resulted in a titanium coating which was 0.03–0.04 mm thick being incorporated and welded on the implant surface.

The ability of TPS implant surfaces to establish and maintain osseointegration was proven by many experimental animal studies. A long-term *in-vivo* study revealed that titanium sprayed coatings had the ability to osseointegrate and maintain strong contact with bone, even under functional loading (Schroeder *et al.*, 1981). The effect of these porous coatings on connective and epithelial tissues was also investigated, both under light and electron microscopy, confirming the strong anchorage between titanium sprayed surface and epithelium, connective tissues. This effect was maintained and was not jeopardised by the loading conditions.

An *in-vivo* study carried out by Gotfredsen *et al.* (2001) investigated the effect of applying static lateral load through an expansion screw. This was undertaken using

4 TPS implants connected to crowns that had expansion screws fitted on them under 3 different loads. The loaded sides were compared to the unloaded sides for 24 weeks. Bone density and bone-to-implant contact results reflected the adaptive capacity of these TPS implants to lateral loading when compared to the unloaded sides. Similarly, another study by the same group of researchers using the same technique compared TPS implants to machined surfaces. The load tested was set to 0.6 mm for a period of 24 weeks. The results of this study showed inferior BIC values and average bone density, along with the occurrence of angular bone defects around machined implants in comparison to TPS implants.

Another *in-vivo* study compared machined implant surfaces to three different TPS surfaces: TPS, TPS plus acid treated, and TPS with HA coating. The results did not reveal any difference in bone response between the TPS and machined surfaces (Vercaigne *et al.*, 1998).

However, the findings from a 3 year clinical study comparing TPS (ITI) implants to machined (Branemark) implants were in contrast to those obtained in the animal studies. The outcome of this study did not support the superiority of TPS implants over machined implants in terms of bone loss or survival rates. Moreover, it revealed that TPS surfaces demonstrated a statistically higher tendency for peri-implantitis in comparison to machined implants (Åstrand *et al.*, 2004).

1.9.4 Bioceramic coatings

In general, the term bioceramic is used to describe a biocompatible ceramic material, which can be used for biomedical or clinical purposes. Based on the chemical components, bioceramics are categorised into two main groups: 1) the calcium phosphate (CaP) group, including HA; and 2) others (Tanaka and Yamashita, 2008). Bioceramics used for dental implant coatings are based on the CaP group and HA, which is part of the normal composition of bone and teeth (Campbell, 2003). Interest in bioceramic coatings for dental implants has increased over the years, mainly due to their ability to release calcium phosphate that stimulates osteogenesis at the bone-implant interface, thus accelerating the implant biomechanical fixation (Surmenev *et al.*, 2014).

1.9.4.1 Hydroxyapatite (HA) $Ca_{10}(PO_4)_6(OH)_2$

Hydroxyapatite is a calcium phosphate bioceramic material that has been sprayed onto dental implants due to its similarity in composition to human bone, leading to the formation of an apatite-like bond with the underlying bone (Kokubo *et al.*, 2003). This coating showed the best morphometric results for bone implant anchorage when compared to other surfaces *in-vivo* (Buser *et al.*, 1991). It also revealed higher degrees of surface roughness when compared to TiO_2 blasted implants and machined implants (Gotfredson *et al.*, 1995). The R_a values reported in the latter study for the HA, TiO_2, and machined surfaces were 1.89 µm, 0.61 µm, and 0.31 µm, respectively. In addition, the HA coating demonstrated a higher

removal torque value after healing and better fixation in comparison to the TiO_2 blasted and machined surfaces (Gotfredson *et al.*, 1995).

Hydroxyapatite powders used in biomedical fields have been produced using several methods and are generally classified as dry methods, wet methods, energy input methods, and other methods (Fihri *et al.*, 2017).

1.9.4.1.1 Coating deposition methods

Several deposition techniques have been developed to deposit HA coatings such as plasma spraying (Hung *et al.*, 2013), ion beam sputtering, electrophoretic deposition, flame spraying, dip coating, high velocity oxy-fuel combustion spraying, hot isostatic pressing, ion beam dynamic mixing (Tsui *et al.*, 1998), and blasting (Ishikawa *et al.*, 1997).

1.9.4.1.2 Plasma sprayed hydroxyapatite coatings

Plasma spraying technique is the optimum method used for applying HA coatings to dental implants. This method will result in the formation of crystalline and amorphous phases of calcium phosphate combined with other phases such as tricalcium phosphate (α or β), tetracalcium phosphate (TTCP), calcium deficient hydroxyapatite (CDHA), and calcium oxide (CaO) (Prevéy, 2000; Liu *et al.*, 2004). The HA coating thickness resulting from plasma spraying reported in the literature ranges from 50 to 200 µm (Jansen and Leon, 2009).

Despite the biocompatibility of plasma sprayed hydroxyapatite (PSHA) coatings, there are still concerns regarding their use due to issues related to the quality of

the coatings, and specifically the thickness, crystallinity and purity, dissolution, adhesion, and fatigue failure (Jansen and Leon, 2009). The characteristics of the PSHA coatings will vary according to the spray parameters used such as the gas flow rate, spray distance, and powder feed rate (Levingstone *et al.*, 2017). Investigations using different substrate temperatures and cooling conditions resulted in HA coatings with different residual stresses. Studies highlighted that the increase in residual stress was associated with increased susceptibility to fracture in the bond between the coating and titanium substrate (Yang and Chang, 2001). Tensile testing revealed a weak mechanical bond between HA and titanium (Khor *et al.*, 2003). In addition, it was noted that increased thicknesses of the coatings reduced its fatigue resistance (Lynn and DuQuesnay, 2002). Nevertheless, the adhesion of HA coatings to the titanium substrate is an essential factor in preventing the mechanical failure of HA coating.

The major limitation associated with HA coatings is their partial resorption or dissolution over time (Gottlow *et al.*, 2012). After implantation, the dissolution of the bioceramic coatings is essential to induce a cascade of biological events, leading to the precipitation of apatite on the implant surface (LeGeros, 2002). However, the main issue in this aspect is to control the rate of dissolution to prevent coating degradation and maintain the bond between the implant and coating, ensuring long-term stability (Sun *et al.*, 2001). Research showed that the crystallinity and phase composition of the HA coating determines its dissolution, whereby the higher the crystallinity, the lower the dissolution (Steinemann and Perren, 1977).

Therefore, research has been directed towards altering the crystallinity of HA coatings.

Flame vapour treatment was used by Xue *et al.* (2004) to increase the crystallinity of PSHA coatings: vapour flame treatment of PSHA coatings increased the crystallinity of the HA coatings by 33 %, which resulted in higher shear strength and better bone contact. The results noted distinguishable dissolution of the sprayed coating in comparison to vapour flame-treated coating, which was related to the phase composition of the coating (Al-Nawas *et al.*, 2012). Hung *et al.* (2013) examined a series of methods to enhance the properties of HA coatings on titanium alloys. This was done by first increasing the crystallinity and calcium ion concentrations of the coatings by immersing them in simulated body fluids for 28 days. This decreased the surface roughness from 9.36 µm to 8.41 µm. Then, they tested different nozzle transverse speeds. The resultant HA coating demonstrated a high density and uniformity. When HA coatings were applied using plasma spraying, better bone response was also reported in comparison to TPS surfaces (Vercaigne *et al.*, 1998). Moreover, PSHA-coated implants demonstrated better BIC length both before loading and after 1 year of loading, when compared to TPS and Ti implants. However, the pull-out test did not reveal any difference between any of the surfaces in terms of interfacial strength (Ong *et al.*, 2004).

An *in-vivo* experiment comparing HA coatings to TPS coatings by Darimont *et al.* (2002) studied the coating thickness and bone contact, in their study the behaviour of the above coatings in cortical, trabecular and marrow bone was followed for 1 year. During the period of study, the HA coatings demonstrated a significant

reduction in its overall thickness in areas of reduced bone contact, trabecular, and marrow bone, while the TPS coatings did not show any reduction in their coating thickness. However, the HA coatings demonstrated better contact to bone than the TPS coating.

To overcome the limitations associated with the use of thick PSHA coatings, research has focused on the production of thin CaP coatings (Junker *et al.*, 2009). Thin CaP coatings demonstrated their ability to enhance the bone response at implant sites (Coelho and Suzuki, 2005). However, mechanical testing did not reveal any statistical difference between thin CaP-coated and uncoated samples in terms of biomechanical fixation (Coelho *et al.*, 2009).

1.9.4.1.3 Clinical performance of HA-coated dental implants

Several long-term studies were conducted on the survival and success of HA-coated implants. A study by Tinsley *et al.* (2001) involving 181 HA-coated implants placed in the mandible found that their survival rate was 100 %. However, the success rates reduced from over 96 % in the first 4 years to 83 % after 6 years. Similarly, Artzi *et al.* (2006) found a reduction in both the survival and success rates over time. Furthermore, the accumulative success rate decreased dramatically from 5 years to 10 years in function from 89.9 % to 54 %, respectively.

Conversely, survival rates reported for HA-coated implants followed up for 6–10 years after placement in mandibles were shown to be 99 %, and the mean annual bone loss calculated was less than 0.2 mm per year (Leventi *et al.*, 2014). Histomorphometric studies found that 52–70 % of HA coatings remain on implant

surfaces after 11 years in function (Baker *et al.*, 2010). Moreover, immediately loaded HA-coated implants in maxillary premolar regions showed 100 % success rates after 3 years following placement (Proussaefs and Lozada, 2004). In order to avoid all the limitations associated with PSHA coatings, research is directed towards finding alternative methods of depositing HA coatings onto metal implants that do not alter the structure of the primary HA powders.

1.9.4.1.4 Blasted hydroxyapatite coatings

Several alternatives have been developed to avoid the disadvantages associated with the use of high temperatures during HA deposition (Harun *et al.*, 2018). Blasting is one of the methods that has been proposed. In 1997, Ishikawa *et al.* (1997) sprayed HA coating on grade 4 titanium plates using a sandblasting unit. The blasting was carried out at 0.54 MPa for 10 seconds at a distance of 2 mm from the sample. The surface analysis of the coated samples revealed the effectiveness of this method in depositing a uniform homogenous HA coating onto the titanium surface. Further *in-vivo* assessment of these coatings at 6 weeks also demonstrated significant differences in BIC when compared to non-coated titanium surfaces. The reported roughness parameter R_a was also less than that of the non-coated titanium surfaces (Mano *et al.*, 2002).

Histological examination showed better bone contact with blasted surfaces when compared to flame sprayed coatings. The BIC ratios reported were 75.5 % and 30.8 %, respectively. However, when comparing the calcium and phosphate release in SBF, the blasted samples tended to release their coatings faster (Ishikawa *et al.*,

2011). Another *in-vivo* study by Nakada *et al.* (2007) using backscattered imaging revealed enhanced bone tissue formation around all the coated surfaces.

Gbureck *et al.* (2003) evaluated the change in surface topography of the coated samples and their adhesion to CpTi substrates using the sandblasting method. The coatings were found to be homogenous and thin with an average surface roughness of 10–15 µm. In addition, the SEM, EDS, and XRD analyses confirmed their stability on the surface, even after ultrasonic cleaning. One explanation for this was that the blasting process produced a combination of physical and chemical-mechanical bond to the underlying substrate. In contrast, when the same method was used on zirconia surfaces the coating was thin and non-uniform in comparison to the thermal spraying method (Azari *et al.*, 2017).

O'Donoghue and Haverty (2012) developed a new micro-blasting method named CoBlast™. This deposition method involves blasting a surface with a simultaneous flow of both abrasive powder and a dopant stream. The abrasive powder (usually Al_2O_3) roughens the surface, while the dopant enhances the osteoconductivity of the surface resulting in a thin bioactive layer. Dunne *et al.* (2014) demonstrated the effectiveness of this method by producing HA coatings with enhanced surface roughness, crystallinity, and adhesion in comparison to PSHA coatings. Similar to the sandblasting method, it was suggested that CoBlast™ bioceramic coatings bind to the underlying substrate by mechanical and chemical bonding. However, the adhesion of the CoBlast™ coating is significantly stronger than sandblasted coatings (O'Sullivan *et al.*, 2011). Furthermore, *in-vitro* assessment revealed their ability to enhance cell proliferation (Barry *et al.*, 2013), and enhance osteoblast cell

proliferation and differentiation (Umeda *et al.*, 2017). Recently, the CoBlast™ method has been used to deposit HA coatings on commercial orthopaedic and dental implants, and marketed under the name OsteoZip+™.

1.9.5 Biochemical treatments

Titanium surfaces have been subjected to biochemical treatments using different bioactive organic and inorganic components of natural bone (Gaviria *et al.*, 2014). When applying these compounds, the cellular activity in the surrounding biological environment will be altered to promote bone formation (Yeo, 2014). The aim of the biochemical surface treatment is to control the healing process after implant placement through delivering molecules to the tissue-implant interface (Wirth *et al.*, 2017). The inorganic components include the HA and CaP-based coatings previously discussed (in §1.9.4). Other forms of biochemical treatments involve the incorporation of bioactive drugs or antibiotics onto the implant surface (Anil *et al.*, 2011).

1.9.5.1 Organic coatings

Numerous organic molecules such as peptides, extracellular matrix proteins (ECM), bone morphogenetic proteins (BMPs), and growth factors (GFs) have been coated onto implant surfaces to trigger a specific tissue response (Bagno and Di Bello, 2004; Morra, 2006). Generally, immobilisation of these molecules on the implant surface will result in a functionally and biologically active implant surface that regulates the signalling cascade of cellular responses at the bone-implant interface (De Jonge *et al.*, 2008).

Research has showed that GFs and ECM proteins like fibronectin, vitronectin, and collagen play a remarkable role in enhancing bone regeneration, through modulating the osteoblast cell adhesion, proliferation and differentiation on implant surfaces (Stanford and Keller, 1991; Petrie *et al.*, 2009; Agarwal and García, 2015). A study by Ku *et al*. (2005) evaluated the response of mouse osteoblast cells on titanium discs coated with fibronectin or vitronectin. The study showed that the osteoblast adhesion, proliferation, and differentiation were faster when using these coatings. Furthermore, this effect was significantly higher with fibronectin-coated surfaces.

Coating acid-etched titanium discs with collagen type I enhanced the BIC after 2 weeks of implantation in a rabbit femur in comparison to the control acid-etched surface (Morra *et al.*, 2010). However, this effect was not sustained at 4 weeks. The alkaline phosphatase activity (biochemical marker of bone formation) indicated that collagen type I coatings did accelerate the bone formation. Moreover, this study highlighted that the surface microstructure played a more significant role in guiding

the cellular adhesion and proliferation of the osteoblast-like cells than its chemical composition. Another *in-vivo* study tested collagen type I on anodised titanium discs, with the results proving the enhanced bone apposition with such coatings after 4 weeks. Furthermore, the same study confirmed this effect *in-vitro* using human mesenchymal cells (Morra *et al.*, 2006).

In order to optimise the ability of implant surfaces to osseointegrate, several ECM components and calcium phosphate have been combined with collagen coatings. Ferguson *et al*. (2008) examined the effect of different modifications including collagen type I coatings with chondroitin sulfate (ECM proteoglycan). Their study compared this coating with Ti, Zr, and Ti coated with CaP and Ti treated with anodic plasma, and Ti coated with bisphosphonate. All implants were sandblasted and acid etched before treatment except, the Ti surface treated with anodic plasma which was only sandblasted. The removal torque results suggested that both collagen chondroitin sulfate and bisphosphonate coatings could enhance peri-implant bone formation. However, this effect was not found to be significantly different from Ti sandblasted and acid-etched surfaces, both in bone density and removal torque values at 8 weeks.

The effect of combining collagen type I coatings with other GFs was examined using acid-etched implants inserted in a pig skull by Mueller *et al*. (2011). The biological markers of bone formation (collagen type I and osteocalcin expression) were used to evaluate the enhanced biological performance of collagen type I coated implants. The study revealed that the addition of other GFs to the collagen type I coatings

failed to increase their ability to express collagen type I or osteocalcin. In fact, collagen type I coating alone produced a significant effect.

The addition of HA to collagen type I coatings showed considerable potential to increase BIC after 6 weeks of placement (Lee *et al.*, 2014). Similarly, bone density and BIC were enhanced when using combined calcium phosphate and collagen type I coatings after 1 and 3 months of placement (Schliephake *et al.*, 2006).

Coating implant surfaces with the osteogenic peptide sequence arginine-glycine-aspartic acid (RGD) found in many ECM proteins significantly increased bone formation at 2 and 4 weeks when compared to smooth titanium surfaces (Ferris *et al.*, 1999). A histomorphometric study using pig maxilla demonstrated that RGD peptide-modified surfaces increased BIC at 2 weeks when compared to the control SLA surface (Germanier *et al.*, 2006). However, this effect was not significant after 4 weeks. Another study comparing RGD coatings implanted in dog's mandible revealed a significant increase in bone quality and quantity in the first month, when using high concentrations of RGD peptides (Schliephake *et al.*, 2005).

Conversely, some *in-vivo* studies reported insignificant effects of RGD peptides on bone formation when compared to other bioactive coatings (Jenny *et al.*, 2016). Barros *et al.* (2009) examined two concentrations of RGD peptides (20 and 200 µg/ml) on grit-blasted and acid-etched control implants. The peptide coatings were added to the control implants after being treated with HA. Their results did not report any significant effect on BIC or bone density between the control and peptide-coated implants with different concentration. In contrast, another study examining the same surfaces and concentrations using another peptide known as

15-residue peptide reported that peptide-coated implants significantly increased the BIC for up to 30 days in comparison to the control (Lutz *et al.*, 2010).

Several GFs including: transforming growth factor (TGF), insulin-like growth factor (IGF), platelet-derived growth factor (PDGF), fibroblast growth factors (FGF), and vascular endothelial growth factor (VEGF), have been reported to be important factors in bone formation (Deschaseaux *et al.*, 2009; Agarwal and García, 2015; Tahriri *et al.*, 2017). Applying GFs on surface-modified implants shows some positive results *in-vivo*. Anodised titanium implants soaked in fibroblast growth factor-fibronectin (FGF-FN) revealed higher removal torque and BIC when compared to the control anodised implants after 12 weeks (Park *et al.*, 2006). Schliephake *et al*. (2015) reported an increase in the rate of BIC in the first month of healing with sandblasted implants coated with recombinant human vascular endothelial growth factor (rhVEGF) in comparison to the control sandblasted titanium implants. This study concluded that the use of rhVEGF enhanced the bone regeneration at the implant site.

Contrarily, histological and histomorphometric analysis by Nikolidakis *et al*. (2009) reported a statistically lower BIC values with different concentrations of coatings in comparison to uncoated acid-etched implants after 6 weeks of placement. Additionally, connective tissue formation was observed around some of the implants coated with TGF-β1 and not around the uncoated implants. Moreover, the conjunction of TGF-β1 to CaP coatings on titanium implants did not produce any statistical effect on the peri-implant bone formation (Schouten *et al.*, 2009).

The most common GFs studied are bone morphogenetic proteins (BMPs), which are members of the transforming growth factor family (Boyne and Jones, 2004). This group of proteins is known to stimulate the undifferentiated mesenchymal cells to differentiate into osteoblasts to form bone (Urist, 1965; Simon and Watson, 2002). Among these BMPs, most trials in the field of maxillofacial applications and dental implants are focused on bone morphogenic protein-2 (BMP-2) due to its major role in osteogenesis (Kelly *et al.*, 2016; Haimov *et al.*, 2017; De Queiroz Fernandes *et al.*, 2018).

In-vivo observations using a synthesised form of BMP-2 known as recombinant human bone morphogenetic protein-2 (rhBMP-2) proved its ability to improve osseointegration when used on modified titanium surfaces (e.g. sandblasted dual acid etched, anodised, SLA, and PSHA surfaces) (Jae-Kwan *et al.*, 2013; Jiang *et al.*, 2013; Kim *et al.*, 2013b; Yoo *et al.*, 2014). Nevertheless, titanium surface modifications could affect the osteogenic properties of rhBMP-2, due to the difference in the amount of rhBMP-2 adsorbed on these surfaces (Xiao *et al.*, 2016).

For implant applications, rhBMP-2 can be applied directly (adsorbed) to implant surfaces or delivered with carriers like collagen and osseoconductive coatings (CaP and HA) (Jennissen, 2002; Hunziker *et al.*, 2012). Histomorphometric and microscopic evaluations show that the delivery method has a significant effect on the amount of bone deposited around rhBMP-2 coated implants (Liu *et al.*, 2007). Several studies have examined the effect of combining rhBMP-2 with other GFs. Lan *et al*. (2006) focused on combining rhBMP-2 with either recombinant FGF or IGF-1. Their study showed that by combining GFs an increase in bone formation can be

achieved up to 8 weeks post-implantation. Ramazanoglu *et al*.'s (2011) microradiography indicated that bone density could be enhanced with combined rhBMP-2 and rhVEGF coatings on CaP-coated implants.

A meta-analysis by Jenny *et al.* (2016) investigated the effect of different biological coatings (inorganic, ECM, peptides, and GF-coated surfaces) on BIC in comparison to uncoated surfaces. Their study concluded a significant increase in BIC percentages with inorganic and ECM coatings, whereas peptides and GFs did not show any significant effect.

Although the application of ECM components or GFs to the implant surface is advantageous, their therapeutic success depends on the delivery system, dose and concentration (Alenezi *et al.*, 2018). The release of such organic molecules should be controlled, in order to maintain its concentration until new bone formation is established (Luginbuehl *et al.*, 2004). However, the optimum dose, concentration, delivery method, and time needed for tissue repair are still under investigation.

1.9.5.2 Drug coatings

Recent approaches for dental implant biochemical treatments include the use of bioactive drugs like bisphosphonates and statins. Bisphosphonates are drugs that are regularly used to treat osteoporosis, due to their ability to decrease bone resorption by inhibiting osteoclast activity (Russell *et al.*, 2007). Coating implants with bisphosphonates shows considerable potential to enhance peri-implant bone mineralisation *in-vivo* and *in-vitro* (Yoshinari *et al.*, 2002; Ferguson *et al.*, 2008; Langhoff *et al.*, 2008; Abtahi *et al.*, 2010; Abtahi *et al.*, 2012; Kellesarian *et al.*,

2017). However, limited evidence is available to confirm that this is a clinically significant effect (Xuereb *et al.*, 2015; Najeeb *et al.*, 2017). Stadlinger *et al*. (2013) evaluated the osseointegration of sandblasted acid-etched implants with various treatments including bisphosphonates. Computed tomography and histomorphometric examinations indicated that implants coated with bisphosphonates produced a significant increase in BIC in rats. Radiographical examination of bisphosphonate-coated implants placed in 14 patients after 5 years was studied by Abtahi *et al*. (2016). The results revealed that the amount of marginal bone loss was lower around the bisphosphonate-coated implants compared to the uncoated implants.

Statins are cholesterol-inhibiting drugs that are reported to enhance osteogenesis through increasing the expression of the BMP-2 of osteoblast cells (Mundy *et al.*, 1999). Experimental attempts evaluating the effect of statins on titanium surfaces demonstrated that their systematic or local use holds a potential advantage to improve osseointegration (Ayukawa *et al.*, 2004; Fang *et al.*, 2015; Moraschini *et al.*, 2018). Histomorphometric analysis of the bone-implant interfaces demonstrated that systemic administration of simvastatin significantly improved the BIC and bone density around titanium implants in rats (Ayukawa *et al.*, 2004; Du *et al.*, 2009; Ayukawa *et al.*, 2010). Yang *et al*. (2011) evaluated the effect of simvastatin applied locally on sandblasted acid-etched titanium surfaces on osteoblast-like mice cells. The results showed that simvastatin increased the expression of osteoblast differentiation markers: ALP, osteocalcin, and collagen type I. This is in agreement with the study by Zhao *et al*. (2014b).

The use of antibiotics has also been studied as a possible coating for dental implants, to decrease the biofilm formation and possible risk of infection around dental implants (Zhang *et al.*, 2014; Saghiri *et al.*, 2016; Yarramaneni *et al.*, 2016). Coating titanium surfaces with vancomycin was effective in reducing bacterial growth (Zhang *et al.*, 2014). A study by Lee *et al*. (2013a) revealed that the deposition of amoxicillin on titanium oxide surfaces could reduce the risk of early implant failure due to its bactericidal effect.

1.9.6 Laser treatment

One of the recent developments in modern implant production is 3D implants, which are produced by rapid prototyping and direct metal forming processing by harnessing computer-aided design (CAD) technology. Mangano (2009) evaluated porous dental implants fabricated using a direct laser metal forming technique, known as direct metal laser sintering. In this method, the implants were made by the coalescence of layers created by the fusion of titanium powders using a computer-guided laser beam. The implants were implanted in a human maxilla, and demonstrated a significantly enhanced mean BIC in comparison to CpTi. Shibli *et al*. (2013) reported similar results and indicated that immediately loaded implants made by direct laser metal sintering had increased BIC percentages.

Figliuzzi *et al*. (2012) and Mangano *et al*. (2012) evaluated the effect of direct metal laser sintering in conjunction with computed tomography to fabricate customised root-shaped implants to replace missing teeth. Both studies showed successful integration of these implants after 1 year follow up. Traini *et al*. (2008)

demonstrated that the direct laser metal sintering technique can produce dental implants with controlled surface roughness and elastic modulus.

The direct laser fabrication technique used for implant production was assessed by Ricci *et al*. (2012) using AFM analysis to qualitatively assess the surface topography using different images and 3D ranges of different dimensions, namely 30 µm, 10 µm, and 5 µm, where the R_a values were 0.6 µm, 133.4 nm, 68.5 nm, respectively. They concluded that surfaces produced by this technique had topographic characteristics at the nanometre scale.

Femtosecond laser technology was applied to ZrO_2 surfaces to create grooves on the surface (Calvo-Guirado *et al.*, 2013). SEM and EDS analyses were used to assess the difference between laser-treated ZrO_2 implants and sandblasted acid-etched Ti implants. The BIC values were 51.36 % for Ti at 1 month and 61.73 % after 3 months, whereas the BIC for ZrO_2 was 44.68 % at 1 month and 47.94 % after 3 months. However, crestal bone resorption was generally greater with the laser-treated ZrO_2 implants than the Ti implants after 90 days. Moritz *et al.* (2003) reported successful results when CO_2 laser treatment was used to enhance the bioactivity of TiO_2 coatings. Using laser with acid-etched treatments showed enhanced BIC in comparison to laser treatments only (Rong *et al.*, 2009).

Dental implant surface roughness can also be modified by laser treatment (Braga *et al.*, 2007; Faeda *et al.*, 2009), which uses a laser beam to produce a surface with two levels of surface roughness at the micro and nano levels (Mariscal-Muñoz *et al.*, 2016). Furthermore, surfaces produced by laser treatment enhanced the osteoblast differentiation and subsequent bone formation (Hindy *et al.*, 2017). Laser

irradiation was also used to modify dental implant collars to establish a good biological seal around the dental implants and to minimise the risk of infection (Heinrich *et al.*, 2008; Pecora *et al.*, 2009; Botos *et al.*, 2011; Guarnieri *et al.*, 2014).

1.10 Implant surface characteristics and their biological influences

Implant surface properties are one of the factors that could optimise the host biological response to dental implants during healing (Albrektsson *et al.*, 1981; Davies, 2003). After implant insertion, the healing process is initiated by the adsorption of proteins and exchange of signals that result in the recruitment and migration of mesenchymal stem cell and osteoprogenitor cells on the implant surface arriving from the surrounding blood clot (Boyan *et al.*, 2016). Implant surface properties including roughness, surface energy, wettability, and chemistry are known factors that regulate and determine these early cellular responses at the bone-implant interface (Schwartz and Boyan, 1994; Rompen *et al.*, 2006).

Numerous studies showed that rough implant surfaces can affect osteoblast cell differentiation, proliferation, and migration (Schwartz *et al.*, 1999; Mustafa *et al.*, 2001; Bächle and Kohal, 2004; Kim *et al.*, 2006; Wennerberg and Albrektsson, 2009), adhesion (Cooper, 2000; Anselme and Bigerelle, 2005), morphology and growth orientation (Martin *et al.*, 1995; Zhao *et al.*, 2007; Lukaszewska-Kuska *et al.*, 2018).

Comparisons of the surface morphology of osteoblast cells cultured on rough (SLA) and smooth surfaces showed that rough surfaces can enhance osteoblast cell differentiation on their surfaces by having different cell morphologies and elevating the cell differentiation markers (Lai *et al.*, 2015). A similar conclusion was reported by Andrukhov *et al*. (2016), when they examined sandblasted acid-etched titanium surfaces with different levels of surface roughness. Significantly enhanced osteoblast proliferation and increased production of osteoblast differentiation markers (ALP, osteocalcin, and VEGF) were associated with the moderately rough surfaces in comparison to smooth or rough implant surfaces. This agrees with studies by Boyan *et al*. (2002), Kim *et al*. (2006), Rausch-Fan *et al*. (2008), and Lukaszewska-Kuska *et al*. (2018), which reported a significant increase in the secretion of osteoblast differentiation markers on rough surfaces in comparison to smooth surfaces.

In addition, *in-vitro* results demonstrated that the implant surface microstructure induces significant changes in the expression of specific osteogenic cytokines and GFs like prostaglandin E_2 (PGE_2), transforming growth factor β_1 (TGF-β_1), and BMPs (Kieswetter *et al.*, 1996; Takebe *et al.*, 2003; Zinger *et al.*, 2005; Rausch-Fan *et al.*, 2008). The growth of osteoblastic cells on rough surfaces tends to be scattered and not follow the surface orientation compared to smooth surfaces (Martin *et al.*, 1995; Lukaszewska-Kuska *et al.*, 2018). Furthermore, some studies demonstrated that osteoblasts have greater adhesion and proliferation on rough surfaces as a result of increases in the surface area available for bone growth (Rosales-Leal *et al.*, 2010).

In order to modulate the surface topography including roughness, many manufacturers have produced surface treatments that resulted in dental implants with combined changes in surface roughness, chemical composition, and physical properties (surface energy and wettability) (Morra *et al.*, 2003; Albrektsson and Wennerberg, 2004). Therefore, the effect of surface treatment on host tissues could be due to the synergistic effect of all these properties (Palmquist *et al.*, 2012; Rupp *et al.*, 2017). Furthermore, these properties will predetermine the matrix protein adsorption of the molecules in the local environment that influences the cellular attachment, adhesion, and subsequent osseointegration process (Boyan *et al.*, 1996).

Surface analysis studies of the implant surfaces revealed that the chemical composition of the implant surface is different from the bulk materials' composition due to surface modifications (Massaro *et al.*, 2002; Roach *et al.*, 2007). Variation in the surface treatment techniques will produce surfaces with different impurities that alter the chemical composition of the implant's titanium oxide surface layer, which influences the biological response (Sader *et al.*, 2005; Palmquist *et al.*, 2010; Zareidoost *et al.*, 2012). The chemical composition of the implant surface is known to effect the first stage of serum protein adsorption after implantation, which modulates the subsequent osteoblast cell behaviour (Boyan *et al.*, 2001).

One of the approaches to changing the implant surface topography and chemistry that can modulate the biological response is by incorporating CaP-based bioceramics on the implant surfaces (Citeau *et al.*, 2005; Le Guehennec *et al.*, 2008; Surmenev *et al.*, 2014; Lukaszewska-Kuska *et al.*, 2018). The dissolution of CaP ions

into the peri-implant region promotes the precipitation of biological apatite on the implanted surfaces that act as a matrix for bone formation (Anselme *et al.*, 2010). This process are associated with the adsorption of different biological molecules at the bioceramic-tissue interface (Ducheyne and Qiu, 1999). Kilpadi *et al*. (2001) demonstrated that the enhanced biological response of HA surfaces could be attributed to their ability to adsorb higher amounts of serum ECM adhesive proteins that allow the subsequent attachment of surrounding undifferentiated osteoblast cells.

Surface energy is affected by surface roughness (Lim *et al.*, 2001). Surfaces with increased surface roughness are associated with higher surface energy and show an increase in the number of osteoblasts (Feng *et al.*, 2003). Moreover, dental implant surfaces with high surface energy promoted better osteoblast differentiation based on increased levels of alkaline phosphatase, osteocalcin, PGE2, and TGF-β1 (Zhao *et al.*, 2005). The surface energy of a surface can be evaluated by the wettability, which is assessed by a direct or indirect measurement of the contact angle of a liquid drop on the surface (Gittens *et al.*, 2014). The values of the contact angle determine the nature of the surface (wettability) being hydrophilic or hydrophobic (Rupp *et al.*, 2014).

The wettability of the surface plays a significant role in the protein adsorption and subsequent cellular attachment (Roach *et al.*, 2005; Xu and Siedlecki, 2007). Accordingly, modification of wettability leads to hydrophilic surfaces with higher removal torque values in comparison to hydrophobic surfaces (Elias *et al.*, 2008). Enhanced blood coagulation, which is important for bone formation, was also

correlated with increased wettability and hydrophilic surfaces (Schwarz *et al.*, 2007; Milleret *et al.*, 2011; Kopf *et al.*, 2015).

Numerous treatments have been used to increase the hydrophilicity of dental implants by using gas treatments and storage in different solutions (Buser *et al.*, 2004; Rupp *et al.*, 2004; Zhao *et al.*, 2005; Schwarz *et al.*, 2009c), ultraviolet light (Sawase *et al.*, 2008), alkaline solutions (Tugulu *et al.*, 2010), and heat treatments (Feng *et al.*, 2003). Sandblasting and acid etching is one of the common commercial modifications used to produce moderately rough surfaces that are hydrophobic and with low surface energy and wettability in comparison to the modified hydrophilic SLActive surface (Rupp *et al.*, 2004). These surface characteristics were attributed to the contamination of the titanium oxide surface layer when exposed to air and the difference in surface roughness (Rupp *et al.*, 2006).

Many studies have compared the biological response to SLA (hydrophobic) and SLActive (hydrophilic) surfaces (Schwarz *et al.*, 2007; Schwarz *et al.*, 2009c; Raines *et al.*, 2010; Zhang *et al.*, 2010). Hydrophilic SLActive surfaces increase the expression of specific genes associated with improved angiogenesis and osteogenesis in comparison to SLA surfaces *in-vivo* (Wall *et al.*, 2009; Donos *et al.*, 2011). In addition, human osteoblast and osteoblast-like cells seeded on SLA and SLActive surfaces show higher levels of angiogenesis GFs associated with SLActive surfaces (Raines *et al.*, 2010). Similarly, significantly enhanced levels of ALP and osteocalcin and lower numbers of osteoblast cells are reported with hydrophilic SLA surfaces compared to hydrophobic SLA surfaces (Rausch-Fan *et al.*, 2008).

1.11 Implant success and failure

The success of dental implants depends on the ability of an implant to establish a firm contact with the bone (osseointegration) (Jensen, 2017). When a dental implant fails to form, this contact with the bone is considered an early implant failure. Any disruption of this contact after establishing osseointegration and loading will lead to late implant failure (Tonetti and Schmid, 1994; Zitzmann and Berglundh, 2008). Many factors have been suggested to cause or influence implant failure (Montes *et al.*, 2007). Esposito *et al.* (1998) highlighted the factors that result in biological implant failure as the patient, operator, or implant.

1.12 Early implant failure

Various factors related to the host have been considered as a potential cause of early implant failure. A 5 year retrospective study indicated a significant relationship between the occurrence of early implant failure in men regardless of their age (Olmedo-Gaya *et al.*, 2016). In contrast, a 10-year study suggested that implant failure was higher in females and in patients aged 41–60 years (Noguerol *et al.*, 2006). Similarly, another study found that early implant failure was associated with young females (Manor *et al.*, 2009). Alsaadi *et al.* (2007) in their retrospective study reported a significant relationship between smoking, osteoporosis, Crohn's disease, implant length and diameter and the occurrence of early implant failure.

Other studies are divergent, with no significant relationship between implant diameter, length, location, need of additional intervention, and implant failure

(Bornstein *et al.*, 2008a; Pabst *et al.*, 2015). Furthermore, lower success rates have been reported with short implants (6–9 mm) (Olate *et al.*, 2010).

Patient-related factors most commonly reported to cause early implant failure are quality and quantity of bone (Sakka and Coulthard, 2009), systemic conditions, smoking (Noda *et al.*, 2015), and pre-existing periodontal condition (Al-Sabbagh and Bhavsar, 2015).

Several studies also identified surgical technique, infection, and premature loading as the main risk factors causing early implant failure (Sakka and Coulthard, 2011; Antoun *et al.*, 2017). Fürst *et al.* (2007) found that bacterial colonisation can occur in the first 30 minutes after fixture insertion. Nevertheless, a recent systematic review did not find enough evidence on the relationship between bacterial contamination during surgery and implant prognosis (Johansson *et al.*, 2017).

1.13 Late implant failure

The most common causes of late implant failure are either microbial colonisation of the implant surface or implant overload (Sakka *et al.*, 2012). A literature review focusing on the prevalence of peri-implantitis over 5–10 years found that it occurred in 10 % of the implants and 20 % of patients (Mombelli *et al.*, 2012), with cumulative survival rates for implants after 10 years in function being 94.0 % (Noda *et al.*, 2015). Bacterial invasion and colonisation on the implant surface may lead to inflammation of the soft tissues surrounding the implant (peri-implant mucositis), or more progressive loss of the bony tissues surrounding the implant (peri-implantitis) (Lindhe and Meyle, 2008). Clinical studies on humans highlighted that

bacterial biofilms are responsible for the occurrence of peri-implant mucositis (Zitzmann *et al.*, 2001; Salvi *et al.*, 2012; Renvert and Polyzois, 2015a).

With regard to the implant surface properties, research has highlighted the effect of implant surface properties on the amount of biofilm adherence (Subramani *et al.*, 2009). Surface roughness, topography, and surface energy, are considered to play a potential role in the adherence of biofilms to implant surfaces (Kloss *et al.*, 2011; Han *et al.*, 2016), with increased surface roughness being considered the primary surface property contributing to increased biofilm adherence (Teughels *et al.*, 2006).

Rough implant surfaces show more favourable results in terms of the interaction with salivary proteins and enhanced osseointegration properties (Cavalcanti *et al.*, 2015). The increased level of surface roughness above 0.2 µm was found to be associated with more biofilm formation (Teughels *et al.*, 2006). Zhao *et al*. (2014a) examined the effect of different implant materials (Ti, TiZr, and ZrO_2) with different surface treatments on biofilm formation. Their results showed that biofilms adhere to all implant surfaces tested, regardless of their surface roughness or wettability. Furthermore, the implant material played a more significant role in biofilm formation than the other surface properties, where the ZrO_2 implants had the highest amount of biofilm volume compared to Ti and TiZr.

Conflicting findings have been reported regarding the implant length and diameter, and their effect on implant failure. Some systematic reviews suggested that implant survival rates decrease with short and wide diameter implants, when other factors such as the implant surface properties, design and operator skill were not optimised

(Renouard and Nisand, 2006). Moreover, length does not have any effect on implant survival when using rough implants (Kotsovilis *et al.*, 2009). A systematic review by Sun *et al*. (2011) did not indicate any significant effect of the implant length on implant failure rates in maxilla and mandibles. This is in agreement with the studies by (Olate *et al.*, 2010; Baqain *et al.*, 2012; Grisar *et al.*, 2017). Lops *et al.* (2012) compared the 20 year prognosis of short and long implants in maxilla and mandible, where survival rates did not reveal any significant differences when using short or long implants. Similarly, this finding was also reported in a systematic review and meta-analysis conducted by Lemos *et al*. (2016) that indicated no significant difference in survival rates between short and long implants in posterior maxilla and mandibles. Recent results from an animal study concluded that increased implant length significantly enhanced implant primary stability in areas of poor bone quality (Bataineh and Al-dakes, 2017). A retrospective study found that implants with reduced diameter (3.3 mm) and less than 10 mm length showed a 93.4 % cumulative survival rate after 3 years of placement (Maló *et al.*, 2017).

Many systematic reviews focusing on smoking and the presence of previous periodontal disease found a correlation between these factors and the increased prevalence of peri-implantitis (Safii *et al.*, 2010; Chrcanovic *et al.*, 2014; Chrcanovic *et al.*, 2015; Cheng, 2016). Occlusal overloading of a dental implant without considering its biomechanical factors will ultimately lead to implant failure. Such factors are 1) bone quality and quantity to withstand loading; 2) implant material, position, diameter, length, and number; and 3) the definitive prosthesis (Kim *et al.*, 2005). Higher failure rates and peri-implant bone loss were seen in patients with

parafunctional habits such as bruxism (Zhou *et al.*, 2016; Chrcanovic *et al.*, 2017; Passanezi *et al.*, 2017), highlighting that increased functional load may influence failure rates.

Several complications may arise after implant placements, which are manifested as veneer fracture, screw loosening, or abutment fracture (Pjetursson *et al.*, 2014; Tey *et al.*, 2017). Many implant complications are related to overloading the implant and/or the implant prosthesis (Liaw *et al.*, 2015). Hence, in order to avoid implant complications and subsequent implant failure, careful patient selection and implant planning is mandatory (Weber *et al.*, 2015; Clark and Levin, 2016).

1.14 Peri-implant disease

Peri-implant diseases are classified into peri-implant health, peri-implant mucositis, peri-implantitis, and peri-implant soft and hard tissue deficiencies (Caton *et al.*, 2018). Peri-implant diseases (peri-implant mucositis and peri-implantitis) are inflammatory conditions diagnosed based on the clinical signs of inflammation, probing depths, and bleeding on probing, in conjunction with the radiological assessment of crestal bone levels (Heitz-Mayfield and Salvi, 2018).

Typically, peri-implant mucositis and peri-implantitis present clinically as inflammation and bleeding on probing of the soft tissues surrounding the dental implant (Lindhe and Meyle, 2008). In addition, peri-implantitis is characterised by an increase in probing depths from the base line, which could be associated with suppuration (Heitz-Mayfield, 2008; Berglundh *et al.*, 2018; Hashim *et al.*, 2018; Schwarz *et al.*, 2018). Continuous evaluation of probing depths and alveolar bone

levels is essential to determine the progression of peri-implant mucositis to peri-implantitis (Lang *et al.*, 2011a). Any subsequent increase in the probing depth of ≥ 5 mm and progressive bone loss after the establishment of physiological healing are the manifestation of peri-implantitis (Koldsland *et al.*, 2010; Renvert *et al.*, 2018).

1.15 Peri-implant diseases and bacterial biofilms

Microbial biofilm has been recognised as the main aetiological factor for both periodontal and peri-implant diseases (Pérez-Chaparro *et al.*, 2016; Lafaurie *et al.*, 2017). Once exposed to the oral environment, dental implants are prone to microbial invasion and subsequent biofilm formation, similar to teeth and other biomaterials (Subramani *et al.*, 2009; Busscher *et al.*, 2010). However, significantly more micro-organisms are found around teeth than around dental implants immediately after implant placement (Fürst *et al.*, 2007). Adjacent teeth could be one of the sources of bacteria that play a role in the inflammation process around dental implants (Botero *et al.*, 2005). Bacteria might ingress from the supragingival part of the dental implant if the biological seal between the implant and the soft tissues is interrupted (Lindhe and Berglundh, 1998; Atsuta *et al.*, 2016).

In 1987, Gristina described a theory that was coined the “race for the surface”, in which the bacteria will compete with the surrounding body cells for the implant surface. The implant surface could be either dominated by the bacteria and result in a biofilm formation, or the host tissue will win the race and initiate the physiological healing process (Gristina, 1987).

The development of biofilms on a dental implant surface starts with the acquired pellicle formation, which is mediated by the adsorption of several proteins (Steinberg *et al.*, 1995). This acquired pellicle will permit bacteria known as early colonisers that are mainly gram-positive cocci, rods and actinomyces species, to adhere to the implant surface (Dhir, 2013). The early colonisers provide the sites for cell-to-cell adhesion for other types of bacteria known as late colonisers (Kohavi *et al.*, 1995; Costerton *et al.*, 2005; Lee and Wang, 2010).

Various microbial species have been isolated from dental implant surfaces, where healthy peri-implant tissues mainly harbour gram-positive cocci, rods and spirochetes (Mombelli *et al.*, 1987). Infected implant sites are found to be associated with the same microbiota as in periodontal infections, such as *prevotella intermedia, porphyromonas gingivalis, actinobacillus actinomycetemcomitans, bacteroides forsythus, treponema denticola, and fusobacterium species* (Leonhardt *et al.*, 1999; Hultin *et al.*, 2002; Mombelli and Décaillet, 2011). However, other species that are not commonly involved in the periodontal infections have been isolated from peri-implant lesions (Renvert *et al.*, 2008b; Albertini *et al.*, 2015). In general, the published literature has shown that peri-implant mucositis and peri-implantitis sites are mainly harboured by gram-negative anaerobic bacteria (Heitz-Mayfield and Lang, 2010; Mombelli and Décaillet, 2011; Kumar *et al.*, 2012; Hahnel, 2017).

1.16 Management of peri-implant diseases

No universal protocol has been established for the treatment of peri-implant diseases (Romanos *et al.*, 2015), however, published approaches to treat peri-implant diseases are based on the management of periodontal diseases, as they are both initiated by bacterial invasion and have similar pathogenesis (Heitz-Mayfield and Lang, 2010; Salvi *et al.*, 2017). Therefore, to resolve the inflammatory condition the primary aim of treatment is to reduce bacterial colonisation. Treatment of peri-implant mucositis and peri-implantitis is categorised into non-surgical and surgical approaches (Mishler and Shiau, 2014; Smeets *et al.*, 2014).

With respect to peri-implant mucositis, evidence has proved that non-surgical therapy with or without adjunctive antimicrobial treatments is sufficient to resolve the inflammatory condition (Heitz-Mayfield *et al.*, 2011; Hallström *et al.*, 2012; Figuero *et al.*, 2014). On the other hand, a non-surgical approach is not clinically predictable in halting the progression of peri-implantitis (Lindhe and Meyle, 2008; Persson *et al.*, 2010; Suárez-López Del Amo *et al.*, 2016; De Almeida *et al.*, 2017). This can be attributed to the incomplete removal of bacterial biofilm from implant surfaces by existing non-surgical methods (Renvert *et al.*, 2008c; Subramani and Wismeijer, 2012; Mellado-Valero *et al.*, 2013). Hence, surgical intervention may be indicated. However, various outcomes and surgical protocols have been proposed with the lack of a standard surgical protocol for treating peri-implantitis (Romanos and Weitz, 2012).

1.16.1 Non-surgical approach

The non-surgical approach is recognised as the initial intervention for managing peri-implant inflammatory diseases. It involves the decontamination of the implant surface by removing the bacterial biofilm using several methods. These include mechanical debridement of the implant surfaces utilising curettes, titanium brushes, rubber cups, ultrasonic devices, air powder abrasion, and burs for implantoplasty (Mellado-Valero *et al.*, 2013; Suarez *et al.*, 2013). Detoxification of implant surfaces can be achieved with chemical treatments such as antimicrobial or antiseptic agents (chlorohexidine, citric acid, hydrogen peroxide, local or systematic antibiotic), and saline to eliminate the micro-organisms and their by-products (Lang *et al.*, 2000; Mombelli, 2002; Kolonidis *et al.*, 2003). In addition, supplemental antimicrobial therapy has been suggested to reduce the bacterial load on implant surfaces, especially in areas with restricted access (Heitz-Mayfield and Lang, 2004; Renvert *et al.*, 2008a).

Novel techniques such as laser and photodynamic therapy (low-level laser) have also been employed in both non-surgical and surgical approaches for treating peri-implantitis due to their bactericidal effects (Takasaki *et al.*, 2009; Chambrone *et al.*, 2018; Mills *et al.*, 2018). Different lasers have been recommended for decontamination in cases of peri-implantitis, most commonly carbon dioxide (CO_2) and erbium-doped yttrium aluminium garnet (Er:YAG) (Takasaki *et al.*, 2007; Romanos *et al.*, 2009; Natto *et al.*, 2015). The Er:YAG laser demonstrated a high bactericidal effect with no changes in surface morphology when used to decontaminate sandblasted, acid- etched, HA, and TPS surfaces (Kreisler *et al.*,

2002). The Er:YAG laser treatment shows comparable results to air abrasion in terms of surface change, clinical improvement, and the reduction of pathogens when treating peri-implantitis (Persson *et al.*, 2011; Renvert *et al.*, 2011), and can lead to significant reductions in bleeding on probing when compared to non-surgical decontamination using plastic curettes and chlorhexidine (Schwarz *et al.*, 2005).

All the above decontamination methods and agents have been reported as effective methods for decontaminating implant surfaces with varying outcomes, with no evidence indicating the optimum treatment modality (Claffey *et al.*, 2008; Renvert *et al.*, 2009b; Gosau *et al.*, 2010; Louropoulou *et al.*, 2014). Nevertheless, the cleaning efficacy of non-metal instruments is inferior to some of the metal instruments (Louropoulou *et al.*, 2014; Schmage *et al.*, 2014). Mechanical cleaning with metal instruments results in a considerable change in the surface morphology (roughness) of the implant in comparison to other methods (Augthun *et al.*, 1998; Kawashima *et al.*, 2007; Duarte *et al.*, 2009b; Schmidt *et al.*, 2017). Therefore, non-metal instruments and air abrasion are recommended for cleaning rough implant surfaces (Louropoulou *et al.*, 2012).

1.16.2 Surgical approach

The primary aim of surgical treatment is to preserve the implant by preventing the progress of the disease and subsequent bone destruction that will ultimately lead to implant loss. Surgical treatment involves the elevation of a mucoperiosteal flap in order to gain direct access for debriding and decontaminating the implant surface, which could be followed by resective or regenerative procedures if needed (Renvert *et al*., 2018b).

Similar to non-surgical treatment, different mechanical interventions have been used for the surgical debridement of implant surfaces including air abrasion (Maximo *et al*., 2009), curettes (Louropoulou *et al*., 2012), implantoplasty (Romeo *et al*., 2007; Schwarz *et al*., 2011), titanium brushes (An *et al*., 2017) and ultrasonics (Serino and Turri, 2011). The combination of mechanical treatment and chemical agents such as citric acid (Gosau *et al*., 2010), hydrogen peroxide (Leonhardt *et al*., 2003), saline gauzes (Heitz-Mayfield *et al*., 2012), chlorohexidine (De Waal *et al*., 2013) and antibiotics (Salvi *et al*., 2007) are effective in reducing the microbial load and reducing the probing depth (Heitz-Mayfield *et al*., 2012; Mellado-Valero *et al*., 2013; Ramanauskaite *et al*., 2016a).

The adjunctive use of laser and photodynamic therapy with surgical treatment shows positive outcomes in the treatment of peri-implantitis (Dörtbudak *et al*., 2001; Hayek *et al*., 2005; Shibli *et al*., 2006; Romanos and Nentwig, 2008). Re-osseointegration of infected implants has been shown after CO_2 (Deppe *et al*., 2001; Stübinger *et al*., 2005) or Er:YAG laser irradiation (Takasaki *et al*., 2007). Although

better clinical results have been reported with laser treatments, the results of systematic reviews and meta-analyses do not conclude any superiority in clinical outcome with lasers over other decontamination methods in treating peri-implantitis (Esposito *et al*., 2012; Muthukuru *et al*., 2012; Kotsakis *et al*., 2014; Mailoa *et al*., 2014).

Following biofilm elimination, some surgical protocols suggest the effectiveness of resective surgical procedures to manage peri-implantitis. These procedures may involve apically re-positioning flaps (De Waal *et al*., 2013), and re-contouring of the bone with surgical burs with or without smoothening of the infected implant surface (implantoplasty) (Romeo *et al*., 2005; Romeo *et al*., 2007). Other surgical protocols propose the use of a regenerative approach to eliminate the peri-implant pocket, correct the bone defect, and induce bone regeneration after surface debridement (Froum *et al*., 2012; Ramanauskaite *et al*., 2016b; Renvert *et al*., 2018b). Several techniques have been used including the use of bone grafts (Khoury and Buchmann, 2001; An *et al*., 2017) or bone substitutes either used alone or protected from the soft tissues with resorbable or non-resorbable membranes with guided bone generation (GBR) (Schwarz *et al*., 2006; Sahrmann *et al*., 2011; Aghazadeh *et al*., 2012; Roos-Jansåker *et al*., 2014). However, recent meta-analysis and systematic reviews indicated the lack of clinical evidence to support regenerative procedures having merit over non-regenerative procedures (Daugela *et al*., 2016; Khoshkam *et al*., 2016). The combination of resective and regenerative approaches has shown some advantages in terms of bone fill in large bone defects.

Animal studies show that combining regenerative approaches with bioactive molecules such as BMP-2 could be beneficial to enhance re-osseointegration (Jung *et al*., 2015; Park *et al*., 2015). Clinical improvement in bone levels has been noted with a surgical protocol combining air abrasion and the application of enamel matrix derivatives and bone graft or bone substitute hydrated with platelet-derived factors and collagen membranes (Froum *et al*., 2015).

1.17 Air-powder abrasion

The air abrasion method uses kinetic energy to deliver an abrasive powder introduced in a stream of compressed air, to remove part of the surface in order to clean or polish it (Rainey, 2002) (Figure 1.7). Air abrasion is considered one of the conservative methods used for conditioning and the removal of stains, caries and plaque from teeth surfaces (Hegde and Khatavkar, 2010; Moëne *et al.*, 2010; Fumes *et al.*, 2017; Ng *et al.*, 2018). Therefore, its use has been extended to the decontamination and removal of bacterial biofilms from infected dental implant surfaces.

Air abrasion has been reported as one of the effective decontamination techniques used in the treatment of peri-implant mucositis and peri-implantitis both *in-vivo* and *in-vitro* (Parham *et al.*, 1989; Renvert *et al.*, 2011; Sahrmann *et al.*, 2013; Louropoulou *et al.*, 2014; Riben-Grundstrom *et al.*, 2015; Ronay *et al.*, 2017). Various abrasive powders have been used to clean implant surfaces with air abrasion systems. The two most commonly used powders are sodium bicarbonate and glycine amino acid (Schwarz *et al.*, 2015a; Schmidt *et al.*, 2017). Other powders

such as hydroxyapatite, calcium phosphate (Tastepe *et al.*, 2013; Tastepe *et al.*, 2018b), and bioceramic powders (Koller *et al.*, 2007) have also been reported.

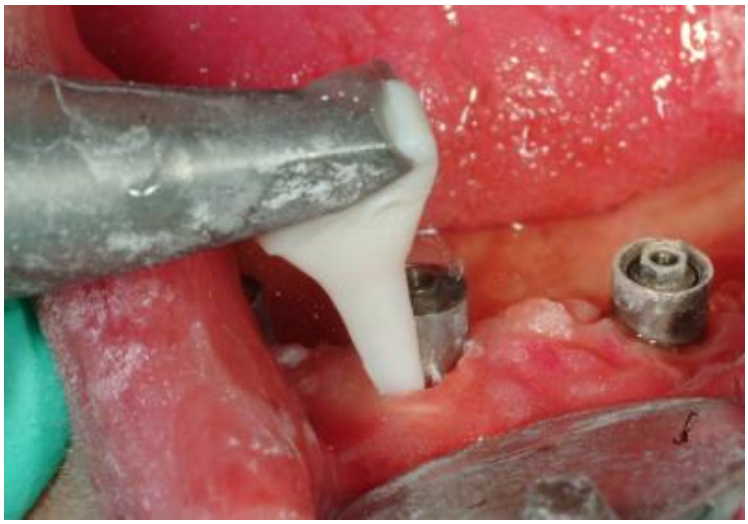

Figure 1.7 Air abrasion unit cleaning an implant surface (non-surgically) (Renvert *et al.*, 2011)

1.17.1 Air abrasion as a non-surgical decontamination method

The use of air powder abrasion systems to decontaminate titanium surfaces as a non-surgical method have been assessed for treating peri-implantitis (Klinge *et al.*, 2002), and the effectiveness of air abrasion to reduce bacterial biofilms, and improve the inflammatory condition on different implant surfaces has been proven (Kreisler *et al.*, 2005; Muthukuru *et al.*, 2012; Tastepe *et al.*, 2012; Schwarz *et al.*, 2015a).

Zablotsky *et al.* (1992) demonstrated that air abrasion achieved significant results when used for decontaminating grit blasted, hydroxyapatite-coated titanium strips in comparison to other methods. The air abrasion of HA surfaces was compared to

using topical citric acid, chloramine-T, and sterile water. This is in agreement with the study by Dennison *et al.* (1994), which reported superior cleaning with air abrasion when used on machined, plasma sprayed and HA surfaces. The air abrasion was compared to citric acid, chlorhexidine, and water. However, using citric acid treatment was equally effective as air abrasion on HA surfaces. Quintero *et al*. (2017) reported a 99.9 % reduction of *streptococcus sanguinis* after using air powder abrasion on acid-etched implant surfaces using glycine and sodium bicarbonate powders.

Scanning electron microscopic examination of failed implants also reveals successful cleaning of machined implant surfaces with air abrasion (Mouhyi *et al.*, 1998). Another study reported the effectiveness of air abrasion to produce 100 % clean SLA surfaces previously contaminated with human biofilms. In this study, the effectiveness of this method was related to the type of powder used for air abrasion (Schwarz *et al.*, 2009a). This is in agreement with the studies by Dennison *et al*. (1994) and Augthun *et al.* (1998), which reported complete removal of biofilms with air abrasion. On the other hand, a study by Sahrmann *et al*. (2015) showed a significant cleaning efficacy for air abrasion in comparison to steel curettes and ultrasonic devices in simulated bone defects. However, complete decontamination of the SLA implant surfaces was not achieved with air abrasion. This could be attributed to the restricted access as the implants were imbedded in acrylic resin, or the different simulated angulations of the bone defects.

In-vivo, air abrasion can reduce bacterial counts associated with peri-implantitis in the first month of treatment, but not after 6 months (Persson *et al.*, 2011). Sahm *et*

al. (2011) demonstrated a reduction in bleeding on probing after 12 months from 99.0 % to 47.8 % following air abrasion treatment in patients with peri-implantitis conditions, this is consistent with the clinical randomised studies conducted by Renvert *et al*. (2011) and John *et al*. (2015). Renvert *et al*. (2011) evaluated the clinical effect of air abrasion as a non-surgical cleaning method after 6 months. The implant superstructures were removed and then the implant surfaces were cleaned with air abrasion. In their study, a significant reduction in bleeding on probing, probing depths and suppuration was reported. John *et al*. (2015) reported a significant reduction in bleeding on probing after 3, 6, and 12 months of non-surgical treatment of peri-implantitis with air powder abrasion, and a reduction in pocket depths and initial gain in clinical attachment levels with air abrasion.

Available systematic reviews focusing on randomised clinical trials have demonstrated the efficacy of air abrasion as one of the non-surgical methods for treating peri-implant mucositis and peri-implantitis in comparison to other debridement methods. These reviews concluded a clinical improvement in peri-implant conditions associated with air abrasion, which was manifested as a reduction in bleeding on probing (Muthukuru *et al.*, 2012) and probing depth (Faggion *et al.*, 2014; Schwarz *et al.*, 2015a).

1.17.2 Air abrasion as a surgical debridement method

Limited clinical research is available on the use of air abrasion systems after surgical access (open flap) as a debridement method for treating peri-implantitis. Schou *et al*. (2003) reported that air abrasion was equally effective as other debridement methods when used in surgical debridement for treating simulated peri-implantitis in monkeys.

Significant reduction of pocket depths, bleeding scores, attachment levels, and the amount of pathogens has been observed when using Teflon curettes and air abrasion *in-vivo* for surgical debridement in 10 patients (Maximo *et al.*, 2009). The effect of the surgical debridement of dental implants with air abrasion on clinical parameters was investigated in another clinical study by Duarte *et al.* (2009a). Six parameters were evaluated: probing depth, clinical attachment level, marginal bleeding, bleeding on probing, suppuration, and plaque accumulation. The results revealed a significant reduction of all clinical parameters after 3 and 12 months, which was also associated with a reduction of inflammatory cytokines. This is in agreement with the study by De Mendonça *et al*. (2009), which evaluated the clinical effect following surgical debridement using resin curettes and air abrasion with sodium bicarbonate powder. Significant improvements in plaque indices, bleeding on probing, marginal bleeding, suppuration, pocket depths, and relative clinical attachment levels were reported. Moreover, in this study the peri-implantitis sites showed a significant reduction in the pro-inflammatory marker TNF-α over time.

The efficacy of the combined use of surgical debridement and air abrasion with glycine powder in 22 implants on plaque indices, gingival indices, and pocket depths was evaluated in a retrospective study by Toma *et al*. (2014). Access flaps were reflected and the granulation tissues were first removed, before the debridement method was performed. Clinical examination showed a significant improvement in gingival indices and probing depths at the implant level after 12 months. Nevertheless, the improvement in clinical parameters did not reach the level of re-osseointegration and no bone fill was reported.

Taschieri *et al*. (2015) presented a case report which investigated the outcome of surgical debridement with air abrasion using erythritol-enriched powder combined with guided bone regeneration. Clinical examination and radiographic assessment performed at 6 and 12 months concluded a positive treatment outcome in terms of re-osseointegration ability.

1.17.3 Air abrasion and surface changes

Air abrasion can change the implant surface micromorphology when assessed by profilometry or SEM technology (Ramaglia *et al.*, 2006; Duarte *et al.*, 2009a; Schwarz *et al.*, 2009a; Tastepe *et al.*, 2012). Chairay *et al*. (1997) examined the effect of air abrasion on the surface morphology of machined and plasma-sprayed dental implants. The degree of surface change did vary from the smoothing of the surface to the flattening of the ridges according to the type of implant, area examined, and air abrasion time. The same smoothing effect was also reported by Kreisler *et al.* (2005) when examining SLA surfaces. Ramaglia *et al*. (2006) reported a decrease in the R_a parameter when air abrasion was used on TPS surfaces, however, in the same study HA surface showed an increase in the R_a parameter as a result of coating removal.

Schwarz *et al*. (2009a) noted a flattening of the sharp elevations of SLA discs after air abrasion with sodium bicarbonate powder. However, no surface change was noted when using glycine powders. This is in agreement with the SEM findings by Sahrmann *et al*. (2015), which reported no significant changes in the SLA implant surfaces when using glycine powders with air abrasion with a simulated bony defect. In the study by Tastepe *et al*. (2013), SEM examination revealed that SLA titanium discs treated with air abrasion produced a rounding of the sharp edges regardless of the powder used, which were TiO_2, amino acid glycine, HA, and CaP. In their study, the degree of surface change and morphology of the surfaces were attributed to the powder used for air abrasion. Significant increases in the surface roughness of smooth titanium discs was reported following air abrasion with

bioceramic powders (Koller *et al.*, 2007). Cafiero *et al*. (2017) reported a smoothing effect associated with the use of air abrasion on dental implant collars.

1.17.4 Limitations of air abrasion

Despite the reported efficacy of air powder abrasion for decontamination it also has some limitations, including the powder deposits left on the surface after treatment (Koller *et al.*, 2007; Tastepe *et al.*, 2013; Louropoulou *et al.*, 2015; Sahrmann *et al.*, 2015). It is not known if this retained powder will adversely affect the biological healing process (Sygkounas *et al.*, 2017). Surgical emphysema could be one of the potential disadvantages related to the use of air abrasion (Bergendal *et al.*, 1990; Liebenberg and Crawford, 1997). However, clinical studies do not report any adverse effect or surgical emphysema when using air abrasion for treating peri-implantitis (Maximo *et al.*, 2009; Persson *et al.*, 2011; Renvert *et al.*, 2011; Sahm *et al.*, 2011; Toma *et al.*, 2014). Table 1.2 provides a summary of the studies that used air abrasion as a decontamination method.

Table 1.2 Studies that used air abrasion on different surfaces as a decontamination method

Study	Type of study	Sample surface	Air abrasion powder
(Zabtotsky *et al.*, 1992)	*In-vitro*	Grit blasted, HA coated	Sodium bicarbonate
(Quintero *et al.*, 2017)	*In-vitro*	Acid-etched Osseotite implant	Glycine, sodium bicarbonate
(Dennison *et al.*, 1994)	*In-vitro*	Machined, HA plasma sprayed	Sodium bicarbonate
(Augthun *et al.*, 1998)	*In-vivo*	Smooth, plasma sprayed, HA	Sodium hydrocarbonate solution
(Maximo *et al.*, 2009)	*In-vivo*	Machined	Sodium carbonate
(Mouhyi *et al.*, 1998)	*In-vitro*	Machined	Sodium bicarbonate
(Persson *et al.*, 2011)	*In-vivo*	Machined, medium rough	Glycine based grain of aluminium oxide
(Schwarz *et al.*, 2009a)	*In-vivo*	SLA	Glycine, sodium bicarbonate
(De Mendonça *et al.*, 2009)	*In-vitro*	Machined, sandblasted /acid etched	Sodium bicarbonate
(Kreisler *et al.*, 2005)	*In-vitro*	Sandblasted/acid etched	Glycine, sodium bicarbonate
(Sahm *et al.*, 2011)	*In-vivo*	Machined, micro rough	Glycine
(Tastepe *et al.*, 2013)	*In-vitro*	SLA	HA, HA/CaP, TiO2, amino acid glycine
(John *et al.*, 2015)	*In-vivo*	Machined, micro rough	Amino acid glycine powder
(Duarte *et al.*, 2009a)	*In-vivo*	Machined	Sodium carbonate
(Renvert *et al.*, 2011)	*In-vivo*	Machined, medium rough	Hydrophobic glycine powder
(Sahrmann *et al.*, 2013)	*In-vitro*	Double acid etched	Glycine
(Sahrmann *et al.*, 2015)	*In-vitro*	SLA	Glycine
(Koller *et al.*, 2007)	*In-vitro*	Machined	Bioceramic powder
(De Mendonça *et al.*, 2009)	*In-vivo*	Implants surface not stated	Sodium carbonate
(Toma *et al.*, 2014)	*In-vivo*	Micro-rough	Amino acid glycine
(Taschieri *et al.*, 2015)	*In-vivo*	Implant surface not stated	Erythritol enriched powder

1.18 Re-osseointegration attempts and the implant surface

The re-osseointegration of rough implant surfaces previously affected by peri-implantitis could be achieved if the surface was thoroughly debrided and decontaminated, regardless of the decontamination method or surgical protocol used (Kolonidis *et al.*, 2003; Alhag *et al.*, 2008; Claffey *et al.*, 2008). Many factors could affect the re-osseointegration process including the type of bone defect (Schwarz *et al.*, 2010; Schwarz *et al.*, 2012), surgical protocol and regenerative material used (Khoshkam *et al.*, 2013; Madi *et al.*, 2018), implant surface characteristics and decontamination method (Parlar *et al.*, 2009; Subramani and Wismeijer, 2012).

Parlar *et al.* (2009) compared the effect of decontamination on turned, SLA, and TPS surfaces, and their re-osseointegration in dogs. The treatment included the use of curettes and chlorhexidine, followed by one of the tested methods, which were the replacement of infected implants with a new implant, spraying in situ with sterile saline, spraying with saline outside the mouth and autoclave. Significant re-osseointegration and BIC was reported with SLA surfaces cleaned in situ for 3 minutes with sterile saline. This is in agreement with the study by Persson *et al.* (2001) that reported 84 % re-osseointegration with SLA implants compared to 22 % for turned surfaces (both decontaminated with saline cotton pellets and systemic antibiotics in dogs). Similar clinical results have been reported with complete bone fill in 25 % of SLA implants versus no bone fill on TPS surfaces treated with

combined mechanical, chemical, and regenerative approaches (Roccuzzo *et al.*, 2011). The re-osseointegration of machined, SLA, and TPS surfaces treated with surgical debridement using curettes and chlorhexidine alone or in combination with GBR has been evaluated in dogs (Wetzel *et al.*, 1999). Histological examination revealed regenerative changes on all surfaces using both protocols, with no significant differences in the re-osseointegration outcome. This is in contrast with the study by Shibli *et al*. (2006), which reported that the implant surface had no significant effect on the re-osseointegration ability when the implants were treated with combined GBR and photodynamic therapy. The implant surfaces tested were CpTi, TPS, and acid etched.

Nociti *et al*. (2001) concluded that there was no significant difference in re-osseointegration with surgical debridement alone using air abrasion or in combination with GBR, with or without bone grafts, resorbable or non-resorbable membranes in acid-etched implant surfaces. This is in agreement with the study by Schou *et al*. (2003), which reported no significant difference in re-osseointegration when using surgical debridement alone (including air abrasion, air abrasion and citric acid, gauze with saline and citric acid, gauze with chlorohexidine and then saline) or the use of bone graft covered with a membrane.

Schwarz *et al*. (2012), and Matarasso *et al*. (2014) assessed the concomitant use of resective (implantoplasty) and regenerative (bovine-bone mineral or natural bone covered with resorbable membranes) procedures *in-vivo.* The studies concluded a reduction in clinical parameters (pocket depth and bleeding on probing), and a 93.3 % fill of the bone defect (Matarasso *et al.*, 2014).

Two clinical studies by Schwarz and colleagues (Schwarz *et al.*, 2008; Schwarz *et al.*, 2009b) compared the clinical and radiographical outcome of using a natural bone substitute (Bio-Oss®) or nanocrystalline hydroxyapatite for bone augmentation with a resorbable barrier at 2 and 4 years follow up. The results showed that the use of either technique produced a significant improvement in clinical attachment levels and bone gain after 2 years. However, after 4 years of follow up, the clinical outcome and bone refill were better in the bone augmentation with resorbable barrier group. Another study by Wiltfang *et al.* (2012) evaluated the regenerative efficacy of combining human bone grafts and bone substitutes with GFs in filling the osseous defect. Radiographical examination revealed a 3.5 mm implant defect fill after 1 year of treatment. The effect of porous titanium granules as a potential bone graft substitute to enhance bone regeneration was examined by Wohlfahrt *et al*. (2012). The study demonstrated significant bone fill ability with the use of porous titanium granules. However, the study did not indicate that this outcome could be equivocal to re-osseointegration.

To date, the optimum surgical approach for the complete resolution of peri-implantitis and its long-term effect are still unknown (Renvert and Polyzois, 2015b). However, considering the systematic reviews and meta-analyses of published *in-vivo* and *in-vitro* studies, it is suggested that the combination of mechanical and chemical decontamination in conjunction with regenerative approaches demonstrates the most promising clinical outcome (Renvert *et al.*, 2009a; Chan *et al.*, 2014; Schwarz *et al.*, 2015b; Mahato *et al.*, 2016; Madi *et al.*, 2018).

Chapter 2

Statement of the Problem and the Aim and Objectives

2.1 Statement of the problem

Different implants vary in biocompatibility, as well as the physical, mechanical, and chemical properties (Saini *et al.*, 2015). Titanium and zirconia have been used as dental implants with comparable osseointegration and biocompatibility (Gahlert *et al.*, 2007; Osman and Swain, 2015; Bosshardt *et al.*, 2017). Furthermore, their mechanical properties have been extensively investigated (Hisbergues *et al.*, 2009). However, certain clinical situations demand different implant size, geometry, mechanical properties, and surface characteristics. Commercially pure titanium (CpTi) and its alloys are considered the gold standard for implant materials. There is a trend of using reduced sized implants to allow minimal reduction in bone volume during preparation and reduce post-operative complications, however this increases the possibility of mechanical complications such as fracture (Schiegnitz and Al-Nawas, 2018). Therefore, different alloys with enhanced mechanical properties, such as titanium zirconia (TiZr) alloy, have been investigated to avoid these limitations (Badran *et al.*, 2017; Iegami *et al.*, 2017).

A new binary TiZr alloy (Roxolid®) has proven to be biocompatible, non-toxic, and to osseointegrate similarly to titanium, but with enhanced strength (Grandin *et al.*, 2012; Brizuela-Velasco *et al.*, 2017), although less is known about the mechanical properties of this alloy. Furthermore, there are no studies investigating the effect of different surface treatments (manufacturing process) on the sub-surface mechanical properties of the TiZr alloy, such as elastic modulus, hardness, and fatigue. As a consequence, more research on the mechanical properties of this alloy after undergoing the manufacturing process in comparison to CpTi are required in order to gain further knowledge and predict its behaviour in load-bearing situations.

Hardness of the implant material is important when reducing implant size, and the elastic modulus of implant materials has a significant influence on osseointegration (Zhang *et al.*, 2013; Dai *et al.*, 2016; Brizuela *et al.*, 2019). Therefore, these two properties deserve investigation in order to investigate if they are influenced by surface processing at both the nano and micro-nano levels.

The surface of an implant is the first part that comes into contact with host tissue, and is one of the important factors in establishing bone-implant contact (osseointegration). Thus, most of the developments in dental implants over the last decade are related to surface modifications to create an optimum surface for osseointegration. Several surface modifications have been suggested to alter the surface characteristics and composition of dental implants and to enhance bone anchorage. These modifications are either physical, chemical, or a combination of more than one treatment (Albrektsson and Wennerberg, 2003; Wirth *et al.*, 2017). Surface roughness is one of the factors known to be altered due to such treatments. Rough surfaces are known to enhance osseointegration, as documented in the literature (Grizon *et al.*, 2002; Saghiri *et al.*, 2016; Rupp *et al.*, 2017). However, there is no agreement regarding which roughness parameter correlates to enhanced molecular and biological response to surface-modified dental implants (Wennerberg and Albrektsson, 1999). Most studies use average surface roughness (S_a/R_a) to characterise surface topography, although such a parameter alone does not provide sufficient detail about the different levels of surface textures (Wennerberg and Albrektsson, 2009). A combination of more than one parameter can provide better insight into the effect of implant roughness on the surface interactions (Elias *et al.*, 2008; Jimbo *et al.*, 2015; Mendoza-Arnau *et al.*, 2016). Average surface roughness (S_a/R_a) does not

provide information about peaks and valleys, as different surface treatments produce different peaks and valleys (Mendoza-Arnau *et al.*, 2016). Thus, surfaces with the same S_a/R_a could have different surface textures and subsequent biological responses.

Although various studies have investigated the S_p, S_v, R_p, and R_v parameters for dental implants (Biasotto *et al.*, 2005; Mints *et al.*, 2014; Montero *et al.*, 2015), there are no reports comparing the effect of the material and surface modification on the S_p, S_v, R_p, and R_v roughness parameters.

The two most common reasons for implant failure are implant mucositis and peri-implantitis (Derks and Tomasi, 2015; Salvi *et al.*, 2017). The prevalence of mucositis was noted in 46.83 % of subjects, while the prevalence of peri-implantitis was noted in 19.83 % of subjects (Lee *et al.*, 2017). The first stage of treatment in peri-implant disease involves the mechanical debridement of the implant surface (Renvert *et al.*, 2008c; Suarez *et al.*, 2013; Smeets *et al.*, 2014). The ability of air abrasion using abrasive powders to clean and polish titanium surfaces has been reported (Zabtotsky *et al.*, 1992; Augthun *et al.*, 1998; Schwarz *et al.*, 2009a; Sahm *et al.*, 2011; Ronay *et al.*, 2017), and several air abrasive mediums have been used with air abrasion, such as amino glycine powder and sodium bicarbonates (Sahm *et al.*, 2011).

Recent attempts have been directed towards using osseoconductive powders such as bioglass and hydroxyapatite with air abrasion to restore the implant surface bioactivity and potential re-osseointegration ability (Koller *et al.*, 2007; Tastepe *et al.*, 2018a; Tastepe *et al.*, 2018b). These studies applied such powders on untreated titanium surfaces and SLA treated titanium, with no studies using air abrasion with bioceramic abrasives on TiZr (Roxolid®) implants or CpTi with other surface treatments. Furthermore, the influence of such treatment on the surface properties of different materials and

surfaces, and its dissolution behaviour, has not been assessed to date. Therefore, the use of air abrasion with a bioceramic abrasive in order to modify the implant surface properties and introduce a potential surface that might favour re-osseointegration (after affected by peri-implantitis) deserves further study.

2.2 Aim and objectives

The aim of this thesis was to investigate the effect of using different implant materials and surface modifications on selected surface and mechanical properties. The objectives were as follows:

- To obtain quantitative surface roughness profiles of different implant materials and surfaces using a 3D optical profilometer.
- To evaluate the effect of manufacturer processes on the bulk material sub-surface mechanical properties (hardness and elastic modulus) using nanoindentation and micro-nanoindentation.
- To assess the effect of air abrasion using a bioceramic abrasive on the surface characteristics of the implant surfaces using optical profilometry and SEM-EDS analysis.
- To investigate the dissolution behaviour of the deposited bioceramic treatment in deionised water using ICP-OES.

The outline of this thesis is illustrated by the flow chart presented in Figure 2.1.

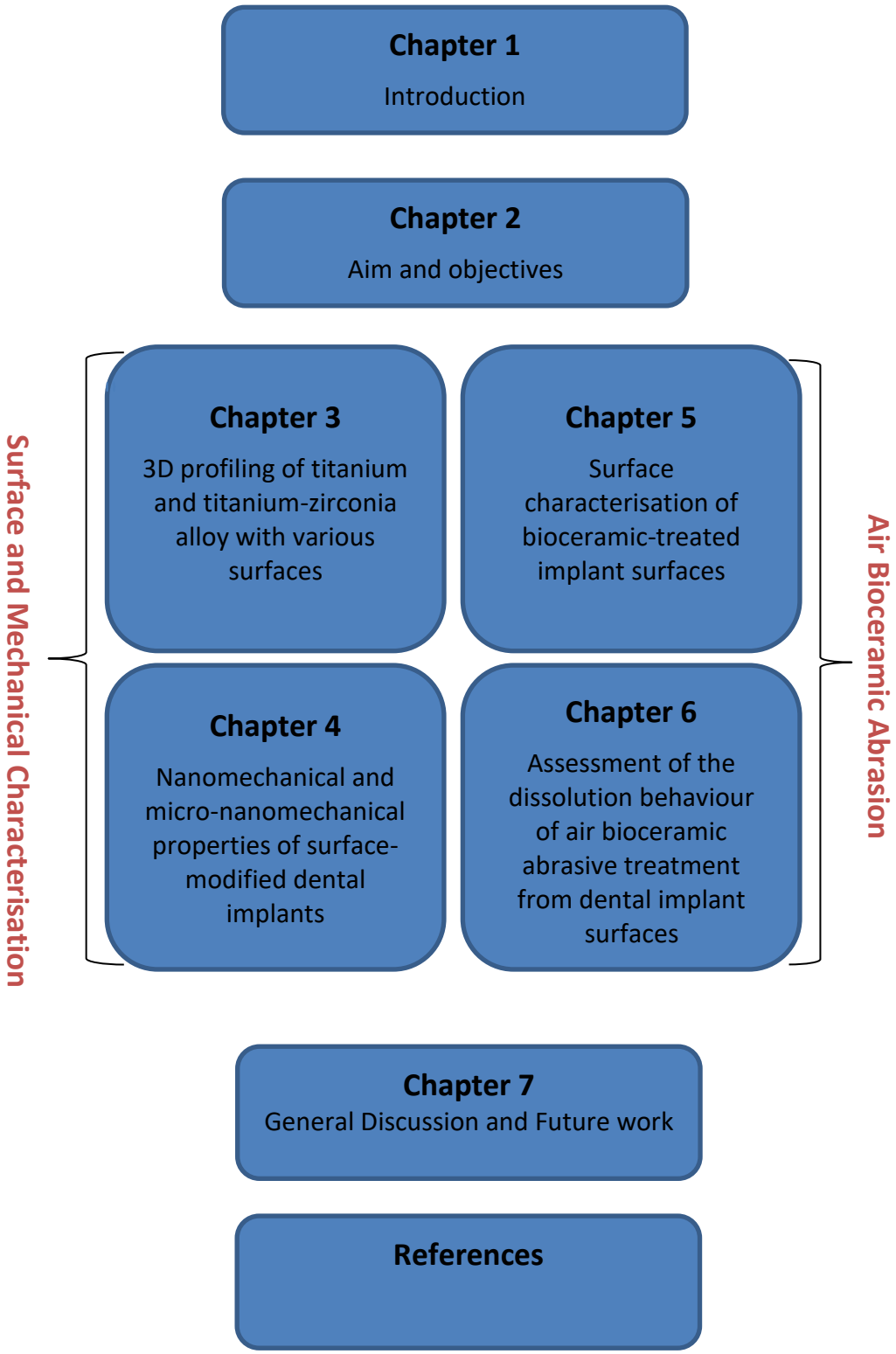

Figure 2.1 A flow chart illustrating the outline of this thesis

Chapter 3

3D Profiling of Titanium and Titanium–Zirconia Alloys with Various Surfaces

3.1 Introduction

Different implant surface modifications affect surface topography: both physical and/or chemical surface treatments produce different levels of surface roughness (Wirth *et al.*, 2017). It is also well documented that increased surface roughness has a direct effect on increasing the implant anchorage (Barfeie *et al.*, 2015; Shibata and Tanimoto, 2015). In this study, the effects of implant material and surface modifications on the surface roughness were investigated.

The topography of the tested surfaces were quantitatively measured using a non-contact laser optical profilometer. The use of optical profilometry in measuring the surface roughness of dental implants is well documented (Li *et al.*, 2002), where both 2D and 3D profiles can be obtained (Wennerberg and Albrektsson, 1999).

3.2 Aim of the study

The aim of this study was to investigate the effect of the implant substrate and surface modification on the surface roughness. The objectives were as follows:

- To obtain the 2D and 3D surface roughness measurements of the CpTi and TiZr alloys with different surfaces.
- To compare the 2D and 3D surface roughness parameters.

The null hypothesis was that there is no significant difference in surface roughness parameters between different implant materials and surfaces.

3.3 Materials and methods

3.3.1 Substrate materials and surface modifications

Three substrate implant materials from two different companies were used in this study:

1) Commercially pure titanium 1 grade 2 (Cp) ASTM F67 discs, 7 mm in diameter and 4 mm thick (S&S Biomat, Manchester, UK)

2) Commercially pure titanium 2 grade 2 (Ti) discs, 5 mm in diameter and 1 mm thick (Institut Straumann AG, Basel, Switzerland)

3) Titanium-zirconia alloy (13–17 % Zr) (R) (commercially known as the Roxolid®), discs 5 mm in diameter and 1 mm thick (Institut Straumann AG, Basel, Switzerland)

All surface modifications were applied to the discs by the companies following the same methods used for the respective commercial products. Each material thus had different existing surface modifications, which were sensitive company data and limited details about the surface preparation were provided by the companies. The materials and available detail regarding surfaces used in this study are summarised in Table 3.1, and are detailed below:

Commercially pure titanium 1 grade 2 (Cp):

- Control (no treatment) (CpC)
- Sandblasted with 250 µm Al_2O_3 particles at 5 mm distance and a pressure of 8 bar, followed by ultrasonic cleaning for 20 minutes using an environmentally friendly detergent (15–30 % anionic surfactants, 5–15 % non-ionic surfactants), then washed with hot water and air pressure 3 times and dried in the oven (SB)

- Sandblasted as above, followed by acid etching in 3 % hydrofluoric acid/17.5 % nitric acid solution, followed by wash in distilled water and heat treatment at 200 °C in an oven for 1 hour (SBE).

Commercially pure titanium 2 grade 2 (Ti):

- Acid etched with a boiling mixture of sulfuric/hydrochloric acids (concentration not provided by the company) (TiA)
- Acid etched as above, followed by rinsing in NaCl solution under nitrogen treatment, then stored in 0.9 % NaCl solution, where this type of treatment resulted in a hydrophilic surface (TiMOD)
- Sandblasted with large grit 250–500 µm Al_2O_3 particles and acid etched with a boiling mixture of sulfuric/hydrochloric acids (concentrations not provided by the company), then cleaned in nitric acid, rinsed in deionised water and air dried (TiSLA)
- Same sandblasting and acid-etching treatment as the TiSLA surface, followed by rinsing in NaCl solution under nitrogen treatment and storage in 0.9 % NaCl solution (TiSLACT)

Titanium-zirconia alloy (R):

- Acid etched with a boiling mixture of sulfuric/hydrochloric acids (concentrations not provided by the company) (RA)
- Acid etched as above, followed by rinsing in NaCl solution under nitrogen treatment, then stored in 0.9 % NaCl, where this type of treatment resulted in a hydrophilic surface (RMOD)

- Sandblasted with large grit 250–500 µm Al_2O_3 particles and acid etched with a boiling mixture of sulfuric/hydrochloric acids (concentrations not provided by the company), then cleaned in nitric acid, rinsed in deionised water and air dried (RSLA)
- Same sandblasting and acid-etching treatment as the RSLA surface, followed by rinsing in NaCl solution under nitrogen treatment and storage in 0.9 % NaCl solution (RSLACT)

All discs received were wrapped and sealed in foil, except the discs with SLActive surfaces and the acid-etched hydrophilic discs, which were received in plastic bottles filled with saline solution. Representative images of the CpTi1, CpTi2, and TiZr discs are presented below in Figure 3.1.

(a) **(b)** **(c)**

Figure 3.1 Representative images of the samples: a) CpTi1, b) CpTi2, and 3) TiZr

Table 3.1 Materials and surface modifications used in the study

Material	Surface			
CpTi1	(CpC) Control (no treatment)	(SB) Sandblasted with 250 µm Al_2O_3	(SBE) Sandblasted with 250 µm Al_2O_3/etched (3 % HF/17.5 % HNO_3)	
CpTi2 (Ti)	(TiA) acid-etched (H_2SO_4/HCl)	(TiMOD) (Hydrophilic) acid-etched (H_2SO_4/HCl) /rinsed with NaCl under N_2/stored 0.9% NaCl	(TiSLA) Sandblasted 250–500 µm Al_2O_3/etched (H_2SO_4/HCl)/ cleaned in HNO_3/rinsed with deionised water	(TiSLACT) Sandblasted 250–500 µm Al_2O_3/etched (H_2SO_4/HCl) /rinsed with NaCl under N_2 /stored 0.9 % NaCl
TiZr (R)	(RA) acid-etched (H_2SO_4/HCl)	(RMOD) (Hydrophilic) acid-etched (H_2SO_4/HCl)/ rinsed with NaCl under N_2/stored 0.9% NaCl	(RSLA) Sandblasted 250–500 µm Al_2O_3/etched (H_2SO_4/HCl)/ cleaned in HNO_3/rinsed with deionised water	(RSLACT) Sandblasted 250–500 µm Al_2O_3/etched (H_2SO_4/HCl) /rinsed with NaCl under N_2/ stored 0.9 % NaCl

3.3.2 Talysurf CLI 1000 optical profilometer

The Talysurf CLI 1000 optical profilometer (Taylor Hobson Precision, UK) was used in this study. This profilometer is composed of several parts, as illustrated below in Figure 3.2:

Figure 3.2 3D optical profilometer: (a) gauge cover, (b) gauge selection, (c) vertical *Z* slide, (d) horizontal *X*-*Y* slides, (e) remote control keypad, (f) emergency stop button, and (g) granite base and gantry

The profilometer had 3 different gauges: chromatic length aberration (CLA) gauge, inductive gauge, and laser gauge.

3.3.2.1 Non-contacting conofocal gauge measurement

Surface measurements were obtained using the (CLA) gauge and involved passing a light beam focused by a beam splitter traveling through a fibre optic cable. The light then passes through spectral aberration lenses to the surface examined. Any difference in the surface texture is identified as a change in the reflected beam (Leena *et al.*, 2016). This type of measurement has the advantage of producing high accuracy and resolution. The CLA gauge (300 µm) was selected with the following specifications: 10 nm resolution at 30 mm/second speed.

3.3.3 Experimental setting

Three samples from each group (n=3) were tested. The samples were placed on the horizontal *X*-*Y* slide table of the profilometer. The machine was first calibrated before each sample. Following calibration, the scanning light beam was focused on the sample using the keypad on the machine. The sample position, area to be scanned and resolution parameters were specified and entered into the software before scanning. The time needed for scanning was automatically calculated according to the area and resolution specified.

Different areas and resolution settings were tested. The resolution was optimised to obtain the best result, which was 1,001 points/mm. All measurements were standardised to be made over an area of 1 mm x 1 mm with 1 µm spacing at a bidirectional speed. The Gaussian filter used was 0.8 mm with 0.250 mm cut-off. Each disc was scanned 3 times over a randomly selected area. The scanned images were analysed using the Talymap Platinum software, which allowed 2D and 3D quantitative parameters of the surface

roughness to be evaluated. The 3D surface roughness parameters chosen were S_a, S_p, and S_v and their equivalent 2D parameters R_a, R_p, and R_v.

3.4 Data analysis

The data collected from the means of the three measurements per sample for each group were entered into a statistical software package (SPSS® Ver.23, SPSS Inc., Chicago, IL, USA) for analysis. The test of normality revealed that the data were not normally distributed, and therefore a non-parametric test was used. The Kruskal–Wallis test with multiple pairwise comparisons was used to compare the medians, with the level of significance set to p= 0.05.

3.5 Results

The medians and range of the surface roughness parameters S_a and R_a (µm) for all groups are presented below in Table 3.2. The medians are presented graphically in Figure 3.3. The commercially pure sandblasted acid etched (SBE) showed the highest overall S_a (3.70 µm), while the TiZr acid etched (RA) had the lowest overall S_a (1.14 µm). For the overall R_a medians, the Ti sandblasted large grit acid etched (TiSLA) showed the highest R_a (2.47 µm), whereas the commercially pure titanium control (CpC) had the lowest overall R_a (0.19 µm). Statistical analysis of the data revealed statistically significant differences in the S_a and R_a parameters between groups (p = 0.002 and 0.002, respectively).

The multiple pairwise comparisons for the S_a parameter showed that RA and RMOD were significantly different from CpC, SB, SBE, TiSLA, and TiSLACT. In addition, a statistically significant difference was found between the TiA, TiMOD and SBE. The RSLA was also noted to be statistically different from TiSLACT, SB, and SBE, while the RSLACT was only significantly different from the SBE. The multiple pairwise comparisons for the R_a parameter indicated a significant difference between CpC, RA, and RMOD, and the SB, TiA, TiSLA, TiSLACT, and RSLACT. The TiMOD showed a further difference from the TiSLA.

Table 3.2 Median of the S_a and R_a parameters

Group (n=3)	Median S_a µm (range)	Median R_a µm (range)	Material
CpC	3.00 (1.53)$^{a, b, d, 1}$	0.19 (0.14)^{a,1}	
SB	3.37 (2.70)^{a,b,1}	1.85 (1.32)^{b,c,2}	CpTi1
SBE	3.70 (0.23)^{a,1}	1.48 (0.40)^{a,b,c,1,2}	
TiA	2.44 (0.17)^{b,c,d,2}	1.91 (0.58)^{b,c,3,4}	
TiMOD	2.45 (0.81)^{b,c,d,2}	0.80 (0.50)^{a,b,3}	CpTi2
TiSLA	2.96 (0.08)^{a,b,d,2}	2.47 (0.49)^{c,4}	
TiSLACT	3.24 (0.20)^{a,b,2}	1.96 (0.51)^{b,c,3,4}	
RA	1.14 (0.15)^{c,3}	0.30 (0.09)^{a,5}	
RMOD	1.27 (0.41)^{c,3}	0.31 (0.12)^{a,5}	TiZr
RSLA	2.19 (0.35)^{c,d,3}	1.45 (0.17)^{a,b,c,5,6}	
RSLACT	2.56 (0.70)^{b,c,3}	1.90 (0.50)^{b,c,6}	

NOTE: the different superscript letters within the same column indicate significant differences between all the groups. Different numbers within the same column indicate significant differences between the surface of the same material (p<0.05)

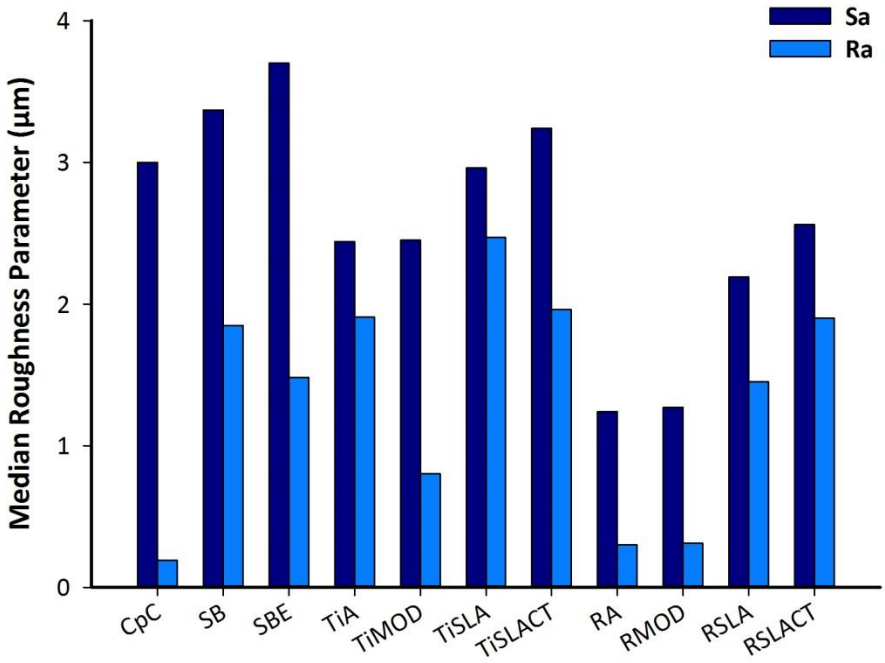

Figure 3.3 Bar chart representing the medians of the S_a and R_a roughness parameters for all groups

Table 3.3 shows the medians and range for the S_p, S_v, R_p, and R_v parameters for all groups. The medians are presented graphically in Figure 3.4. Overall, the R_a, R_p, and R_v showed the same trend in relation to the highest and lowest values. The same trend was also observed among the highest values of S_P and S_v which were associated with SB. The lowest values S_a and S_p were associated with the same group, the RA. The highest and lowest 3D peaks S_p were for the SB and RA at 24.70 µm and 5.50 µm, respectively. For the 3D valleys S_v, the highest value was for the SB (29.33 µm), while the RMOD showed the lowest valley S_v (4.89 µm). For both the highest 2D peaks and valleys R_p and R_V, the highest values were for the TiSLA at 6.67 µm and 7.04 µm, respectively. Similarly, the lowest R_p and R_v were associated with the CpC at 0.61 µm and 0.64 µm, respectively. The statistical analysis of the data revealed significant differences in all parameters across all groups: S_p, S_v, R_p, and R_v where p= 0.015, 0.002, 0.002, and 0.002, respectively.

The results of the multiple pairwise comparisons of all parameters S_p, S_v, R_p, and R_v across groups were between the RMOD and RA, and the TiSLA, TiSLACT, and RSLACT. The only exception was in the S_p parameter that did not show any difference between the RMOD, RA and RSLACT. When comparing the S_v and R_v parameters across the groups, both RMOD and RA were also significantly different from the TiA and SB. In addition, for the S_v parameter, the RA and RMOD were statistically different from the SBE as well. The RA and RMOD were significantly different from the SB, SBE, TiSLA, and TiSLACT in the S_p. The RA group showed a further statistical difference from the TiA both in the S_p and R_p parameters across groups. The CpC was statistically different from the SBE, SB, TiA, TiSLA, TiSLACT, and RSLACT in both the R_p and R_v parameters. When comparing the S_v parameter across groups, the CpC was noted to be significantly different from the TiA, SB, and SBE. For the S_p, the CpC was different from TiSLA and SB. There were some statistical

differences noted in the TiMOD as well in the S_v values, where the TiMOD was statistically different from SB and SBE. For the R_p parameter, the TiMOD showed a significant difference from the TiSLA, TiSLACT, and RSLACT. Similarly, in the R_v parameter, the TiMOD was statistically different from the TiSLA.

The effect of the surface modifications on the tested surfaces can clearly be seen in the representative 3D images (Figures 3.5–3.15). The difference in implant material and surface modification on the surface topography is demonstrated when comparing the control sample CpC (Figure 3.5) with the other surfaces. The CpC has a smother surface with deep orientation grooves from the machining process, whereas the other surfaces clearly appear different in their level of roughness and homogeneity, with multiple peaks and valleys.

Table 3.3 Medians of the surface roughness parameters S_p, S_v, R_p, and R_v for all tested groups

Group (n=3)	Median S_p µm (range)	Median S_v µm (range)	Median R_p µm (range)	Median R_v µm (range)	Material
CpC	9.65 (4.40)^{a,c,1}	8.63 (6.29)^{a,d,1}	0.61 (0.28)^{a,1}	0.64 (0.40)^{a,1}	
SB	24.70 (10.20)^{b,2}	29.33 (26.90)^{b,2}	4.27 (3.23)^{b,c,d,2}	6.45 (2.51)^{b,c,2}	CpTi1
SBE	15.93 (3.00)^{a,b,1,2}	27.73 (6.30)^{b,2}	3.90 (1.59) ^{b,c,d,2}	4.58 (2.54)^{b,c,d,2}	
TiA	14.76 (0.60)^{a,b,d,3}	22.93 (14.30)^{b,c,3}	4.47 (1.90)^{b,c,3,4}	6.13 (3.79)^{b,c,3,4}	
TiMOD	20.59 (29.83)^{a,b,c,3}	11.03 (1.50)^{a,c,d,3}	1.94 (0.65)^{a,b,3}	2.86 (1.77)^{a,b,3}	CpTi2
TiSLA	19.43 (3.70)^{b,3}	18.63 (3.20)^{a,b,3}	6.67 (3.28)^{c,4}	7.04 (1.29)^{c,4}	
TiSLACT	19.00 (7.90)^{a,b,3}	19.70 (7.70)^{a,b,3}	5.21 (0.78)^{c,4}	5.53 (0.69)^{b,c,3,4}	
RA	5.50 (2.49)^{c,4}	6.06 (3.86)^{d,4}	1.02 (0.47)^{a,d,5}	1.11 (0.40)^{a,d,5}	
RMOD	6.40 (6.55)^{c,d,4}	4.89 (0.45)^{d,4}	1.36 (0.97)^{a,b,5}	0.95 (0.20)^{a,d,5}	TiZr
RSLA	19.40 (22.40)^{a,b,c,4}	14.96 (5.40)^{a,b,d,4,5}	3.63 (0.62)^{a,b,c,5,6}	3.92 (0.66)^{a,b,c,5,6}	
RSLACT	13.60 (6.20)^{a,b,c,4}	19.30 (7.00)^{a,b,5}	5.26 (2.19)^{c,6}	6.08 (3.86)^{b,c,6}	

NOTE: The different superscript letters within the same column indicate significant differences between all groups. Different numbers within the same column indicate significant differences between surfaces of the same material ($p<0.05$)

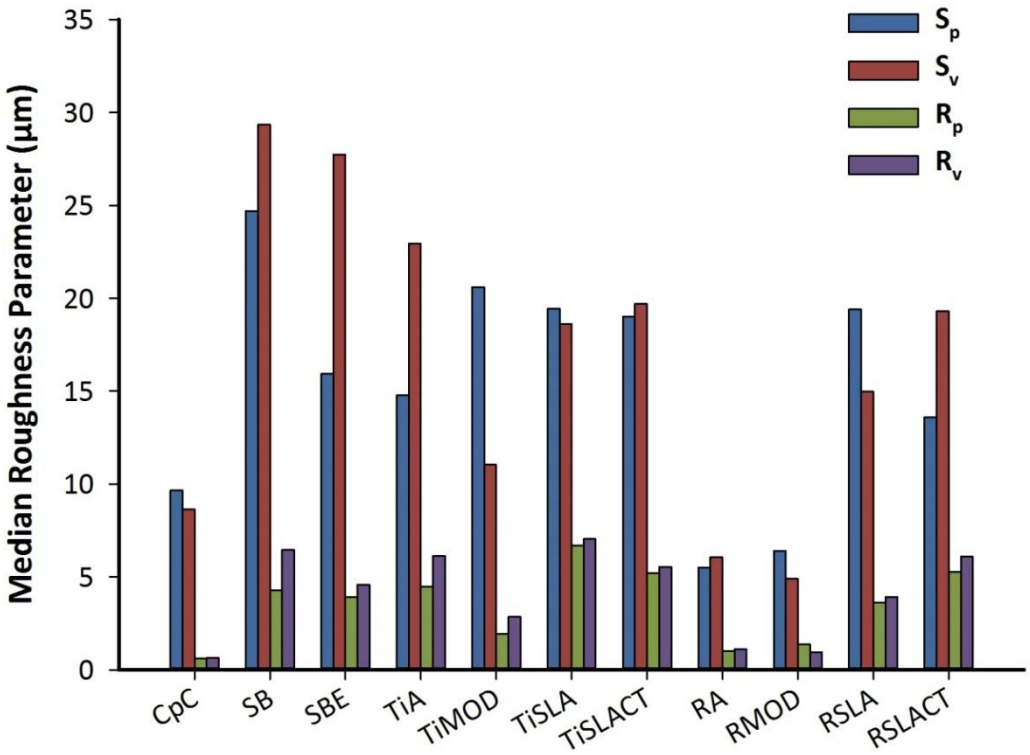

Figure 3.4 Bar chart representing the medians of the roughness parameters for all groups

The surface roughness test produced a large amount of 3D surface roughness profile images. A representative 3D profile from each group is presented below in Figures 3.5–3.15.

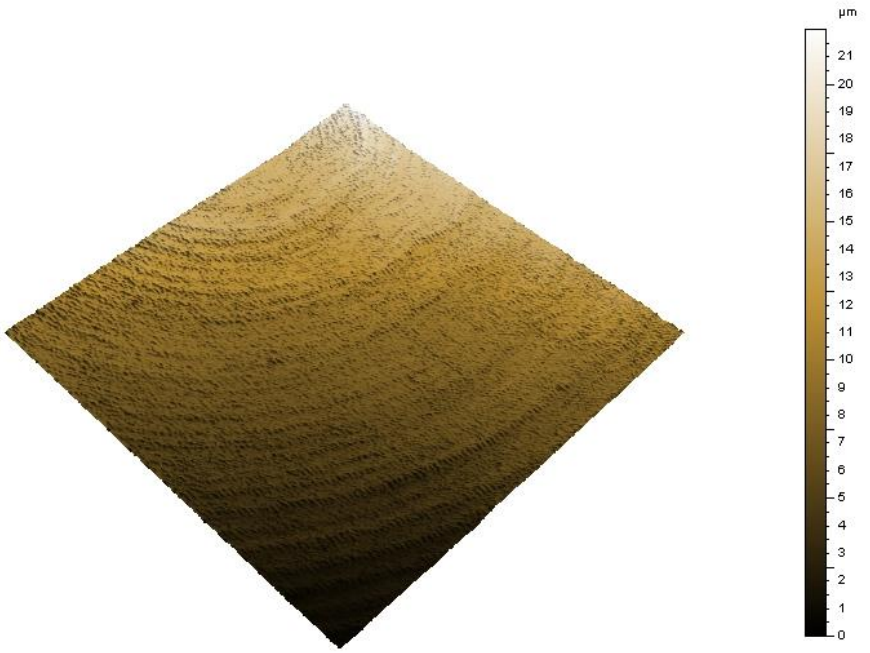

Figure 3.5 A representative 3D view of the CpC group

Figure 3.6 A representative 3D view of the SB group

Figure 3.7 A representative 3D view of the SBE group

Figure 3.8 A representative 3D view of the TiA group

Figure 3.9 A representative 3D view of the TiMOD group

Figure 3.10 A representative 3D view of the TiSLA group

Figure 3.11 A representative 3D view of the TiSLACT group

Figure 3.12 A representative 3D view of the RA group

Figure 3.13 A representative 3D view of the RMOD group

Figure 3.14 A representative 3D view of the RSLA group

Figure 3.15 A representative 3D view of the RSLACT group

3.6 Discussion

The ability of dental implants to osseointegrate is strongly related to the surface topography (Barfeie *et al.*, 2015). This relationship has been demonstrated in many studies (Buser *et al.*, 1991; Saghiri *et al.*, 2016). The results of this study showed that different implant materials and surface modifications had a significant effect on the surface roughness. Therefore, the null hypothesis was rejected.

The methodology selected for this study followed the guidelines for measuring surface topography published by Wennerberg and Albrektsson (1999). The optical profilometer used in this study was a non-contacting type, which has the advantage of being more accurate and non-destructive to the surface (Wennerberg *et al.*, 2015). Three disc specimens per group was chosen based on previous similar studies to assess the surface roughness of dental implants (Rupp *et al.*, 2006; Elias *et al.*, 2008; Rosales-Leal *et al.*, 2010; Dos Santos *et al.*, 2011; Sista *et al.*, 2011; Saulacic *et al.*, 2012; Park *et al.*, 2013; Wennerberg *et al.*, 2013; Elias *et al.*, 2015; Zahran *et al.*, 2016). Three readings were taken from each disc in line with existing research (Rupp *et al.*, 2006; Sista *et al.*, 2011; Saulacic *et al.*, 2012; Wennerberg *et al.*, 2013; Hotchkiss *et al.*, 2017; Lotz *et al.*, 2017).

S_a versus R_a parameter

In general, this study demonstrated that surface modifications changed the surface roughness of the tested materials, in agreement with the majority of studies in the literature (Elias *et al.*, 2008; Rupp *et al.*, 2017). When comparing the median 2D and 3D roughness parameters R_a and S_a, it was noted that the highest and lowest S_a were for the SBE and RA groups, respectively. Meanwhile, the highest and lowest R_a were for the TiSLA and CpC groups, respectively. These findings also noted that both the 2D and 3D

parameters of the same groups using the same device gave different values and significant differences among different groups. This might be partially explained by how the parameters are calculated, as the 2D parameters are calculated from a profile of the surface, whereas the 3D parameters are calculated from the areal surface. Thus, different results are expected. This is consistent with other studies suggesting that 3D parameters are more accurate in representing the surface than 2D parameters (Wennerberg *et al.*, 2015).

Although the CpC surface is a machined surface and is considered to be a smooth surface (Albrektsson and Wennerberg, 2004; Takeuchi *et al.*, 2005), its S_a in the present study was high and significantly different from RA and RMOD. Meanwhile, when comparing the R_a for the CpC, lower values were obtained, indicating its smoother texture with no significant difference from RA or RMOD, and significant differences from other groups. This variation could be related to the concentric ridges on its surface (Figure 3.5) representing the machining process increasing the surface roughness (Elias *et al.*, 2008), or other unknown factors in the manufacturing process of CpC, which might have influenced its surface texture. Furthermore, when comparing the CpC to the CpTi2 (TiA, TiMOD) groups having the same surface as TiZr (RA, RMOD), there were no significant difference in the S_a between CpC and TiA, and TiMOD. While for R_a, a significant difference was noted between the CpC and TiA, in line with the study by Takeuchi *et al*. (2005). The variation in the results between the CpC and (RA, RMOD/TiA, TiMOD) reflects that different results were obtained from the R_a and S_a parameters. In addition, the implant material could affect the S_a and R_a parameters when the same treatment is applied.

The RSLACT group showed lower S_a values than the TiSLA or TiSLACT groups. This is in agreement with another study that used the same materials and surfaces supplied by the same company (Wennerberg *et al.*, 2013). Similarly, in the present study, lower S_a values were noted for the TiMOD group in comparison to the TiSLA, TiSLACT, and RSLACT groups. This is in agreement with the results of the study by Wennerberg *et al.* (2013). However, the S_a values were higher in the present study with no significant differences between TiSLACT and (TiMOD, RSLACT), nor between TiSLA and TiMOD, which is different from the Wennerberg *et al.* (2013) study and this could be attributed to the use of different techniques and scanning areas. Another study by Zhao *et al.* (2005) also reported lower S_a values for the TiSLA and TiSLACT surfaces in comparison to the present study.

When comparing the R_a values, the TiA surface was smoother (R_a= 1.91 µm) than the TiSLA surface (R_a= 2.47 µm) with no significant difference. The same outcome was observed in a study by Li *et al.* (2002) who reported the R_a for TiA and TiSLA at 1.57 µm and 2.18 µm, respectively, where this difference in R_a was one of the reasons that explained the greater biomechanical performance of TiSLA. Similarly, the TiA was smoother than the TiSLA for S_a, with no significant difference.

Previous studies have reported that hydrophilic surfaces have enhanced biological responses compared to hydrophobic surfaces (Lang *et al.*, 2011b; Lotz *et al.*, 2016; Saghiri *et al.*, 2016). However, in this study the hydrophilicity of the surface when comparing the (TiSLA/TiSLACT, TiA/TiMOD, RA/RMOD, and RSLA/RSLACT) groups did not have a significant effect on any 2D or 3D surface roughness parameters. No significant difference was noted for all the 2D and 3D surface roughness parameters for the TiSLA and TiSLACT surfaces of the same material. This coincides with results obtained from other studies

using a light confocal microscope to compare the TiSLA and TiSLACT surfaces (Buser *et al.*, 2004; Zhao *et al.*, 2005), or using an optical profilometer (Rupp *et al.*, 2006). Furthermore, consistent with the study by Rupp *et al.* (2006), no differences in the R_a parameter were found between the TiA (hydrophobic) and TiMOD (hydrophilic) groups supplied and modified by the same company.

In general, it has been noted that the titanium-zirconia alloy (R) exhibited lower average roughness S_a values than all the treated CpTi1 and CpTi2 (Ti) groups, with the only exception being the RSLACT group. These lower S_a values could be due to the composition of the alloy, as previous research showed greater S_a values were associated with CpTi compared to the Roxolid® alloy with the same surface treatment (Lotz *et al.*, 2017). Saulacic *et al.* (2012) observed that the implant material composition had a significant effect on the microtopography and surface roughness parameters of TiZr and CpTi implants when the same surface (SLActive) was examined; this was suggested as one of the factors that could explain the improved bone apposition associated with the TiZr alloy compared to CpTi.

Comparing different materials, CpTi2 (Ti) and TiZr (R) groups (TiA/RA, TiMOD/RMOD, TiSLA/RSLA, TiSLACT/RSLACT) provided by the same company with the same surface modification showed different S_a values with no statistical differences. This is in agreement with the studies by Jimbo *et al*. (2015) and Lotz *et al*. (2017), which indicated different values of S_a with no significant difference when comparing the CpTi and TiZr (Roxolid®) implants with the same SLActive surface. However, when comparing the CpTi2 (Ti) and TiZr (R) groups with different materials and different surfaces, some significant differences were noted in both the S_a and R_a parameters. This indicates that the implant

material and surface modification together might have a significant effect on the S_a and R_a parameters.

Similarly, when comparing the CpTi1 and R groups with different surface modifications and materials, some significant differences were also noted in both the S_a and R_a parameters. Nevertheless, whether this effect was due to difference in the bulk material or the surface modification could only be confirmed if the CpTi1 were exposed to the same surface modification and compared to the R substrate, as in the case of CpTi2. This could be a limitation of the study, however to ensure that the surface modifications were identical to the commercial implants all the samples were prepared by the aforementioned companies, and this limitation had to be accepted.

The two CpTi being identified by the manufacturers as CpTi grade 2 (i.e. the same material) with different surfaces showed significant differences between some groups in S_a and R_a. This could be explained by the variation in surface modifications examined. However, no significant differences were noted in the S_a and R_a when comparing the SBE and TiSLA groups having the same type of treatment (sandblast/acid-etched) despite the difference in the sandblasted and acid-etched protocols.

S_p, S_v, R_p, R_v versus S_a/R_a

Generally, the analysis of S_p, S_v, R_p, and R_v across all surfaces showed that RA and RMOD had lower values compared to all the other modified surfaces, even the surfaces with the same treatment (TiA, TiMOD). The RA/TiA and RMOD/TiMOD did not show a significant difference in their S_a values, although their S_p, S_v, R_p, and R_v were much higher with a significant difference between RA and TiA. This reflects that the maximum peaks and valleys could be influenced by the material composition when the same modifications are applied. In contrast, the same effect was not seen between the TiSLA/RSLA and TiSLACT/RSLACT in S_a, S_p, S_v, R_a, R_p, and R_v. This could be related to the difference in the level of surface roughness produced by the two modifications. The sandblast and acid-etched modification produces more complex surfaces with larger cavity diameters than the acid-etched modification alone (Li *et al.*, 2002; Rupp *et al.*, 2006).

The overall variation in the extreme height peaks and valleys between groups could be attributed to manufacturer modification protocols (Czan *et al.*, 2017). Research has shown that different acid-etching protocols and sandblasting will result in a variation in the maximum peaks and valleys (Mendoza-Arnau *et al.*, 2016). Using different particle sizes for sandblasting is known to produce different roughness levels that affect the subsequent BIC (Wennerberg, 1998; Mustafa *et al.*, 2001; Rønold and Ellingsen, 2002). Additionally, the variation in the blasting parameters during blasting can affect the roughness parameters significantly (Valverde *et al.*, 2013), and Zahran *et al.* (2016) demonstrated that an increase in etching times with HF acid influences the S_a, S_p, and S_v values and cellular response.

Further analysis of the profiles/surfaces revealed that all the CpTi2 (Ti) samples with the same material and different surface showed no significant difference in the S_a, S_p, and S_v

parameters. The same trend was observed with all the TiZr (R) groups with the same material and different surface in the S_a and S_p parameters, whereas in the S_v a significant difference was evident between the RA, RMOD and RSLACT group. The CpTi2 (Ti) and TiZr (R) with different materials and the same surface (TiA/RA, TiMOD/RMOD, TiSLA/RSLA, and TiSLACT/RSLACT) did not show any statistical differences among all the groups in the S_a, while for all groups the same was noted for the S_p and S_v, with the only exception a significant difference between RA and TiA in S_p and S_v.

The combination of different material and surfaces of the CpTi2 (Ti) and TiZr (R) showed the same trend of being significantly different in S_a, S_p, and S_v between some groups. Similarly, when comparing the CpTi1 and TiZr (R) with different materials and surfaces, the same trend was observed in S_a, S_p, and S_v between some groups. The CpTi1 and CpTi2 (same material and different surface) also showed significant differences in all the S_a, S_p, and S_v parameters in some groups.

The S_p and S_v parameters did not show the same trend as S_a for CpTi1. Although the S_a did not show any significant differences between the CpTi1-treated groups and control, which should not be the case as the CpC sample was not treated, the analysis of the S_p and S_v revealed that both the SB and SBE surfaces were extremely different in their textures to CpC. Thus, examining the S_p and S_v parameters could be useful to provide better understanding about the biological responses to different implant surfaces. This is in line with the suggestion of using other roughness parameters to provide more details about the surface roughness of an implant surface (Löberg *et al.*, 2010; Hansson and Hansson, 2011).

Regarding the 2D parameters, the same trend was evident in all the material and surface combinations, with significant differences between some groups in R_a, R_p, and R_v. The R_a,

R_p and R_v parameters did not demonstrate whether the change in the surface roughness was influenced by the material, surface, or a combination of both.

3.7 Conclusions

Within the limitations of this study, the following conclusions were drawn:

- The mean 2D and 3D surface roughness profiles S_a and R_a provide an informative overview about surface roughness. The analysis of the highest peaks and valleys can provide more information about the surface roughness.
- The variation in the surface treatment within the same material had no significant effect on the S_a value. The combination of different implant material and surface modification had a significant effect on S_a.
- The variation in the implant material, surface, or combination thereof had a significant influence on the 2D parameters (R_a, R_p, and R_v).
- The different modification within the same material in the CpTi and TiZr groups did not have a significant effect on S_p. However, different materials could have a significant effect on the S_p and S_v when the same surface modification is applied.

Chapter 4

Nanomechanical and Micro-Nanomechanical Properties of Surface-Modified Dental Implants

4.1 Introduction

Surface modification of dental implants at the manufacturing stage results in different levels of surface texture and chemical compositions at the micrometre and nanometre scales (Svanborg *et al.*, 2010). These modifications are mainly used to enhance the BIC and subsequent healing process. Although the manufacturing processes are surface modifications aimed at providing a moderately roughened surface, it remains unknown what effect, if any, these processes have on the sub-surface bulk properties of the implant body. Such effects are seen in different materials such as stainless steel and nickel titanium endodontic instruments (Zinelis *et al.*, 2008), and titanium alloys including titanium-zirconia alloys (Cáceres *et al.*, 2008; Majumdar *et al.*, 2008; Cordeiro *et al.*, 2018). However, surface modifications and their effect on the sub-surface elastic modulus and hardness properties of bulk dental implant materials have not been investigated.

A successful dental implant should be able to withstand a functional load without resulting in fracture or deformation. Evaluating the mechanical properties of dental implants in terms of elastic modulus and hardness is essential for their stability (Niinomi and Nakai, 2011). One of the essential requirements of dental implant materials is a low elastic modulus in comparison to bone to avoid bone shielding and subsequent implant loss (Niinomi, 1998; Shibata *et al.*, 2015). The effect of zirconia on lowering the elastic modulus and increasing the hardness of titanium alloys was shown by various studies (Ho *et al.*, 2008; Lee *et al.*, 2016).

Nanoindentation technology has been applied in dentistry to investigate the mechanical characteristics of different restorative materials such as resin composites and endodontic files (Zinelis *et al.*, 2008; El-Safty *et al.*, 2012a). Attention was directed toward studying

the mechanical properties of thin coatings at the micro and nanometre scales (Mayo *et al.*, 1990; Saber-Samandari *et al.*, 2011). Depth sensing indentation has established itself as a valuable method to assess both elastic modulus (*E*), and hardness (*H*), not only for materials but even for human bone and teeth (Rho *et al.*, 1997; Zysset *et al.*, 1999; Cuy *et al.*, 2002). Data derived from nanoindentation has been used to assess other mechanical properties such as creep, phase transformation, cracking, and energy absorption (Fischer-Cripps, 2011; El-Safty *et al.*, 2012b).

Limited studies have been conducted to assess the elastic modulus and hardness properties of different dental implant materials using nanoindentation (Jíra *et al.*, 2015; Fiuza *et al.*, 2017). Moreover, none of the available studies focused on using nanoindentation to compare TiZr alloy and CpTi with various surfaces.

A new generation of indentation instruments (i.e. the micro-nanoindenter) has been marketed; these devices apply the same principle of indentation testing as detailed in (§ 1.7.2.1). A load is placed on the indenter head to make an indent on the surface with a small diamond indenter. The data are then collected from the load-depth curves and the hardness and elastic modulus are automatically calculated. This new micro-nanoindenter applies a load lower than the microhardness testers and higher than a conventional nanoindenter.

The main advantage of this machine in comparison to microhardness testers is the lack of any need to visualise the indent to calculate the elastic modulus and hardness. Therefore, the chance of introducing any errors in this stage is eliminated. Furthermore, this machine is smaller, more compact and easier to use in comparison to a conventional nanoindenter. Additionally, it is automated, gives instant results and is less sensitive to noise and other external factors. Therefore, using the new micro-nanoindenter could

represent a potential alternative to the conventional nanoindenter if comparable results are obtained. Furthermore, this device is able to assess the mechanical properties at a micro-nanometre scale.

4.2 Aims of the study

The aims of this study were to a) investigate the effect of the manufacturer processes on the sub-surface mechanical properties, and b) investigate the effect of implant composition on the sub-surface mechanical properties. The objectives were:

- To assess the elastic modulus (*E*) using nanoindentation and micro-nanoindentation.
- To assess the hardness (*H*) using nanoindentation and micro-nanoindentation.
- To compare the elastic modulus and hardness profiles at the nano and micro-nano levels.

The null hypothesis was that there is no difference in the sub-surface elastic modulus and hardness properties between different manufacturer processes and implant compositions using nanoindentation and micro-nanoindentation.

4.3 Materials and methods

The implant materials and surfaces were the same as detailed in Chapter 3 (Table 3.1), namely CpC, SB, SBE, TiA, TiMOD, TiSLA, TiSLACT, RA, RMOD, RSLA, and RSLACT. Three samples from each group (n=3) were tested. The Nanoindenter G200 (Agilent Technologies Ltd, UK) and the Nanovea M3 micro-nanoindenter (Nanovea Inc., MA, USA), both equipped with a Berkovich indenter, were used to carry out the mechanical testing.

4.3.1 Nanoindenter G200

The Nanoindenter G200 (Agilent Technologies UK Ltd) in Figure 4.1 was used in this study. The nanoindenter is composed of three main components: 1) cabinet, 2*) X-Y-Z* table, and 3) indentation head that carries all the elements necessary to carry out the measurement.

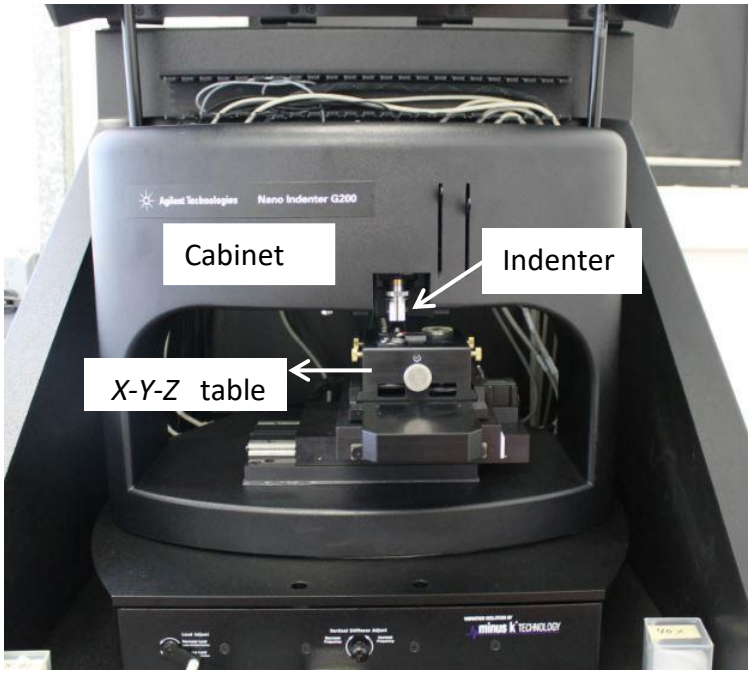

Figure 4.1 Nanoindenter components

4.3.2 Nanovea M3 micro-nano mechanical tester

The Nanovea M3 micro-nanoindenter (Nanovea Inc., MA, USA) (Figure 4.2) equipped with a Berkovich indenter was used to carry out the mechanical testing. The machine has a *Y-Z* axes to move the sample stage, where the *Y* axis is for the horizontal movement and the *Z* axis is for the vertical movements. Each axis has 4 mm travel and 5 µm resolution. The machine specifications (Table 4.1) were as follows: depth sensor range 250 µm, 0.003 nm resolutions with 0.5 nm noise floor. The load sensors have two different ranges (400 mN or 200 mN) and a resolution of 0.03 µN or 0.30 µN, with a noise floor of 10 µN and 50 µN, respectively.

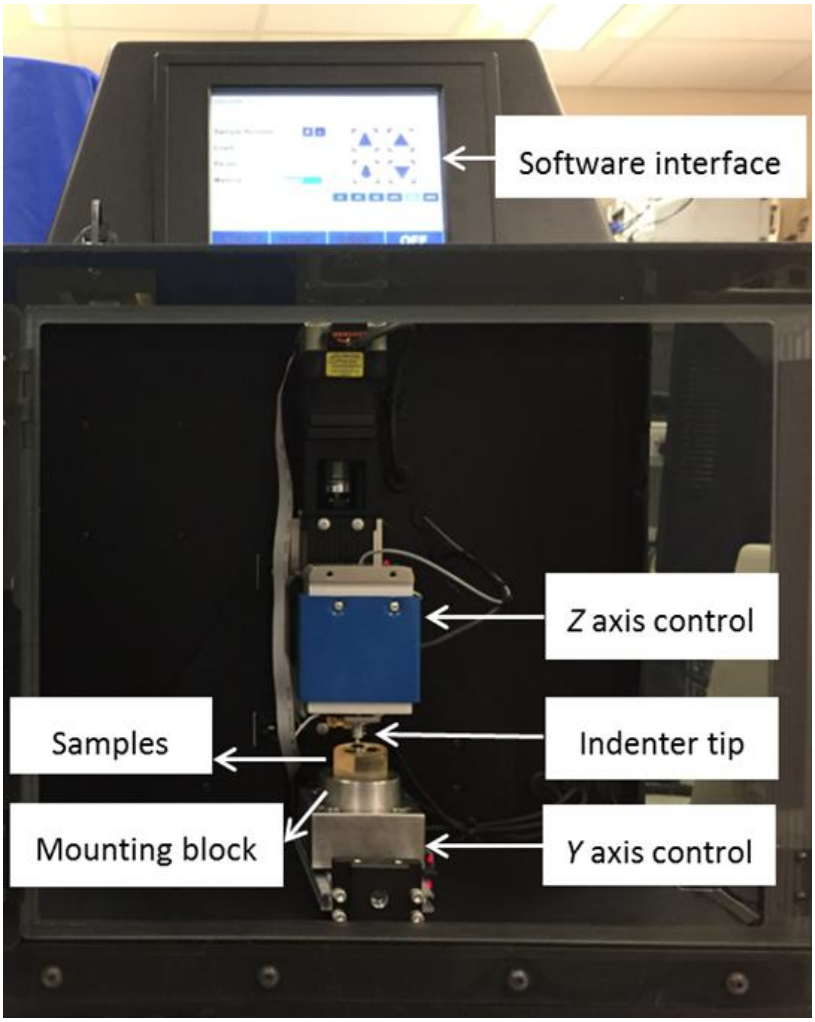

Figure 4.2 The Nanovea M3 micro-nanoindenter components

Table 4.1 The Nanovea M3 micro-nanoindenter specifications

Specifications	Depth sensor	Load sensor
Range	250 µm	400 mn / 2000 mN
Resolution	0.003 nm	0.03 µN / 0.30 µN
Noise floor	0.5 nm	10 µN / 50 µN

4.3.3 Sample preparation

In order to grind/polish the samples, they were embedded in low heat acrylic resin EpoxiCure 2 (Buehler, UK). The acrylic was left to set for 24 hours, and after setting the samples were labelled and ready for grinding and polishing.

The MetaServ 250 (Buehler, UK) grinder/polisher was used to prepare the samples. The protocol for grinding and polishing was performed using CarbiMet (Buehler, UK) silicon carbide (SiC) abrasive papers (sequence: 280, 400, 600, 1,000, 1,200, 4,000 PSA) using water as a lubricant at 1 bar load and 300 rpm speed. Each paper was used until the marks from the previous one had disappeared. After that, polishing was done using a cloth and diamond suspension (sequence: 1 µm, 0.25 µm) with MetaDi fluid (Buehler, UK) as a lubricant. Finally, the samples were ultrasonically cleaned using an ultrasonic cleaner (L&R Ultrasonics, New Jersey, USA) with distilled water for 15 seconds. The thickness of the samples before and after grinding/polishing was measured using a digital calliper (H Roberts & Sons, UK). The typical amount of surface removed was approximately 50 µm.

4.3.4 Mechanical testing

Nanoindentation

The samples were mounted on the *X*-*Y* table and tested using the Nanoindenter G200 (Agilent Technologies, UK Ltd) seen in Figure 4.3.

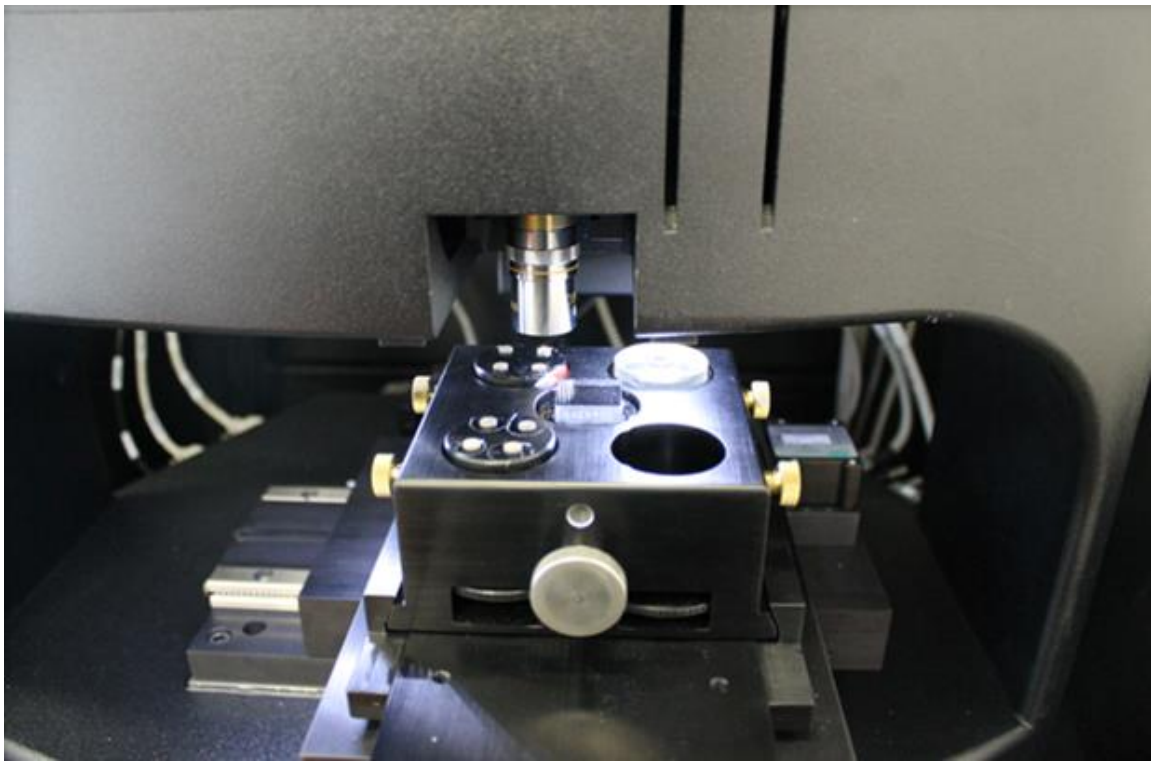

Figure 4.3 Samples mounted on the nanoindenter

Indents were made using a Berkovich diamond indenter tip with a 20 nm nominal radius. The indenter was first calibrated using fused silica block with known specifications. After that, the samples were placed on the *X*-*Y* table for testing. Thirty indents (Figure 4.4) were taken from each specimen on a randomly selected area at 30 microns distance from each other, to avoid creating any residual impression that might affect the accuracy of measurement. The measurement profiles for hardness (*H*) and elastic moduli (*E*) started from the outer surface to a depth of 2,000 nm, using the settings shown in Table 4.2. Means and standard deviations of elastic modulus and hardness of the 30 indents per

sample were calculated automatically from the load–depth curves using the NanoSuite 6.2 Agilent software. The Oliver and Pharr's method was used to analyse the load-depth curves.

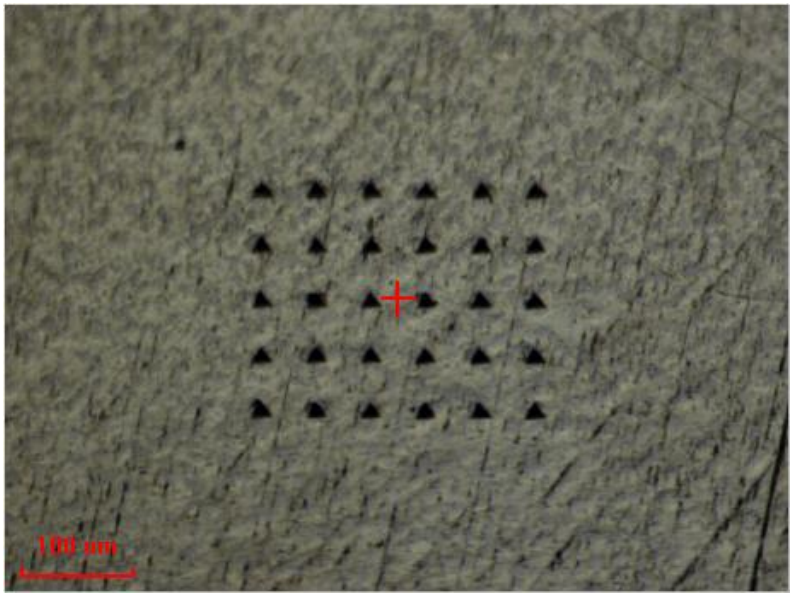

Figure 4.4 Image taken for the 30 indents

Table 4.2 Nanoindenter setting

Parameter	Value
Strain rate	0.05 1/s
Depth limit	2000 nm
Surface approach velocity	10 nm/s
Surface detect stiffness	200 N/m
Poisson's ratio for Ti alloy	0.34
Poisson's ratio for TiZr alloy	0.33
Frequency	0.00
Number of indents	43 Hz
Space between indents	30 microns

Micro-nanoindentation

After polishing and grinding, the samples were loaded on the mounting block inside the machine as in Figure 4.2. The *Y-Z* axes controllers were used to adjust the sample position in relation to the indenter tip. The machine was first calibrated using a fused silica block before each test. After that, the software interface was used to adjust the test parameters (Figure 4.5). Different test parameters were tested and the parameters selected were as follows: metal for tested material at 100 g load and 20 second pause. The indents were made using a Berkovich diamond tip. Five continuous indents for each sample were made on a randomly selected area at 250 µm spacing (Table 4.3).

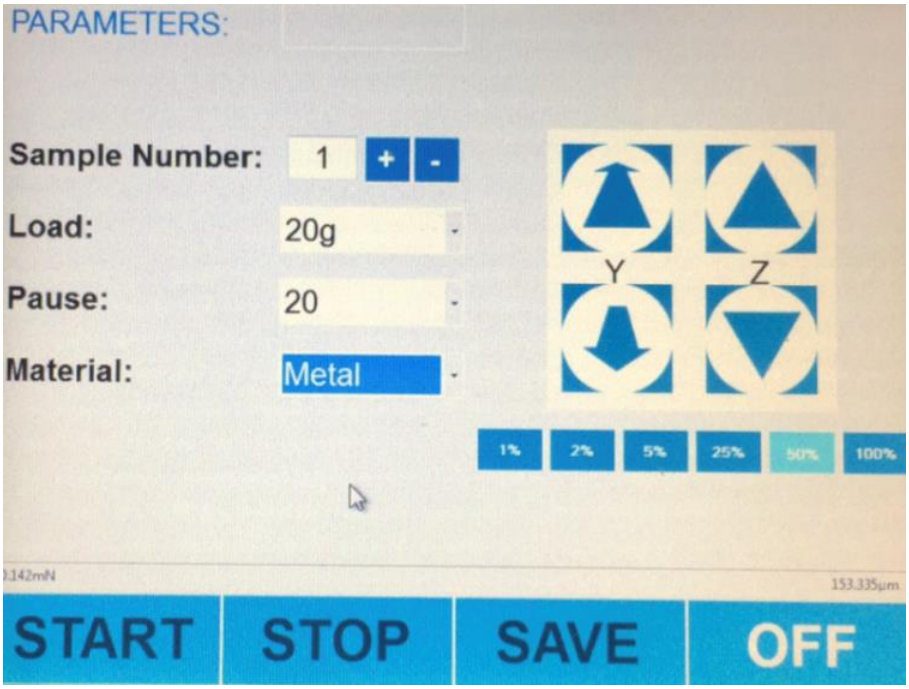

Figure 4.5 The M3 Nanovea software interface

Table 4.3 Micro-nanoindenter settings

Parameter	Value
Indenter type	Berkovich
Indenter core angle	130.54
Indenter Poisson's ratio	0.07
Indenter elastic modulus	1140 GPa
Sample Poisson's ratio	0.3
Number of indents	5
Space between indents	250 microns

The measurements of the elastic modulus and hardness of the 5 indents per sample were calculated automatically from the load–depth curves. The measurements were calculated by the machine using Nanovea Nano Hardness software (Ver.1.6.2). The Oliver and Pharr's method was used for analysis. The data were then saved on an external flash drive.

4.4 Data analysis

The means of 90 indents per group for the nanoindentation, and the means of 15 indents per group for the micro-nanoindentation, were entered into a statistical software package (SPSS® Ver.23, SPSS Inc., Chicago, IL) for analysis. The test of normality revealed that the data were not normally distributed, and therefore a non-parametric test was used. The Kruskal–Wallis test with multiple pairwise comparisons was used to compare the medians with the level of significance set to p= 0.05. Scatter plots and the Spearman's correlation test were used to assess the relationship between the sub-surface E and H values obtained by micro-nanoindentation and the nanoindentation.

4.5 Results

Nanoindentation

The elastic modulus and hardness measurements were automatically calculated from the load-depth curves. A representative load–depth curve is presented in Figure 4.6. The medians and range for the elastic modulus and hardness for all groups are presented in Tables 4.4 and 4.5, and the medians are presented graphically in Figures 4.8 and 4.9. The elastic modulus range was 60.49 GPa and 108.04 GPa, with the lowest value for RA and the highest value for SB, respectively. The hardness profiles ranged between 2.20 GPa for TiSLA and 3.36 GPa for the RSLA. Statistical analysis of the data revealed a significant difference in the elastic modulus and hardness between samples (p= 0.006 and 0.002, respectively). The pairwise comparisons of elastic modulus among groups revealed a significant difference between RA and RSLACT, and CpC, SB, SBE, TiA, and TiSLACT. Similarly, RMOD was also statistically different from the same groups, apart from TiSLACT. The TiSLA and TiMOD were both significantly different from SB.

For the hardness profiles, the pairwise comparisons between groups showed that the TiSLA and TiMOD were statistically different from the SB, RA, RMOD, RSLA, and RSLACT. Similarly, the TiSLACT was statistically different from the SB, RMOD, RSLA, and RSLACT. A statistical difference was also noted between the TiA and RSLA.

Micro-nanoindentation

The elastic modulus and hardness measurements were automatically calculated from the load–depth curves. A representative load–depth curve is presented in Figure 4.7. The medians and range for elastic modulus and hardness are presented in Tables 4.4 and 4.5, and the medians are presented graphically in Figures 4.8 and 4.9. Generally, the elastic modulus ranged from 37.23 GPa for the CpC to 170.65 GPa for the SBE. The Kruskal–Wallis test showed that there was a significant difference in elastic modulus between all groups (p= 0.001). The pairwise comparisons for elastic modulus revealed a significant difference between the CpC and RSLA, and SB, SBE, TiA, and TiSLACT. The RA showed a similar pattern to RSLA, with the TiSLACT being the only exception by not being statistically different from RA. The RMOD, TiSLA, and RSLACT showed a statistical difference from the SBE.

For hardness, the RMOD showed the highest value of 2.74 GPa, whereas the RSLA had the lowest value of 1.98 GPa. The Kruskal–Wallis test showed that there was a significant difference in hardness between groups (p= 0.010). The multiple pairwise comparisons revealed a statistical difference between the (CpC, SBE, TiMOD, and RSLA) and (SB, RA, RMOD, and RSLACT). In addition, a statistical difference was noted between TiSLA and RMOD and RSLACT.

Generally, when comparing the micro-nanoindentation and nanoindentation median measurements (Table 4.4 and Figure 4.10), a positive weak correlation was noted in the elastic modulus with no significant effect (r_s= 0.46, p= 0.15). For the hardness (Table 4.5 and Figure 4.11), a positive weak correlation was noted between the two methods with no significant effect (r_s= 0.32, p= 0.32). Thus, there is insufficient evidence to suggest there is a correlation between the two methods when measuring *E* and *H*.

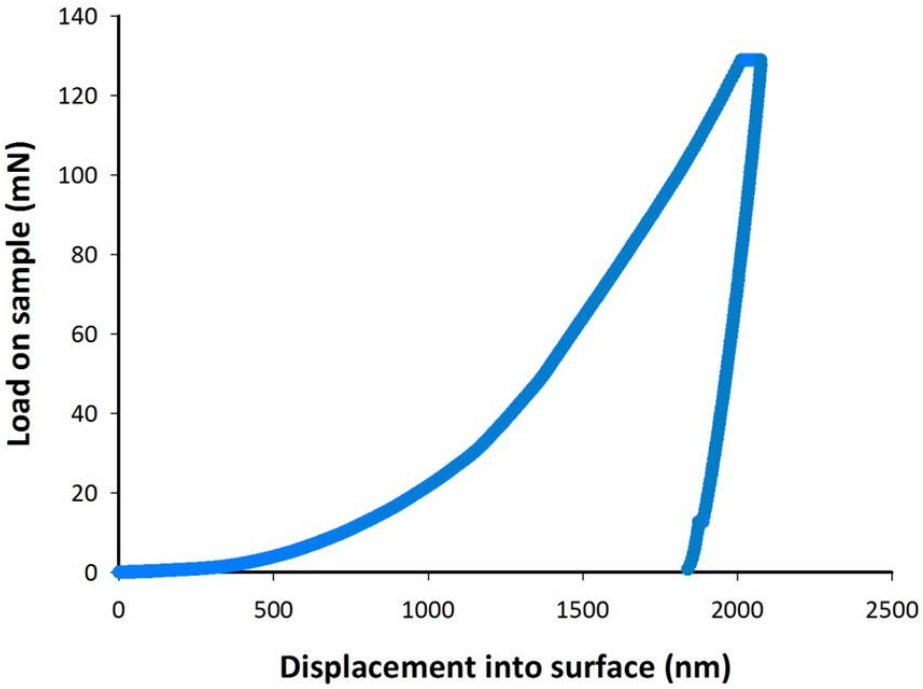

Figure 4.6 A representative load–depth curve for the nanoindentation

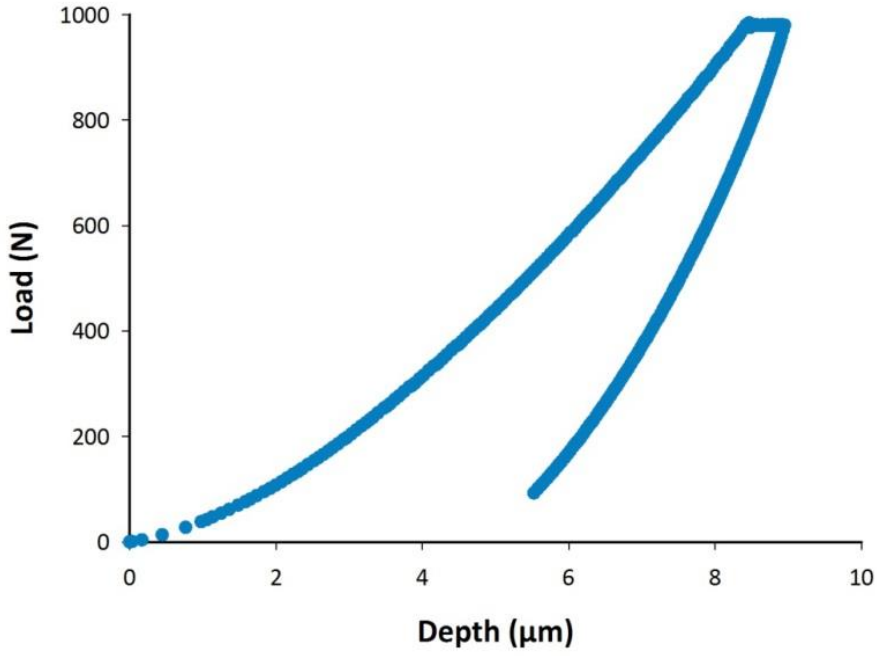

Figure 4.7 A representative load–depth curve for the micro-nanoindentation

Table 4.4 Representing the medians (range) of the elastic modulus using micro-nanoindentation and nanoindentation

Group	Micro-nanoindentation	Nanoindentation	Material
	Elastic modulus (GPa) Median (range)	Elastic modulus (GPa) Median (range)	
CpC	37.23 (4.82)^{a,1}	101.52 (16.32)^{a,b,1}	
SB	147.16 (35.53)^{b,c,2}	108.04 (4.23)^{a,1}	CpTi1
SBE	170.65 (17.98)^{b,2}	101.38 (12.50)^{a,b,1}	
TiA	149.23 (42.85)^{b,c,3}	103.06 (9.79)^{a,b,2}	
TiMOD	97.75 (35.70)^{a,b,3}	82.25 (50.96)^{b,c,2}	CpTi2
TiSLA	84.38 (9.53)^{a,c,3}	87.30 (8.97)^{b,c,2}	
TiSLACT	113.99 (21.77)^{b,c,d,3}	99.82 (5.80)^{a,b,d,2}	
RA	54.41 (3.85)^{a,d,4}	60.49 (4.33)^{c,3}	
RMOD	81.94 (12.44)^{a,c,4}	75.56 (27.13)^{c,d,3}	TiZr
RSLA	38.22 (2.73)^{a,4}	91.58 (5.31)^{a,b,c,3}	
RSLACT	84.29 (3.12)^{a,c,4}	65.49 (39.77)^{c,3}	

NOTE: The different superscript letters within the same column indicate significant differences between all groups. Different numbers within the same column indicate significant differences between the surface of the same material (p<0.05)

Table 4.5 Representing the medians (range) of the hardness using micro-nanoindentation and nanoindentation

Group	Micro-nanoindentation	Nanoindentation	Material
	Hardness (GPa) Median (range)	Hardness (GPa) Median (range)	
CpC	2.01 (0.59)^{a,1}	2.87 (0.65)^{a,b,d,1}	
SB	2.66 (0.54)^{b,c,2}	3.22 (0.56)^{a,d,1}	CpTi1
SBE	2.06 (0.09)^{a,1}	2.89 (0.25)^{a,b,d,1}	
TiA	2.41 (0.78)^{a,b,c,3}	2.53 (0.16)^{a,b,2}	
TiMOD	2.05 (0.16)^{a,3}	2.31 (0.34)^{b,2}	CpTi2
TiSLA	2.03 (0.39)^{a,b,3}	2.20 (0.06)^{b,2}	
TiSLACT	2.46 (0.43)^{a,b,c,3}	2.34 (0.08)^{b,c,2}	
RA	2.59 (0.06)^{b,c,4}	3.09 (0.19)^{a,c,d,3}	
RMOD	2.74 (0.54)^{c,4}	3.20 (0.27)^{a,d,3}	TiZr
RSLA	1.98 (0.50)^{a,5}	3.36 (0.06)^{d,3}	
RSLACT	2.67 (0.18)^{c,4}	3.23 (0.45)^{a,d,3}	

NOTE: The different superscript letters within the same column indicate significant differences between all groups. Different numbers within the same column indicate significant differences between the surface of the same material (p<0.05)

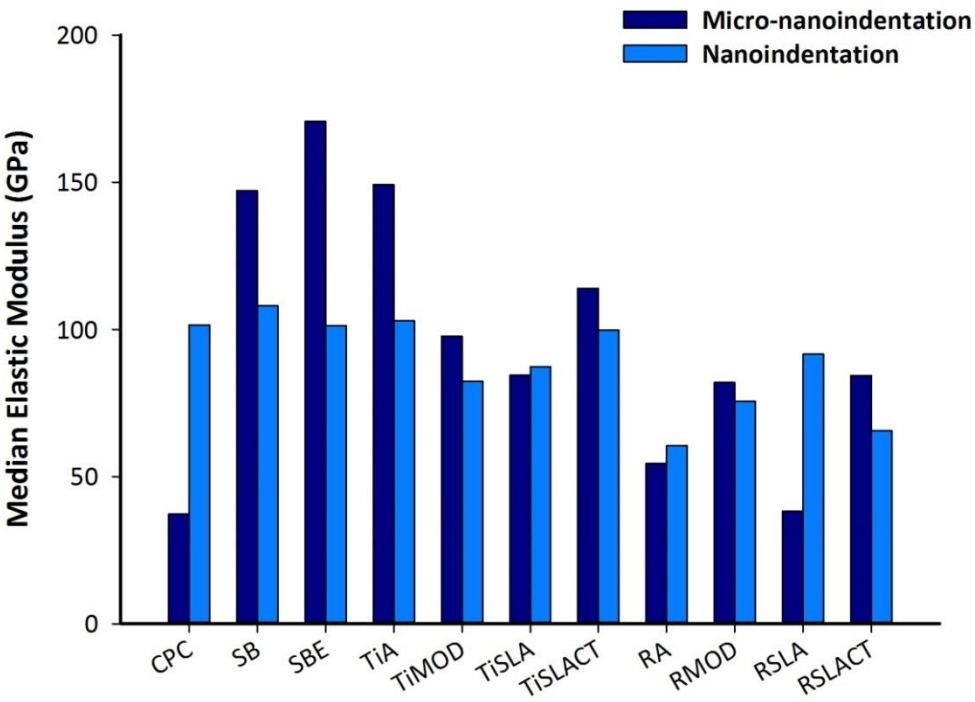

Figure 4.8 Bar chart representing the medians of elastic modulus for all groups using nano and micro-nanoindentation

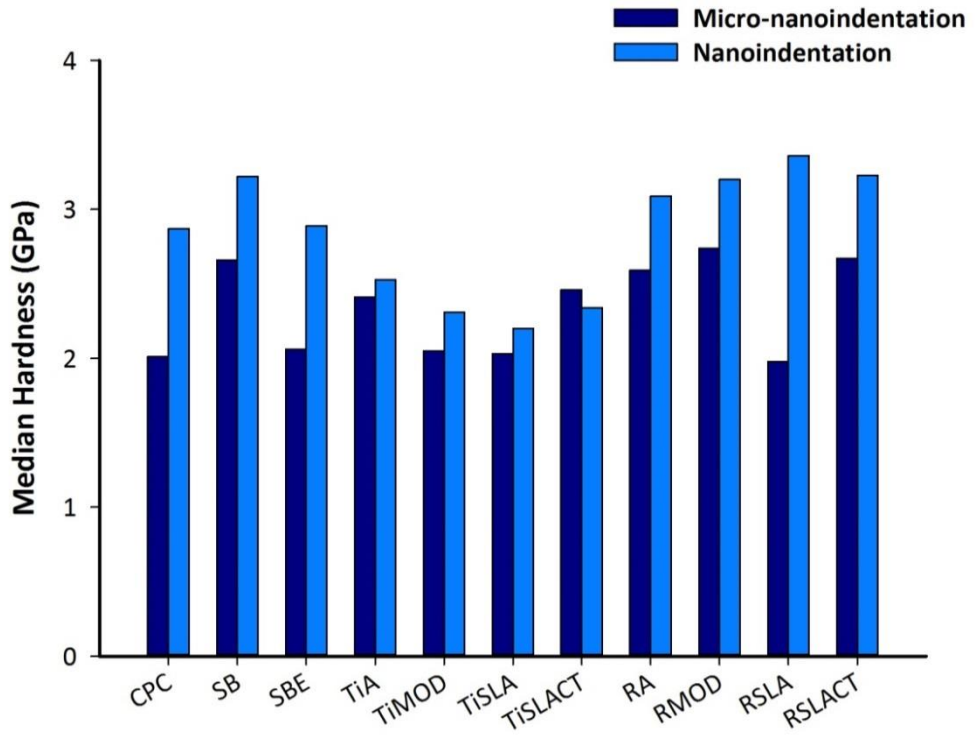

Figure 4.9 Bar chart representing the medians of hardness for all groups using nano and micro-nanoindentation

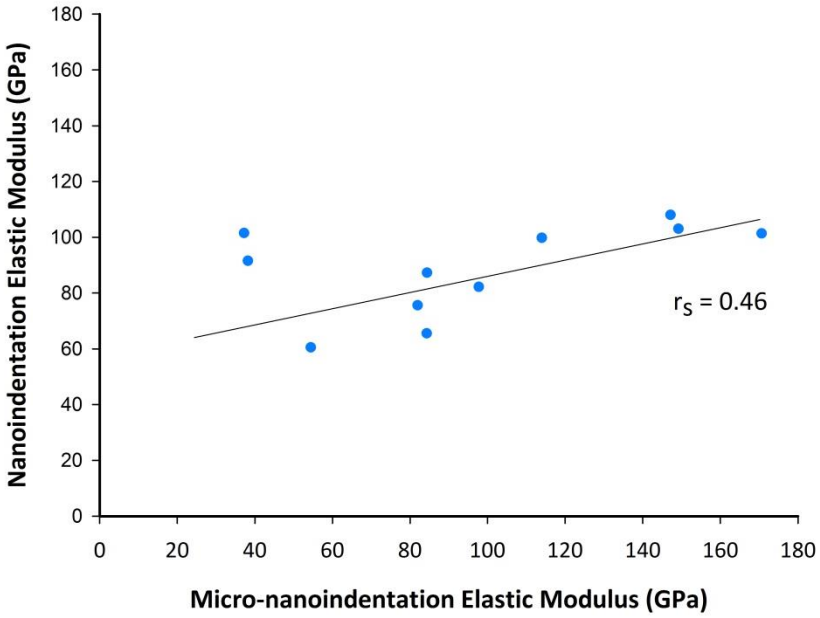

Figure 4.10 Scatterplot of the elastic modulus medians using micro-nanoindentation and nanoindentation

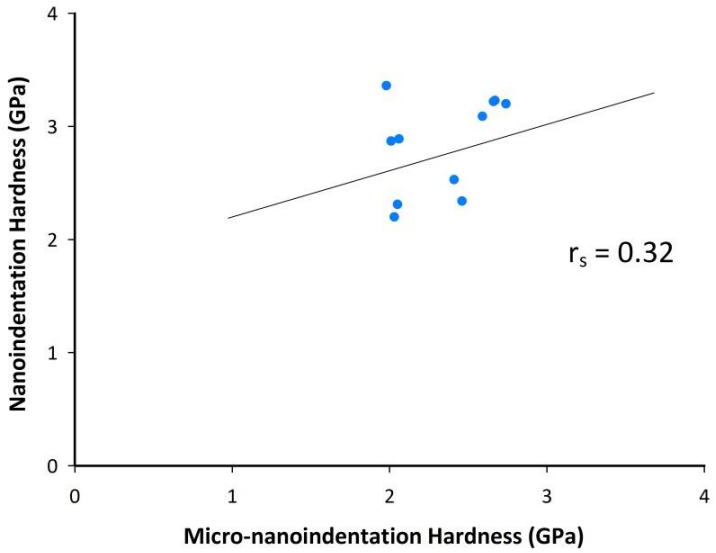

Figure 4.11 Scatterplot of the hardness medians using micro-nanoindentation and nanoindentation

4.6 Disscussion

The material used to fabricate a dental implant should possess a high strength (hardness) to withstand load and a lower elastic modulus, which is closer to bone, to avoid implant failure. Dai *et al.* (2016) demonstrated that low elastic modulus and variation in surface modification can effect implants osseointegration.

Nanoindentation

Nanoindentation is a well-established technique used in the field of biomaterials to quantitatively assess the mechanical properties of a given material (Schuh, 2006). Investigations into the mechanical properties of dental implant materials, especially hardness and elastic modulus, are a key element to predict their behaviour in the oral environment under load. Nanoindentation have been widely used due to their simplicity, reproducibility, and flexibility in obtaining a wide range of mechanical characteristics (Gouldstone *et al.*, 2007), as well as the other advantages such as a small amount of material being required for testing, with the ability to monitor the amount of load and displacement at all times. Furthermore, different experimental options can be selected (Oyen and Cook, 2009). For these reasons, this method was used to measure the sub-surface mechanical properties. Micro-nanoindentation was used in this study to provide better insight into the behaviour of the material, in order to investigate the mechanical properties at a deeper level than nanoindentation.

Samples in the form of discs were used for the mechanical testing, in line with other research using discs to assess the hardness and elastic modulus properties of dental implant alloys (Takeuchi *et al.*, 2003; Elias *et al.*, 2015; Dai *et al.*, 2016; Cordeiro *et al.*, 2018). Three samples were prepared and chosen for the mechanical testing based on

other research using nanoindentation (Takeuchi *et al.*, 2005; Cattani-Lorente *et al.*, 2014). The number of indents per sample used with nanoindentation studies vary in the literature from 5 indents (Takeuchi *et al.*, 2005; Sasani *et al.*, 2014; Mazur *et al.*, 2015; Cordeiro *et al.*, 2018), to 10 indents (Cáceres *et al.*, 2008), and 30 indents (Masouras *et al.*, 2008; El-Safty *et al.*, 2012a; Cattani-Lorente *et al.*, 2014; Grubova *et al.*, 2016). In the present study, after pilot testing and considering the dimensions of the samples, indentation force and leaving sufficient spacing between indents, it was decided to perform 30 indents for the nanoindentation and 5 indents for the micro-nano testing.

Recent research showed that different surface processing can alter the micro structure of the surface layer, which can consequently influence the hardness and elastic properties of the implant material (Grubova *et al.*, 2016; Cordeiro *et al.*, 2018), thus different surface modifications can produce different effects on the mechanical properties of the bulk material.

Every method has its limitation: in the case of depth sensing indentation, it was reported to be sensitive to noise and changes in room temperature (Fischer-Cripps, 2011), thus affecting the accuracy of measurement as a result of increased thermal drift due to the expansion or contraction of any component in the load frame (Trenkle *et al.*, 2010; Fischer-Cripps, 2011). The accuracy of nanoindentation testing is affected by many factors, such as the surface finish and setting the point of contact where the indenter head reaches the tested surface (Menčík, 2007). Thus, the accuracy of elastic modulus and hardness measurements could be smaller or larger than expected depending on whether the material tested is soft or hard (Menčík, 2007). All these factors could explain the difference seen in the data range for the different groups.

Nanoindentation studies on dental implants are mainly directed towards studying the change in elastic modulus and hardness of bone surrounding dental implants (Butz *et al.*, 2006; Anchieta *et al.*, 2013). Furthermore, some nanoindentation studies investigated the elastic modulus of zirconia dental implants after hydrothermal aging (Sevilla *et al.*, 2010).

The results of the present study showed that the manufacturer processing and different implant compositions had a significant effect on the sub-surface elastic modulus and hardness. Therefore, the null hypothesis was rejected. Several studies are available on CpTi, Ti alloys, Zr, and TiZr mechanical properties as a substrate material for dental implants (Niinomi, 1998; Niinomi, 2002; Niinomi, 2003; Niinomi, 2008; Niinomi *et al.*, 2012; Breme *et al.*, 2016; Lee *et al.*, 2016). However, insufficient data exist about different Ti and TiZr treated surfaces (Takeuchi *et al.*, 2003; De Souza *et al.*, 2005; Majumdar *et al.*, 2008; Medvedev *et al.*, 2016a). In addition, most of the studies were conducted on Ti alloys containing different concentrations of Zr, with no studies available on the TiZr alloy (Roxolid®) with the surface treatments tested in this study.

When comparing the hardness values of all groups, the TiZr alloy tended to have higher hardness values than the CpTi, with the exception of the CpTi1 sandblasted (SB). Statistical difference was also noted between the TiZr alloy and other CpTi groups. This is in agreement with a previous study that reported increased hardness with Zr availability (Ho *et al.*, 2008). Similarly, the elastic modulus of the TiZr alloy tended to be lower than the CpTi samples, which is consistent with other studies (Kirmanidou *et al.*, 2016; Lee *et al.*, 2016). The only exception was in the RSLA, which did not show any significant difference from the CpTi groups.

Some statistical differences were noted in (*E*) and (*H*) between the grade 2 CpTi supplied by the two different companies with different surfaces, which could be explained by the different surface modifications or different methods used when preparing the surfaces. However, no differences in elastic modulus were observed between the two CpTi types: acid-etched TiA and control CpC. This is in agreement with the study conducted by Takeuchi *et al.* (2003), which concluded no significant changes in the elastic modulus between acid-etched and non-treated Ti samples tested using nanoindentation. Furthermore, when comparing the CpC (with no treatment) to all the other treated CpTi groups (SB, SBE, TiA, TiMOD, TiSLA, and TiSLACT) no significant differences were noted in both elastic modulus and hardness.

To date, no data are available about the elastic moduli of the TiZr (Roxolid®) alloy obtained by nanoindentation. In this study, no statistical differences in the sub-surface elastic modulus and hardness values were noted between all surfaces made from the same alloy at the nano level. However, when comparing the TiZr with the Ti some significant differences were noted between the groups (different bulk material and with the same surface prepared by the same company). Additionally, when comparing the TiZr (R) with the CpTi1 and CpTi2 with different bulk material and surface, some significant differences were noted. This suggests that the substrate material could influence the sub-surface elastic modulus and hardness more than the surface modification. Therefore, the use of TiZr alloys in areas of insufficient bone width might be preferable to the CpTi implants in terms of elastic modulus and hardness.

Micro-nanoindentation

Generally, for the micro-nanoindentation study the control group (CpC) had the lowest elastic modulus across all tested groups. Furthermore, it was statistically different from the groups made from the same material and with different surface (SB and SBE) for elastic modulus, and different from SB for the hardness. The SB was significantly different from the SBE in the hardness property. The CpTi2 (Ti) and TiZr (R) groups did not show any statistical differences in the elastic modulus between different surface-modified groups with the same bulk material. The opposite was seen in the hardness measurements for the TiZr groups, as the RSLA group was statistically different from the other R groups.

When comparing the Ti and R groups with the same surface and different bulk materials, lower elastic modulus values were noted with the TiZr groups. This is in agreement with previous research highlighting the enhanced hardness and reduced elastic modulus associated with the addition of zirconia (Ho *et al.*, 2008; Saini *et al.*, 2015; Lee *et al.*, 2016). However, the only significant difference observed between the same surfaces and different alloys was between the RA and TiA for the elastic modulus, and a difference between the TiMOD and RMOD for the hardness.

Overall, the TiZr showed a tendency for decreased elastic modulus and increased hardness when the same modifications were applied, using both nanoindentation and micro-nanoindentation techniques. The average elastic modulus ranges for the CpTi, Ti, and TiZr groups using micro-nanoindentation were 37–170 GPa, 84–149 GPa, and 38–84 GPa, respectively. When compared to nanoindentation, the elastic modulus ranges for the same groups were 101–108 GPa, 82–103 GPa, and 60–91 GPa, respectively. The ranges for the hardness using micro-nanoindentation for all groups were 1–2 GPa,

whereas the nanoindentation hardness ranges for all groups were 2–3 GPa. These different ranges underscore, that different manufacturer processes and material composition could influence the sub-surface elastic modulus and hardness, which could be different at the nano and micro-nano levels. Nevertheless, when comparing the control CpC with no treatment to all the treated CpTi groups (SB, SBE, TiA, TiMOD, TiSLA, and TiSLACT) using micro-nanoindentation, it is evident that the same material composition can have different sub-surface elastic modulus and hardness when exposed to different manufacturing processes. However, this effect was not the same at the nano level, as no significant differences in elastic modulus (*E*) and hardness (*H*) were noted between CpC and the other CpTi-modified samples.

The results of this study have shown a variation in elastic modulus and hardness measurements across all groups, irrespective of the method used for testing. However, the variability in the results was more pronounced in the elastic modulus measurements. This variation in the hardness and elastic modulus measurements could be attributed to several factors: 1) the surface finish or the surface modification, 2) the oxide layer phase composition, 3) difference in the machine used for measurement, or 4) the bulk material microstructure characteristics (Han *et al.*, 2014; Medvedev *et al.*, 2016a; Medvedev *et al.*, 2016b; Cordeiro *et al.*, 2018). A previous nanoindentation study showed that elastic modulus varies as a result of different surface modification and phase composition (Majumdar *et al.*, 2008).

The only studies available that investigated the hardness and elastic modulus of surface-modified dental implants using nanoindentation were performed on hydroxyapatite-coated dental implants (Gross *et al.*, 2010; Saber-Samandari *et al.*, 2011). These showed that lower hardness values were obtained from nanoindentation testing in comparison to

microhardness; this is in contrast to the present study, as the micro-nanoindentation gave slightly lower values for hardness for most of the groups when compared to nanoindentation. For the elastic modulus the opposite trend was noted as higher values were associated with most of the groups. Possibly, this variation is due to the higher force used with the micro-nanoindenter that penetrates deeper into the surface, whereas the nanoindenter uses less force and measures the first nanometres of the material. Thus, it could be concluded that the changes in the sub-surface bulk mechanical properties due to different implant compositions and/or the manufacturer processes are different at the nano and micro-nano levels. In addition, the micro-nanoindenter tester could be considered as a measuring tool falling between the microhardness tester and the nanoindenter. However, further assessment of the indents over larger areas is needed to confirm this conclusion.

Although the correlation is weak, the scatter plots in Figures 4.10 and 4.11, and values for elastic modulus and hardness are comparable. Thus, demonstrating that the elastic modulus and hardness measured using both techniques have a trend to increase and decrease in the same direction, and if the sample size is increased the correlation might improve.

4.7 Conclusions

Within the limitations of this study, the following conclusions were drawn:

- Different manufacturer processes had no significant influence on the sub-surface elastic modulus within the same bulk material composition at both the nano and micro-nanometre levels.
- Variation in manufacturer processes within the same material could affect the hardness of the bulk material at the micro-nano level, but not at the nano level.
- The variation in material composition alone or in combination with different manufacturer processes might influence the sub-surface elastic modulus and hardness of the bulk material at both the nano and the micro-nanometre levels.
- Titanium-zirconia alloy showed a tendency to increase the hardness and decrease the elastic modulus compared to commercially pure titanium, irrespective of the mechanical testing method used.

Chapter 5

Surface Characterisation of Bioceramic-Treated Implant Surfaces

5.1 Introduction

Peri-implantitis is one of the most common inflammatory conditions leading to implant failure, which is mainly caused by bacterial colonisation of the peri-implant site (Pérez-Chaparro *et al.*, 2016). The mechanical removal of the adherent bacterial biofilm is essential to resolve the inflammatory condition when treating peri-implantitis (Lindhe and Meyle, 2008; Subramani and Wismeijer, 2012). The optimal treatment of peri-implantitis is to detoxify and create a surface that can attract the osteoprogenitor cells in order to re-osseointegrate. Air abrasion with abrasive powders is one of the effective mechanical methods used to decontaminate the infected implant surface during the management of peri-implantitis (Zabtotsky *et al.*, 1992; Duarte *et al.*, 2009a; Tastepe *et al.*, 2012; Schwarz *et al.*, 2015a). After air abrasion, the surface morphology and surface characteristics will change depending on the type of powder used, which could influence the cellular interaction at the bone-implant interface (Schwarz *et al.*, 2009a; Tastepe *et al.*, 2013; John *et al.*, 2016). In addition, air abrasion with CaP (HA) particles can alter the surface roughness of previously infected titanium surfaces, leaving behind some powder deposits (Tastepe *et al.*, 2013; Tastepe *et al.*, 2018b).

The clinical success of dental implants is strongly related to the surface characteristics, including the surface morphology, topography and chemistry, and its interaction with osteoblastic cells (Saghiri *et al.*, 2016). Thus, it is vital to assess the change in surface characteristics that could be associated with air abrasion and bioceramic abrasives on implant surfaces. Several studies demonstrated the ability of a bioceramic apatite abrasive as a blasting material to change the implant surface characteristics (Koller *et al.*, 2007; O'Sullivan *et al.*, 2011; Kulkarni Aranya *et al.*, 2017). Although air abrasion with

bioceramic powders has not yet been applied clinically, *in-vivo* studies have shown that the cellular response and biocompatibility of titanium surfaces could be enhanced by blasting CaP-based bioceramics (Piattelli *et al.*, 2002; Citeau *et al.*, 2005; Le Guehennec *et al.*, 2008; O'Sullivan *et al.*, 2011; Tastepe *et al.*, 2018a; Tastepe *et al.*, 2018b). However, none of these studies assessed or compared the effect of air abrasion with a bioceramic abrasive on TiZr and CpTi with different surfaces.

5.2 Aim of the study

The aim of this study was to use air abrasion to deposit a bioceramic powder (with a possible osseoconductive effect) on implant substrates with different surface characteristics, followed by the surface characterisation of the resulting surfaces, in order to investigate the potential to create an alternative bioactive surface that could enhance the surface characteristics and tissue repair for the treatment of peri-implantitis. The objectives were as follows:

- To evaluate the influence of air abrasion with bioceramic abrasives on the surface characteristics.
- To employ a 3D profilometer to measure the surface roughness of the bioceramic air-abraded samples.
- To assess and compare the surface and elemental differences between treated samples with different materials, surfaces and powder compositions using SEM-EDS analysis.

The null hypotheses were a) air abrasion with bioceramic abrasives of titanium and titanium-zirconia surfaces has no effect on its surface characteristics, and b) using different powder composition has no effect on the surface characteristics.

5.3 Materials and methods

5.3.1 Substrate samples and surfaces

The tested materials and surfaces were from the same samples detailed in Chapter3 (§ 3.3.1), namely: CpTi1: control (CpC), sandblasted (SB), and sandblasted acid etched (SBE); CpTi2: (TiSLACT) and TiZr Roxolid® (RSLACT). Three samples from each group (n=3) were treated with air abrasion**,** with two different powders.

5.3.2 Apatite abrasive (bioceramic) powders

Two apatite abrasive powders of sintered CaP (particle size: 53 µm) were used to treat the samples. The chemical formulas of the powders were:

1. 95 % hydroxyapatite (HA), Ca_{10} $(PO_4)_6(OH)_2$ mixed with 5 % CaO (MCD) (Hitemco Medical Applications, Inc., USA)
2. 90 % hydroxyapatite (HA) (Ca_{10} $(PO_4)_6(OH)_2$ mixed with 10 % CaO (MCD) (Hitemco Medical Applications, Inc., USA)

These samples will be referred to as 95 % HA/5 % CaO and 90 % HA/10 % CaO.

Before blasting the samples, the powders used in this study were analysed using SEM-EDS.

5.3.3 Air abrasion experimental setting

All discs were rinsed with deionised water and dried with an air dryer before air abrasion. Bioceramic powders were deposited by blasting them onto the samples. The PrepAir™ air abrasion unit (Danville, CA, USA) connected to an air compressor was used for blasting. In order to simulate the clinical situation, the distance between the spraying nozzle and the sample was standardised to be 1–2 mm. This was done by clamping the air abrasion unit at two points: one at the body and the other at the tip. The sample and the abrasion unit were all housed in a plastic box. The blasting was performed using a nozzle (tip size 0.48 mm x 80˚) at 0.41 MPa pressure, as recommended by the manufacturer. After pilot testing, the spraying time was standardised to be 2 minutes over the whole sample. The custom made experimental setup for the air abrasion process is presented in Figure 5.1.

The surface and chemical characterisation were examined using an optical profilometer and SEM-EDS.

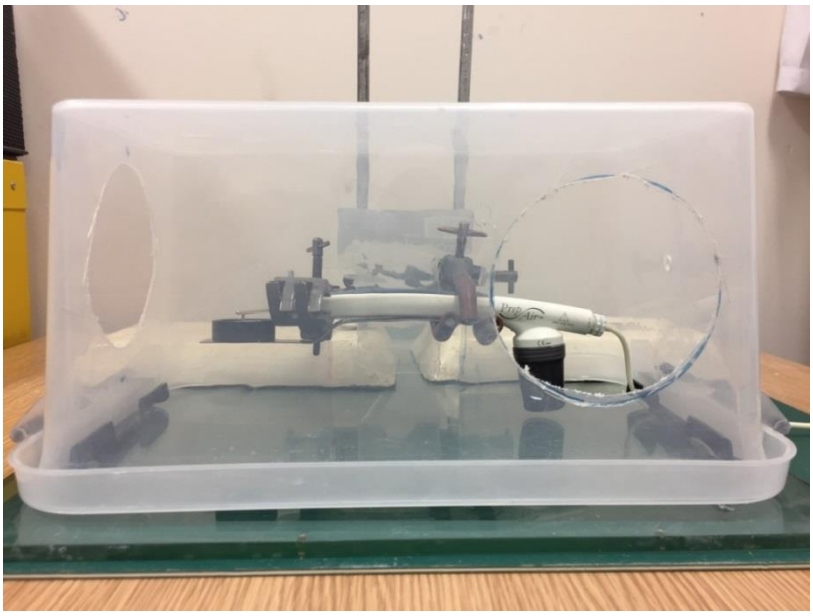

Figure 5.1 The experimental setup for air abrasion

5.3.4 Surface roughness

The surface topography of the treated samples was examined using an optical profilometer (Talysurf CLI 1000, Taylor Hobson Precision, UK) previously described in Chapter 3 (§ 3.3.2). The same settings described in Chapter 3 (§ 3.3.3) were applied. Three samples from each group (n=3), with 3 randomly selected areas per sample were tested.

5.3.5 Scanning electron microscopy and energy dispersive spectroscopy

A scanning electron microscope (FEI Quanta 650 FEG) equipped with an energy dispersive spectroscope (SEM-EDS, FEI Quanta 650 FEG, Oxford Instruments, UK) (Figure 5.2) was used in this study. Four samples (n=4) comprising 1 control (no treatment) and 3 treated samples from each group per powder were used for the SEM-EDS surface characterisation.

Figure 5.2 The SEM-EDS, FEI Quanta 650 FEG

5.3.5.1 Experimental setting

The treated samples were mounted on aluminium stubs and loaded on the metal holder inside the machine (Figure 5.3). The samples were tested at different levels of magnification at an accelerated voltage of 20 kV and spot size of 3.5 nm, using both high and low vacuum modes. The samples viewed under high vacuum mode were coated with carbon at approximately 10 nm thickness. A representative sample from each group was randomly selected for microphotography using both the secondary electron and backscattered modes.

The elemental analysis was performed using energy dispersive spectroscope (EDS) analysis software (Aztec Software, Ver.3.1) provided with the device for point analysis. All EDS analysis was performed on the samples as received, with no conductive coatings. Four random points from the tested areas were selected for the analysis.

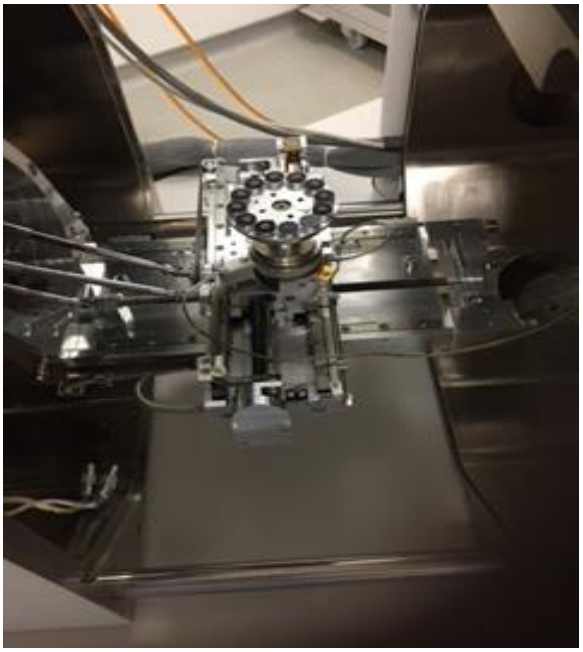

Figure 5.3 Samples mounted on the machine holder

5.4 Data analysis

All data collected were entered into a statistical software package (SPSS® Ver.23, SPSS Inc., Chicago, IL) for analysis. The test of normality revealed that data were not normally distributed, and therefore a non-parametric test was used. The Kruskal–Wallis test with multiple pairwise comparisons was used to compare the medians with the level of significance set to p= 0.05.

- Surface roughness data

  The surface roughness measurements S_a, S_v, S_p, R_a, R_v, and R_p were chosen for analysis. The means of the 3 samples per group were used for the statistical analysis.

- Elemental analysis data

  The element weight percentages of Ti, Ca, and P were recorded. The means from the 4 measurements for each sample were used for the statistical analysis.

5.5 Results

5.5.1 SEM-EDS

Control samples

Representative SEM images of the samples before treatment are presented below in Figures 5.4 and 5.5.

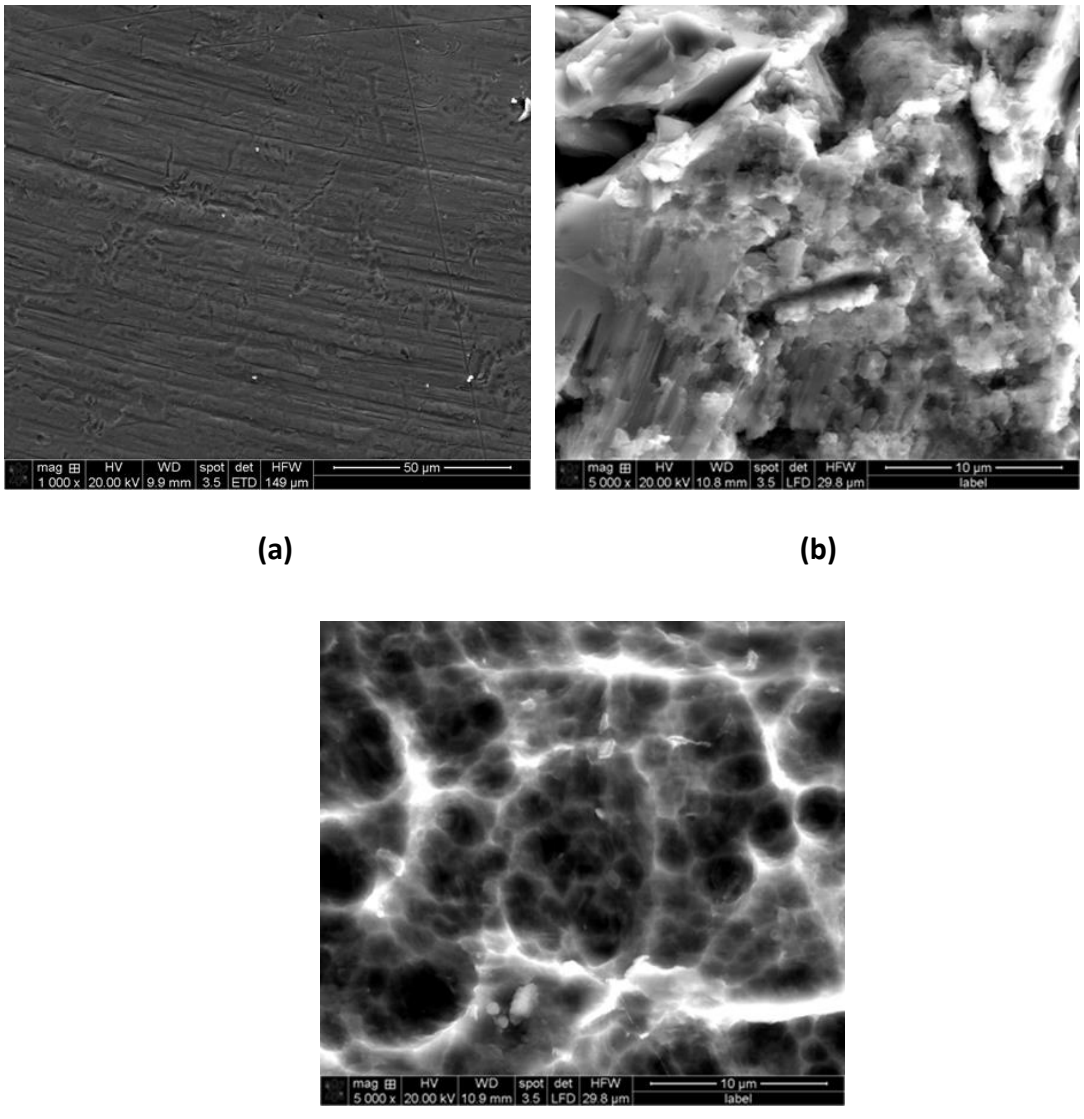

(a) **(b)**

(c)

Figure 5.4 Representative SEM images of the commercially pure titanium samples before treatment: a) CpC at 1,000x magnification, b) SB at 5,000x magnification, and c) SBE at 5,000x magnification

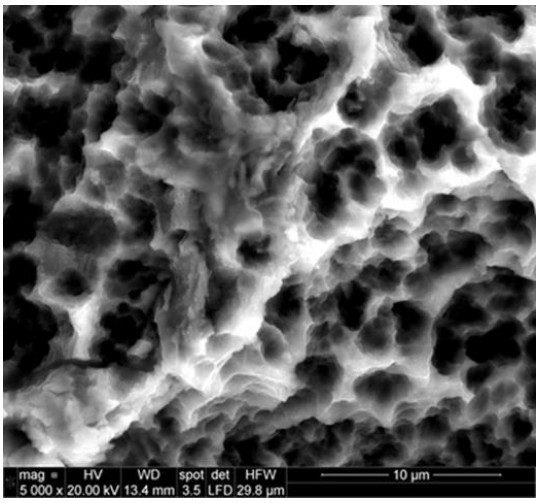

(a)

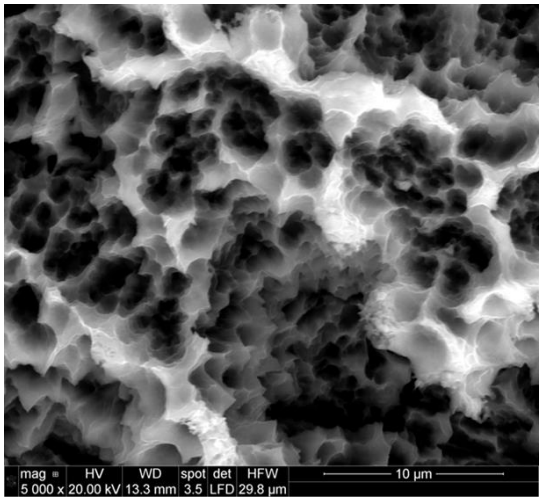

(b)

Figure 5.5 Representative SEM images at 5,000x magnification of the a) TiSLACT and b) RSLACT samples before treatment

The EDS analysis of the control samples (no treatment) for CpC, SB, SBE, TiSLACT, and RSLACT showed the predominance of Ti and O as the main elements. Other trace elements were present at less than 1 % (carbon, magnesium, aluminium, vanadium, and silicon). Representative images of the control sample EDS spectrum are presented in Figure 5.6. A small peak of zirconia was seen in the compositional analysis of the RSLACT samples.

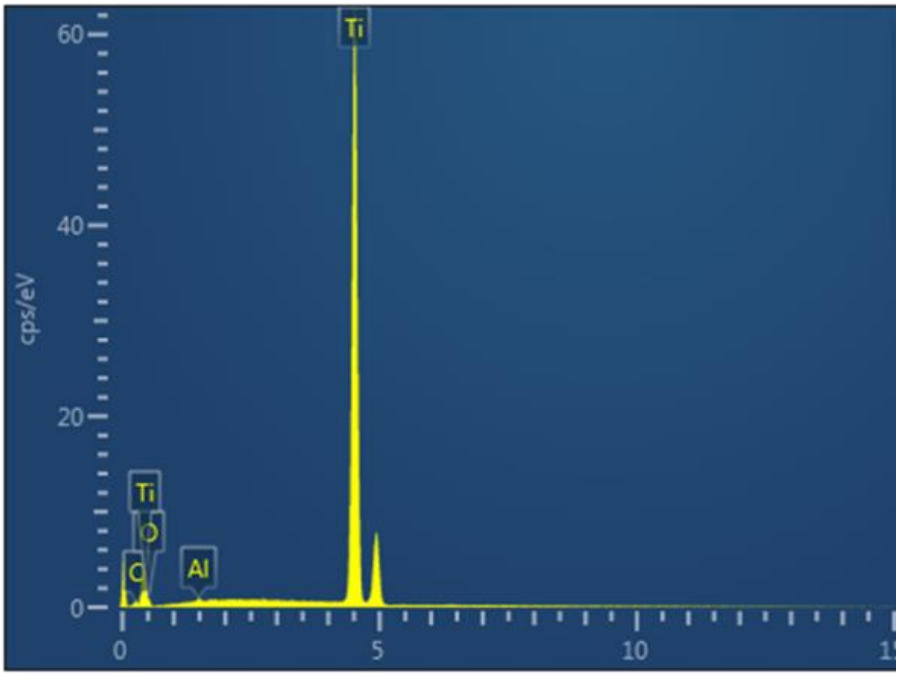

Figure 5.6 Representative EDS spectrum of SBE control (no treatment) sample showing the peaks of titanium as the main element

Powder analysis

The elemental composition of the bioceramic powders in atomic percentages (at %) using EDS analysis is presented in Table 5.1. The two powders were mainly composed of O, Ca, and P, with some traces of Mg, Al, and Si (less than 1 %). Representative SEM images of the bioceramic powders are presented in Figure 5.7. The XRD pattern (provided by the company) of the powders as shown in Figures 5.8 and 5.9 revealed narrow well- defined peaks of HA powders and CaO, indicating their high crystallinity.

Table 5.1 Elemental composition (at %) of the bioceramic powders obtained by EDS analysis with Ca/P ratios

Powder	O at %	Ca at %	P at %	Ca/P ratio
95 % HA/5 % CaO	63.76	22.79	13.45	1.69
90 % HA/10 % CaO	78.14	15.59	6.26	2.49

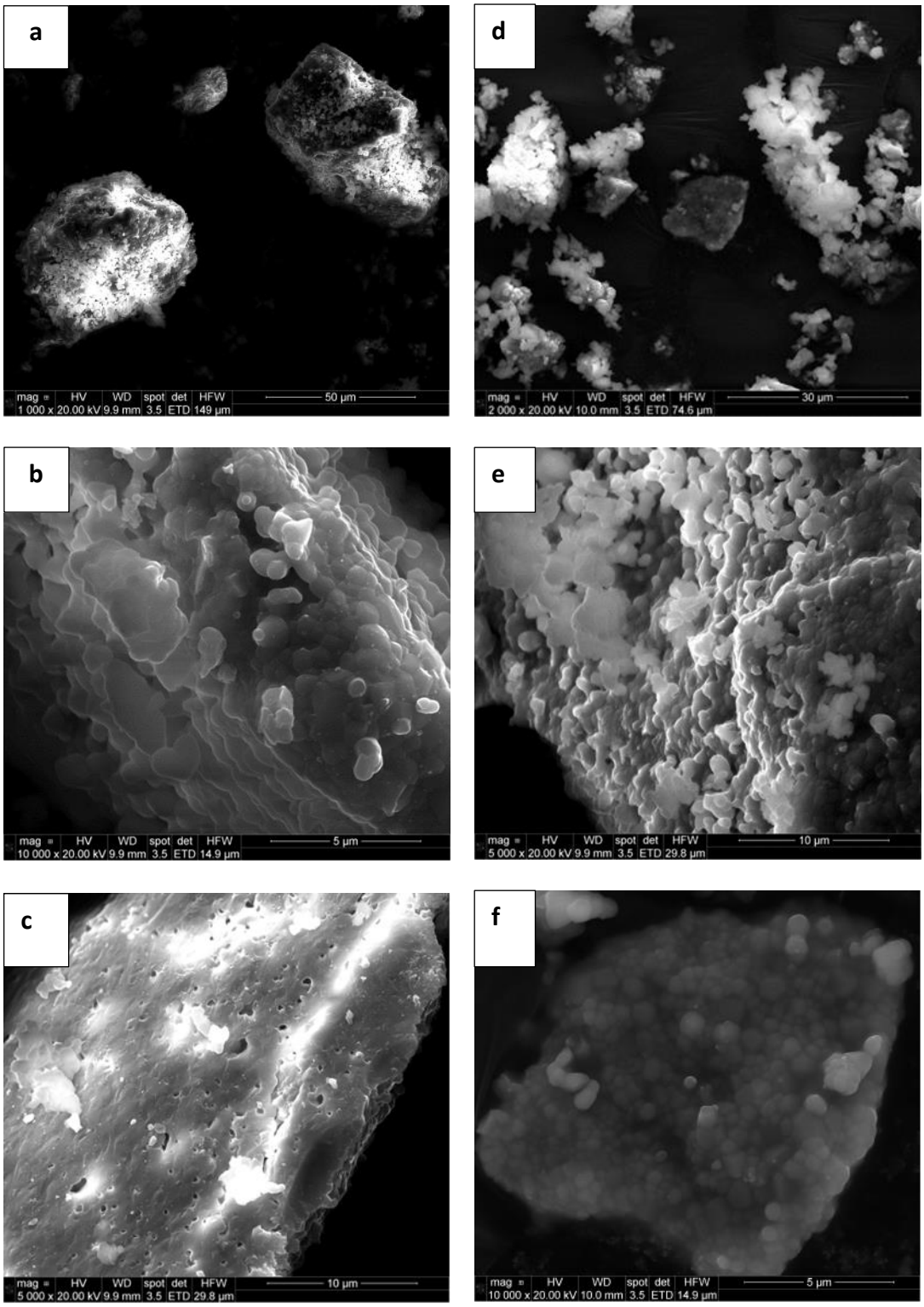

Figure 5.7 SEM images of the bioceramic powders at different magnifications: (a) 1,000x, (b) 50,000x, (c) 5,000x representing the 95 % HA/5 % CaO powder, (d) 2,000x, (e) 5,000x, and (f) 10,000x representing the 90 % HA/10 % CaO powder

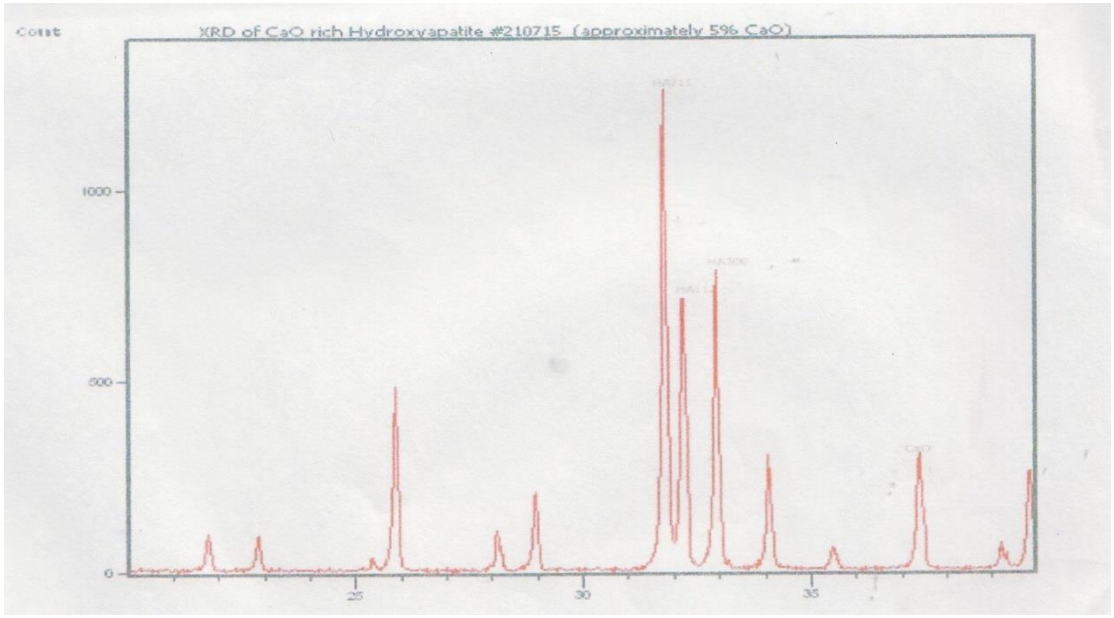

Figure 5.8 X-ray diffraction image of the 95 % HA/5 % CaO powder (image courtesy of Hitemco Medical Applications Inc.)

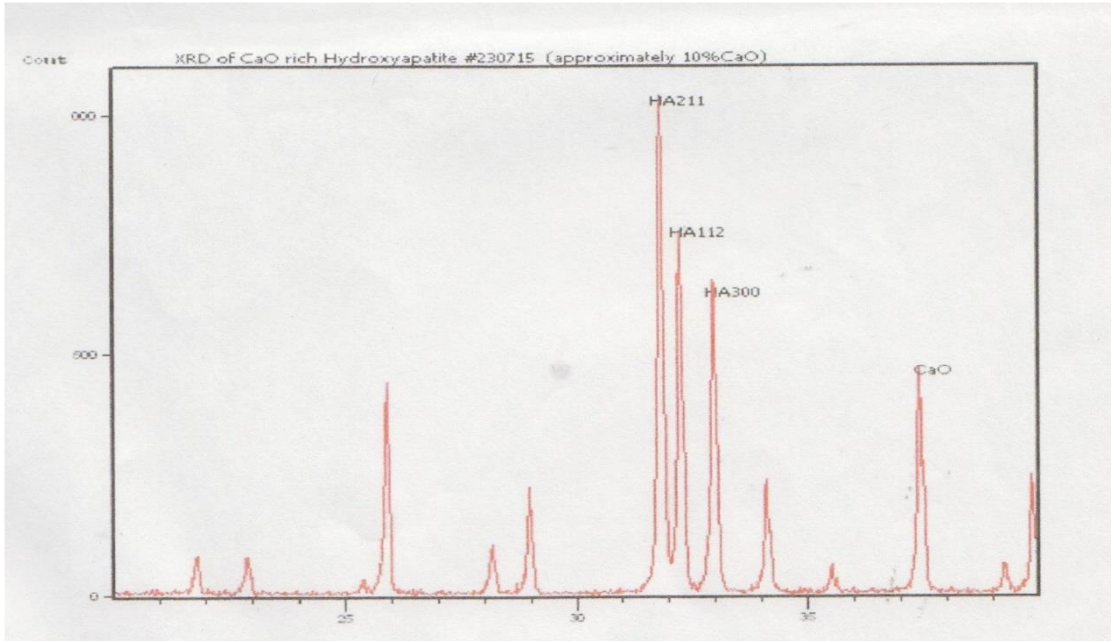

Figure 5.9 X-ray diffraction image of the 90 % HA/10 % CaO powder (image courtesy of Hitemco Medical Applications Inc.)

Air abrasion sample analysis

Representative SEM images of the treated samples are shown below (Figures 5.10–5.12). The images demonstrate that the samples were covered by the bioceramic powders. A non-uniform distribution of the bioceramic powders was noted on the surface layer of the samples.

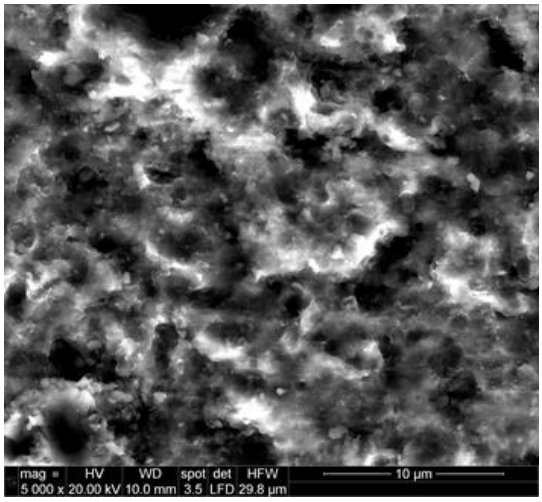

(a)

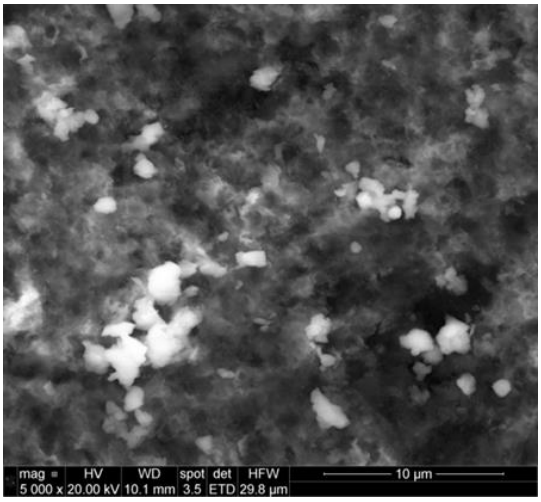

(b)

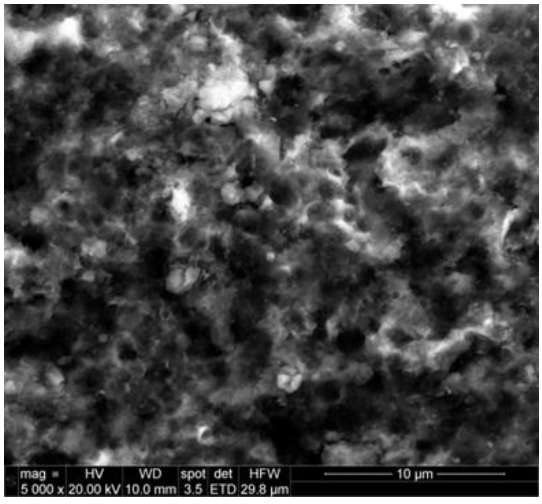

(c)

Figure 5.10 Representative SEM images at 5,000x magnification of the commercially pure samples: a) CpC, b) SB, and c) SBE treated with 95 % HA/5 % CaO

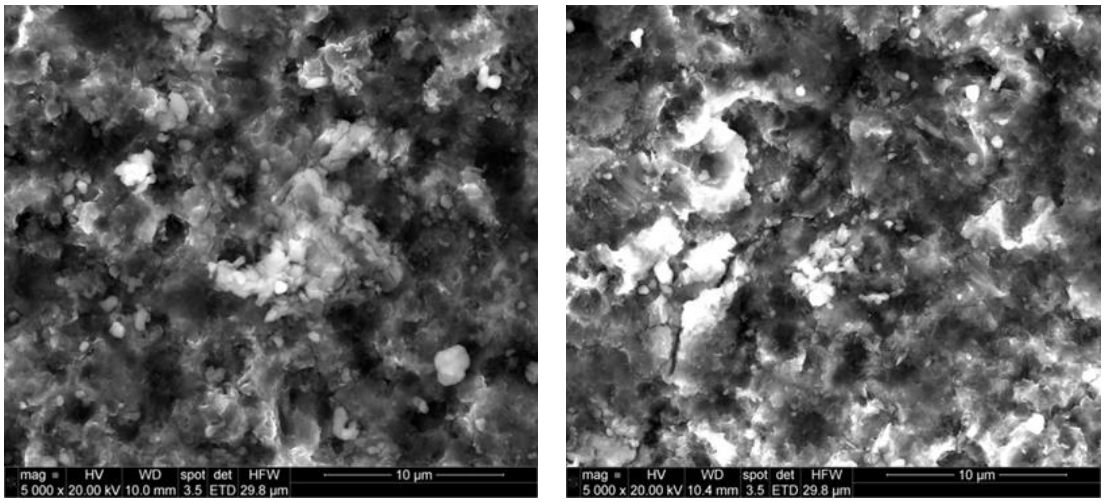

(a) **(b)**

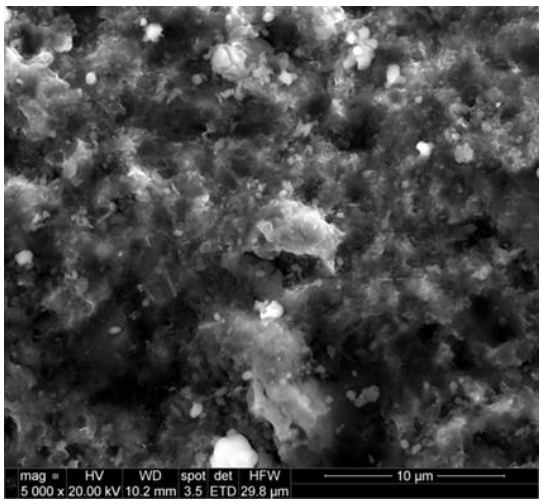

(c)

Figure 5.11 Representative SEM images at 5,000x magnification of the commercially pure samples: a) CpC, b) SB, and c) SBE treated with 90 % HA/10 % CaO

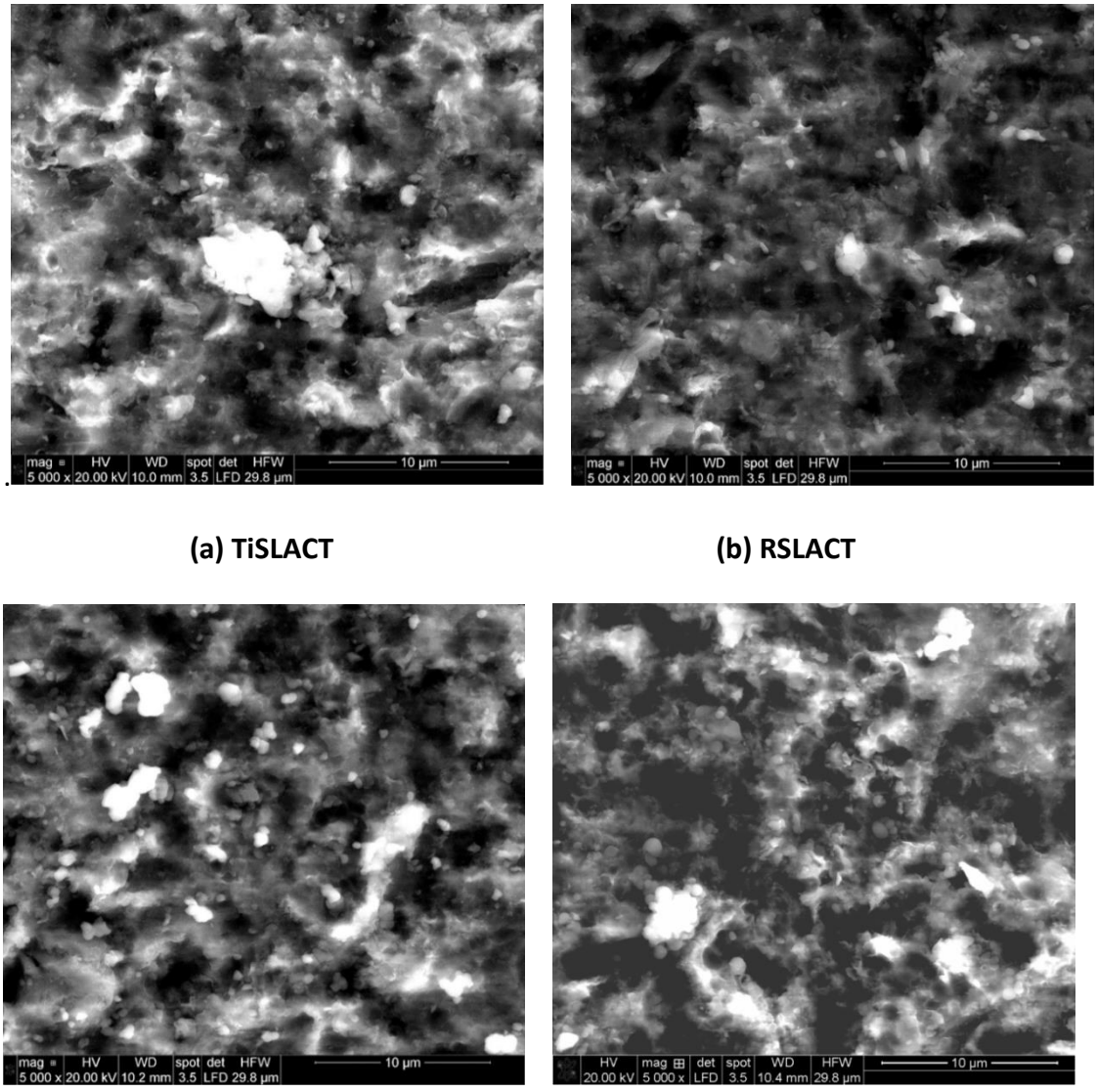

(a) TiSLACT **(b) RSLACT**

(c) TiSLACT **(d) RSLACT**

Figure 5.12 Representative SEM images of the treated samples at 5,000x magnifications: a) TiSLACT, b) RSLACT treated with 95 % HA/5 % CaO, c) TiSLACT, and d) RSLACT at 20,000x magnification treated with 90 % HA/5 % CaO

Representative mapping of the bioceramic treatment distribution of each powder is presented in Figures 5.13 and 5.14. These images highlight the qualitative distribution of the elements within the samples that were detected by the EDS analysis. From these maps, it can be observed that the Ca and P were detected and distributed all over the sample, confirming that the powders are present on the surface.

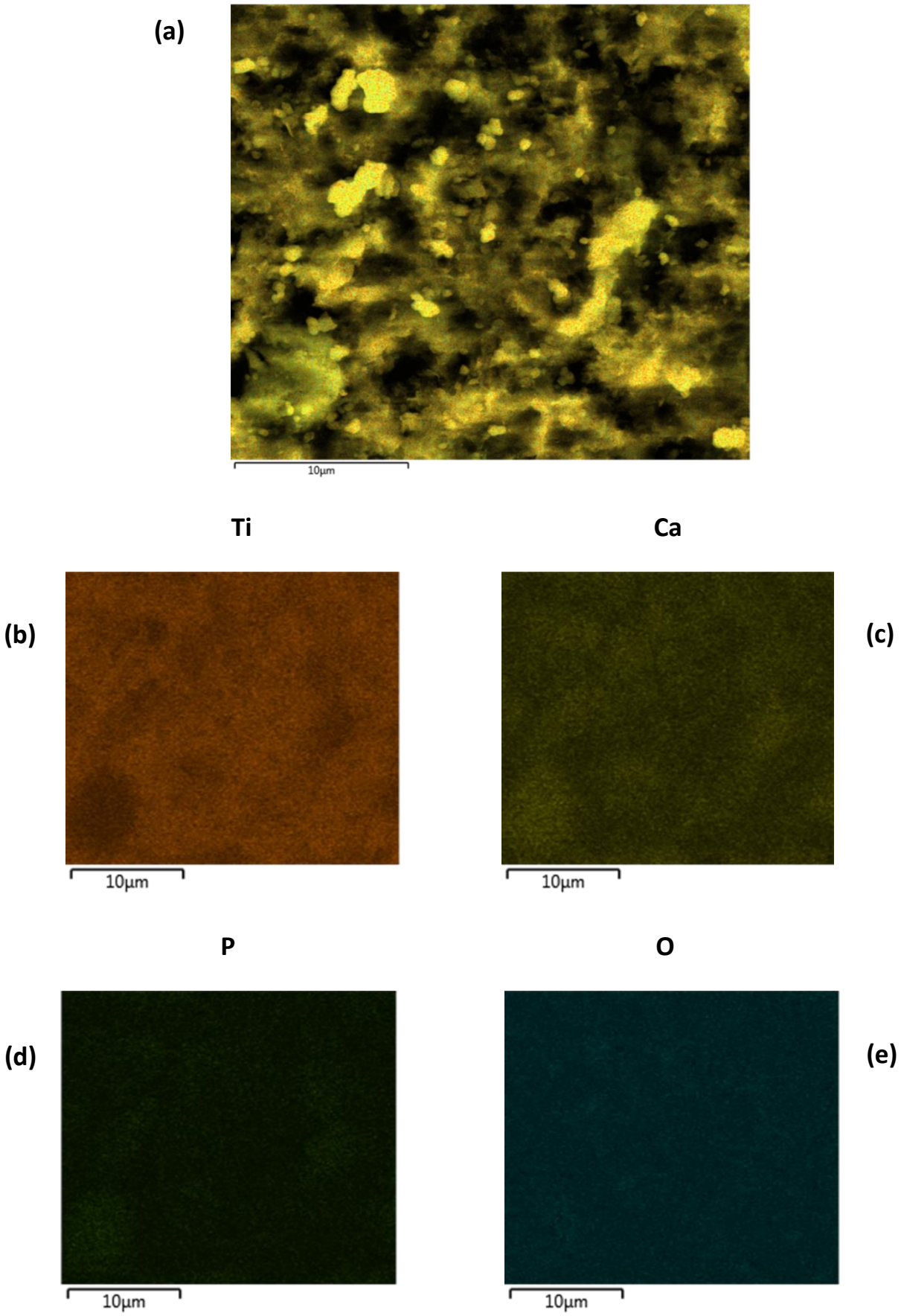

Figure 5.13 Representative map of the bioceramic elemental distribution on the TiSLACT surface treated with 90 % HA/10 % CaO: a) representing the layered SEM image, and b) titanium, c) calcium, d) phosphate, e) oxygen

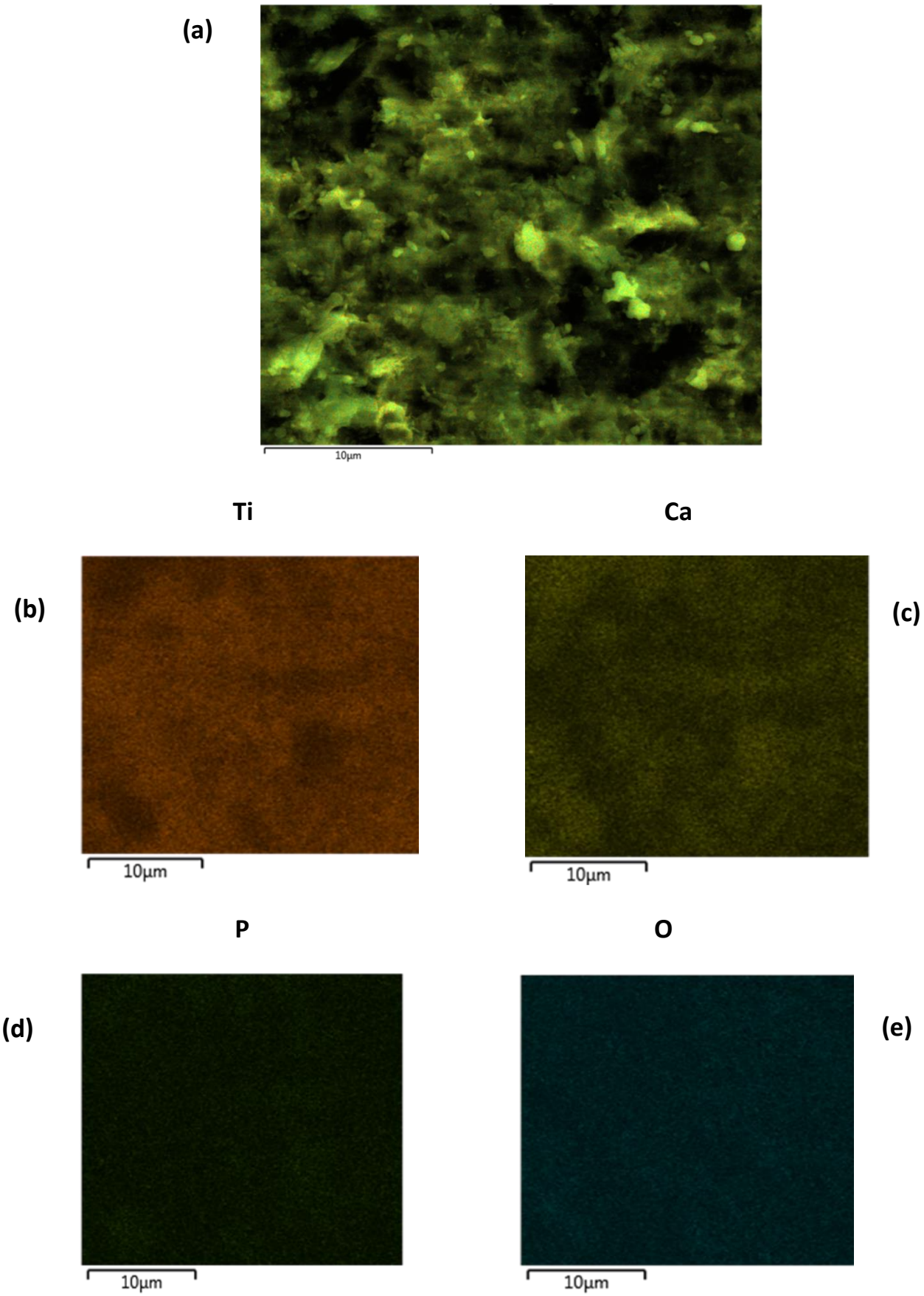

Figure 5.14 Representative map of the bioceramic elemental distribution on the RSLACT surface treated with 95 % HA/5 % CaO: a) representing the layered SEM image, and b) titanium, c) calcium, d) phosphate, e) oxygen

After applying the bioceramic treatment, Ca and P peaks appeared on the EDS spectrum as shown in the representative spectrums (Figures 5.15 & 5.16). EDS elemental analysis of the samples treated with 95 % HA/5 % CaO and 90 % HA/10 % CaO showed different median calcium and phosphate ratios on the surfaces (Tables 5.2 & 5.3). The median weight percentages (wt %) and ranges of Ca, P, and Ti from the EDS analysis for all groups treated with the different powders (95 % HA/ 5% CaO, 90 % HA/ 10 % CaO) are presented in Tables 5.2 and 5.3, and the median values presented graphically in Figures 5.17 and 5.18. There were no significant differences in the Ca and P wt % between all groups and powders 95 % HA/5 % CaO and 90 % HA/10 % CaO (p= 0.14, 0.18, and p= 0.15, 0.12, respectively).

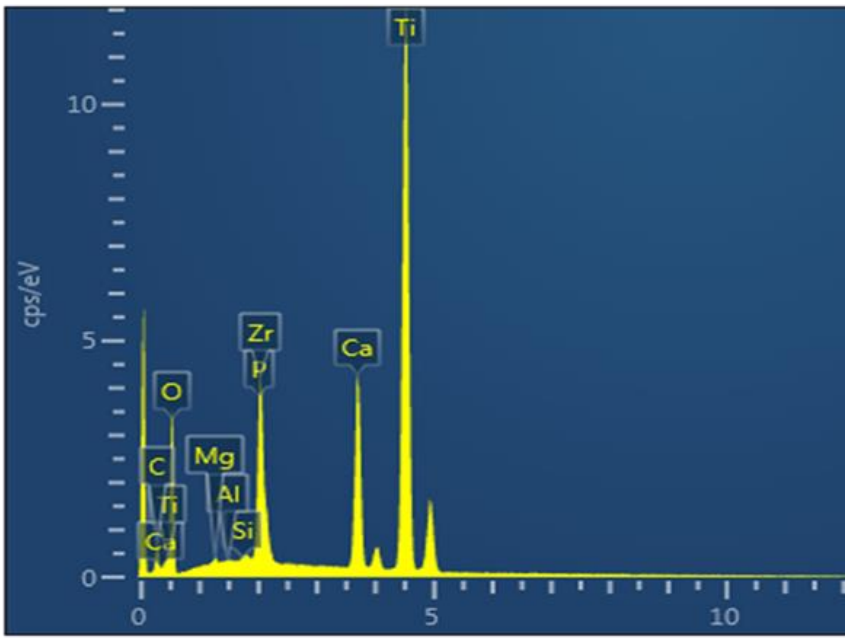

Figure 5.15 Representative EDS spectrum of the RSLACT sample treated with 95 % HA/5 % CaO showing the Ca and P peaks

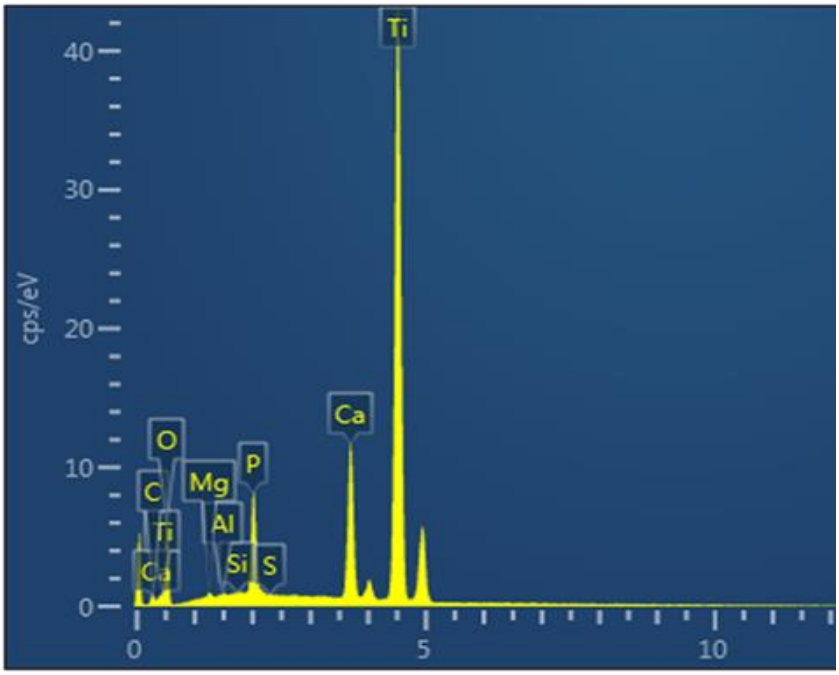

Figure 5.16 Representative EDS spectrum of the TiSLACT sample treated with 90 % HA/10 % CaO showing the Ca and P peaks

Table 5.2 Medians and range of the elemental (wt %) of titanium, calcium, phosphate and calcium phosphate ratios of the samples treated with 95 % HA/5 % CaO

Group treated 95 % HA/5 % CaO	Titanium Median wt % (range)	Calcium Median wt % (range)	Phosphate Median wt % (range)	Ca/P ratio
CpC	55.53 (33.02)	24.50 (17.40)	7.99 (5.20)	3.06
SB	57.31 (9.79)	8.33 (11.44)	2.51 (1.56)	3.31
SBE	72.04 (10.53)	13.18 (4.65)	4.70 (1.61)	2.80
TiSLACT	47.31 (19.66)	11.88 (8.20)	3.61 (3.23)	3.29
RSLACT	50.32 (10.13)	8.45 (2.58)	2.41 (1.38)	3.50

Table 5.3 Medians and range of elemental (wt %) of the titanium, calcium, phosphate, and calcium phosphate ratios of the samples treated with 90 % HA/10 % CaO

Group treated 90 % HA/10 % CaO	Titanium Median wt % (range)	Calcium Median wt % (range)	Phosphate Median wt % (range)	Ca/P ratio
CpC	76.74 (22.34)	11.43 (13.74)	4.62 (4.86)	2.47
SB	72.74 (14.31)	11.50 (6.69)	3.01 (4.05)	3.82
SBE	69.95 (17.24)	14.65 (9.56)	6.15 (4.06)	2.38
TiSLACT	60.98 (10.85)	7.90 (3.86)	3.18 (0.72)	2.48
RSLACT	50.89 (8.90)	8.65 (4.59)	2.78 (1.76)	3.11

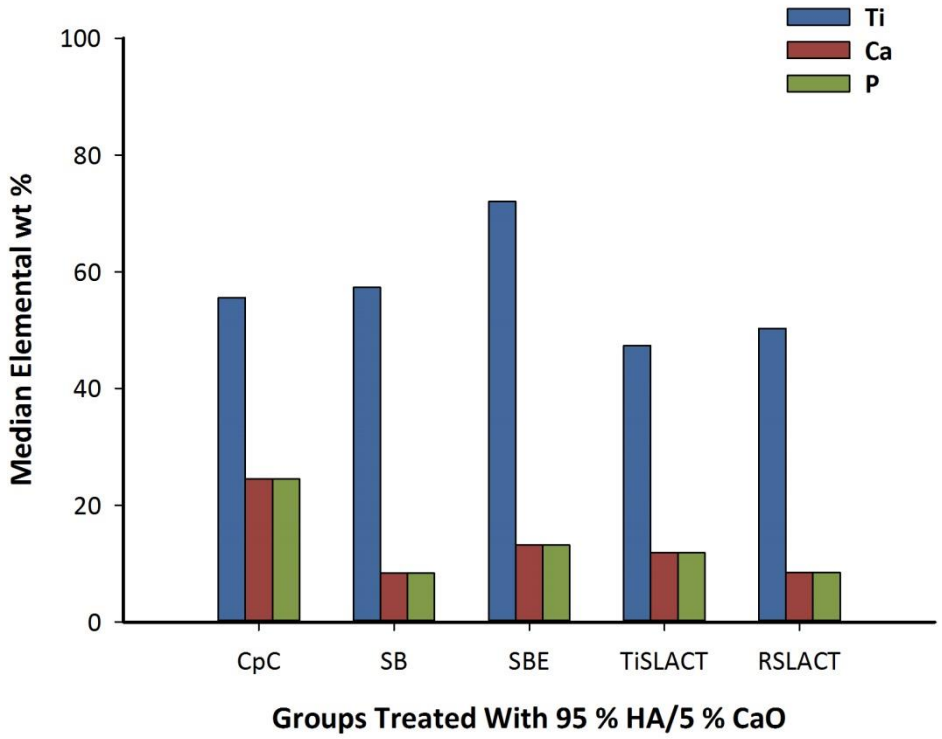

Figure 5.17 Bar chart for the median of the elemental wt % of the groups coated with 95 % HA/5 % CaO

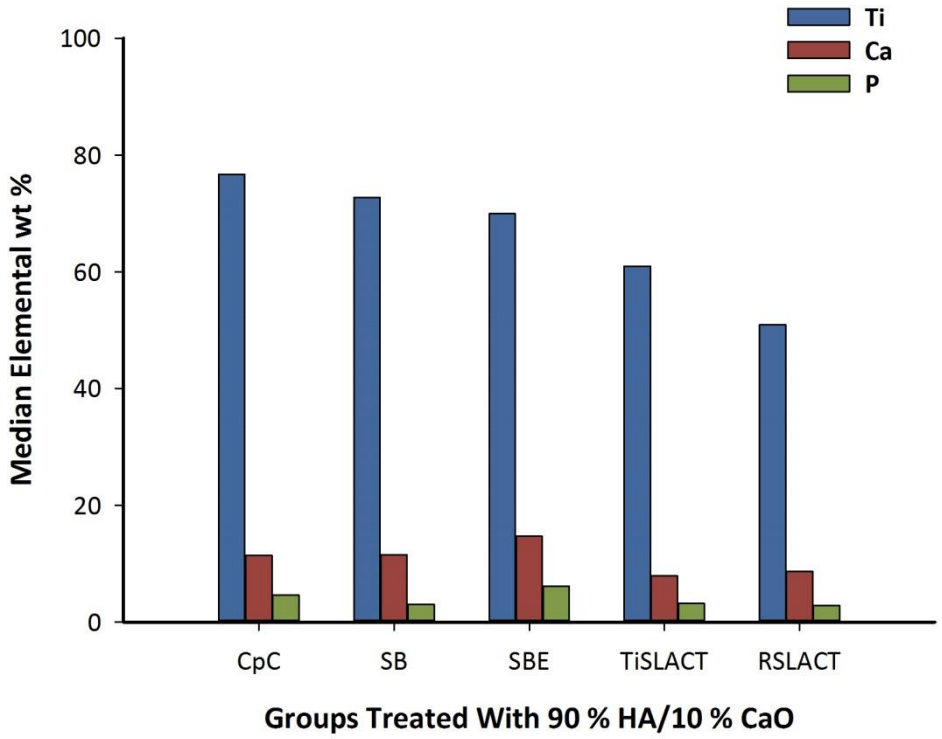

Figure 5.18 Bar chart for the medians of the elemental wt % of the groups coated with 90 % HA/10 % CaO

5.5.2 Surface roughness

The surface roughness medians and ranges for the samples treated with 95 % HA/5 % CaO are summarised in Table 5.4 and Figure 5.19. The highest S_a was recorded for TiSLACT (5.80 µm), whereas the lowest S_a was recorded for the SBE (3.24 µm). The highest S_p, was recorded for the CpC (58.03 µm), whereas the lowest S_p was recorded for the RSLACT (16.53 µm). For the S_v measurements, the TiSLACT group showed the highest value of 22.23 µm, while the lowest S_v value of 9.97 µm was recorded for CpC.

There was no statistically significant difference in the S_a, S_v, R_a, and R_v measurements across all material groups. The only statistically significant differences between the material groups were found in the S_p and R_p parameters (p= 0.03 and 0.04, respectively). The pairwise comparisons for the S_p revealed a statistically significant difference between CpC and (SB, SBE, and RSLACT). CpC was also statistically different from the SBE for R_p.

Table 5.4 Medians and range of the surface roughness measurements for all groups treated with 95 % HA/5 % CaO

Group coated 95 % HA/5 % CaO	S_a µm Median (range)	S_p µm Median (range)	S_v µm Median (range)	R_a µm Median (range)	R_p µm Median (range)	R_v µm Median (range)
CpC	3.45 (1.44)[a]	58.03 (11.00)[a]	9.97 (3.27)[a]	2.80 (2.17)[a]	11.65 (10.33)[a]	3.63 (3.36)[a]
SB	3.77 (3.39)[a]	17.97 (23.49)[b]	14.83 (7.10)[a]	1.62 (2.24)[a]	3.33 (1.88)[a,b]	3.21 (1.87)[a]
SBE	3.24 (4.48)[a]	16.90 (22.49)[b]	14.14 (16.58)[a]	0.83 (0.49)[a]	2.22 (0.90)[b]	2.38 (1.10)[a]
TiSLACT	5.80 (5.02)[a]	32.30 (14.40)[a,b]	22.23 (14.80)[a]	1.53 (1.19)[a]	3.64 (3.01)[a,b]	5.14 (5.85)[a]
RSLACT	3.89 (4.70)[a]	16.53 (3.90)[b]	15.16 (11.50)[a]	1.18 (0.37)[a]	4.02 (3.10)[a,b]	3.00 (0.84)[a]

NOTE: **The different superscript letters within the same column indicate significant differences between all groups**

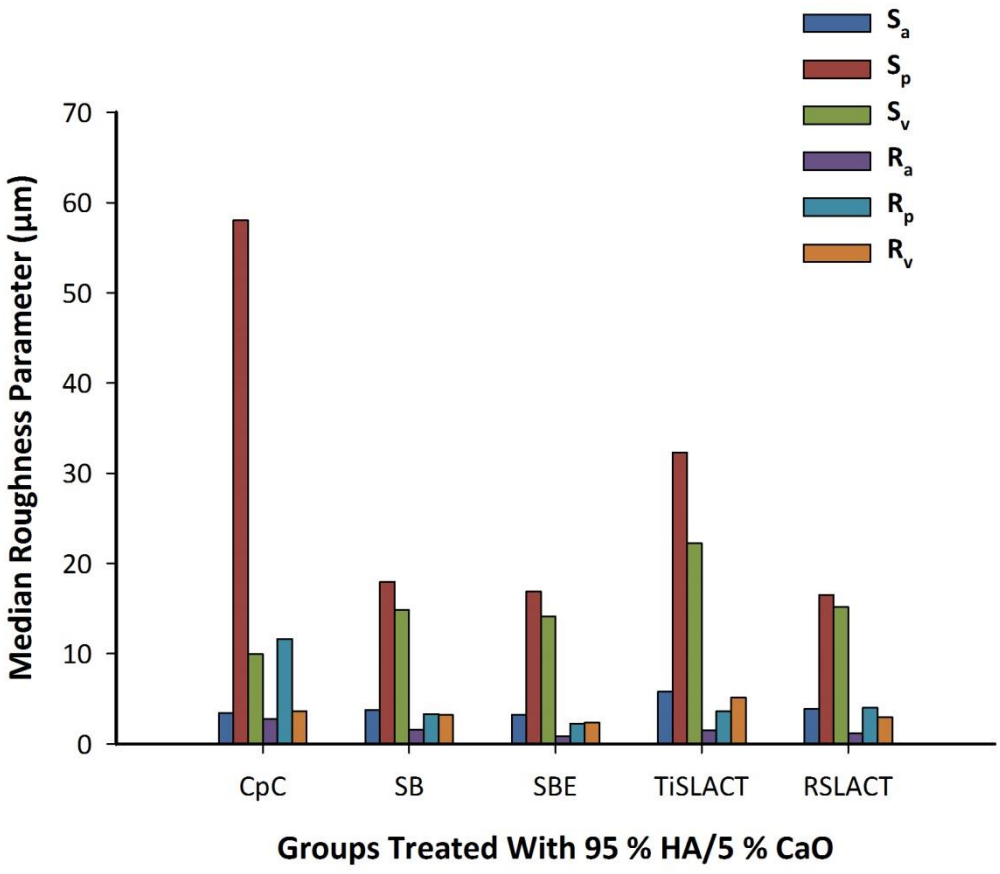

Figure 5.19 Bar chart representing the median roughness parameter for each group treated with 95 % HA/5 % CaO

As shown in Table 5.5 and Figure 5.20, different measurements were recorded for the groups treated with 90 % HA/10 % CaO powders. The SBE group showed the highest S_a (6.30 µm) and SB showed the lowest S_a (3.35 µm). The highest S_p was recorded for SBE (35.80 µm), whereas the lowest S_p was recorded for the TiSLACT (20.80 µm). Similarly, the highest S_v was recorded for the SBE (31.06 µm), while CpC showed the lowest S_v (14.63 µm). There were no significant differences for all the 2D and 3D roughness measurements across all groups.

When comparing the S_a values of all material groups treated with the two different powders, there were no statistical differences between all groups (p= 0.40 and 0.40, respectively).

Table 5.5 Medians and range of surface roughness measurements for all groups treated with 90 % HA/10 % CaO

Group coated 90 % HA/10 % CaO	S_a µm Median (range)	S_p µm Median (range)	S_v µm Median (range)	R_a µm Median (range)	R_p µm Median (range)	R_v µm Median (range)
CpC	3.40 (0.35)	20.83 (2.90)	14.63 (3.10)	0.36 (0.08)	1.83 (0.99)	1.05 (0.26)
SB	3.35 (2.15)	28.60 (11.40)	17.13 (10.00)	1.31 (0.92)	4.56 (5.60)	3.59 (2.83)
SBE	6.30 (0.39)	35.80 (13.50)	31.06 (40.40)	0.97 (0.23)	4.03 (3.44)	2.79 (0.72)
TiSLACT	3.93 (3.95)	20.80 (19.20)	16.13 (9.90)	1.63 (0.96)	4.80 (4.61)	4.28 (1.12)
RSLACT	4.70 (5.01)	28.23 (28.50)	19.56 (10.90)	1.89 (2.83)	8.20 (16.51)	4.34 (5.31)

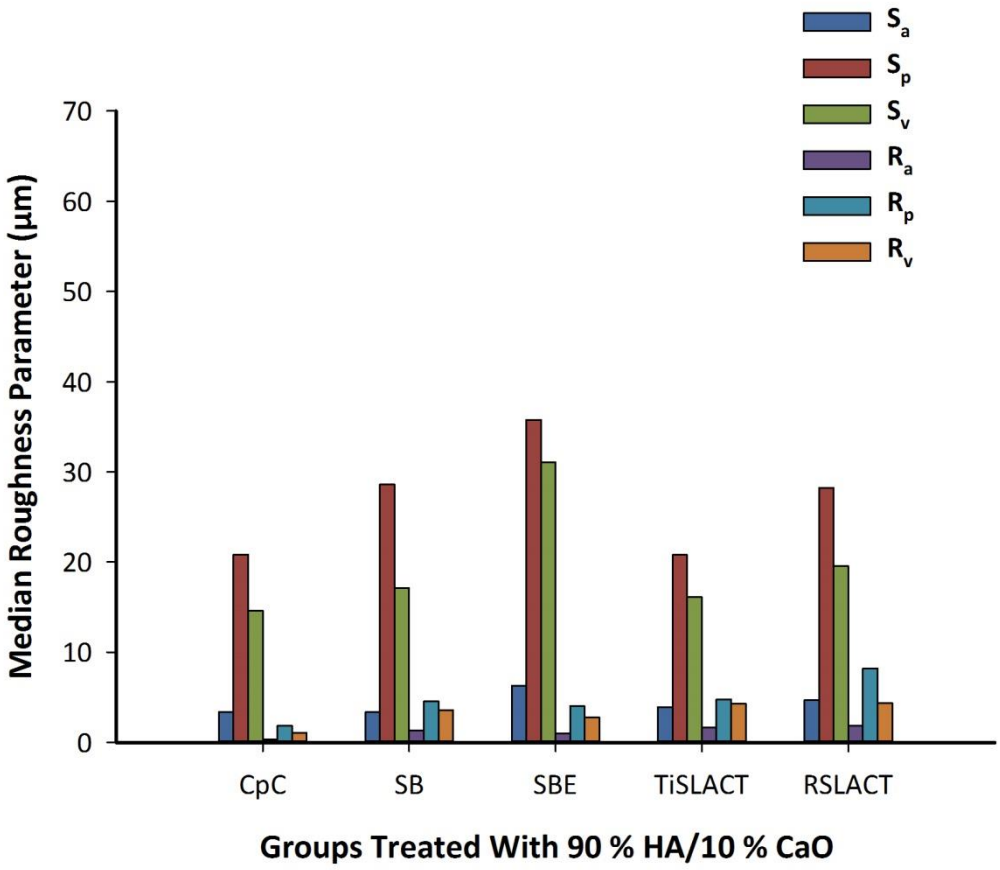

Figure 5.20 Bar chart representing the median roughness parameter for each group treated with 90 % HA/10 % CaO

Comparison of the median differences in the average 3D roughness parameter S_a values before and after the bioceramic treatment is presented in Table 5.6. No significant differences were noted in the median difference of S_a between the pre-treatment and post-treatment with the 95 % HA/5 % CaO and 90 % HA/10 % CaO (p= 0.40 and 0.40, respectively). Further analysis of the S_p, and S_v parameters is presented in Appendix I.

Table 5.6 Medians of the S_a parameter for all groups before and after treatment with the bioceramic powders

Group	Median S_a (µm)	Median S_a (µm)	Median S_a (µm)
	Before treatment	After treatment with 95 % HA/5 % CaO	After treatment with 90 % HA/10 % CaO
CpC	3.00	3.45	3.40
SB	3.37	3.77	3.35
SBE	3.70	3.24	6.30
TiSLACT	3.24	5.80	3.93
RSLACT	2.56	3.89	4.70

Representative 3D surface roughness profile images from each tested surface are presented below in Figures 5.21–5.30.

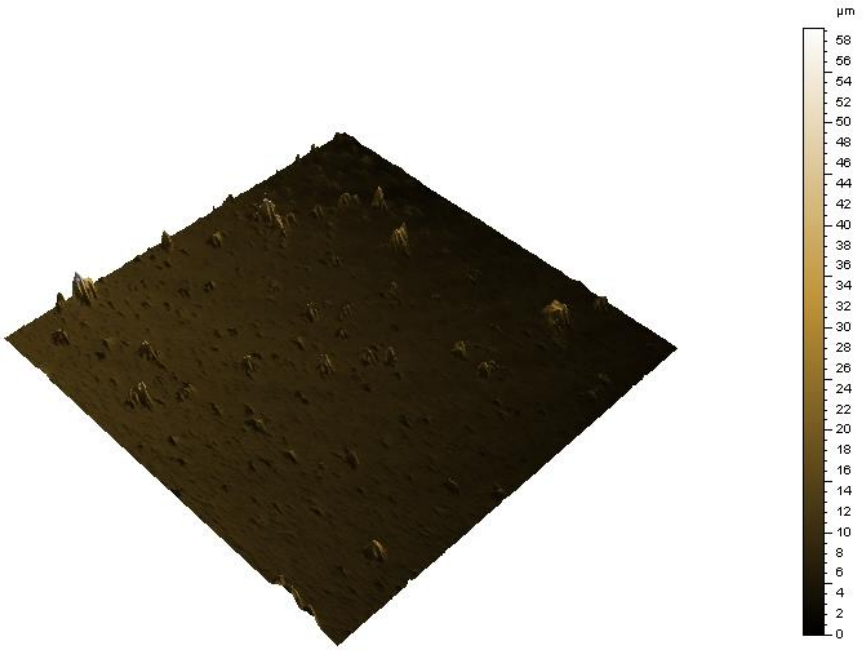

Figure 5.21 Representative 3D image of CpC treated with 95 % HA/5 % CaO

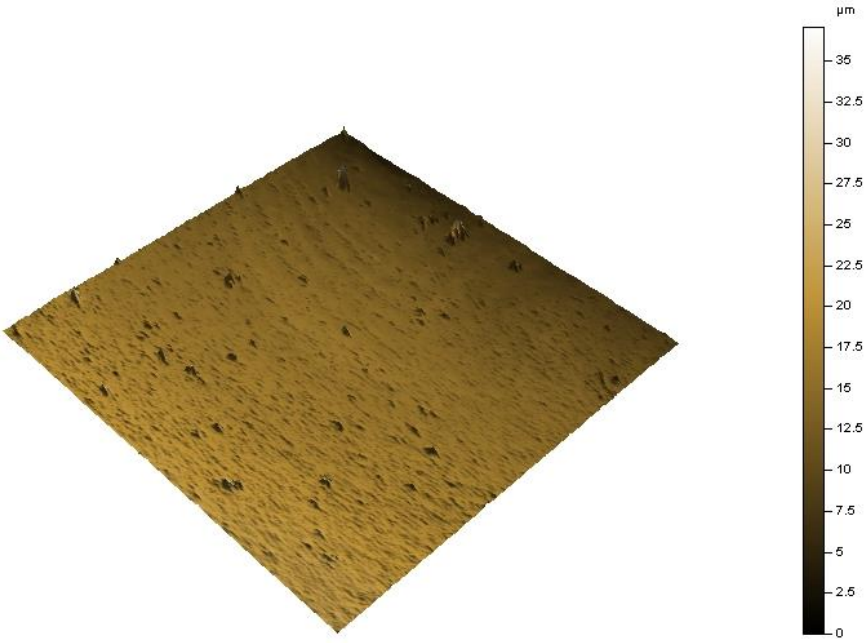

Figure 5.22 Representative 3D image of CpC treated with 90 % HA/10 % CaO

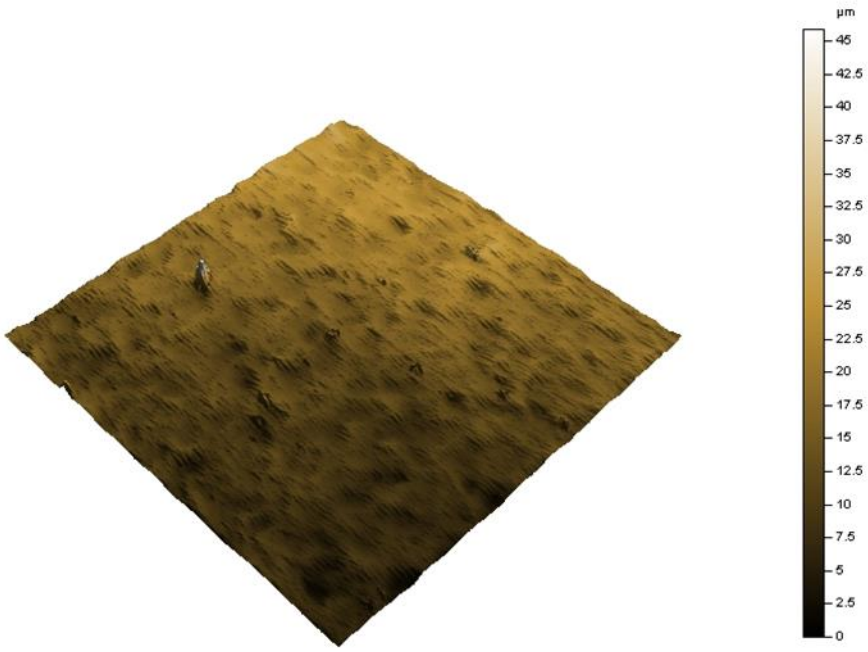

Figure 5.23 Representative 3D image of SB treated with 95 % HA/5 % CaO

Figure 5.24 Representative 3D image of SB treated with 90 % HA/10 % CaO

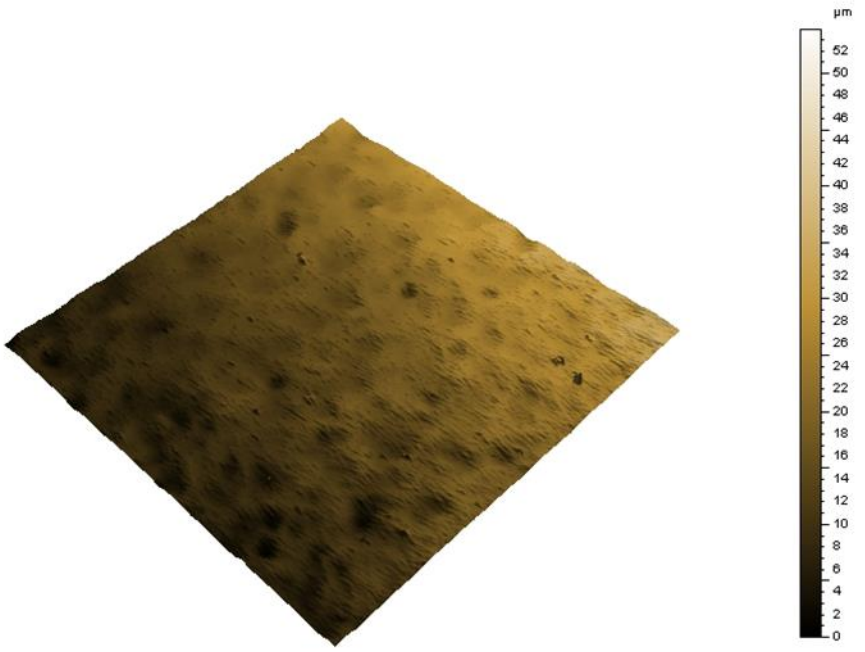

Figure 5.25 Representative 3D image of SBE treated with 95 % HA/5 % CaO

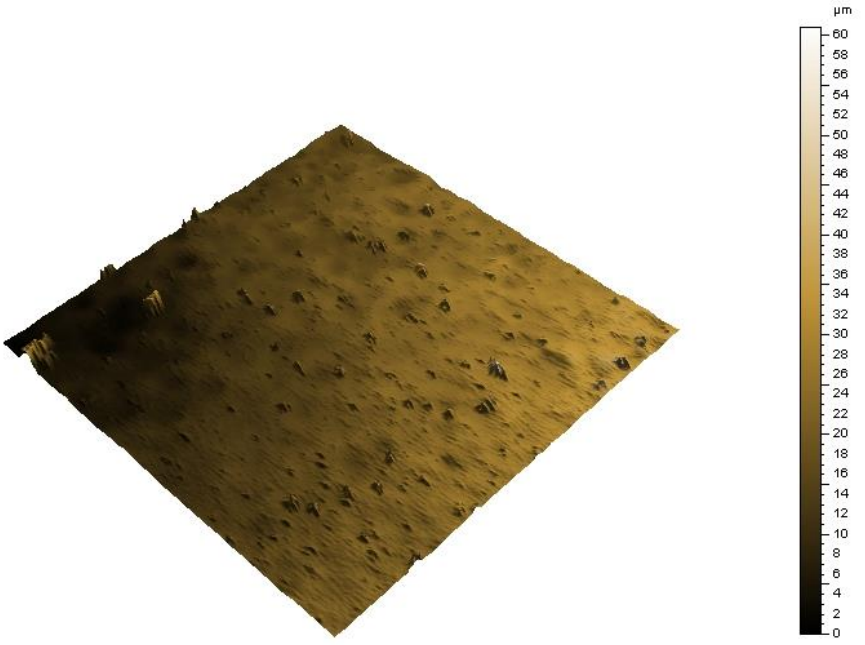

Figure 5.26 Representative 3D image of SBE treated with 90 % HA/10 % CaO

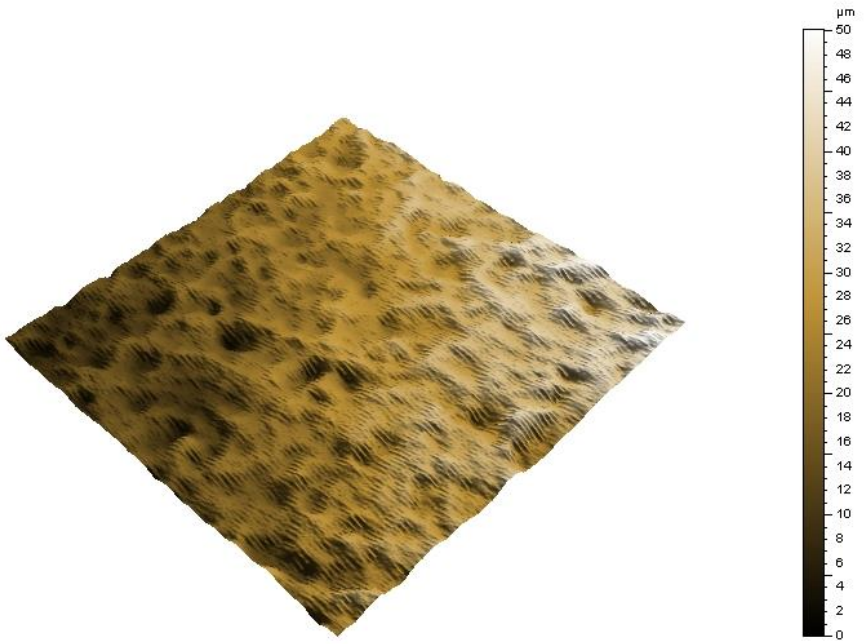

Figure 5.27 Representative 3D image of TiSLACT treated with 95 % HA/5 % CaO

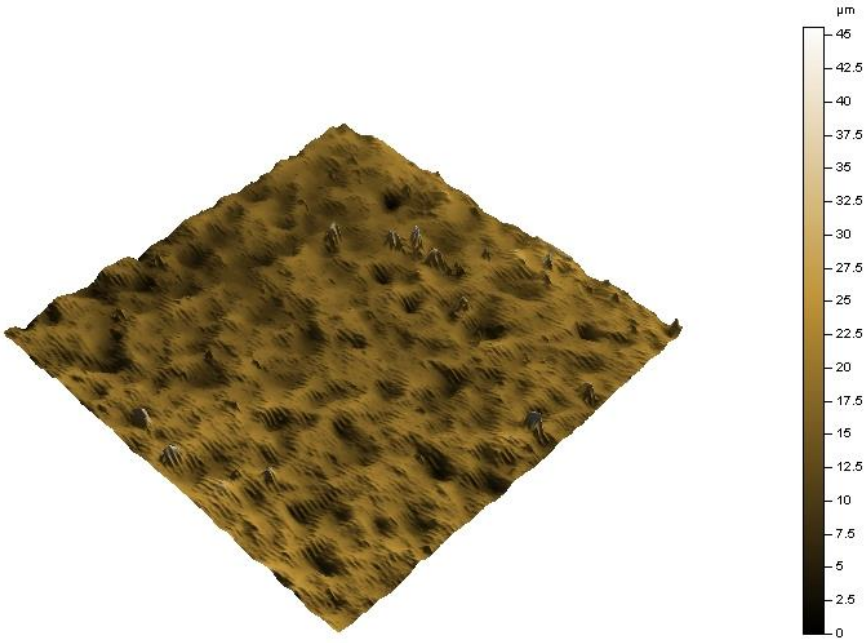

Figure 5.28 Representative 3D image of TiSLACT treated with 90 % HA/10 % CaO

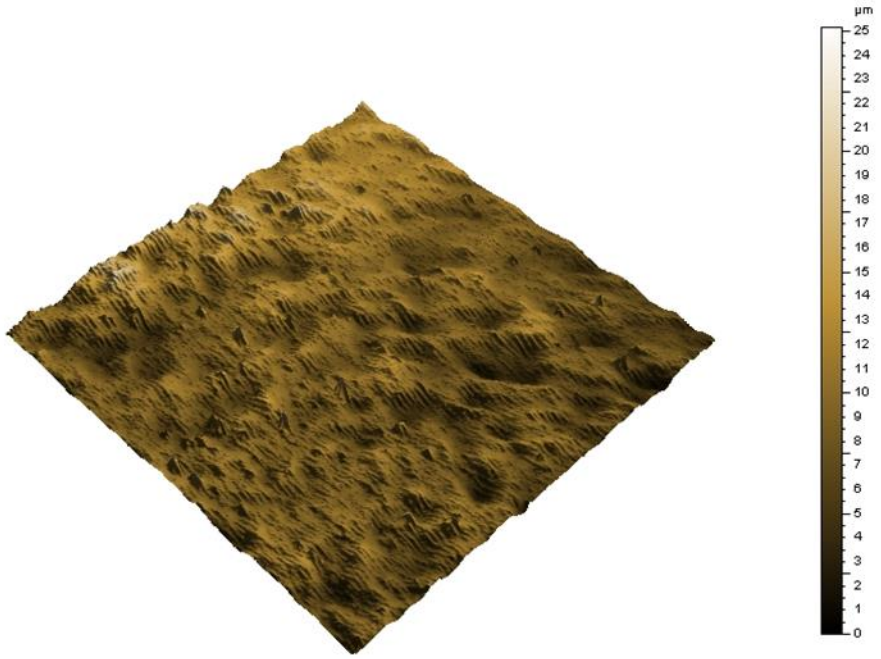

Figure 5.29 Representative 3D image of RSLACT treated with 95 % HA/5 % CaO

Figure 5.30 Representative 3D image of RSLACT treated with 90 % HA/10 % CaO

5.6 Discussion

The combined effect of changing the surface characteristics and osseoconductive properties of HA-based bioceramics has led to their continuous use as a coating material for dental implants (Subramani *et al.*, 2018). This study presents a bioceramic treatment that could be applied on an implant surface for treating peri-implantitis, in order to enhance its bioactivity. Three samples were chosen in this study based on previous similar studies using 3 samples to evaluate the surface characteristics of implant surfaces (Rupp *et al.*, 2006; Coelho and Lemons, 2009; Coelho *et al.*, 2011; Schmage *et al.*, 2012; Barry *et al.*, 2013; Tastepe *et al.*, 2013; Kopf *et al.*, 2015; John *et al.*, 2016; Hakki *et al.*, 2017; Kulkarni Aranya *et al.*, 2017; Lotz *et al.*, 2017).

Previous research has demonstrated that varying air abrasives powder parameters, including the powder formulation and particle size, might influence the surface characteristics (Schwarz *et al.*, 2009a; O'Sullivan *et al.*, 2011; Tastepe *et al.*, 2013; Dunne *et al.*, 2015b; Menini *et al.*, 2015). The addition of CaO to HA powders resulted in different Ca/P ratios that were correlated to the dissolution rate of CaP coatings (Lee *et al.*, 2000; Hwang *et al.*, 2013); therefore, two formulations of bioceramic powders were chosen. Previous studies have been published using similar bioceramic powders but without specifying the exact formulas used (Ahn *et al.*, 2009; O'Sullivan *et al.*, 2011; Barry *et al.*, 2013). Therefore, the composition was systematically varied to 5 % and 10 % CaO. This was in order to examine the effect of CaO concentration on the properties studied. There are no reported adverse effects on osteoblast cells with these abrasive powders both *in-vivo* and *in-vitro* (Ahn *et al.*, 2009; O'Sullivan *et al.*, 2011; Tan *et al.*, 2012; Barry *et al.*, 2013; Dunne *et al.*, 2015b).

The results of this study have demonstrated that air abrasion can deposit bioceramic powders on the surfaces of a previously modified implant and change its surface characteristics. This was confirmed by the SEM and EDS surface analyses that demonstrated the incorporation of abrasive powders on the treated surfaces. However, the material substrate and existing surface modification had no significant effect on the change in surface characteristics produced by air abrasion when using the 90 % HA/10 % CaO. Therefore, the null hypothesis was accepted, whereas when using the 95 % HA/5 % CaO powder the material substrate and existing surface had a significant effect on the S_p and R_p parameters only. This significant effect on S_p and R_p could be related to the different powder composition used. Although the samples had different microstructures before treatment (Figures 5.4 and 5.5), after treatment (Figures 5.10–5.12) the morphological appearance of all air-abraded samples regardless of the material and existing surface appeared similar: all were rough and irregular, with several depressions and projections observed across the surface.

The use of the air blasting to deposit bioceramics on titanium surfaces has been proven in many studies (Ishikawa *et al.*, 1997; O'Neill *et al.*, 2009; O'Sullivan *et al.*, 2010; Barry *et al.*, 2013; Dunne *et al.*, 2015a). However, previously blasted HA treatments were deposited on titanium substrates and not TiZr alloy. To date limited studies have used air abrasion to deposit bioceramic abrasive powders on surface-modified CpTi, with no studies using the method employed in this study or bioceramic powders on TiZr alloy with different surfaces.

Air abrasion with bioceramic demonstrated some changes in the surface roughness of the tested samples. This effect can be seen when comparing the values of surface roughness parameters before treatment (Chapter 3: Tables 3.2 and 3.3), with those after treatment

(Chapter 5: Tables 5.4 and 5.5). The values of all parameters post-treatment were either higher or lower than pre-treatment. However, when statistically comparing the S_a (Table 5.6), and S_p and S_v values (Appendix I) no significant differences were noted between the before and after treatment for both powders. This could be explained by the non-uniformity of the coating on the surface, where some areas might have more particles than others, and different powder composition might also have produced different effects on the surface.

When looking at the 3D views of the bioceramic-treated samples (Figures 5.21–5.30) and the untreated samples (Figures 3.5–3.15), the change in surface topography is presented as projections that most likely represent the deposited bioceramic powder that was present on the surfaces, as confirmed by the EDS analysis.

The average surface roughness measurements (S_a/R_a) obtained by the 3D optical profilometer used in this study recorded different S_a/R_a values between all materials and surface treatments tested. However, no significant differences were noted in the S_a/R_a with different powders across all groups. For the 95 % HA/5 % CaO powder, the TiSLACT group represented the highest value of S_a (5.80 µm), while the lowest S_a value (3.24 µm) was associated with the SBE group. The opposite was seen for the powder with 90 % HA/ 10 % CaO, where the highest S_a (6.30 µm) was obtained in the SBE group, whereas the lowest S_a (3.35 µm) was for the SB. This difference in the median roughness parameters could be attributed to the different level of surface roughness due to the previous surface modifications or the different amounts of powder blasted on each surface.

The qualitative SEM images before (Figures 5.4 and 5.5) and after the bioceramic abrasion (Figures 5.10–5.12) showed that the bioceramic treatment changed the surface morphology of the tested samples. This is in agreement with other studies using air

abrasion (Koller *et al.*, 2007; Duarte *et al.*, 2009b). However, the surface morphology of all treated surfaces revealed a non-uniform distribution of the treatment on the surface layer of the samples, with dispersed patches of bioceramic powders spread over the surface. This was confirmed by the EDS analysis that demonstrated the availability of Ca/P rich surfaces at different concentrations from the same sample, and is in agreement with other studies using air abrasion with bioceramic abrasives (Tastepe *et al.*, 2013; Tastepe *et al.*, 2018b).

The EDS analysis of the treated surfaces also showed the peaks of titanium in all the resulting spectrums (e.g. Figures 5.15 & 5.16), which means that the effect of the treatment was limited to the surface layer of the samples.

In general, different materials and surfaces showed different weight percentages of Ca and P, with no statistically significant differences. This could be attributed to the different surfaces or due to the different concentrations of the powders. However, the limitations of the EDS analysis, depth limit, and accuracy should be taken into account.

The CpC surface, which was not exposed to any surface modification before the bioceramic treatment showed a high wt % of both Ca and P for both powders, which was also evident in the 3D view of surface roughness (Figure 5.21 & 5.22). This could be attributed to the nature of its surface being anisotropic and having deep grooves (Elias *et al.*, 2008). However, it did not show any significant difference to the other tested groups in relation to the Ca/P ratios with both powder compositions.

5.7 Conclusions

Within the limitations of this study, the following conclusions were drawn:

- The experimental air abrasion method used in this study has demonstrated that bioceramic abrasion can modify the surface characteristics when used on different implant materials and surfaces. However, the change in the median R_a and S_a surface roughness resulting from such treatment was not significant in all cases.
- Varying the powder composition might affect the resulting surface characteristics. Additionally, the change in surface characteristic resulting from such treatment was not influenced by the implant material or surface modification.
- Air abrasion with CaP-based bioceramic leaves powder deposits on the treated implant surfaces. Further characterisation of implant surfaces and *in-vivo* studies are needed to assess if these deposits will stimulate a beneficial cellular response during tissue healing.

.

Chapter 6

Assessment of the Dissolution Behaviour of Air Bioceramic Abrasive Treatment from Dental Implant Surfaces

6.1 Introduction

Titanium is known to be an inert material that is unable to stimulate any bone formation (Chen *et al.*, 2013). Since the implant surface is the first part to interact with the peri-implant tissues, research is being directed towards incorporating different bioactive treatments to increase implant surface osseoinduction (Avila *et al.*, 2009). The rationale behind incorporating CaP-based treatments is to accelerate osseointegration immediately after implant placement. This is achieved when the Ca/P particles dissolute to the surface, causing apatite precipitation on the implant (Surmenev *et al.*, 2014; Subramani *et al.*, 2018).

Assessment of coating dissolution is achieved by immersing the coated samples in liquid solutions such as SBF (Gu *et al.*, 2003), deionised water, Ringer's solutions, and distilled water (Wang *et al.*, 2006). Several methods have been used to investigate the amount of Ca^{2+} and PO_4^{3+} released from HA coatings. Inductive coupled plasma optic emission spectrometry (ICP-OES) is one of the most extensively used methods to detect trace elements released from treated titanium surfaces (O'Sullivan *et al.*, 2010; Hung *et al.*, 2013; Kim *et al.*, 2013a). The main advantage associated with the use of ICP-OES is its sensitivity and accuracy.

In the previous chapter, it was demonstrated that bioceramic powder can be applied using an air abrasion method. The dissolution of this bioceramic treatment from the implant surface and into the surrounding environment is essential to enhance the bioactivity. Additionally, the dissolution rate of Ca^{2+} and PO_4^{3+} from HA bioceramics is crucial to stimulate the osseoconductive characteristics of the implant surface during tissue healing. The effect of the bioceramic air abrasion method used in the previous

study and the dissolution behaviour of the bioceramic treatment deserve further research.

6.2 Aim of the study

The aim of the study was to assess the effect of material and surface on the stability of bioceramic treatment on dental implant surfaces using air abrasion. The objectives were as follows:

- To quantify the concentration of Ca^{2+} and PO_4^{3+} released from the treated surfaces of different implant materials and surfaces using ICP-OES.
- To evaluate the difference in the concentration of Ca^{2+} and PO_4^{3+} released from the surfaces at 1, 2, and 3 week intervals.

The null hypothesis was that the implant material and surface have no effect on the dissolution of the bioceramic treatment. In addition, there is no difference in the amount of calcium and phosphorous ions released from different implant materials and surfaces at 1, 2, and 3 weeks.

6.3 Materials and methods

6.3.1 Bioceramic-treated samples

The same bioceramic-treated samples studied in Chapter 6 were used for testing.

6.3.2 Sample preparation

A pilot study was conducted where one sample from each group (per powder) was placed in a glass beaker and soaked in 50 ml of deionised water for 3 weeks. All samples were then stored in an incubator at 37 °C. A 10 ml sample was taken from the tested beakers at 1, 2, and 3 weeks and stored in separate labelled bottles for testing.

6.3.3 Inductive coupled plasma optical emission spectrometry (ICP-OES)

The ICP-OES (Perkin-Elmer Optima 5300 dual view, MA, USA) (Figure 6.1) was used in this study. The ICP-OES has the ability to detect a wide range of elements with a 10–100 ppb detection limit and a wavelength range of 163–782 nm. The system has both axial and radial or mixed plasma viewing modes. The liquid sample is introduced into the machine through a pump to a nebuliser that converts it to an aerosol (Figure 6.2). Then, the aerosol is transferred to the plasma, where it is converted into excited atoms and ions that emit radiation. These radiations are then sorted by wavelength and processed in a spectrometer that converts them to electrical signals. After that, the electrical signals are converted into concentrations ready to be analysed by the computer software.

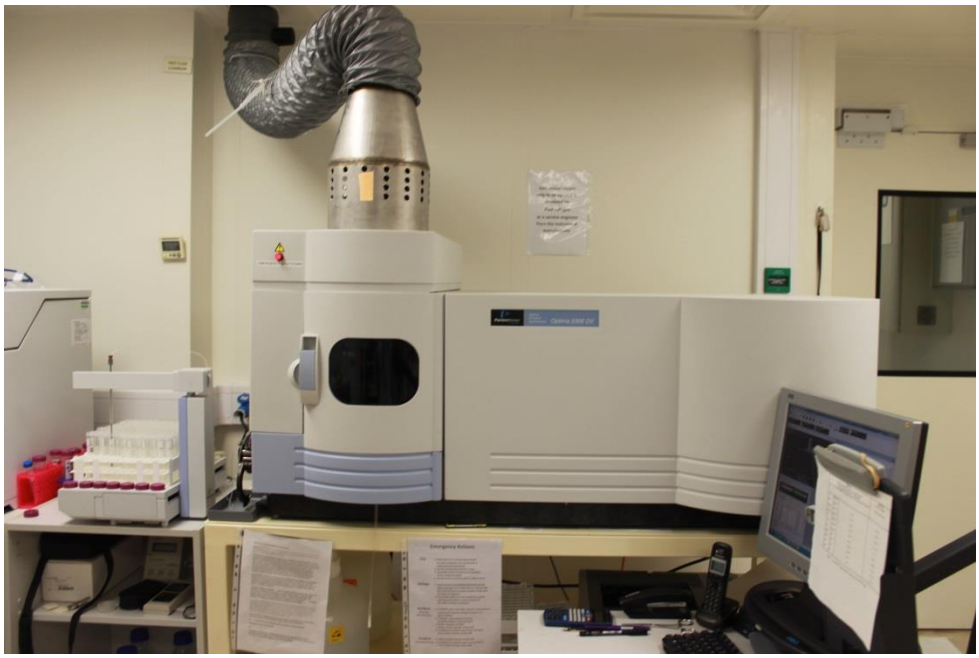

Figure 6.1 ICP-OES Perkin-Elmer Optima 5300

Figure 6.2 The pump and nebuliser that converts the liquid samples to aerosol

All samples were acidified with 2 % HNO_3 and filtered. The analysis was performed using laboratory standardisations. To ensure accuracy, two standards and one blank were prepared by the laboratory and introduced into the machine with the tested samples.

6.4 Data analysis

The amount of Ca^{2+} and PO_4^{3+} concentration was calculated from 3 runs of each sample. The mean of the 3 measurements per sample and standard deviations were calculated. Due to the small sample size, no statistical analysis of the data was carried out.

6.5 Results

The means and standard deviations of the concentrations of Ca^{2+} and PO_4^{3+} from each treated sample are presented in Tables 6.1–6.4, while the concentrations of the Ca^{2+} and PO_4^{3+} released over the 3 weeks are plotted graphically in Figures 6.3–6.8.

Generally, the mean concentration of Ca^{2+} and PO_4^{3+} varied from week 1 to week 3. When comparing all groups, the maximum concentration of Ca^{2+} released over 1, 2, and 3 weeks was from the SBE 5 % samples at 0.58, 0.62, and 0.64 mg/l, respectively. Meanwhile, the minimum concentration of Ca^{2+} released over 1, 2, and 3 weeks was from the SB 10 % samples at 0.22, 0.26, and 0.35 mg/l, respectively. The concentration of PO_4^{3+} varied between the 3 weeks. The highest concentration of PO_4^{3+} released in the first and third weeks was from the RSLACT 5 % samples at 0.13 and 0.19 mg/l, respectively. In the second week, the highest concentration of PO_4^{3+} was from both the SBE 5 %, and TiSLACT 10 % (0.12 mg/l). The pattern of Ca^{2+} release was different between the two powders (5 % and 10 % CaO). The pattern of Ca^{2+} for the 5 % CaO powder in the first week (Figure 6.5) was in the order of SBE> SB> CP> RSLACT> TiSLACT. A similar pattern was noted in the second and third weeks, except that the CpC group released more Ca^{2+} than the SB group. The pattern of Ca^{2+} released from the 10 % CaO powder (Figure 6.6) was different from the 5 % CaO powder. The order of Ca^{2+} release over the 3 week period was CP> TiSLACT> SBE> RSLACT> SB.

Table 6.1 Means and standard deviations (SD) of the amount of calcium released from samples treated with 95 % HA/5 % CaO at 1, 2, and 3 weeks

Group treated 95 % HA/5 % CaO	Week 1 Mean Ca^{2+} mg/l (SD)	Week 2 Mean Ca^{2+} mg/l (SD)	Week 3 Mean Ca^{2+} mg/l (SD)
CpC	0.43 (0.06)	0.54 (0.06)	0.58 (0.06)
SB	0.45 (0.08)	0.52 (0.08)	0.48 (0.05)
SBE	0.58 (0.05)	0.62 (0.05)	0.64 (0.07)
TiSLACT	0.26 (0.04)	0.30 (0.05)	0.37 (0.06)
RSLACT	0.27 (0.06)	0.37 (0.05)	0.40 (0.07)

Table 6.2 Means and standard deviations (SD) of the amount of calcium released from samples treated with 90 % HA/10 % CaO at 1, 2, and 3 weeks

Group treated 90 % HA/10 % CaO	Week 1 Mean Ca^{2+} mg/l (SD)	Week 2 Mean Ca^{2+} mg/l (SD)	Week 3 Mean Ca^{2+} mg/l (SD)
CpC	0.47 (0.08)	0.59 (0.08)	0.62 (0.11)
SB	0.22 (0.06)	0.26 (0.06)	0.35 (0.07)
SBE	0.35 (0.06)	0.44 (0.06)	0.48 (0.06)
TiSLACT	0.44 (0.08)	0.49 (0.05)	0.56 (0.08)
RSLACT	0.31 (0.O4)	0.38 (0.08)	0.44 (0.07)

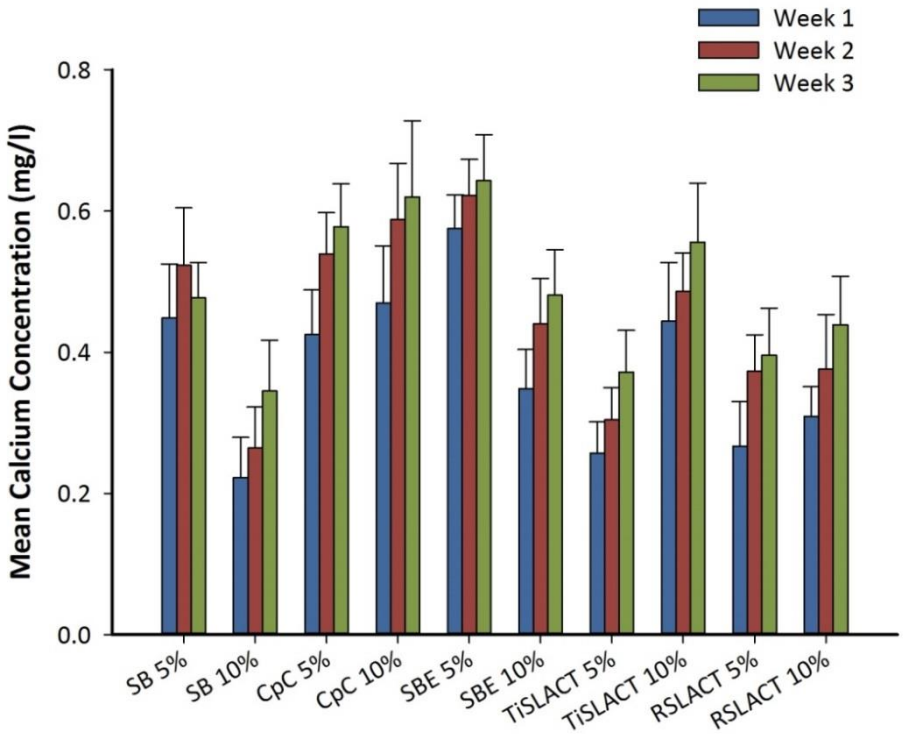

Figure 6.3 Bar chart comparing the mean amount of calcium ion dissolute from all groups at 1, 2, and 3 weeks, with error bars representing the standard deviations

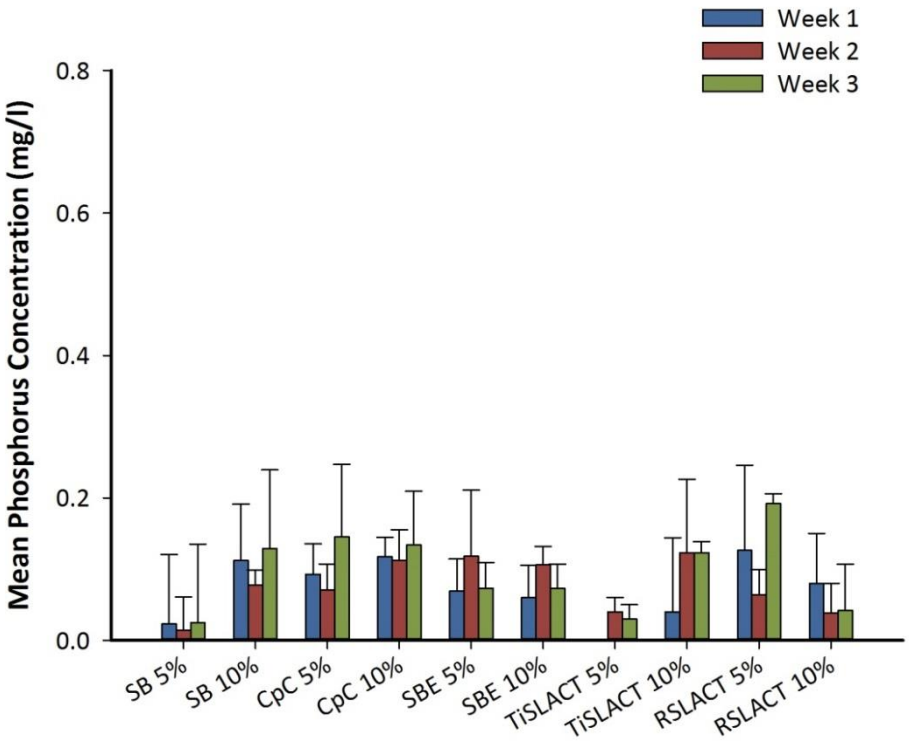

Figure 6.4 Bar chart comparing the mean amount of phosphorous ion dissolute from all groups at 1, 2, and 3 weeks, with error bars representing the standard deviations

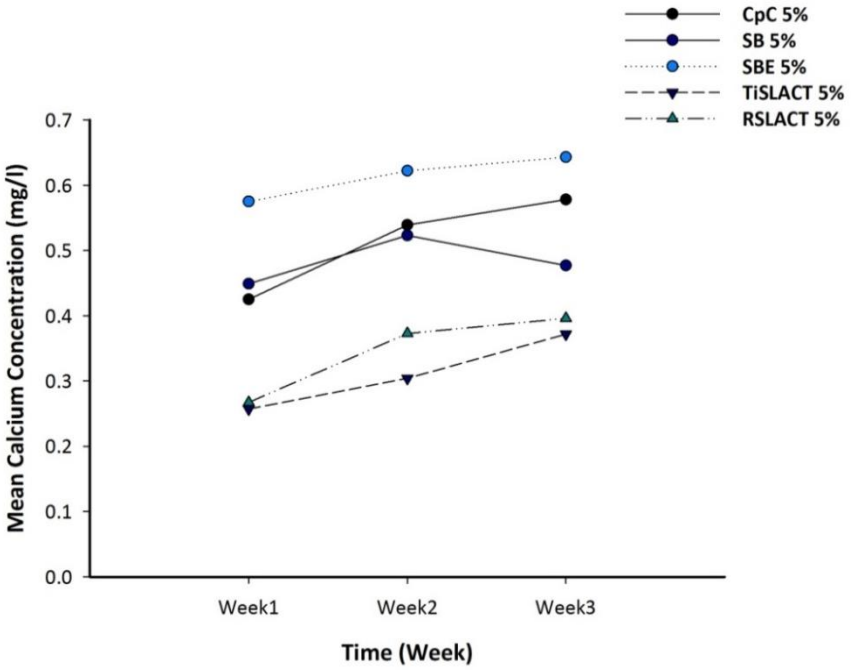

Figure 6.5 Mean calcium ion release from the samples treated with 95 % HA/5 % CaO over 3 weeks

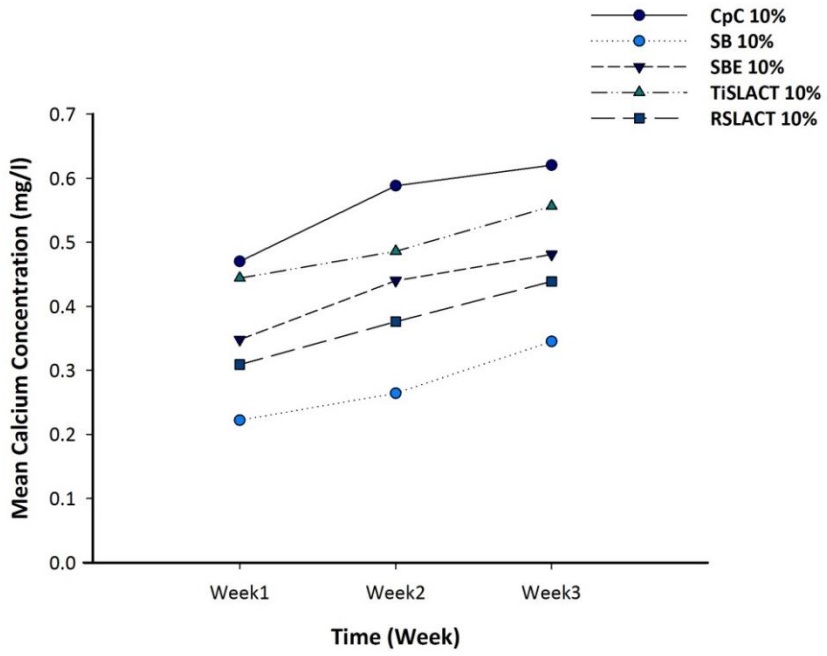

Figure 6.6 Mean calcium ion release from the samples treated with 90 % HA/10 % CaO over 3 weeks

Table 6.3 Means and standard deviations (SD) of the amount of phosphorous released from samples treated with 95 % HA/5 % CaO at 1, 2, and 3 weeks

Group treated 95 % HA/5 % CaO	Week 1 Mean PO_4^{3+}mg/l (SD)	Week 2 Mean PO_4^{3+} mg/l (SD)	Week 3 Mean PO_4^{3+} mg/l (SD)
CpC	0.09 (0.04)	0.07 (0.04)	0.15 (0.10)
SB	0.02 (0.10)	0.01 (0.05)	0.03 (0.11)
SBE	0.07 (0.05)	0.12 (0.09)	0.07 (0.04)
TiSLACT	0.00 (0.09)	0.04 (0.02)	0.03 (0.02)
RSLACT	0.13 (0.12)	0.06 (0.04)	0.19 (0.01)

Table 6.4 Means and standard deviations (SD) of the amount of phosphorous released from samples treated with 90 % HA/10 % CaO at 1, 2, and 3 weeks

Group treated 90 % HA/10 % CaO	Week 1 Mean PO_4^{3+} mg/l (SD)	Week 2 Mean PO_4^{3+}mg/l (SD)	Week 3 Mean PO_4^{3+} mg/l (SD)
CpC	0.12 (0.03)	0.11 (0.04)	0.13 (0.08)
SB	0.11 (0.08)	0.08 (0.02)	0.13 (0.11)
SBE	0.06 (0.05)	0.11 (0.03)	0.07 (0.03)
TiSLACT	0.04 (0.10)	0.12 (0.10)	0.12 (0.02)
RSLACT	0.08 (0.07)	0.04 (0.04)	0.04 (0.06)

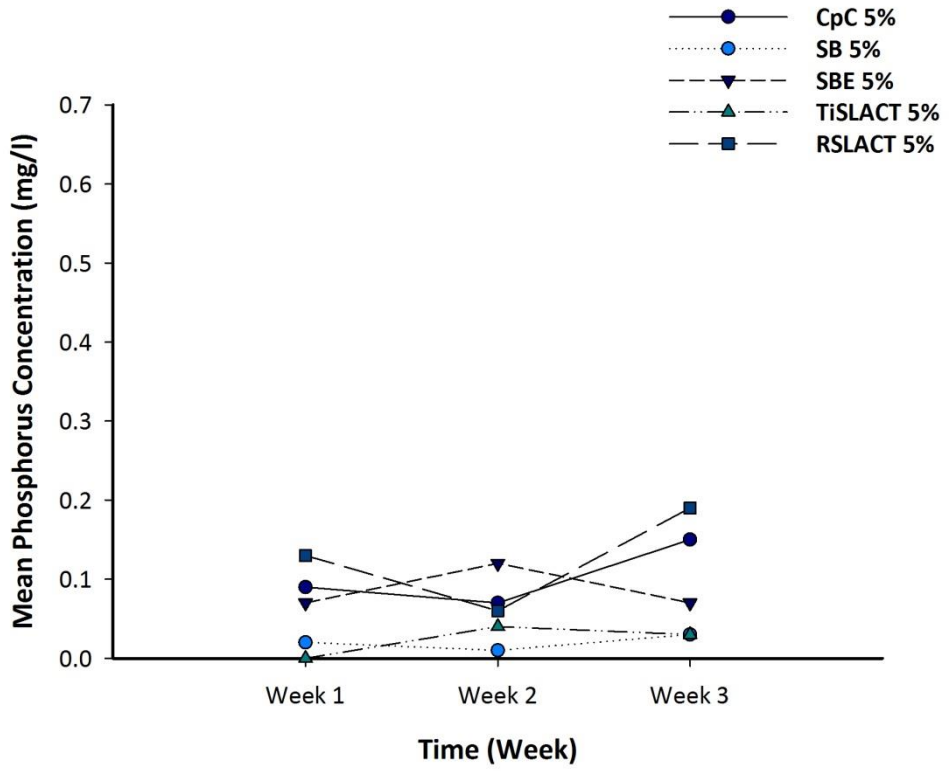

Figure 6.7 Mean phosphorous ion release from the samples treated with 95 % HA/5 % CaO over 3 weeks1

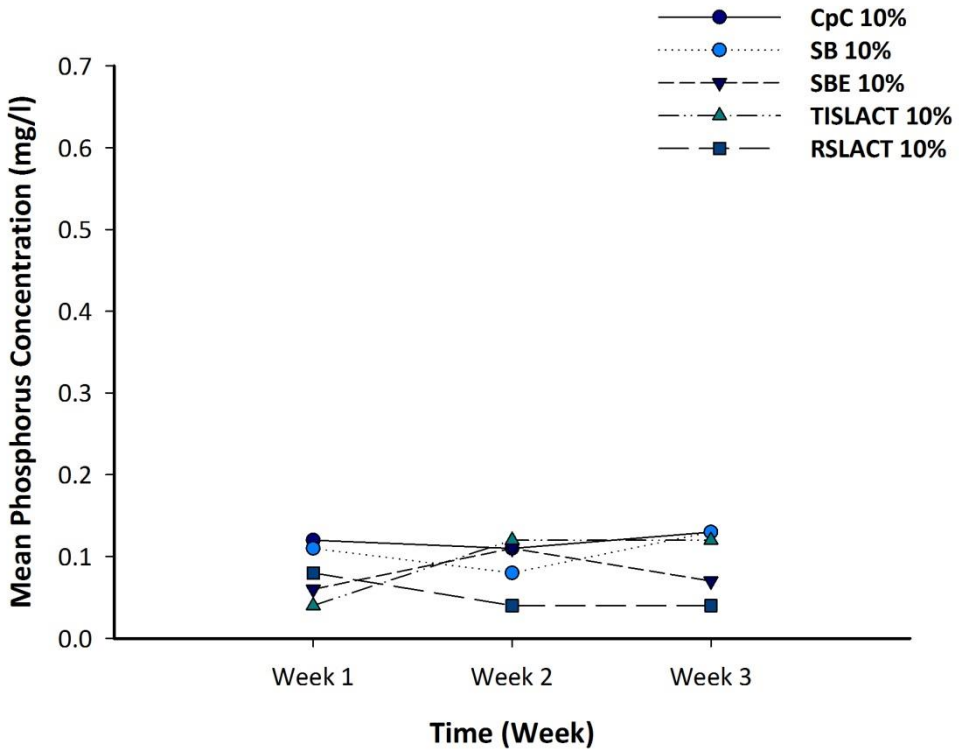

Figure 6.8 Mean phosphorous ion release from the samples treated with 90 % HA/10 % CaO over 3 weeks

6.6 Discussion

The dissolution of the Ca/P from the bioceramic-treated samples in the previous study (Chapter 5) was evident in all the tested samples, thus confirming that the air abrasion method used did deposit the bioceramic powders on the previously modified implant surfaces.

The dissolved Ca^{2+} and PO_4^{3+} ions were assessed in deionised water, in line with other research (Kim *et al.*, 2010), to avoid any possible interference that may result from different electrolytes in the immersion media. There is no standard protocol for the amount of immersion media, where different amounts have been used in previous research: 25 ml (Mohedano *et al.*, 2014), 30 ml (Hung *et al.*, 2013), and 50 ml (Gu *et al.*, 2005). Thus, to allow for 10 ml withdraw for each time interval a 50 ml immersion solution was chosen.

The concentrations of Ca^{2+} and PO_4^{3+} released from the different treated surfaces varied between samples and bioceramic powders. Every treated surface behaved differently from the other. In general, the amount of Ca^{2+} released over the 3 weeks was higher than the amount of PO_4^{3+} released. This could be due to the difference in the Ca/P ratios, as demonstrated by the EDS analysis (Tables 5.2 & 5.3), which might be due to the different concentrations of CaO added to the bioceramic powders by the company (i.e. the Ca^{2+} released could be from the HA and the extra CaO, where the PO_4^{3+} originates from the HA component). Thus, a lower concentration of PO_4^{3+} was noted in comparison to Ca^{2+}.

The amount of Ca^{2+} released tended to increase slowly from week 1 to week 3 for all the tested samples. The only group which behaved differently was the SB group that was

treated with 95 % HA/5 % CaO. This group showed a slight decrease in the Ca^{2+} concentration from 0.52 mg/l at week 2 to 0.48 mg/l at week 3.

The concentrations of PO_4^{3+} released from the surfaces were fluctuant as it was higher in the first week for some samples and lower in the others (Figures 6.7 & 6.8). The same trend was seen in the second and third weeks. This could be attributed to the previous surface modification and level of surface roughness of the samples before applying the bioceramic treatment. However, whether this effect is significant or not can only be concluded if more samples are studied.

CaP dissolution from implant surfaces coated with hydroxyapatite starts early after implantation during the first 3 hours (Porter *et al.*, 2002), and bone mineralisation has been observed 1 to 2 weeks post-implantation (Wang *et al.*, 2006). The latter study also linked the dissolution behaviour of bioactive coatings to bone apposition. Coatings with low dissolution rates had lower bone apposition rates. Therefore, any treatment should stay in place for the first 2 weeks post-implantation to ensure the enhancement of bone apposition. Thus, the 3 week observation period was chosen in this study based on these previous in-vivo studies. In this study it was confirmed that the treatment was still available and continued to release Ca/P for up to 3 weeks in deionised water.

In the present study, the amount of Ca^{2+} and PO_4^{3+} released tended to increase, decrease or stabilise from the first week to the third week, although it is unknown whether this release will continue to increase, decrease or stabilise after 3 weeks. Kim *et al.* (2010) reported that thin CaP films tended to dissolve rapidly in the first two days of immersion in deionised water, and then dissolution decreased when assessed over a 2 week period. Dumelie *et al.* (2008) observed that Ca^{2+} dissolution behaviour is different from PO_4^{3+} dissolution. Their study indicated that Ca^{2+} dissolution will start early after immersion in

SBF and in the first day of immersion, after which it will continue to decrease for up to 14 days and then stabilise, while PO_4^{3+} dissolution was stable during the 3 week observation period. The findings of Dumelie *et al.* (2008) are not consistent with the present study as the dissolution of both Ca^{2+} and PO_4^{3+} ions increased, decreased or stabilised during the 3 week period. This could be due to the different immersion media or the deposition method used. Nevertheless, the present study did not account for any precipitation, as samples were withdrawn by the immersion of a pipette into the liquid. Therefore, the amount of Ca^{2+} and PO_4^{3+} might be underestimated.

Research has shown that blasted bioceramic particles enhance osteoblast cell early differentiation and viability at 8 and 15 days of observation, without altering the surface cytocompatibility (Citeau *et al.*, 2005; Le Guehennec *et al.*, 2008). Similarly, the abrasive powders used in the present study have not shown any adverse effect on osteoblast cells both *in-vivo* and *in-vitro* (Ahn *et al.*, 2009; O'Sullivan *et al.*, 2011; Tan *et al.*, 2012; Barry *et al.*, 2013; Dunne *et al.*, 2015b). Tastepe *et al.* (2018a) concluded that CaP-based bioceramics applied by air abrasion start to enhance cell viability at 6 days post-treatment. Therefore, the dissolution of the bioceramic abrasives in the present study for 3 weeks should be sufficient to induce apatite precipitation, in order to enhance the cellular response and subsequent implant bioactivity. The Ca^{2+} and PO_4^{3+} may continue to be released from the thin coating on the treated surfaces after 3 weeks, although any such sustained release is unlikely to have any negative effect on the healing process, unlike the previously used thick HA coatings which were prone to failure (Artzi *et al.*, 2006).

One factor that could contribute to the dissolution rate of the bioceramic treatment is the Ca/P ratio, as a result of the addition of CaO to the HA powder. Research has highlighted

that the variation in the Ca/P ratios is an important factor that could influence its dissolution behaviour (Lee *et al.*, 2002). The slow dissolution rate of the bioceramic treatment in this study could be related to the crystallinity of the HA powder. It was shown that the crystallinity of the HA has a significant effect on its stability and dissolution, namely that the crystalline coatings dissolved slower *in-vivo* and *in-vitro* (Gross *et al.*, 1997; Gledhill *et al.*, 2001; Dunne *et al.*, 2014). Nevertheless, no XRD analysis was undertaken for the treated samples. However, the XRD pattern supplied by the company for the initial powders in Chapter 5 (Figures 5.8 & 5.9) clearly shows the sharp narrow peaks of the HA, indicating their high crystallinity. Further analysis of the treated samples is needed to confirm whether the treatment did or did not undergo any changes in crystallinity or phase composition after air abrasion.

6.7 Conclusions

Within the limitations of this study, the following conclusions were drawn:

- The ionic release of calcium and phosphorous from the bioceramic-treated surfaces confirms that air abrasion incorporated the bioceramic abrasives on all samples.
- Continuous Ca/P dissolution over 3 weeks confirms that the treatment did stay on the treated surfaces for this period of time, thus indicating the possibility of using bioceramic air abrasion to treat peri-implantitis in order to enhance the osteoconductivity of implant surfaces. Further analysis of dissolution behaviour using larger groups and different solutions is needed to confirm the effect of the bioceramic air abrasion and its dissolution.

Chapter 7

General Discussion, Conclusions and Future Work

7.1 General discussion

Over the last two decades, the demand to replace missing teeth with dental implants has increased significantly (Buser *et al.*, 2017). The need to replace missing teeth continues to grow and is partly due to the increase in life expectancy and an aging population. This, in turn, generates higher expectations for the performance and longevity of dental implants. As a result, research has been directed towards developing different implant systems to help clinicians in choosing the optimum implant design, material type and surface for each treatment need.

The selection of a dental implant is dependent on the material, surface characteristics, and geometry. The ideal dental implant material should be inert and biocompatible, have enhanced mechanical and chemical properties, as well as superior wear and corrosion resistance, and have sufficient strength and elastic modulus (Ananth *et al.*, 2015). To date, commercially pure titanium and its alloys are the material of choice and fulfil most of these requirements.

Numerous studies have been conducted on commercially pure titanium and its alloys. Although they have been considered the gold standard for dental implant material, they still have some limitations. Commercially pure titanium has a higher elastic modulus compared to bone, and lower strength, whereas the most commonly used titanium alloy (Ti-6Al-4V) with enhanced mechanical properties can cause a toxic effect due to the presence of aluminium and vanadium (Elias *et al.*, 2015). To overcome these limitations, other alloying elements have been suggested. However, the only alloy in the dental implant field that has been marketed and used in the fabrication of dental implants is the TiZr alloy (Roxolid®).

The host response to an implant is governed by the nature of its surface and properties. Therefore, to ensure the clinical success of an implant, research is directed towards enhancing the surface properties including the surface topography, chemistry, surface energy, and bioactivity (Bruschi *et al.*, 2015).

With the above knowledge in mind, the work conducted in this thesis investigated the effect of implant material and surface modifications on selected surface and mechanical properties. The selected implant materials and surfaces were chosen from the systems available in the market.

The biological response to dental implants is driven by their ability to form a firm contact with bone (osseointegration). For this to take place, several biological and biomechanical factors need to be considered; some are related to the patient, while others are related to the implant or surgical procedure (Porter and Von Fraunhofer, 2005). Patient age and the presence of systemic conditions could jeopardise the bone quality and quantity (Schimmel *et al.*, 2017), elderly patients with severely resorbed alveolar ridges are one of the major groups that are in need of implants to support their dentures (Srinivasan *et al.*, 2017).

Nowadays, the rehabilitation of elderly patients with an implant-supported overdenture is a routine treatment (Thomason *et al.*, 2009). These cases are often in need of narrow and shorter implants to fit their ridges. Furthermore, they require implants made of a material with higher mechanical strength to withstand mechanical occlusal loads. The advances in dental implant alloys have led to the introduction of TiZr implants that fulfil these requirements. Their clinical success is well documented in the literature (Grandin *et al.*, 2012; Altuna *et al.*, 2016; Badran *et al.*, 2017; Iegami *et al.*, 2017).

The effect of the alloy material was observed in the mechanical testing (hardness and elastic modulus) in this thesis (Chapter 4). The TiZr alloy showed slightly higher hardness and lower elastic modulus than CpTi when the same modification was applied to different bulk materials at the nano and micro-nano levels. This is in line with previous studies, confirming the increased hardness and lower elastic modulus associated with the addition of zirconia (Grandin *et al.*, 2012). Therefore, this supports the use of TiZr alloy as a bulk material when the implant size and length are crucial. Nevertheless, the osseointegration of TiZr alloy as a material irrespective of the surface treatment was not reported to be significantly different from commercially pure titanium (Gottlow *et al.*, 2012; Saulacic *et al.*, 2012; Galli *et al.*, 2017).

The micro-nanoindentation and nanoindentation experiments demonstrated comparable results, especially in relation to the hardness measurements (Chapter 4) (Table 4.5). Therefore, micro-nanoindentation evaluation could be an alternative to conventional nanoindentation instruments, as the former is compact, fast, and cost effective.

Efforts are focused around enhancing, accelerating and maintaining osseointegration for as long as possible, this has been well documented *in-vivo* and *in-vitro* to be related to implant surface modifications (Novaes Jr *et al.*, 2010; Gittens *et al.*, 2013; Bosshardt *et al.*, 2017). The most important influence that results from the surface modifications is the change in surface topography. This was clearly seen in the different surface roughness measurements obtained in this study (Tables 3.2 & 3.3) and the 3D images presented in Chapter 3 (Figures 3.5–3.15). The results of this study demonstrated that surface modifications significantly affected the surface roughness of the tested materials. Moreover, further changes in the surface roughness was noted when the bioceramic treatment was applied to the previously modified samples in Chapter 5 (Tables 5.4 & 5.5).

Research has demonstrated that rough surfaces enhance cell adhesion, adsorption, and differentiation (Raines *et al.*, 2010). Thus, the aim of the studies in Chapters 3 and 5 was to assess the effect of the implant material and surface modification on the level of surface roughness, in order to predict its behaviour after implantation. However, the optimum level of surface roughness has not been specified in the literature. Most implant systems available in the market are moderately rough with an S_a of 1–2 µm. It was reported that implants with this level of roughness could behave better *in-vivo* than other surfaces, although these results are not considered to be statistically significant (Albrektsson and Wennerberg, 2004).

A recent study suggested that moderately rough surfaces showed the most favourable results in terms of osteoblast cell proliferation. Nevertheless, the same study did not conclude any significant effect of increased R_a up to 4 µm on osteoblast cells differentiation or proliferation (Andrukhov *et al.*, 2016). Generally, higher S_a values were noted in this study in Chapter 3 (Table 3.2) than the values reported in the literature for the same surfaces, where the S_a range was 1.14–3.70 µm. This could be attributed to the different filters and machines used or scanning errors. When looking at CpC, which is a machined surface and considered a minimally rough surface, the S_a value in this study revealed this to be a rough surface. This could be related to the grooves on its surface (see Figure 3.5) that represent the manufacturing process (Elias *et al.*, 2008), or other factors related to the machining process. However, as demonstrated in this thesis (Chapters 3 & 5), the S_a and R_a values give a general description of the surface roughness, while further analysis of the surface using other roughness parameters provides more details about the surface.

Most of the studies in the literature used flat discs to obtain the S_a and R_a values, although surface roughness values obtained from measuring flat discs are significantly different when compared to those measured on implants, as the threads on the implant surface give different values than flat discs (Barbosa *et al.*, 2017). Furthermore, the different measuring methods and filters used gave statistically different results (Matteson *et al.*, 2016; Kournetas *et al.*, 2017).

Over the years, the continuous development in implant surface modifications has reduced the healing times and accelerated osseointegration, thus enabling the operator to load the implant early or even immediately without the need to wait for the conventional loading times. However, the implant surface properties should be optimised to ensure fast and successful osseointegration (Morton and Pollini, 2017).

The SLA and SLActive surfaces in particular show better results in both human and animal studies when compared to other surfaces (Raines *et al.*, 2010; Lang *et al.*, 2011b; Van Velzen *et al.*, 2015; Hicklin *et al.*, 2016; Alayan *et al.*, 2017). Recent research has shown that both Ti and TiZr alloys with SLActive surfaces induce rapid osteoblast differentiation (Kaluđerović *et al.*, 2017). This enhanced host response is attributed to the hydrophilicity of the SLActive surfaces. This reflects that the surface modification is more important than the material in respect to osseointegration. Therefore, a titanium implant could be as effective as a TiZr implant when having the same surface treatment.

In this study (Chapter 3), when comparing the hydrophilic and hydrophobic surfaces in terms of surface roughness (Table 3.2), this property did not have a significant effect on the surface roughness.

Another way of stimulating tissue responses and increasing primary stability after implant placement is by using bioceramic coatings on the titanium surface (Strnad *et al.*, 2000; Zhou *et al.*, 2011). Over the years, several attempts have been made to deposit HA coatings on titanium surfaces. However, these coatings had the disadvantage of being thick and dissolving quickly after implantation, leaving a gap at the bone-implant interface. This subsequently leads to implant failure (Sun *et al.*, 2001). Alternatively, other methods to produce thin stable bioactive coatings have been suggested. One of these methods is air abrasion of bioceramic coatings on titanium surfaces.

Implant treatment could fail due to peri-implant disease; if the disease is not resolved it might lead to the loss of osseointegration, as well as implant mobility and loss. Polishing and decontamination of the implant surface are needed as a first attempt to resolve the inflammatory condition. Applying a treatment to the implant surface that is able to clean and produce a surface with enhanced osseoconductive properties could potentially help in the treatment. The aim of the studies in Chapters 5 and 6 was to assess the effect of air abrasion with a bioceramic abrasive on different implant materials and surfaces. The air abrasion method was successful in depositing the bioceramic treatment on the tested surfaces. This was accompanied by a change in the surface characteristics (i.e. surface roughness and composition). Meanwhile, by observing the dissolution of this treatment it was shown that it continuously released over the 3 week testing period. However, this behaviour was tested in deionised water, and further research will be required to determine whether this will also occur when in the oral environment.

With the abundance of implant systems with different bulk materials and surface modifications, the selection of the implant is driven by the clinical situation. The type and amount of bone available will determine the geometry of the implant, and after that the

implant material will be chosen according to the biomechanical needs. Recent studies recommend the selection of an implant to be based on implant design (El-Anwar *et al.*, 2017), or the load it will be exposed to (Kumararama and Chowdhary, 2017).

Within the limitations of this thesis, it is recommended that when enhanced mechanical properties are needed, the TiZr alloy might be the most favourable choice, as it has shown increased hardness and decreased elastic modulus compared to CpTi. In terms of surface roughness, different surface modifications produce different levels of surface roughness. It could not be concluded whether one surface is better than the other in terms of surface roughness. In addition, a bioceramic-treated surface could be an option to enhance the surface properties and bioactivity, although animal and clinical testing are required to confirm this. In an ideal clinical situation, surface-treated CpTi or TiZr implants could be successfully used. According to the literature, no surface has been reported to be superior over another (Esposito *et al.*, 2014; Coe, 2017).

In summary, there is no optimal implant material or surface treatment. However, implant selection should be based on maximum strength, load resistance and osseointegration ability, which can be altered by using different materials and surface modification.

7.2 Conclusions

- The average 3D surface roughness parameter S_a was significantly affected by the combined effect of material composition and surface modification.
- Irrespective of the manufacturer surface modification, different alloys (CpTi and TiZr) showed significant differences in the 3D surface roughness parameters (S_p, and S_v).
- 2D parameters (R_a, R_p, and R_v) were significantly influenced by the surface modification, alloy and their interaction.
- Nanoindentation and micro-nanoindentation methods could detect the different effects of manufacturer processing on the sub-surface elastic modulus and hardness at nano and micro-nano levels.
- The variation in material composition with the same surface modification, or the variation of both material and manufacturer processing could have a significant effect on the sub-surface elastic modulus and hardness at both nano and micro-nano levels. Furthermore, the manufacturer processing produced a significant effect on the sub-surface elastic modulus and hardness of the same material at the micro-nano level.
- Air abrasion did embed the bioceramic abrasives on CpTi and TiZr surfaces, with a minimal change in the surface characteristics.
- Dissolution of Ca^{2+} and PO_4^{3+} from the bioceramic-treated samples confirmed the stability and the continuous release of the bioceramic treatment over 3 weeks.

7.3 Future work

The following research is suggested for future work:

- Investigation of the effect of different implant materials and surface modifications on fatigue and corrosion properties.
- Assess the correlation between fatigue crack propagation, and the elastic modulus and hardness.
- Assess the effect of air abrasion with bioceramic powders *in-vivo* to confirm the possibility of applying it to infected dental implant surfaces.
- Evaluate the effect of using different air abrasion parameters and powders on the characteristics of implant surfaces.

References

Abrahamsson, I., Berglundh, T., Linder, E., Lang, N. P. & Lindhe, J. (2004). Early bone formation adjacent to rough and turned endosseous implant surfaces. *Clinical Oral Implants Research,* 15(4)**,** 381-392.

Abtahi, J., Henefalk, G. & Aspenberg, P. (2016). Randomised trial of bisphosphonate-coated dental implants: radiographic follow-up after five years of loading. *International Journal of Oral & Maxillofacial Surgery,* 45(12)**,** 1564-1569.

Abtahi, J., Tengvall, P. & Aspenberg, P. (2010). Bisphosphonate coating might improve fixation of dental implants in the maxilla: a pilot study. *International Journal of Oral and Maxillofacial Surgery,* 39(7)**,** 673-677.

Abtahi, J., Tengvall, P. & Aspenberg, P. (2012). A bisphosphonate-coating improves the fixation of metal implants in human bone. A randomized trial of dental implants. *Bone,* 50(5)**,** 1148-1151.

Adell, R., Lekholm, U., Rockler, B. & Brånemark, P. I. (1981). A 15-year study of osseointegrated implants in the treatment of the edentulous jaw. *International Journal of Oral Surgery,* 10(6)**,** 387-416.

Agarwal, R. & García, A. J. (2015). Biomaterial strategies for engineering implants for enhanced osseointegration and bone repair. *Advanced Drug Delivery Reviews,* 94**,** 53-62.

Ahn, S., Vang, M.-S., Yang, H.-S., Park, S.-W. & Lim, H.-P. (2009). Histologic evaluation and removal torque analysis of nano-and microtreated titanium implants in the dogs. *Journal of Advanced Prosthodontics,* 1(2)**,** 75-84.

Al-Nawas, B., Domagala, P., Fragola, G., Freiberger, P., Ortiz-Vigón, A., Rousseau, P. & Tondela, J. (2015). A prospective noninterventional study to evaluate survival and success of reduced diameter implants made from titanium-zirconium alloy. *Journal of Oral Implantology,* 41(4)**,** e118-e125.

Al-Sabbagh, M. & Bhavsar, I. (2015). Key local and surgical factors related to implant failure. *Dental Clinics,* 59(1)**,** 1-23.

Al-Amleh, B., Lyons, K. & Swain, M. (2010). Clinical trials in zirconia: a systematic review. *Journal of Oral Rehabilitation,* 37(8)**,** 641-652.

Al-Nawas, B., Brägger, U., Meijer, H. J., Naert, I., Persson, R., Perucchi, A., Quirynen, M., Raghoebar, G. M., Reichert, T. E. & Romeo, E. (2012). A double-blind randomized controlled trial (RCT) of Titanium-13 Zirconium versus Titanium Grade IV small-diameter bone level implants in edentulous mandibles–results from a 1-year observation period. *Clinical Implant Dentistry and Related Research,* 14(6)**,** 896-904.

Alayan, J., Vaquette, C., Saifzadeh, S., Hutmacher, D. & Ivanovski, S. (2017). Comparison of early osseointegration of SLA® and SLActive® implants in maxillary sinus augmentation: a pilot study. *Clinical Oral Implants Research,* 28(11)**,** 1325-1333

Albertini, M., López-Cerero, L., O'sullivan, M. G., Chereguini, C. F., Ballesta, S., Ríos, V., Herrero-Climent, M. & Bullón, P. (2015). Assessment of periodontal and opportunistic flora in patients with peri-implantitis. *Clinical Oral Implants Research,* 26(8)**,** 937-941

Albrektsson, T., Brånemark, P.-I., Hansson, H.-A. & Lindström, J. (1981). Osseointegrated titanium implants: requirements for ensuring a long-lasting, direct bone-to-implant anchorage in man. *Acta Orthopaedica,* 52(2)**,** 155-170.

Albrektsson, T., Chrcanovic, B., , J., M & , W., A (2017a). Osseointegration of implants - A biological and clinical overview. *Journal of Science Medical,* 2(3)**,** 1022-1027.

Albrektsson, T., Chrcanovic, B., Östman, P. O. & Sennerby, L. (2017b). Initial and long-term crestal bone responses to modern dental implants. *Periodontology 2000,* 73(1)**,** 41-50.

Albrektsson, T. & Johansson, C. (2001). Osteoinduction, osteoconduction and osseointegration. *European Spine Journal,* 10(2)**,** S96-S101.

Albrektsson, T. & Wennerberg, A. (2003). Oral implant surfaces: Part 2-review focusing on clinical knowledge of different surfaces. *International Journal of Prosthodontics,* 17(5)**,** 544-564.

Albrektsson, T. & Wennerberg, A. (2004). Oral implant surfaces: Part 1-review focusing on topographic and chemical properties of different surfaces and in vivo responses to them. *International Journal of Prosthodontics,* 17(5)**,** 536-543.

Albrektsson, T. & Zarb, G. (1993). Current interpretations of the osseointegrated response: clinical significance. *International Journal of Prosthodontics,* 6(2)**,** 95-105.

Albrektsson, T., Zarb, G., Worthington, P. & Eriksson, A. (1986). The long-term efficacy of currently used dental implants: a review and proposed criteria of success. *International Journal of Oral & Maxillofacial Implants,* 1(1)**,** 11-25.

Albrektsson, T. O., Johansson, C. B. & Sennerby, L. (1994). Biological aspects of implant dentistry: osseointegration. *Periodontology 2000,* 4(1)**,** 58-73.

Alenezi, A., Chrcanovic, B. & Wennerberg, A. (2018). Effects of Local Drug and Chemical Compound Delivery on Bone Regeneration Around Dental Implants in Animal Models: a systematic review and meta-analysis. *International Journal of Oral & Maxillofacial Implants,* 33(1)**,** e1-e18.

AlFarraj, A. A., Sukumaran, A., Al Amri, M. D., Van Oirschot, A. B. & Jansen, J. A. (2018). A comparative study of the bone contact to zirconium and titanium implants after 8 weeks of implantation in rabbit femoral condyles. *Odontology,* 106(1)**,** 37-44.

Alhag, M., Renvert, S., Polyzois, I. & Claffey, N. (2008). Re-osseointegration on rough implant surfaces previously coated with bacterial biofilm: an experimental study in the dog. *Clinical Oral Implants Research,* 19(2)**,** 182-187.

Allum, S. R., Tomlinson, R. A. & Joshi, R. (2008). The impact of loads on standard diameter, small diameter and mini implants: a comparative laboratory study. *Clinical Oral Implants Research,* 19(6)**,** 553-559.

Alsaadi, G., Quirynen, M., Komárek, A. & Van Steenberghe, D. (2007). Impact of local and systemic factors on the incidence of oral implant failures, up to abutment connection. *Journal of Clinical Periodontology,* 34(7)**,** 610-617.

Altuna, P., Lucas-Taulé, E., Gargallo-Albiol, J., Figueras-Álvarez, O., Hernández-Alfaro, F. & Nart, J. (2016). Clinical evidence on titanium–zirconium dental implants: a systematic review and meta-analysis. *International Journal of Oral and Maxillofacial Surgery,* 45(7)**,** 842-850.

Ananth, H., Kundapur, V., Mohammed, H., Anand, M., Amarnath, G. & Mankar, S. (2015). A review on biomaterials in dental implantology. *International Journal of Biomedical Science,* 11(3)**,** 113-120.

Anchieta, R. B., Baldassarri, M., Guastaldi, F., Tovar, N., Janal, M. N., Gottlow, J., Dard, M., Jimbo, R. & Coelho, P. G. (2013). Mechanical property assessment of bone healing around a Titanium–Zirconium alloy dental implant. *Clinical Implant Dentistry and Related Research,* 16(6)**,** 913-919.

Andrukhov, O., Huber, R., Shi, B., Berner, S., Rausch-Fan, X., Moritz, A., Spencer, N. D. & Schedle, A. (2016). Proliferation, behavior, and differentiation of osteoblasts on surfaces of different microroughness. *Dental Materials,* 32(11)**,** 1374-1384.

Anil, S., Anand, P., Alghamdi, H. & Jansen, J. (2011). Dental implant surface enhancement and osseointegration, *In:* Turkyilmaz, I. (ed.) *Implant dentistry-A rapidly evolving practice.* Croatia: In Tech Open Access Publisher, 83-108. [Online]. Available: https://www.intechopen.com/books/implant-dentistry-a-rapidly-evolving-practice/dental-implant-surface-enhancement-and-osseointegration.

Anitua, E., Tapia, R., Luzuriaga, F. & Orive, G. (2010). Influence of implant length, diameter, and geometry on stress distribution: a finite element analysis. *International Journal of Periodontics & Restorative Dentistry,* 30(1)**,** 89-95.

Anselme, K. & Bigerelle, M. (2005). Topography effects of pure titanium substrates on human osteoblast long-term adhesion. *Acta Biomaterialia,* 1(2)**,** 211-222.

Anselme, K., Ponche, A., Bigerelle, M., Tanner, K. E. & Dalby, M. J. (2010). Relative influence of surface topography and surface chemistry on cell response to bone implant materials. Part 2: Biological aspects. *Proceedings of the Institution of Mechanical Engineers.,* 224(12)**,** 1487-1507.

Antoun, H., Karouni, M., Abitbol, J., Zouiten, O. & Jemt, T. (2017). A retrospective study on 1592 consecutively performed operations in one private referral clinic. Part I: Early inflammation and early implant failures. *Clinical Implant Dentistry and Related Research,* 19(3)**,** 404-412.

Aparicio, C., Javier Gil, F., Fonseca, C., Barbosa, M. & Planell, J. A. (2003). Corrosion behaviour of commercially pure titanium shot blasted with different materials and sizes of shot particles for dental implant applications. *Biomaterials,* 24(2)**,** 263-273.

Aparicio, C., Padrós, A. & Gil, F.-J. (2011). In vivo evaluation of micro-rough and bioactive titanium dental implants using histometry and pull-out tests. *Journal of the Mechanical Behavior of Biomedical Materials,* 4(8)**,** 1672-1682.

Artzi, Z., Carmeli, G. & Kozlovsky, A. (2006). A distinguishable observation between survival and success rate outcome of hydroxyapatite-coated implants in 5–10 years in function. *Clinical Oral Implants Research,* 17(1)**,** 85-93.

Arısan, V., Bölükbaşı, N., Ersanlı, S. & Özdemir, T. (2010). Evaluation of 316 narrow diameter implants followed for 5–10 years: a clinical and radiographic retrospective study. *Clinical Oral Implants Research,* 21(3)**,** 296-307.

Åstrand, P., Engquist, B., Anzén, B., Bergendal, T., Hallman, M., Karlsson, U., Kvint, S., Lysell, L. & Rundcranz, T. (2004). A three-year follow-up report of a comparative study of ITI dental implants® and Brånemark system® implants in the treatment of the partially edentulous maxilla. *Clinical Implant Dentistry and Related Research,* 6(3)**,** 130-141.

Atsuta, I., Ayukawa, Y., Kondo, R., Oshiro, W., Matsuura, Y., Furuhashi, A., Tsukiyama, Y. & Koyano, K. (2016). Soft tissue sealing around dental implants based on histological interpretation. *Journal of Prosthodontic Research,* 60(1)**,** 3-11.

Augthun, M., Tinschert, J. & Huber, A. (1998). In vitro studies on the effect of cleaning methods on different implant surfaces. *Journal of Periodontology,* 69(8)**,** 857-864.

Avila, G., Misch, K., Galindo-Moreno, P. & Wang, H.-L. (2009). Implant surface treatment using biomimetic agents. *Implant Dentistry,* 18(1)**,** 17-26.

Ayllón, J. M., Navarro, C., Vázquez, J. & Domínguez, J. (2014). Fatigue life estimation in dental implants. *Engineering Fracture Mechanics,* 123**,** 34-43.

Ayukawa, Y., Ogino, Y., Moriyama, Y., Atsuta, I., Jinno, Y., Kihara, M., Tsukiyama, Y. & Koyano, K. (2010). Simvastatin enhances bone formation around titanium implants in rat tibiae. *Journal of Oral Rehabilitation,* 37(2)**,** 123-130.

Ayukawa, Y., Okamura, A. & Koyano, K. (2004). Simvastatin promotes osteogenesis around titanium implants: a histological and histometrical study in rats. *Clinical Oral Implants Research,* 15(3)**,** 346-350.

Azari, A., Jamnani, S. N., Yazdani, A., Atri, F., Rasaie, V. & Yazdi, A. F. A. (2017). Deposition of crystalline hydroxyapatite nanoparticles on Y-TZP ceramic: a potential solution to enhance bonding characteristics of Y-TZP ceramics. *Journal of Dentistry,* 14(2)**,** 62-68.

Bächle, M. & Kohal, R. J. (2004). A systematic review of the influence of different titanium surfaces on proliferation, differentiation and protein synthesis of osteoblast-like MG63 cells. *Clinical Oral Implants Research,* 15(6)**,** 683-692.

Badran, Z., Struillou, X., Strube, N., Bourdin, D., Dard, M., Soueidan, A. & Hoornaert, A. (2017). Clinical performance of narrow-diameter Titanium-Zirconium implants: a systematic review. *Implant Dentistry,* 26(2)**,** 316-323.

Bagno, A. & Di Bello, C. (2004). Surface treatments and roughness properties of Ti-based biomaterials. *Journal of Materials Science: Materials in Medicine,* 15(9)**,** 935-949.

Baker, M. I., Eberhardt, A., Martin, D., McGwin, G. & Lemons, J. (2010). Bone properties surrounding hydroxyapatite-coated custom osseous integrated dental implants. *Journal of Biomedical Materials Research Part B: Applied Biomaterials,* 95(1)**,** 218-224.

Baqain, Z. H., Moqbel, W. Y. & Sawair, F. A. (2012). Early dental implant failure: risk factors. *British Journal of Oral and Maxillofacial Surgery,* 50(3)**,** 239-243.

Barbosa, T. P., Naves, M. M., Menezes, H. H. M., Pinto, P. H. C., de Mello, J. D. B. & Costa, H. L. (2017). Topography and surface energy of dental implants: a methodological approach. *Journal of the Brazilian Society of Mechanical Sciences and Engineering,* 39(6)**,** 1895-1907.

Barfeie, A., Wilson, J. & Rees, J. (2015). Implant surface characteristics and their effect on osseointegration. *British Dental Journal,* 218(5)**,** e9-e9.

Barros, R. R., Novaes Jr, A. B., Papalexiou, V., Souza, S. L., Taba Jr, M., Palioto, D. B. & Grisi, M. F. (2009). Effect of biofunctionalized implant surface on osseointegration: a histomorphometric study in dogs. *Brazilian Dental Journal,* 20(2)**,** 91-98.

Barry, J., Twomey, B., Cowley, A., O'Neill, L., McNally, P. & Dowling, D. (2013). Evaluation and comparison of hydroxyapatite coatings deposited using both thermal and non-thermal techniques. *Surface and Coatings Technology,* 226(15)**,** 82-91.

Barter, S., Stone, P. & Brägger, U. (2012). A pilot study to evaluate the success and survival rate of titanium–zirconium implants in partially edentulous patients: results after 24 months of follow-up. *Clinical Oral Implants Research,* 23(7)**,** 873-881.

Bataineh, A. B. & Al-dakes, A. M. (2017). The influence of length of implant on primary stability: An in vitro study using resonance frequency analysis. *Journal of Clinical and Experimental Dentistry,* 9(1)**,** e1-e6.

Bennani, V., Hwang, L., Tawse-Smith, A., Dias, G. J. & Cannon, R. D. (2015). Effect of air-polishing on titanium surfaces, biofilm removal, and biocompatibility: a pilot study. *BioMed Research International,* 2015. Article ID 491047.

Bergendal, T., Forsgren, L., Kvint, S. & Löwstedt, E. (1990). The effect of an airbrasive instrument on soft and hard tissues around osseointegrated implants. A case report. *Swedish Dental Journal,* 14(5)**,** 219-223.

Berglundh, T., Abrahamsson, I., Lang, N. P. & Lindhe, J. (2003). De novo alveolar bone formation adjacent to endosseous implants. *Clinical Oral Implants Research,* 14(3)**,** 251-262.

Berglundh, T., Armitage, G., Araujo, M. G., Avila-Ortiz, G., Blanco, J., Camargo, P. M., Chen, S., Cochran, D., Derks, J., Figuero, E., Hämmerle, C. H. F., Heitz-Mayfield, L. J. A., Huynh-Ba, G., Iacono, V., Koo, K.-T., Lambert, F., McCauley, L., Quirynen, M., Renvert, S., Salvi, G. E., Schwarz, F., Tarnow, D., Tomasi, C., Wang, H.-L. & Zitzmann, N. (2018). Peri-implant diseases and conditions: consensus report of workgroup 4 of the 2017 World Workshop on the Classification of Periodontal and Peri-Implant Diseases and Conditions. *Journal of Clinical Periodontology,* 45(s20)**,** s286-s291.

Biasotto, M., Sandrucci, M., Antoniolli, F., Stebel, M., Grill, V., Di Lenarda, R. & Dorigo, E. (2005). Titanium implants with two different surfaces: histomorphologic and histomorphometric evaluation in rabbit tibia. *Journal of Applied Biomaterials and Biomechanics,* 3(3)**,** 168-175.

Block, M. S. (2018). Dental Implants: The Last 100 Years. *Journal of Oral and Maxillofacial Surgery,* 76(1)**,** 11-26.

Bornstein, M. M., Halbritter, S., Harnisch, H., Weber, H.-P. & Buser, D. (2008a). A retrospective analysis of patients referred for implant placement to a specialty clinic: indications, surgical procedures, and early failures. *International Journal of Oral and Maxillofacial Implants,* 23(6)**,** 1109-1116.

Bornstein, M. M., Schmid, B., Belser, U. C., Lussi, A. & Buser, D. (2005). Early loading of non-submerged titanium implants with a sandblasted and acid-etched surface. *Clinical Oral Implants Research,* 16(6)**,** 631-638.

Bornstein, M. M., Valderrama, P., Jones, A. A., Wilson, T. G., Seibl, R. & Cochran, D. L. (2008b). Bone apposition around two different sandblasted and acid-etched titanium implant surfaces: a histomorphometric study in canine mandibles. *Clinical Oral Implants Research,* 19(3)**,** 233-241.

Bosshardt, D. D., Chappuis, V. & Buser, D. (2017). Osseointegration of titanium, titanium alloy and zirconia dental implants: current knowledge and open questions. *Periodontology 2000,* 73(1)**,** 22-40.

Botero, J. E., González, A. M., Mercado, R. A., Olave, G. & Contreras, A. (2005). Subgingival microbiota in peri-implant mucosa lesions and adjacent teeth in partially edentulous patients. *Journal of Periodontology,* 76(9)**,** 1490-1495.

Botos, S., Yousef, H., Zweig, B., Flinton, R. & Weiner, S. (2011). The effects of laser microtexturing of the dental implant collar on crestal bone levels and peri-implant health. *International Journal of Oral & Maxillofacial Implants,* 26(3)**,** 492-498.

Boyan, B., Bonewald, L., Paschalis, E., Lohmann, C., Rosser, J., Cochran, D., Dean, D., Schwartz, Z. & Boskey, A. (2002). Osteoblast-mediated mineral deposition in culture is dependent on surface microtopography. *Calcified Tissue International,* 71(6)**,** 519-529.

Boyan, B., Cheng, A., Olivares-Navarrete, R. & Schwartz, Z. (2016). Implant surface design regulates mesenchymal stem cell differentiation and maturation. *Advances in Dental Research,* 28(1)**,** 10-17.

Boyan, B. D., Dean, D. D., Lohmann, C. H., Cochran, D. L., Sylvia, V. L. & Schwartz, Z. (2001). The titanium-bone cell interface in vitro: the role of the surface in promoting osteointegration, *In:* Brunette, D., Tengvall, P., Textor, M. & Thomsen, P. (eds.) *Titanium in medicine: material science, surface science, engineering, biological responses and medical applications.* Berlin: Springer, 561-585. [Online]. Available: https://doi.org/10.1007/978-3-642-56486-4_17.

Boyan, B. D., Hummert, T. W., Dean, D. D. & Schwartz, Z. (1996). Role of material surfaces in regulating bone and cartilage cell response. *Biomaterials,* 17(2)**,** 137-146.

Boyne, P. & Jones, S. D. (2004). Demonstration of the Osseoinductive Effect of Bone Morphogenetic Protein Within Endosseous Dental Implants. *Implant Dentistry,* 13(2)**,** 180-184.

Braem, A., Chaudhari, A., Vivan Cardoso, M., Schrooten, J., Duyck, J. & Vleugels, J. (2014). Peri- and intra-implant bone response to microporous Ti coatings with surface modification. *Acta Biomaterialia,* 10(2)**,** 986-995.

Braga, F. J., Marques, R. F., de A Filho, E. & Guastaldi, A. C. (2007). Surface modification of Ti dental implants by Nd: YVO4 laser irradiation. *Applied Surface Science,* 253(23)**,** 9203-9208.

Branemark, P.-I. (1983). Osseointegration and its experimental background. *Journal of Prosthetic Dentistry,* 50(3)**,** 399-410.

Breme, H., Biehl, V., Reger, N. & Gawalt, E. (2016). Metallic biomaterials: titanium and titanium alloys, *In:* Murphy, W., Black, J. & Hastings, G. W. (eds.) *Handbook of biomaterial properties.* Second ed. New York: Springer, 167-189. [Online]. Available: https://doi.org/10.1007/978-1-4939-3305-1_16.

Briggs, D. (1990). A perspective on the analysis of surfaces and interfaces. *In:* Briggs, D. & Seah, M. (eds.) *Practical surface analysis: auger and X-ray photoelectron spectroscopy volume 1.* Second ed. New York: John Wiley & Sons, 1-15.

Brizuela-Velasco, A., Pérez-Pevida, E., Jiménez-Garrudo, A., Gil-Mur, F. J., Manero, J. M., Punset-Fuste, M., Chávarri-Prado, D., Diéguez-Pereira, M. & Monticelli, F. (2017). Mechanical characterisation and biomechanical and biological behaviours of Ti-Zr binary-alloy dental implants. *BioMed Research International,* 2017**,** 1-10. Article ID 2785863.

Brizuela, A., Herrero-Climent, M., Rios-Carrasco, E., Rios-Santos, J. V., Pérez, R. A., Manero, J. M. & Gil Mur, J. (2019). Influence of the elastic modulus on the osseointegration of dental implants. *Materials,* 12(6)**,** 980.

Bruschi, M., Steinmüller-Nethl, D., Goriwoda, W. & Rasse, M. (2015). Composition and modifications of dental implant surfaces. *Journal of Oral Implants,* 2015**,** 1-14. Article ID 527426.

Buser, D., Broggini, N., Wieland, M., Schenk, R., Denzer, A., Cochran, D., Hoffmann, B., Lussi, A. & Steinemann, S. (2004). Enhanced bone apposition to a chemically modified SLA titanium surface. *Journal of Dental Research,* 83(7)**,** 529-533.

Buser, D., Schenk, R., Steinemann, S., Fiorellini, J., Fox, C. & Stich, H. (1991). Influence of surface characteristics on bone integration of titanium implants. A histomorphometric study in miniature pigs. *Journal of Biomedical Materials Research,* 25(7)**,** 889-902.

Buser, D., Sennerby, L. & De Bruyn, H. (2017). Modern implant dentistry based on osseointegration: 50 years of progress, current trends and open questions. *Periodontology 2000,* 73(1)**,** 7-21.

Busscher, H., Rinastiti, M., Siswomihardjo, W. & Van der Mei, H. (2010). Biofilm formation on dental restorative and implant materials. *Journal of Dental Research,* 89(7)**,** 657-665.

Butz, F., Aita, H., Wang, C. & Ogawa, T. (2006). Harder and stiffer bone osseointegrated to roughened titanium. *Journal of Dental Research,* 85(6)**,** 560-565.

Cáceres, D., Munuera, C., Ocal, C., Jiménez, J. A., Gutiérrez, A. & López, M. (2008). Nanomechanical properties of surface-modified titanium alloys for biomedical applications. *Acta Biomaterialia,* 4(5)**,** 1545-1552.

Cafiero, C., Aglietta, M., Iorio-Siciliano, V., Salvi, G. E., Blasi, A. & Matarasso, S. (2017). Implant surface roughness alterations induced by different prophylactic procedures: an in vitro study. *Clinical Oral Implants Research,* 28(7)**,** e16-e20.

Calvo-Guirado, J. L., Aguilar-Salvatierra, A., Delgado-Ruiz, R. A., Negri, B., Fernández, M. P. R., Maté Sánchez de Val, J. E., Gómez-Moreno, G. & Romanos, G. E. (2013). Histological and histomorphometric evaluation of zirconia dental implants modified by femtosecond laser versus titanium implants: an experimental study in fox hound dogs. *Clinical Implant Dentistry and Related Research,* 17(3)**,** 525-532.

Campbell, A. A. (2003). Bioceramics for implant coatings. *Materials Today,* 6(11)**,** 26-30.

Caton, J. G., Armitage, G., Berglundh, T., Chapple, I. L., Jepsen, S., Kornman, K. S., Mealey, B. L., Papapanou, P. N., Sanz, M. & Tonetti, M. S. (2018). A new classification scheme for periodontal and peri-implant diseases and conditions–Introduction and key changes from the 1999 classification. *Journal of Periodontology,* 89(s1)**,** s1-s8.

Cattani-Lorente, M., Scherrer, S. S., Durual, S., Sanon, C., Douillard, T., Gremillard, L., Chevalier, J. & Wiskott, A. (2014). Effect of different surface treatments on the hydrothermal degradation of a 3Y-TZP ceramic for dental implants. *Dental Materials,* 30(10)**,** 1136-1146.

Cavalcanti, Y., Soare, R., Leite, A. M., Zenóbio, E. & Girundi, F. (2015). Titanium surface roughing treatments contribute to higher interaction with salivary proteins MG2 and Lactoferrin. *Journal of Contemporary Dental Practice,* 16(2)**,** 141-146.

Chairay, J. P., Boulekbache, H., Jean, A., Soyer, A. & Bouchard, P. (1997). Scanning electron microscopic evaluation of the effects of an air-abrasive system on dental implants: a comparative in vitro study between machined and plasma-sprayed titanium surfaces. *Journal of Periodontology,* 68(12)**,** 1215-1222.

Chambrone, L., Wang, H. L. & Romanos, G. E. (2018). Antimicrobial photodynamic therapy for the treatment of periodontitis and peri-implantitis: an american academy of periodontology best evidence review. *Journal of Periodontology,* 89(7)**,** 783-803.

Chan, H. L., Lin, G. H., Suarez, F., MacEachern, M. & Wang, H. L. (2014). Surgical management of peri-implantitis: a systematic review and meta-analysis of treatment outcomes. *Journal of Periodontology,* 85(8)**,** 1027-1041.

Chandar, S., Kotian, R., Madhyastha, P., Kabekkodu, S. P. & Rao, P. (2017). In vitro evaluation of cytotoxicity and corrosion behavior of commercially pure titanium and Ti-6Al-4V alloy for dental implants. *Journal of Indian Prosthodontic Society,* 17(1)**,** 35-40.

Chaturvedi, T. (2009). An overview of the corrosion aspect of dental implants (titanium and its alloys). *Indian Journal of Dental Research,* 20(1)**,** 91-98.

Chen, X., Li, Y. & Aparicio, C. (2013). Biofunctional coatings for dental implants. *In:* Nazarpour, S. & Chaker, M. (eds.) *Thin films and coatings in biology. Biological and medical physics, biomedical engineering.* Dordrecht: Springer, 105-143.

Chen, X. & Mao, S. S. (2007). Titanium dioxide nanomaterials: synthesis, properties, modifications, and applications. *Chemical Reviews,* 107(7)**,** 2891-2959.

Chen, X., Nouri, A., Li, Y., Lin, J., Hodgson, P. D. & Wen, C. (2008). Effect of surface roughness of Ti, Zr, and TiZr on apatite precipitation from simulated body fluid. *Biotechnology and Bioengineering,* 101(2)**,** 378-387.

Cheng, L. L. (2016). Limited evidence suggests higher risk of dental implant failures in smokers than in nonsmokers. *Journal of the American Dental Association,* 147(4)**,** 292-294.

Chiapasco, M., Casentini, P., Zaniboni, M., Corsi, E. & Anello, T. (2012). Titanium–zirconium alloy narrow-diameter implants (Straumann Roxolid®) for the rehabilitation of horizontally deficient edentulous ridges: prospective study on 18 consecutive patients. *Clinical Oral Implants Research,* 23(10)**,** 1136-1141.

Chrcanovic, B. R., Albrektsson, T. & Wennerberg, A. (2014). Periodontally compromised vs. periodontally healthy patients and dental implants: a systematic review and meta-analysis. *Journal of Dentistry,* 42(12)**,** 1509-1527.

Chrcanovic, B. R., Albrektsson, T. & Wennerberg, A. (2015). Smoking and dental implants: a systematic review and meta-analysis. *Journal of Dentistry,* 43(5)**,** 487-498.

Chrcanovic, B. R., Kisch, J., Albrektsson, T. & Wennerberg, A. (2017). Bruxism and dental implant treatment complications: a retrospective comparative study of 98 bruxer patients and a matched group. *Clinical Oral Implants Research,* 28(7)**,** e1-e9.

Cionca, N., Hashim, D. & Mombelli, A. (2017). Zirconia dental implants: where are we now, and where are we heading? *Periodontology 2000,* 73(1)**,** 241-258.

Citeau, A., Guicheux, J., Vinatier, C., Layrolle, P., Nguyen, T. P., Pilet, P. & Daculsi, G. (2005). In vitro biological effects of titanium rough surface obtained by calcium phosphate grid blasting. *Biomaterials,* 26(2)**,** 157-165.

Claffey, N., Clarke, E., Polyzois, I. & Renvert, S. (2008). Surgical treatment of peri-implantitis. *Journal of Clinical Periodontology,* 35(s8)**,** 316-332.

Clark, D. & Levin, L. (2016). Dental implant management and maintenance: How to improve long-term implant success? *Quintessence International,* 47(5)**,** 417-423.

Cochran, D., Schenk, R., Lussi, A., Higginbottom, F. & Buser, D. (1998). Bone response to unloaded and loaded titanium implants with a sandblasted and acid-etched surface: a histometric study in the canine mandible. *Journal of Biomedical Materials Research,* 40(1)**,** 1-11.

Coe, J. M. (2017). Implant success does not differ significantly according to implant type. *Journal of the American Dental Association,* 148(1)**,** 52-53.

Coelho, P. G., Bonfante, E. A., Pessoa, R. S., Marin, C., Granato, R., Giro, G., Witek, L. & Suzuki, M. (2011). Characterization of five different implant surfaces and their effect on osseointegration: a study in dogs. *Journal of Periodontology,* 82(5)**,** 742-750.

Coelho, P. G., Cardaropoli, G., Suzuki, M. & Lemons, J. E. (2009). Early healing of nanothickness bioceramic coatings on dental implants. An experimental study in dogs. *Journal of Biomedical Materials Research Part B: Applied Biomaterials,* 88(2)**,** 387-393.

Coelho, P. G. & Lemons, J. E. (2009). Physico/chemical characterization and in vivo evaluation of nanothickness bioceramic depositions on alumina-blasted/acid-etched Ti-6Al-4V implant surfaces. *Journal of Biomedical Materials Research Part A: An Official Journal of The Society for Biomaterials, The Japanese Society for Biomaterials, and The Australian Society for Biomaterials and the Korean Society for Biomaterials,* 90(2)**,** 351-361.

Coelho, P. G. & Suzuki, M. (2005). Evaluation of an IBAD thin-film process as an alternative method for surface incorporation of bioceramics on dental implants: a study in dogs. *Journal of Applied Oral Science,* 13(1)**,** 87-92.

Comfort, M., Chu, F., Chai, J., Wat, P. & Chow, T. (2005). A 5-year prospective study on small diameter screw-shaped oral implants. *Journal of Oral Rehabilitation,* 32(5)**,** 341-345.

Conrad, H. J., Seong, W.-J. & Pesun, I. J. (2007). Current ceramic materials and systems with clinical recommendations: a systematic review. *Journal of Prosthetic Dentistry,* 98(5)**,** 389-404.

Cooper, L. F. (2000). A role for surface topography in creating and maintaining bone at titanium endosseous implants. *Journal of Prosthetic Dentistry,* 84(5)**,** 522-534.

Cooper, L. F., Zhou, Y., Takebe, J., Guo, J., Abron, A., Holmén, A. & Ellingsen, J. E. (2006). Fluoride modification effects on osteoblast behavior and bone formation at TiO_2 grit-blasted cp titanium endosseous implants. *Biomaterials,* 27(6)**,** 926-936.

Cordeiro, J. M. & Barão, V. A. R. (2017). Is there scientific evidence favoring the substitution of commercially pure titanium with titanium alloys for the manufacture of dental implants? *Materials Science and Engineering,* 71(Supplement C)**,** 1201-1215.

Cordeiro, J. M., Faverani, L. P., Grandini, C. R., Rangel, E. C., da Cruz, N. C., Junior, F. H. N., Almeida, A. B., Vicente, F. B., Morais, B. R. & Barão, V. A. (2018). Characterization of chemically treated Ti-Zr system alloys for dental implant application. *Materials Science and Engineering: C,* 92**,** 849-861.

Costerton, J., Montanaro, L. & Arciola, C. R. (2005). Biofilm in implant infections: its production and regulation. *The International Journal of Artificial Organs,* 28(11)**,** 1062-1068.

Cuy, J. L., Mann, A. B., Livi, K. J., Teaford, M. F. & Weihs, T. P. (2002). Nanoindentation mapping of the mechanical properties of human molar tooth enamel. *Archives of Oral Biology,* 47(4)**,** 281-291.

Czan, A., Babík, O., Miklos, M., Záušková, L. & Mezencevová, V. (2017). Assessment of surface area characteristics of dental implants with gradual bioactive surface treatment. *Technological Engineering,* 14(1)**,** 35-39.

Dai, X., Zhang, X., Xu, M., Huang, Y., Heng, B. C., Mo, X., Liu, Y., Wei, D., Zhou, Y. & Wei, Y. (2016). Synergistic effects of elastic modulus and surface topology of Ti-based implants on early osseointegration. *Royal Society of Chemisty Advances,* 6(49)**,** 43685-43696.

Darimont, G., Cloots, R., Heinen, E., Seidel, L. & Legrand, R. (2002). In vivo behaviour of hydroxyapatite coatings on titanium implants: a quantitative study in the rabbit. *Biomaterials,* 23(12)**,** 2569-2575.

Davarpanah, M., Martinez, H., Tecucianu, J. F., Celletti, R. & Lazzara, R. (2000). Small-diameter implants: Indications and contraindications. *Journal of Esthetic and Restorative Dentistry,* 12(4)**,** 186-194.

Davies, J. E. (2003). Understanding peri-implant endosseous healing. *Journal of Dental Education,* 67(8)**,** 932-949.

De Almeida, J. M., Matheus, H. R., Gusman, D. J. R., Faleiros, P. L., de Araújo, N. J. & Novaes, V. C. N. (2017). Effectiveness of mechanical debridement combined with adjunctive therapies for nonsurgical treatment of periimplantitis: a systematic review. *Implant Dentistry,* 26(1)**,** 137-144.

De Jonge, L. T., Leeuwenburgh, S. C. G., Wolke, J. G. C. & Jansen, J. A. (2008). Organic–Inorganic surface modifications for titanium implant surfaces. *Pharmaceutical Research,* 25(10)**,** 2357-2369.

De Maeztu, M., Braceras, I., Álava, J., Recio, C., Piñera, M. & Gay-Escoda, C. (2013). Human study of ion implantation as a surface treatment for dental implants. *International Journal of Oral and Maxillofacial Surgery,* 42(7)**,** 891-896.

De Maeztu, M. A., Alava, J. I. & Gay-Escoda, C. (2003). Ion implantation: surface treatment for improving the bone integration of titanium and Ti6Al4V dental implants. *Clinical Oral Implants Research,* 14(1)**,** 57-62.

De Mendonça, A. C., Santos, V. R., César-Neto, J. B. & Duarte, P. M. (2009). Tumor necrosis factor-alpha levels after surgical anti-infective mechanical therapy for peri-implantitis: a 12-month follow-up. *Journal of Periodontology,* 80(4)**,** 693-699.

De Queiroz Fernandes, J., de Lima, V. N., Bonardi, J. P., Filho, O. M. & Queiroz, S. B. F. (2018). Bone regeneration with recombinant human bone morphogenetic protein 2: a systematic review. *Journal of Maxillofacial and Oral Surgery,* 17(1)**,** 13-18.

De Souza, G., Foerster, C., Da Silva, S., Serbena, F., Lepienski, C. & Dos Santos, C. (2005). Hardness and elastic modulus of ion-nitrided titanium obtained by nanoindentation. *Surface and Coatings Technology,* 191(1)**,** 76-82.

Degidi, M., Piattelli, A. & Carinci, F. (2008). Clinical outcome of narrow diameter implants: a retrospective study of 510 implants. *Journal of Periodontology,* 79(1)**,** 49-54.

Del Fabbro, M., Taschieri, S., Canciani, E., Addis, A., Musto, F., Weinstein, R. & Dellavia, C. (2017). Osseointegration of titanium implants with different rough surfaces: a histologic and histomorphometric study in an adult minipig model. *Implant Dentistry,* 26(3)**,** 357-366.

Dennison, D. K., Huerzeler, M. B., Quinones, C. & Caffesse, R. G. (1994). Contaminated implant surfaces: an in vitro comparison of implant surface coating and treatment modalities for decontamination. *Journal of Periodontology,* 65(10)**,** 942-948.

Depprich, R., Zipprich, H., Ommerborn, M., Naujoks, C., Wiesmann, H.-P., Kiattavorncharoen, S., Lauer, H.-C., Meyer, U., Kübler, N. R. & Handschel, J. (2008). Osseointegration of zirconia implants compared with titanium: an in vivo study. *Head and Face Medicine,* 4(30)**,** 1-8.

Derks, J. & Tomasi, C. (2015). Peri-implant health and disease. A systematic review of current epidemiology. *Journal of Clinical Periodontology,* 42(S16)**,** S158-S171.

Deschaseaux, F., Sensébé, L. & Heymann, D. (2009). Mechanisms of bone repair and regeneration. *Trends in Molecular Medicine,* 15(9)**,** 417-429.

Dhir, S. (2013). Biofilm and dental implant: The microbial link. *Journal of Indian Society of Periodontology,* 17(1)**,** 5.

Doerner, M. F. & Nix, W. D. (1986). A method for interpreting the data from depth-sensing indentation instruments. *Journal of Materials Research,* 1(04)**,** 601-609.

Dohan Ehrenfest, D. M., Coelho, P. G., Kang, B.-S., Sul, Y.-T. & Albrektsson, T. (2010). Classification of osseointegrated implant surfaces: materials, chemistry and topography. *Trends in Biotechnology,* 28(4)**,** 198-206.

Donos, N., Hamlet, S., Lang, N. P., Salvi, G. E., Huynh-Ba, G., Bosshardt, D. D. & Ivanovski, S. (2011). Gene expression profile of osseointegration of a hydrophilic compared with a hydrophobic microrough implant surface. *Clinical Oral Implants Research,* 22(4)**,** 365-372.

Dos Santos, M. V., Elias, C. N. & Cavalcanti Lima, J. H. (2011). The effects of superficial roughness and design on the primary stability of dental implants. *Clinical Implant Dentistry and Related Research,* 13(3)**,** 215-223.

Du, Z., Chen, J., Yan, F. & Xiao, Y. (2009). Effects of Simvastatin on bone healing around titanium implants in osteoporotic rats. *Clinical Oral Implants Research,* 20(2)**,** 145-150.

Duarte, P. M., de Mendonça, A. C., Máximo, M. B. B., Santos, V. R., Bastos, M. F. & Nociti Jr, F. H. (2009a). Effect of anti-infective mechanical therapy on clinical parameters and cytokine levels in human peri-implant diseases. *Journal of Periodontology,* 80(2)**,** 234-243.

Duarte, P. M., Reis, A. F., de Freitas, P. M. & Ota-Tsuzuki, C. (2009b). Bacterial adhesion on smooth and rough titanium surfaces after treatment with different instruments. *Journal of Periodontology,* 80(11)**,** 1824-1832.

Ducheyne, P. & Qiu, Q. (1999). Bioactive ceramics: the effect of surface reactivity on bone formation and bone cell function. *Biomaterials,* 20(23)**,** 2287-2303.

Dumelie, N., Benhayoune, H., Richard, D., Laurent-Maquin, D. & Balossier, G. (2008). In vitro precipitation of electrodeposited calcium-deficient hydroxyapatite coatings on Ti6Al4V substrate. *Materials Characterization,* 59(2)**,** 129-133.

Dunne, C., Gibbons, J., FitzPatrick, D., Mulhall, K. & Stanton, K. (2015a). On the fate of particles liberated from hydroxyapatite coatings in vivo. *Irish Journal of Medical Science (1971-),* 184(1)**,** 125-133.

Dunne, C. F., Twomey, B., Kelly, C., Simpson, J. C. & Stanton, K. T. (2015b). Hydroxyapatite and fluorapatite coatings on dental screws: effects of blast coating process and biological response. *Journal of Materials Science: Materials in Medicine,* 26(1)**,** 22.

Dunne, C. F., Twomey, B., O'Neill, L. & Stanton, K. T. (2014). Co-blasting of titanium surfaces with an abrasive and hydroxyapatite to produce bioactive coatings: Substrate and coating characterisation. *Journal of Biomaterials Applications,* 28(5)**,** 767-778.

Edamatsu, H., Kawai, T., Matsui, K., Nakai, M., Takahashi, T. & Echigo, S. (2015). High bone bonding ability and affinity of new low-rigidity β-type Ti-29Nb-13Ta-4.6 Zr alloy as a dental implant. *Journal of Dental and Oral Health,* 1(2)**,** 1-7.

El-Anwar, M. I., El-Zawahry, M. M., Ibraheem, E. M., Nassani, M. Z. & ElGabry, H. (2017). New dental implant selection criterion based on implant design. *European Journal of Dentistry,* 11(2)**,** 186-191.

El-Safty, S., Akhtar, R., Silikas, N. & Watts, D. (2012a). Nanomechanical properties of dental resin-composites. *Dental Materials,* 28(12)**,** 1292-1300.

El-Safty, S., Silikas, N., Akhtar, R. & Watts, D. (2012b). Nanoindentation creep versus bulk compressive creep of dental resin-composites. *Dental Materials,* 28(11)**,** 1171-1182.

Elias, C. N., Fernandes, D. J., Resende, C. R. S. & Roestel, J. (2015). Mechanical properties, surface morphology and stability of a modified commercially pure high strength titanium alloy for dental implants. *Dental Materials,* 31(2)**,** e1-e13.

Elias, C. N., Oshida, Y., Lima, J. H. C. & Muller, C. A. (2008). Relationship between surface properties (roughness, wettability and morphology) of titanium and dental implant removal torque. *Journal of the Mechanical Behavior of Biomedical Materials,* 1(3)**,** 234-242.

Esposito, M., Hirsch, J. M., Lekholm, U. & Thomsen, P. (1998). Biological factors contributing to failures of osseointegrated oral implants,(II). Etiopathogenesis. *European Journal of Oral Sciences,* 106(3)**,** 721-764.

Esposito, M., Murray-Curtis, L., Grusovin, M., Coulthard, P. & Worthington, H. (2014). Interventions for replacing missing teeth: different types of dental implants. *Cochrane Database of Systematic Reviews,* (7). CD003815.

Faeda, R. S., Tavares, H. S., Sartori, R., Guastaldi, A. C. & Marcantonio Jr, E. (2009). Evaluation of titanium implants with surface modification by laser beam: biomechanical study in rabbit tibias. *Brazilian Oral Research,* 23(2)**,** 137-143.

Faggion, C. M., Listl, S., Frühauf, N., Chang, H. J. & Tu, Y. K. (2014). A systematic review and Bayesian network meta-analysis of randomized clinical trials on non-surgical treatments for peri-implantitis. *Journal of Clinical Periodontology,* 41(10)**,** 1015-1025.

Fang, W., Zhao, S., He, F., Liu, L. & Yang, G. (2015). Influence of simvastatin-loaded implants on osseointegration in an ovariectomized animal model. *BioMed Research International,* 2015**,** 1-7. Article ID 831504.

Feng, B., Weng, J., Yang, B., Qu, S. & Zhang, X. (2003). Characterization of surface oxide films on titanium and adhesion of osteoblast. *Biomaterials,* 24(25)**,** 4663-4670.

Ferguson, S., Broggini, N., Wieland, M., De Wild, M., Rupp, F., Geis-Gerstorfer, J., Cochran, D. & Buser, D. (2006). Biomechanical evaluation of the interfacial strength of a chemically modified sandblasted and acid-etched titanium surface. *Journal of Biomedical Materials Research Part A,* 78(2)**,** 291-297.

Ferguson, S. J., Langhoff, J. D., Voelter, K., Rechenberg, B. v., Scharnweber, D., Bierbaum, S., Schnabelrauch, M., Kautz, A. R., Frauchiger, V. M. & Mueller, T. L. (2008). Biomechanical comparison of different surface modifications for dental implants. *International Journal of Oral and Maxillofacial Implants,* 23(6)**,** 1037-1046.

Ferris, D., Moodie, G., Dimond, P., Giorani, C., Ehrlich, M. & Valentini, R. (1999). RGD-coated titanium implants stimulate increased bone formation in vivo. *Biomaterials,* 20(23-24)**,** 2323-2331.

Figliuzzi, M., Mangano, F. & Mangano, C. (2012). A novel root analogue dental implant using CT scan and CAD/CAM: selective laser melting technology. *International Journal of Oral and Maxillofacial Surgery,* 41(7)**,** 858-862.

Figuero, E., Graziani, F., Sanz, I., Herrera, D. & Sanz, M. (2014). Management of peri-implant mucositis and peri-implantitis. *Periodontology 2000,* 66(1)**,** 255-273.

Fihri, A., Len, C., Varma, R. S. & Solhy, A. (2017). Hydroxyapatite: a review of syntheses, structure and applications in heterogeneous catalysis. *Coordination Chemistry Reviews,* 347(Supplement C)**,** 48-76.

Fischer-Cripps, A. C. (2011). Nanoindentation testing. *In:* Ling, F. F. (ed.) *Nanoindentation. mechanical engineering series.* Second ed. New York: Springer, 21-37.

Fiuza, C., Fiuza, S., Aramfard, M., Deng, C. & França, R. (2017). Physicochemical characterization of DMLS dental implants. *Dental Materials,* 33(Supplement 1)**,** e31.

Fomin, A., Dorozhkin, S., Fomina, M., Koshuro, V., Rodionov, I., Zakharevich, A., Petrova, N. & Skaptsov, A. (2016). Composition, structure and mechanical properties of the titanium surface after induction heat treatment followed by modification with hydroxyapatite nanoparticles. *Ceramics International,* 42(9)**,** 10838-10846.

Fumes, A. C., Longo, D. L., De Rossi, A., Fidalgo, T. K. d. S., de Paula e Silva, F. W. G., Borsatto, M. C. & Küchler, E. C. (2017). Microleakage of sealants after phosphoric acid, Er: YAG laser and air abrasion enamel conditioning: systematic review and meta-analysis. *Journal of Clinical Pediatric Dentistry,* 41(3)**,** 167-172.

Fürst, M. M., Salvi, G. E., Lang, N. P. & Persson, G. R. (2007). Bacterial colonization immediately after installation on oral titanium implants. *Clinical Oral Implants Research,* 18(4)**,** 501-508.

Gadelmawla, E., Koura, M., Maksoud, T., Elewa, I. & Soliman, H. (2002). Roughness parameters. *Journal of Materials Processing Technology,* 123(1)**,** 133-145.

Gahlert, M., Gudehus, T., Eichhorn, S., Steinhauser, E., Kniha, H. & Erhardt, W. (2007). Biomechanical and histomorphometric comparison between zirconia implants with varying surface textures and a titanium implant in the maxilla of miniature pigs. *Clinical Oral Implants Research,* 18(5)**,** 662-668.

Galli, S., Jimbo, R., Naito, Y., Berner, S., Dard, M. & Wennerberg, A. (2017). Chemically modified titanium–zirconium implants in comparison with commercially pure titanium controls stimulate the early molecular pathways of bone healing. *Clinical Oral Implants Research,* 28(10)**,** 1234-1240.

Ganeles, J., Zöllner, A., Jackowski, J., Ten Bruggenkate, C., Beagle, J. & Guerra, F. (2008). Immediate and early loading of Straumann implants with a chemically modified surface (SLActive) in the posterior mandible and maxilla: 1-year results from a prospective multicenter study. *Clinical Oral Implants Research,* 19(11)**,** 1119-1128.

Gaviria, L., Salcido, J. P., Guda, T. & Ong, J. L. (2014). Current trends in dental implants. *Journal of the Korean Association of Oral and Maxillofacial Surgeons,* 40(2)**,** 50-60.

Gbureck, U., Masten, A., Probst, J. & Thull, R. (2003). Tribochemical structuring and coating of implant metal surfaces with titanium oxide and hydroxyapatite layers. *Materials Science and Engineering: C,* 23(3)**,** 461-465.

Geetha, M., Singh, A. K., Asokamani, R. & Gogia, A. K. (2009). Ti based biomaterials, the ultimate choice for orthopaedic implants–a review. *Progress in Materials Science,* 54(3)**,** 397-425.

Geng, J.-P., Tan, K. B. C. & Liu, G.-R. (2001). Application of finite element analysis in implant dentistry: a review of the literature. *Journal of Prosthetic Dentistry,* 85(6)**,** 585-598.

Germanier, Y., Tosatti, S., Broggini, N., Textor, M. & Buser, D. (2006). Enhanced bone apposition around biofunctionalized sandblasted and acid-etched titanium implant surfaces. *Clinical Oral Implants Research,* 17(3)**,** 251-257.

Giannasi, C., Pagni, G., Polenghi, C., Niada, S., Manfredi, B., Brini, A. T. & Rasperini, G. (2018). Impact of dental implant surface modifications on adhesion and proliferation of primary human gingival keratinocytes and progenitor cells. *The International Journal of Periodontics & Restorative dentistry,* 38(1)**,** 127-135.

Giavaresi, G., Fini, M., Cigada, A., Chiesa, R., Rondelli, G., Rimondini, L., Torricelli, P., Aldini, N. N. & Giardino, R. (2003). Mechanical and histomorphometric evaluations of titanium implants with different surface treatments inserted in sheep cortical bone. *Biomaterials,* 24(9)**,** 1583-1594.

Gittens, R. A., Olivares-Navarrete, R., Cheng, A., Anderson, D. M., McLachlan, T., Stephan, I., Geis-Gerstorfer, J., Sandhage, K. H., Fedorov, A. G. & Rupp, F. (2013). The roles

of titanium surface micro/nanotopography and wettability on the differential response of human osteoblast lineage cells. *Acta Biomaterialia,* 9(4)**,** 6268-6277.

Gittens, R. A., Scheideler, L., Rupp, F., Hyzy, S. L., Geis-Gerstorfer, J., Schwartz, Z. & Boyan, B. D. (2014). A review on the wettability of dental implant surfaces II: biological and clinical aspects. *Acta Biomaterialia,* 10(7)**,** 2907-2918.

Gledhill, H., Turner, I. & Doyle, C. (2001). In vitro dissolution behaviour of two morphologically different thermally sprayed hydroxyapatite coatings. *Biomaterials,* 22(7)**,** 695-700.

Goldstein, J. I., Newbury, D. E., Michael, J. R., Ritchie, N. W., Scott, J. H. J. & Joy, D. C. (2017). SEM imaging checklist, *Scanning electron microscopy and X-ray microanalysis.* Fourth ed. New York: Springer, 195-197. [Online]. Available: https://doi.org/10.1007/978-1-4939-6676-9_14.

Gonzalez, J. & Mirza-Rosca, J. (1999). Study of the corrosion behavior of titanium and some of its alloys for biomedical and dental implant applications. *Journal of Electroanalytical Chemistry,* 471(2)**,** 109-115.

Gosau, M., Hahnel, S., Schwarz, F., Gerlach, T., Reichert, T. E. & Bürgers, R. (2010). Effect of six different peri-implantitis disinfection methods on in vivo human oral biofilm. *Clinical Oral Implants Research,* 21(8)**,** 866-872.

Gotfredsen, K., Berglundh, T. & Lindhe, J. (2000). Anchorage of titanium implants with different surface characteristics: an experimental study in rabbits. *Clinical Implant Dentistry and Related Research,* 2(3)**,** 120-128.

Gotfredsen, K., Berglundh, T. & Lindhe, J. (2001). Bone reactions adjacent to titanium implants with different surface characteristics subjected to static load. A study in the dog (II). *Clinical Oral Implants Research,* 12(3)**,** 196-201.

Gotfredson, K., Wennerberg, A., Johansson, C., Skovgaard, L. T. & Hjørting-Hansen, E. (1995). Anchorage of TiO_2-blasted, HA-coated, and machined implants: an experimental study with rabbits. *Journal of Biomedical Materials Research,* 29(10)**,** 1223-1231.

Gottlow, J., Dard, M., Kjellson, F., Obrecht, M. & Sennerby, L. (2012). Evaluation of a new Titanium-Zirconium dental implant: a biomechanical and histological comparative study in the mini pig. *Clinical Implant Dentistry and Related Research,* 14(4)**,** 538-545.

Gouldstone, A., Chollacoop, N., Dao, M., Li, J., Minor, A. M. & Shen, Y.-L. (2007). Indentation across size scales and disciplines: recent developments in experimentation and modeling. *Acta Materialia,* 55(12)**,** 4015-4039.

Grandin, H. M., Berner, S. & Dard, M. (2012). A review of titanium zirconium (TiZr) alloys for use in endosseous dental implants. *Materials,* 5(8)**,** 1348-1360.

Gredes, T., Kubasiewicz-Ross, P., Gedrange, T., Dominiak, M. & Kunert-Keil, C. (2014). Comparison of surface modified zirconia implants with commercially available zirconium and titanium implants: a histological study in pigs. *Implant Dentistry,* 23(4)**,** 502-507.

Griggs, J. A. (2017). Dental Implants. *Dental Clinics of North America,* 61(4)**,** 857-871.

Grisar, K., Sinha, D., Schoenaers, J., Dormaar, T. & Politis, C. (2017). Retrospective analysis of dental implants placed between 2012 and 2014: indications, risk factors, and early survival. *International Journal of Oral & Maxillofacial Implants,* 32(3)**,** 649-654.

Gristina, A. G. (1987). Biomaterial-centered infection: microbial adhesion versus tissue integration. *Science,* 237(4822)**,** 1588-1595.

Grizon, F., Aguado, E., Hure, G., Basle, M. & Chappard, D. (2002). Enhanced bone integration of implants with increased surface roughness: a long term study in the sheep. *Journal of Dentistry,* 30(5)**,** 195-203.

Gross, K. A., Berndt, C. C., Goldschlag, D. D. & Iacono, V. J. (1997). In vitro changes of hydroxyapatite coatings. *International Journal of Oral and Maxillofacial Implants,* 12(5)**,** 1-16.

Gross, K. A., Saber-Samandari, S. & Heemann, K. S. (2010). Evaluation of commercial implants with nanoindentation defines future development needs for hydroxyapatite coatings. *Journal of Biomedical Materials Research Part B: Applied Biomaterials,* 93(1)**,** 1-8.

Grubova, I., Chudinova, E., Surmeneva, M., Surmenev, R., Ivanova, A., Kravchuk, K., Shugurov, V., Teresov, A., Koval, N. & Prymak, O. (2016). Comparative evaluation of the sand blasting, acid etching and electron beam surface treatments of titanium for medical application. *In 2016 11th International Forum on Strategic Technology(IFOST)*, Novosibirsk, Russia. Institute of Electrical and Electronics Engineers 69-72. Available: https://doi.org/10.1109/IFOST.2016.7884191 (Accessed: 1 September 2018).

Gu, Y., Khor, K. & Cheang, P. (2003). In vitro studies of plasma-sprayed hydroxyapatite/Ti-6Al-4V composite coatings in simulated body fluid (SBF). *Biomaterials,* 24(9)**,** 1603-1611.

Gu, Y. W., Tay, B. Y., Lim, C. S. & Yong, M. S. (2005). Biomimetic deposition of apatite coating on surface-modified NiTi alloy. *Biomaterials,* 26(34)**,** 6916-6923.

Guarnieri, R., Serra, M., Bava, L., Grande, M., Farronato, D. & Iorio-Siciliano, V. (2014). The impact of a laser-microtextured collar on crestal bone level and clinical parameters under various placement and loading protocols. *International Journal of Oral & Maxillofacial Implants,* 29(2)**,** 354-363.

Guo, J., Padilla, R. J., Ambrose, W., De Kok, I. J. & Cooper, L. F. (2007). The effect of hydrofluoric acid treatment of TiO_2 grit blasted titanium implants on adherent osteoblast gene expression in vitro and in vivo. *Biomaterials,* 28(36)**,** 5418-5425.

Hahn, H. & Palich, W. (1970). Preliminary evaluation of porous metal surfaced titanium for orthopedic implants. *Journal of Biomedical Materials Research,* 4(4)**,** 571-577.

Hahnel, S. (2017). Biofilms on dental implants. *Biofilms and implantable medical devices: infection and control.* Duxford: Woodhead Publishing is an imprint of Elsevier, 117-140. [Online]. Available: https://doi.org/10.1016/B978-0-08-100382-4.00005-8.

Haimov, H., Yosupov, N., Pinchasov, G. & Juodzbalys, G. (2017). Bone morphogenetic protein coating on titanium implant surface: a systematic review. *Journal of Oral & Maxillofacial Research,* 8(2)**,** e1.

Hakki, S. S., Tatar, G., Dundar, N. & Demiralp, B. (2017). The effect of different cleaning methods on the surface and temperature of failed titanium implants: an in vitro study. *Lasers in Medical Science,* 32(3)**,** 563-571.

Hallab, N. J., Vermes, C., Messina, C., Roebuck, K. A., Glant, T. T. & Jacobs, J. J. (2002). Concentration and composition-dependent effects of metal ions on human MG-63 osteoblasts. *Journal of Biomedical Materials Research,* 60(3)**,** 420-433.

Hallström, H., Persson, G. R., Lindgren, S., Olofsson, M. & Renvert, S. (2012). Systemic antibiotics and debridement of peri-implant mucositis. A randomized clinical trial. *Journal of Clinical Periodontology,* 39(6)**,** 574-581.

Han, A., Tsoi, J. K., Rodrigues, F. P., Leprince, J. G. & Palin, W. M. (2016). Bacterial adhesion mechanisms on dental implant surfaces and the influencing factors. *International Journal of Adhesion and Adhesives,* 69**,** 58-71.

Han, M.-K., Hwang, M.-J., Yang, M.-S., Yang, H.-S., Song, H.-J. & Park, Y.-J. (2014). Effect of zirconium content on the microstructure, physical properties and corrosion behavior of Ti alloys. *Materials Science and Engineering: A,* 616**,** 268-274.

Hannink, R. H., Kelly, P. M. & Muddle, B. C. (2000). Transformation toughening in Zirconia-containing ceramics. *Journal of the American Ceramic Society,* 83(3)**,** 461-487.

Hansson, K. N. & Hansson, S. (2011). Skewness and kurtosis: important parameters in the characterization of dental implant surface roughness—a computer simulation. *International Scholarly Research Notices Materials Science,* 2011**,** 1-6. Article ID 305312.

Harun, W. S. W., Asri, R. I. M., Alias, J., Zulkifli, F. H., Kadirgama, K., Ghani, S. A. C. & Shariffuddin, J. H. M. (2018). A comprehensive review of hydroxyapatite-based coatings adhesion on metallic biomaterials. *Ceramics International,* 44(2)**,** 1250-1268.

Hashim, D., Cionca, N., Combescure, C. & Mombelli, A. (2018). The diagnosis of peri-implantitis: a systematic review on the predictive value of bleeding on probing. *Clinical Oral Implants Research,* 29(S16)**,** 276-293.

Hashim, D., Cionca, N., Courvoisier, D. S. & Mombelli, A. (2016). A systematic review of the clinical survival of zirconia implants. *Clinical Oral Investigations,* 20(7)**,** 1403-1417.

Hegde, V. S. & Khatavkar, R. A. (2010). A new dimension to conservative dentistry: air abrasion. *Journal of Conservative Dentistry,* 13(1)**,** 4-8.

Heinrich, A., Dengler, K., Körner, T., Haczek, C., Deppe, H. & Stritzker, B. (2008). Laser-modified titanium implants for improved cell adhesion. *Lasers in Medical Science,* 23(1)**,** 55-58.

Heitz-Mayfield, L. J. & Lang, N. P. (2004). Antimicrobial treatment of peri-implant diseases. *International Journal of Oral & Maxillofacial Implants,* 19(7)**,** 128-139.

Heitz-Mayfield, L. J. A., Salvi, G. E., Botticelli, D., Mombelli, A., Faddy, M. & Lang, N. P. (2011). Anti-infective treatment of peri-implant mucositis: a randomised controlled clinical trial. *Clinical Oral Implants Research,* 22(3)**,** 237-241.

Heitz-Mayfield, L., Schmid, B., Weigel, C., Gerber, S., Bosshardt, D., Jönsson, J. & Lang, N. (2004). Does excessive occlusal load affect osseointegration? An experimental study in the dog. *Clinical Oral Implants Research,* 15(3)**,** 259-268.

Heitz-Mayfield, L. J. (2008). Peri-implant diseases: diagnosis and risk indicators. *Journal of Clinical Periodontology,* 35(s8)**,** 292-304.

Heitz-Mayfield, L. J. & Lang, N. P. (2010). Comparative biology of chronic and aggressive periodontitis vs. peri-implantitis. *Periodontology 2000,* 53(1)**,** 167-181.

Heitz-Mayfield, L. J. & Salvi, G. E. (2018). Peri-implant mucositis. *Journal of Cinical Periodontology,* 45(s20)**,** S237-S245.

Herrmann, K. (2011). *Hardness testing: principles and applications*. Ohio, USA: ASM International.

Hicklin, S. P., Schneebeli, E., Chappuis, V., Janner, S. F. M., Buser, D. & Brägger, U. (2016). Early loading of titanium dental implants with an intra-operatively conditioned hydrophilic implant surface after 21 days of healing. *Clinical Oral Implants Research,* 27(7)**,** 875-883.

Himmlova, L., Dostálová, T. j., Kácovský, A. & Konvičková, S. (2004). Influence of implant length and diameter on stress distribution: a finite element analysis. *Journal of Prosthetic Dentistry,* 91(1)**,** 20-25.

Hindy, A., Farahmand, F. & sadat Tabatabaei, F. (2017). In vitro biological outcome of laser application for modification or processing of titanium dental implants. *Lasers in Medical Science,* 32(5)**,** 1197-1206.

Hirata, R., Bonfante, E. A., Anchieta, R. B., Machado, L. S., Freitas, G., Fardin, V. P., Tovar, N. & Coelho, P. G. (2016). Reliability and failure modes of narrow implant systems. *Clinical Oral Investigations,* 20(7)**,** 1505-1513.

Hisbergues, M., Vendeville, S. & Vendeville, P. (2009). Zirconia: established facts and perspectives for a biomaterial in dental implantology. *Journal of Biomedical Materials Research Part B: Applied Biomaterials,* 88(2)**,** 519-529.

Ho, W.-F., Chen, W.-K., Wu, S.-C. & Hsu, H.-C. (2008). Structure, mechanical properties, and grindability of dental Ti–Zr alloys. *Journal of Materials Science: Materials in Medicine,* 19(10)**,** 3179-3186.

Hotchkiss, K. M., Ayad, N. B., Hyzy, S. L., Boyan, B. D. & Olivares-Navarrete, R. (2017). Dental implant surface chemistry and energy alter macrophage activation in vitro. *Clinical Oral Implants Research,* 28(4)**,** 414-423.

Huang, H. H., Chen, J. Y., Lin, M. C., Wang, Y. T., Lee, T. L. & Chen, L. K. (2012). Blood responses to titanium surface with TiO_2 nano-mesh structure. *Clinical Oral Implants Research,* 23(3)**,** 379-383.

Hultin, M., Gustafsson, A., Hallström, H., Johansson, L. Å., Ekfeldt, A. & Klinge, B. (2002). Microbiological findings and host response in patients with peri-implantitis. *Clinical Oral Implants Research,* 13(4)**,** 349-358.

Hung, K.-Y., Lo, S.-C., Shih, C.-S., Yang, Y.-C., Feng, H.-P. & Lin, Y.-C. (2013). Titanium surface modified by hydroxyapatite coating for dental implants. *Surface and Coatings Technology,* 231**,** 337-345.

Hunziker, E. B., Enggist, L., Küffer, A., Buser, D. & Liu, Y. (2012). Osseointegration: the slow delivery of BMP-2 enhances osteoinductivity. *Bone,* 51(1)**,** 98-106.

Hwang, J.-W., Lee, E.-U., Lee, J.-S., Jung, U.-W., Lee, I.-S. & Choi, S.-H. (2013). Dissolution behavior and early bone apposition of calcium phosphate-coated machined implants. *Journal of Periodontal & Implant Science,* 43(6)**,** 291-300.

Iegami, C. M., Uehara, P. N., Sesma, N., Pannuti, C. M., Tortamano Neto, P. & Mukai, M. K. (2017). Survival rate of titanium-zirconium narrow diameter dental implants versus commercially pure titanium narrow diameter dental implants: a systematic review. *Clinical Implant Dentistry and Related Research,* 19(6)**,** 1015-1022.

Ikarashi, Y., Toyoda, K., Kobayashi, E., Doi, H., Yoneyama, T., Hamanaka, H. & Tsuchiya, T. (2005). Improved biocompatibility of titanium-zirconium (Ti-Zr) alloy: tissue reaction and sensitization to Ti-Zr alloy compared with pure Ti and Zr in rat implantation study. *Materials Transactions,* 46(10)**,** 2260.

Ilie, N., Hilton, T., Heintze, S., Hickel, R., Watts, D., Silikas, N., Stansbury, J., Cadenaro, M. & Ferracane, J. (2017). Academy of dental materials guidance—Resin composites: Part I—Mechanical properties. *Dental Materials,* 33(8)**,** 880-894.

Imam, M. A. & Fraker, A. C. (1996). Titanium alloys as implant materials. *In Medical applications of titanium and its alloys*: The material and biological Issues, Brown & Lemons, J. (eds.) West Conshohocken. PA: ASTM International, 3-16. Avaliable: https://doi.org/10.1520/STP16066S (Accessed: 20 October 2018).

International Organization for Standardization (2015). ISO 14577-1 *Metallic materials—instrumented indentation test for hardness and materials parameters—part 1*: *Test methods*. Geneva. International Organization for Standardization. Avaliable: https://www.iso.org/standard/30104.html (Accessed: 20 October 2018).

Ishikawa, K., Harada, K., Umeda, H. & Ueyama, Y. (2011). Comparison of apatite-coated titanium prepared by blast coating and flame spray methods—evaluation using

simulated body fluid and initial histological study. *Dental Materials Journal,* 30(4)**,** 431-437.

Ishikawa, K., Miyamoto, Y., Nagayama, M. & Asaoka, K. (1997). Blast coating method: new method of coating titanium surface with hydroxyapatite at room temperature. *Journal of Biomedical Materials Research Part A,* 38(2)**,** 129-134

Ivanoff, C. J., Widmark, G., Hallgren, C., Sennerby, L. & Wennerberg, A. (2001). Histologic evaluation of the bone integration of TiO_2 blasted and turned titanium microimplants in humans. *Clinical Oral Implants Research,* 12(2)**,** 128-134.

Iwaya, Y., Machigashira, M., Kanbara, K., Miyamoto, M., Noguchi, K., Izumi, Y. & Ban, S. (2008). Surface properties and biocompatibility of acid-etched titanium. *Dental Materials Journal,* 27(3)**,** 415-421.

Jae-Kwan, L., Lee-Ra, C., Heung-Sik, U., Beom-Seok, C. & Kyoo-Sung, C. (2013). Bone formation and remodeling of three different dental implant surfaces with escherichia coli-derived recombinant human bone morphogenetic protein 2 in a rabbit model. *International Journal of Oral & Maxillofacial Implants,* 28(2)**,** 424-430.

Jansen, J. A. & Leon, B. (2009). Introduction, *In:* León, B. & Jansen, J. (eds.) *Thin calcium phosphate coatings for medical implants.* New York: Springer, 1. [Online]. Available: https://doi-org.manchester.idm.oclc.org/10.1007/978-0-387-77718-4_1.

Jemat, A., Ghazali, M. J., Razali, M. & Otsuka, Y. (2015). Surface modifications and their effects on titanium dental implants. *BioMed Research International,* 2015**,** 1-11. Article ID 791725.

Jennissen, H. P. (2002). Accelerated and improved osteointegration of implants biocoated with bone morphogenetic protein 2 (BMP-2). *Annals of the New York Academy of Sciences,* 961(1)**,** 139-142.

Jenny, G., Jauernik, J., Bierbaum, S., Bigler, M., Grätz, K. W., Rücker, M. & Stadlinger, B. (2016). A systematic review and meta-analysis on the influence of biological implant surface coatings on periimplant bone formation. *Journal of Biomedical Materials Research Part A,* 104(11)**,** 2898-2910.

Jensen, O. T. (2017). Clinical bone response to dental implant materials, *In:* Piattelli, A. (ed.) *Bone response to dental implant materials.* Woodhead Publishing is an

imprint of Elsevier, 129-138. [Online]. Available: https://www.sciencedirect.com/science/article/pii/B9780081002872000070.

Jiang, Q. H., Liu, L., Peel, S., Yang, G. L., Zhao, S. F. & He, F. M. (2013). Bone response to the multilayer BMP-2 gene coated porous titanium implant surface. *Clinical Oral Implants Research,* 24(8)**,** 853-861.

Jimbo, R. & Albrektsson, T. (2015). Long-term clinical success of minimally and moderately rough oral implants: a review of 71 studies with 5 years or more of follow-up. *Implant Dentistry,* 24(1)**,** 62-69.

Jimbo, R., Naito, Y., Galli, S., Berner, S., Dard, M. & Wennerberg, A. (2015). Biomechanical and histomorphometrical evaluation of TiZr alloy implants: an in vivo study in the rabbit. *Clinical Implant Dentistry and Related Research,* 17(s2)**,** e670-e678.

Jíra, A., Králík, V., Denk, F. & Kopecký, L. (2015). Comparison of micromechanical parameters of different dental implants using nanoindentation, *Key Engineering Materials,* 662, 134-137.

Johansson, K., Jimbo, R., Östlund, P., Tranæus, S. & Becktor, J. P. (2017). Effects of bacterial contamination on dental implants during surgery: a systematic review. *Implant Dentistry,* 26(5)**,** 778-789.

John, G., Becker, J. & Schwarz, F. (2016). Effectivity of air-abrasive powder based on glycine and tricalcium phosphate in removal of initial biofilm on titanium and zirconium oxide surfaces in an ex vivo model. *Clinical Oral Investigations,* 20(4)**,** 711-719.

John, G., Sahm, N., Becker, J. & Schwarz, F. (2015). Nonsurgical treatment of peri-implantitis using an air-abrasive device or mechanical debridement and local application of chlorhexidine. Twelve-month follow-up of a prospective, randomized, controlled clinical study. *Clinical Oral Investigations,* 19(8)**,** 1807-1814.

Junker, R., Dimakis, A., Thoneick, M. & Jansen, J. A. (2009). Effects of implant surface coatings and composition on bone integration: a systematic review. *Clinical Oral Implants Research,* 20(s4)**,** 185-206.

Kaluđerović, M. R., Krajnović, T., Maksimović-Ivanić, D., Graf, H.-L. & Mijatović, S. (2017). Ti-SLActive and TiZr-SLActive dental implant surfaces promote fast osteoblast differentiation. *Coatings,* 7(7)**,** 102.

Kämmerer, P. W., Palarie, V., Schiegnitz, E., Hagmann, S., Alshihri, A. & Al-Nawas, B. (2013). Vertical osteoconductivity and early bone formation of titanium–zirconium and titanium implants in a subperiosteal rabbit animal model. *Clinical Oral Implants Research,* 25(7)**,** 774-780.

Kang, B.-S., Sul, Y.-T., Oh, S.-J., Lee, H.-J. & Albrektsson, T. (2009). XPS, AES and SEM analysis of recent dental implants. *Acta Biomaterialia,* 5(6)**,** 2222-2229.

Kassebaum, N., Bernabé, E., Dahiya, M., Bhandari, B., Murray, C. & Marcenes, W. (2015). Global burden of untreated caries: a systematic review and metaregression. *Journal of Dental Research,* 94(5)**,** 650-658.

Kassebaum, N., Smith, A., Bernabé, E., Fleming, T., Reynolds, A., Vos, T., Murray, C., Marcenes, W. & Collaborators, G. O. H. (2017). Global, regional, and national prevalence, incidence, and disability-adjusted life years for oral conditions for 195 countries, 1990–2015: a systematic analysis for the global burden of diseases, injuries, and risk factors. *Journal of Dental Research,* 96(4)**,** 380-387.

Kawashima, H., Sato, S., Kishida, M., Yagi, H., Matsumoto, K. & Ito, K. (2007). Treatment of titanium dental implants with three piezoelectric ultrasonic scalers: an in vivo study. *Journal of Periodontology,* 78(9)**,** 1689-1694.

Kellesarian, S. V., Abduljabbar, T., Vohra, F., Malignaggi, V. R., Malmstrom, H., Romanos, G. E. & Javed, F. (2017). Role of local alendronate delivery on the osseointegration of implants: a systematic review and meta-analysis. *International Journal of Oral and Maxillofacial Surgery,* 46(7)**,** 912-921.

Kelly, M. P., Vaughn, O. L. A. & Anderson, P. A. (2016). Systematic review and meta-analysis of recombinant human bone morphogenetic protein-2 in localized alveolar ridge and maxillary sinus augmentation. *Journal of Oral and Maxillofacial Surgery,* 74(5)**,** 928-939.

Khan, M., Williams, R. & Williams, D. (1999). Conjoint corrosion and wear in titanium alloys. *Biomaterials,* 20(8)**,** 765-772.

Khor, K. A., Gu, Y. W., Quek, C. H. & Cheang, P. (2003). Plasma spraying of functionally graded hydroxyapatite/Ti–6Al–4V coatings. *Surface and Coatings Technology,* 168(2)**,** 195-201.

Khoshkam, V., Chan, H. L., Lin, G. H., MacEachern, M. P., Monje, A., Suarez, F., Giannobile, W. V. & Wang, H. L. (2013). Reconstructive procedures for treating peri-implantitis. *Journal of Dental Research,* 92(s 12)**,** 131s–138s.

Kieswetter, K., Schwartz, Z., Hummert, T. W., Cochran, D. L., Simpson, J., Dean, D. D. & Boyan, B. D. (1996). Surface roughness modulates the local production of growth factors and cytokines by osteoblast-like MG-63 cells. *Journal of Biomedical Materials Research,* 32(1)**,** 55-63.

Kilpadi, K. L., Chang, P.-L. & Bellis, S. L. (2001). Hydroxylapatite binds more serum proteins, purified integrins, and osteoblast precursor cells than titanium or steel. *Journal of Biomedical Materials Research,* 57(2)**,** 258-267.

Kim, B.-S., Kim, J. S., Park, Y. M., Choi, B.-Y. & Lee, J. (2013a). Mg ion implantation on SLA-treated titanium surface and its effects on the behavior of mesenchymal stem cell. *Materials Science and Engineering: C,* 33(3)**,** 1554-1560.

Kim, H., Choi, S.-H., Chung, S.-M., Li, L.-H. & Lee, I.-S. (2010). Enhanced bone forming ability of SLA-treated Ti coated with a calcium phosphate thin film formed by e-beam evaporation. *Biomedical Materials,* 5(4)**,** 044106.

Kim, H., Miyaji, F., Kokubo, T. & Nakamura, T. (1997). Effect of heat treatment on apatite-forming ability of Ti metal induced by alkali treatment. *Journal of Materials Science: Materials in Medicine,* 8(6)**,** 341-347.

Kim, J.-E., Kang, S.-S., Choi, K.-H., Shim, J.-S., Jeong, C.-M., Shin, S.-W. & Huh, J.-B. (2013b). The effect of anodized implants coated with combined rhBMP-2 and recombinant human vascular endothelial growth factors on vertical bone regeneration in the marginal portion of the peri-implant. *Oral Surgery, Oral Medicine, Oral Pathology and Oral Radiology,* 115(6)**,** e24-e31.

Kim, K.-H. & Ramaswamy, N. (2009). Electrochemical surface modification of titanium in dentistry. *Dental Materials Journal,* 28(1)**,** 20-36.

Kim, M.-J., Kim, C.-W., Lim, Y.-J. & Heo, S.-J. (2006). Microrough titanium surface affects biologic response in MG63 osteoblast-like cells. *Journal of Biomedical Materials Research Part A,* 79A(4)**,** 1023-1032.

Kim, Y., Oh, T. J., Misch, C. E. & Wang, H. L. (2005). Occlusal considerations in implant therapy: clinical guidelines with biomechanical rationale. *Clinical Oral Implants Research,* 16(1)**,** 26-35.

Kirmanidou, Y., Sidira, M., Drosou, M.-E., Bennani, V., Bakopoulou, A., Tsouknidas, A., Michailidis, N. & Michalakis, K. (2016). New Ti-alloys and surface modifications to improve the mechanical properties and the biological response to orthopedic and

dental implants: a review. *BioMed Research International,* 2016**,** 1-21. Article ID 2908570.

Klein, M. O., Schiegnitz, E. & Al-Nawas, B. (2014). Systematic review on success of narrow-diameter dental implants. *International Journal of Oral and Maxillofacial Implants,* 29(Supplement)**,** 43-54.

Klinge, B., Gustafsson, A. & Berglundh, T. (2002). A systematic review of the effect of anti-infective therapy in the treatment of peri-implantitis. *Journal of Clinical Periodontology,* 29(s3)**,** 213-225.

Kloss, F. R., Steinmüller-Nethl, D., Stigler, R. G., Ennemoser, T., Rasse, M. & Hächl, O. (2011). In vivo investigation on connective tissue healing to polished surfaces with different surface wettability. *Clinical Oral Implants Research,* 22(7)**,** 699-705.

Kobayashi, E., Matsumoto, S., Yoneyama, T. & Hamanaka, H. (1995). Mechanical properties of the binary titanium-zirconium alloys and their potential for biomedical materials. *Journal of Biomedical Materials Research,* 29(8)**,** 943-950.

Kohal, R. J. & Klaus, G. (2004). A zirconia implant-crown system: a case report. *International Journal of Periodontics & Restorative Dentistry,* 24(2)**,** 146-153.

Kohavi, D., Klinger, A., Steinberg, D. & Sela, M. N. (1995). Adsorption of salivary proteins onto prosthetic titanium components. *Journal of Prosthetic Dentistry,* 74(5)**,** 531-534.

Kokubo, T., Kim, H.-M. & Kawashita, M. (2003). Novel bioactive materials with different mechanical properties. *Biomaterials,* 24(13)**,** 2161-2175.

Koldsland, O. C., Scheie, A. A. & Aass, A. M. (2010). Prevalence of peri-implantitis related to severity of the disease with different degrees of bone loss. *Journal of Periodontology,* 81(2)**,** 231-238.

Koller, G., Cook, R. J., Thompson, I. D., Watson, T. F. & Di Silvio, L. (2007). Surface modification of titanium implants using bioactive glasses with air abrasion technologies. *Journal of Materials Science: Materials in Medicine,* 18(12)**,** 2291-2296.

Kolonidis, S. G., Renvert, S., Hämmerle, C. H. F., Lang, N. P., Harris, D. & Claffey, N. (2003). Osseointegration on implant surfaces previously contaminated with plaque. *Clinical Oral Implants Research,* 14(4)**,** 373-380.

Kopf, B. S., Ruch, S., Berner, S., Spencer, N. D. & Maniura-Weber, K. (2015). The role of nanostructures and hydrophilicity in osseointegration: in-vitro protein-adsorption

and blood-interaction studies. *Journal of Biomedical Materials Research Part A,* 103(8)**,** 2661-2672.

Kotsovilis, S., Fourmousis, I., Karoussis, I. K. & Bamia, C. (2009). A systematic review and meta-analysis on the effect of implant length on the survival of rough-surface dental implants. *Journal of Periodontology,* 80(11)**,** 1700-1718.

Kournetas, N., Spintzyk, S., Schweizer, E., Sawada, T., Said, F., Schmid, P., Geis-Gerstorfer, J., Eliades, G. & Rupp, F. (2017). Comparative evaluation of topographical data of dental implant surfaces applying optical interferometry and scanning electron microscopy. *Dental Materials,* 33(8)**,** e317-e327.

Kreisler, M., Kohnen, W., Christoffers, A. B., Götz, H., Jansen, B., Duschner, H. & d'Hoedt, B. (2005). In vitro evaluation of the biocompatibility of contaminated implant surfaces treated with an Er: YAG laser and an air powder system. *Clinical Oral Implants Research,* 16(1)**,** 36-43.

Kreisler, M., Kohnen, W., Marinello, C., Götz, H., Duschner, H., Jansen, B. & D'Hoedt, B. (2002). Bactericidal effect of the Er: YAG laser on dental implant surfaces: an in vitro study. *Journal of Periodontology,* 73(11)**,** 1292-1298.

Ku, Y., Chung, C.-P. & Jang, J.-H. (2005). The effect of the surface modification of titanium using a recombinant fragment of fibronectin and vitronectin on cell behavior. *Biomaterials,* 26(25)**,** 5153-5157.

Kubies, D., Himmlová, L., Riedel, T., Chánová, E., Balik, K., Douderova, M., Bártová, J. & Pesakova, V. (2011). The interaction of osteoblasts with bone-implant materials: 1. The effect of physicochemical surface properties of implant materials. *Physiological Research,* 60(1)**,** 95-111.

Kulkarni Aranya, A., Pushalkar, S., Zhao, M., LeGeros, R. Z., Zhang, Y. & Saxena, D. (2017). Antibacterial and bioactive coatings on titanium implant surfaces. *Journal of Biomedical Materials Research Part A,* 105(8)**,** 2218-2227.

Kumar, P. S., Mason, M. R., Brooker, M. R. & O'Brien, K. (2012). Pyrosequencing reveals unique microbial signatures associated with healthy and failing dental implants. *Journal of Clinical Periodontology,* 39(5)**,** 425-433.

Kumararama, S. S. & Chowdhary, R. (2017). Selection of dental implants based on masticatory load of the patient: a novel approach. *Indian Journal of Dental Research,* 28(3)**,** 309-313.

Kuromoto, N. K., Simão, R. A. & Soares, G. A. (2007). Titanium oxide films produced on commercially pure titanium by anodic oxidation with different voltages. *Materials Characterization,* 58(2)**,** 114-121.

Lafaurie, G. I., Sabogal, M. A., Castillo, D. M., Rincón, M. V., Gómez, L. A., Lesmes, Y. A. & Chambrone, L. (2017). Microbiome and microbial biofilm profiles of peri-implantitis: a systematic review. *Journal of Periodontology,* 88(10)**,** 1066-1089.

Lai, M., Hermann, C. D., Cheng, A., Olivares-Navarrete, R., Gittens, R. A., Bird, M. M., Walker, M., Cai, Y., Cai, K., Sandhage, K. H., Schwartz, Z. & Boyan, B. D. (2015). Role of α2β1 integrins in mediating cell shape on microtextured titanium surfaces. *Journal of Biomedical Materials Research Part A,* 103(2)**,** 564-573.

Lamolle, S. F., Monjo, M., Rubert, M., Haugen, H. J., Lyngstadaas, S. P. & Ellingsen, J. E. (2009). The effect of hydrofluoric acid treatment of titanium surface on nanostructural and chemical changes and the growth of MC3T3-E1 cells. *Biomaterials,* 30(5)**,** 736-742.

Lan, J., Wang, Z., Wang, Y., Wang, J. & Cheng, X. (2006). The effect of combination of recombinant human bone morphogenetic protein-2 and basic fibroblast growth factor or insulin-like growth factor-I on dental implant osseointegration by confocal laser scanning microscopy. *Journal of Periodontology,* 77(3)**,** 357-363.

Lang, N. P., Berglundh, T. & Periodontology, W. G. o. t. S. E. W. o. (2011a). Periimplant diseases: where are we now? Consensus of the seventh european workshop on periodontology. *Journal of Clinical Periodontology,* 38(s11)**,** 178-181.

Lang, N. P., Salvi, G. E., Huynh-Ba, G., Ivanovski, S., Donos, N. & Bosshardt, D. D. (2011b). Early osseointegration to hydrophilic and hydrophobic implant surfaces in humans. *Clinical Oral Implants Research,* 22(4)**,** 349-356.

Lang, N. P., Wilson, T. G. & Corbet, E. F. (2000). Biological complications with dental implants: their prevention, diagnosis and treatment. *Clinical Oral Implants Research,* 11(s1)**,** 146-155.

Langhoff, J. D., Voelter, K., Scharnweber, D., Schnabelrauch, M., Schlottig, F., Hefti, T., Kalchofner, K., Nuss, K. & von Rechenberg, B. (2008). Comparison of chemically and pharmaceutically modified titanium and zirconia implant surfaces in dentistry: a study in sheep. *International Journal of Oral and Maxillofacial Surgery,* 37(12)**,** 1125-1132.

Le Guehennec, L., Lopez-Heredia, M.-A., Enkel, B., Weiss, P., Amouriq, Y. & Layrolle, P. (2008). Osteoblastic cell behaviour on different titanium implant surfaces. *Acta Biomaterialia,* 4(3)**,** 535-543.

Le Guéhennec, L., Soueidan, A., Layrolle, P. & Amouriq, Y. (2007). Surface treatments of titanium dental implants for rapid osseointegration. *Dental Materials,* 23(7)**,** 844-854.

Lee, A. & Wang, H.-L. (2010). Biofilm related to dental implants. *Implant Dentistry,* 19(5)**,** 387-393.

Lee, C.-T., Huang, Y.-W., Zhu, L. & Weltman, R. (2017). Prevalences of peri-implantitis and peri-implant mucositis: systematic review and meta-analysis. *Journal of Dentistry,* 62**,** 1-12.

Lee, I.-S., Kim, H.-E. & Kim, S.-Y. (2000). Studies on calcium phosphate coatings. *Surface and Coatings Technology,* 131(1-3)**,** 181-186.

Lee, I.-S., Whang, C.-N., Kim, H.-E., Park, J.-C., Song, J. H. & Kim, S.-R. (2002). Various Ca/P ratios of thin calcium phosphate films. *Materials Science and Engineering: C,* 22(1)**,** 15-20.

Lee, J.-H., Moon, S.-K., Kim, K.-M. & Kim, K.-N. (2013a). Modification of TiO_2 nanotube surfaces by electro-spray deposition of amoxicillin combined with PLGA for bactericidal effects at surgical implantation sites. *Acta Odontologica Scandinavica,* 71(1)**,** 168-174.

Lee, J. S., Kim, H. M., Kim, C. S., Choi, S. H., Chai, J. K. & Jung, U. W. (2013b). Long-term retrospective study of narrow implants for fixed dental prostheses. *Clinical Oral Implants Research,* 24(8)**,** 847-852.

Lee, S.-W., Hahn, B.-D., Kang, T. Y., Lee, M.-J., Choi, J.-Y., Kim, M.-K. & Kim, S.-G. (2014). Hydroxyapatite and collagen combination-coated dental implants display better bone formation in the peri-implant area than the same combination plus bone morphogenetic protein-2–coated implants, hydroxyapatite only coated implants, and uncoated implants. *Journal of Oral and Maxillofacial Surgery,* 72(1)**,** 53-60.

Lee, T. J., Ueno, T., Nomura, N., Wakabayashi, N. & Hanawa, T. (2016). Titanium-Zirconium binary alloy as dental implant material: analysis of the influence of compositional change on mechanical properties and in vitro biologic response. *International Journal of Oral and Maxillofacial Implants,* 31(3)**,** 547-554.

Leena, J., Arumugham, V., Rajesh, R. & Muraleedharan, C. (2016). Nanoscale surface characterization of ceramic/ceramic coated metallic biomaterials using chromatic length aberration technique. *Journal of Metrology Society of India,* 31(3)**,** 231-239.

LeGeros, R. Z. (2002). Properties of osteoconductive biomaterials: calcium phosphates. *Clinical Orthopaedics and Related Research,* 395**,** 81-98.

Lemos, C. A. A., Ferro-Alves, M. L., Okamoto, R., Mendonça, M. R. & Pellizzer, E. P. (2016). Short dental implants versus standard dental implants placed in the posterior jaws: a systematic review and meta-analysis. *Journal of Dentistry,* 47**,** 8-17.

Leonhardt, Å., Renvert, S. & Dahlén, G. (1999). Microbial findings at failing implants. *Clinical Oral Implants Research,* 10(5)**,** 339-345.

Leventi, E., Malden, N. J. & Lopes, V. R. (2014). Periimplant bone-level reduction in relation to hydroxyapatite-coated dental implants that act as mandibular overdenture retainers: results at 6 to 10 years. *Journal of Prosthetic Dentistry,* 112(4)**,** 792-797.

Levingstone, T. J., Barron, N., Ardhaoui, M., Benyounis, K., Looney, L. & Stokes, J. (2017). Application of response surface methodology in the design of functionally graded plasma sprayed hydroxyapatite coatings. *Surface and Coatings Technology,* 313(Supplement C)**,** 307-318.

Li, D., Ferguson, S. J., Beutler, T., Cochran, D. L., Sittig, C., Hirt, H. P. & Buser, D. (2002). Biomechanical comparison of the sandblasted and acid-etched and the machined and acid-etched titanium surface for dental implants. *Journal of Biomedical Materials Research,* 60(2)**,** 325-332.

Liaw, K., Delfini, R. H. & Abrahams, J. J. (2015). Dental implant complications. *Seminars in Ultrasound, CT and MRI,* 36(5)**,** 427-433.

Liebenberg, W. H. & Crawford, B. J. (1997). Subcutaneous, orbital, and mediastinal emphysema secondary to the use of an air-abrasive device. *Quintessence International,* 28(1)**,** 31-38.

Lim, Y. J., Oshida, Y., Andres, C. J. & Barco, M. T. (2001). Surface characterizations of variously treated titanium materials. *International Journal of Oral & Maxillofacial Implants,* 16(3)**,** 333-342.

Lindhe, J. & Berglundh, T. (1998). The interface between the mucosa and the implant. *Periodontology 2000,* 17(1)**,** 47-54.

Lindhe, J. & Meyle, J. (2008). Peri-implant diseases: consensus report of the sixth european workshop on periodontology. *Journal of Clinical Periodontology,* 35(s8)**,** 282-285.

Liu, X., Chu, P. K. & Ding, C. (2004). Surface modification of titanium, titanium alloys, and related materials for biomedical applications. *Materials Science and Engineering: R: Reports,* 47(3)**,** 49-121.

Liu, Y., Enggist, L., Kuffer, A. F., Buser, D. & Hunziker, E. B. (2007). The influence of BMP-2 and its mode of delivery on the osteoconductivity of implant surfaces during the early phase of osseointegration. *Biomaterials,* 28(16)**,** 2677-2686.

Löberg, J., Mattisson, I., Hansson, S. & Ahlberg, E. (2010). Characterisation of titanium dental implants I: critical assessment of surface roughness parameters. *The Open Biomaterials Journal,* 2(1)**,** 18-35.

Lops, D., Bressan, E., Pisoni, G., Cea, N., Corazza, B. & Romeo, E. (2012). Short implants in partially edentulous maxillae and mandibles: a 10 to 20 years retrospective evaluation. *International Journal of Dentistry,* 2012**,** 1-8. Article ID 351793.

Lotz, E. M., Olivares-Navarrete, R., Berner, S., Boyan, B. D. & Schwartz, Z. (2016). Osteogenic response of human MSCs and osteoblasts to hydrophilic and hydrophobic nanostructured titanium implant surfaces. *Journal of Biomedical Materials Research Part A,* 104(12)**,** 3137-3148.

Lotz, E. M., Olivares-Navarrete, R., Hyzy, S. L., Berner, S., Schwartz, Z. & Boyan, B. D. (2017). Comparable responses of osteoblast lineage cells to microstructured hydrophilic titanium–zirconium and microstructured hydrophilic titanium. *Clinical Oral Implants Research,* 28(7)**,** e51-e59.

Louropoulou, A., Slot, D. E. & Van der Weijden, F. (2015). Influence of mechanical instruments on the biocompatibility of titanium dental implants surfaces: a systematic review. *Clinical Oral Implants Research,* 26(7)**,** 841-850.

Louropoulou, A., Slot, D. E. & Van der Weijden, F. A. (2012). Titanium surface alterations following the use of different mechanical instruments: a systematic review. *Clinical Oral Implants Research,* 23(6)**,** 643-658.

Louropoulou, A., Slot, D. E. & Weijden, F. (2014). The effects of mechanical instruments on contaminated titanium dental implant surfaces: a systematic review. *Clinical Oral Implants Research,* 25(10)**,** 1149-1160.

Luginbuehl, V., Meinel, L., Merkle, H. P. & Gander, B. (2004). Localized delivery of growth factors for bone repair. *European Journal of Pharmaceutics and Biopharmaceutics,* 58(2)**,** 197-208.

Lukaszewska-Kuska, M., Wirstlein, P., Majchrowski, R. & Dorocka-Bobkowska, B. (2018). Osteoblastic cell behaviour on modified titanium surfaces. *Micron,* 105**,** 55-63.

Lutz, R., Srour, S., Nonhoff, J., Weisel, T., Damien, C. & Schlegel, K. (2010). Biofunctionalization of titanium implants with a biomimetic active peptide (P-15) promotes early osseointegration. *Clinical Oral Implants Research,* 21(7)**,** 726-734.

Lynn, A. K. & DuQuesnay, D. L. (2002). Hydroxyapatite-coated Ti–6Al–4V: Part 1: the effect of coating thickness on mechanical fatigue behaviour. *Biomaterials,* 23(9)**,** 1937-1946.

Madi, M., Htet, M., Zakaria, O., Alagl, A. & Kasugai, S. (2018). Re-osseointegration of dental implants after periimplantitis treatments: a systematic review. *Implant Dentistry,* 27(1)**,** 101-110.

Mahato, N., Wu, X. & Wang, L. (2016). Management of peri-implantitis: a systematic review, 2010–2015. *Springerplus,* 5(1).

Majumdar, P., Singh, S. & Chakraborty, M. (2008). Elastic modulus of biomedical titanium alloys by nano-indentation and ultrasonic techniques—A comparative study. *Materials Science and Engineering: A,* 489(1)**,** 419-425.

Maló, P. S., de Araújo Nobre, M. A., Lopes, A. V. & Ferro, A. S. (2017). Retrospective cohort clinical investigation of a dental implant with a narrow diameter and short length for the partial rehabilitation of extremely atrophic jaws. *Journal of Oral Science,* 59(3)**,** 357-363.

Mangano, C. (2009). Dental implants from laser fusion of titanium microparticles: from research to clinical applications. *Journal of Osseointegration,* 1(1)**,** 2-14.

Mangano, F. G., Cirotti, B., Sammons, R. L. & Mangano, C. (2012). Custom-made, root-analogue direct laser metal forming implant: a case report. *Lasers in Medical Science,* 27(6)**,** 1241-1245.

Manicone, P. F., Rossi Iommetti, P. & Raffaelli, L. (2007). An overview of zirconia ceramics: basic properties and clinical applications. *Journal of Dentistry,* 35(11)**,** 819-826.

Mano, T., Ueyama, Y., Ishikawa, K., Matsumura, T. & Suzuki, K. (2002). Initial tissue response to a titanium implant coated with apatite at room temperature using a blast coating method. *Biomaterials,* 23(9)**,** 1931-1936.

Manor, Y., Oubaid, S., Mardinger, O., Chaushu, G. & Nissan, J. (2009). Characteristics of early versus late implant failure: a retrospective study. *Journal of Oral and Maxillofacial Surgery,* 67(12)**,** 2649-2652.

Manzano, G., Herrero, R. & Montero, J. (2014). Comparison of clinical performance of zirconia implants and titanium implants in animal models: a systematic review. *International Journal of Oral and Maxillofacial Implants,* 29(2)**,** 311-320.

Marinho, V. C., Celletti, R., Bracchetti, G., Petrone, G., Minkin, C. & Piattelli, A. (2003). Sandblasted and acid-etched dental implants: a histologic study in rats. *International Journal of Oral and Maxillofacial Implants,* 18(1)**,** 75-81.

Marino, L. A. C., Deliberador, T. M., Zielak, J. C., Correr, G. M., Giovanini, A. F. & Gonzaga, C. C. (2012). Microstructural and topographical characterization of different surface treatments of a surgical titanium alloy for dental implants. *Implant Dentistry,* 21(3)**,** 207-212.

Mariscal-Muñoz, E., Costa, C. A., Tavares, H. S., Bianchi, J., Hebling, J., Machado, J. P., Lerner, U. H. & Souza, P. P. (2016). Osteoblast differentiation is enhanced by a nano-to-micro hybrid titanium surface created by Yb: YAG laser irradiation. *Clinical Oral Investigations,* 20(3)**,** 503-511.

Martin, J., Schwartz, Z., Hummert, T., Schraub, D., Simpson, J., Lankford, J., Dean, D., Cochran, D. & Boyan, B. (1995). Effect of titanium surface roughness on proliferation, differentiation, and protein synthesis of human osteoblast-like cells (MG63). *Journal of Biomedical Materials Research,* 29(3)**,** 389-401.

Masouras, K., Akhtar, R., Watts, D. C. & Silikas, N. (2008). Effect of filler size and shape on local nanoindentation modulus of resin-composites. *Journal of Materials Science: Materials in Medicine,* 19(12)**,** 3561-3566.

Massaro, C., Rotolo, P., De Riccardis, F., Milella, E., Napoli, A., Wieland, M., Textor, M., Spencer, N. & Brunette, D. (2002). Comparative investigation of the surface properties of commercial titanium dental implants. Part I: chemical composition. *Journal of Materials Science: Materials in Medicine,* 13(6)**,** 535-548.

Matarasso, S., Iorio Siciliano, V., Aglietta, M., Andreuccetti, G. & Salvi, G. E. (2014). Clinical and radiographic outcomes of a combined resective and regenerative approach in the treatment of peri-implantitis: a prospective case series. *Clinical Oral Implants Research,* 25(7)**,** 761-767.

Matteson, J. L., Greenspan, D. C., Tighe, T. B., Gilfoy, N. & Stapleton, J. J. (2016). Assessing the hierarchical structure of titanium implant surfaces. *Journal of Biomedical Materials Research Part B: Applied Biomaterials,* 104(6)**,** 1083-1090.

Maximo, M. B., De Mendonça, A. C., Renata Santos, V., Figueiredo, L. C., Feres, M. & Duarte, P. M. (2009). Short-term clinical and microbiological evaluations of peri-implant diseases before and after mechanical anti-infective therapies. *Clinical Oral Implants Research,* 20(1)**,** 99-108.

Mayo, M., Siegel, R., Narayanasamy, A. & Nix, W. (1990). Mechanical properties of nanophase TiO_2 as determined by nanoindentation. *Journal of Materials Research,* 5(5)**,** 1073-1082.

Mazur, M., Kalisz, M., Wojcieszak, D., Grobelny, M., Mazur, P., Kaczmarek, D. & Domaradzki, J. (2015). Determination of structural, mechanical and corrosion properties of Nb_2O_5 and (Nb_yCu_{1-y}) Ox thin films deposited on Ti6Al4V alloy substrates for dental implant applications. *Materials Science and Engineering,* 47**,** 211-221.

McCracken, M. (1999). Dental implant materials: commercially pure titanium and titanium alloys. *Journal of Prosthodontics,* 8(1)**,** 40-43.

Medvedev, A. E., Molotnikov, A., Lapovok, R., Zeller, R., Berner, S., Habersetzer, P. & Dalla Torre, F. (2016a). Microstructure and mechanical properties of Ti–15Zr alloy used as dental implant material. *Journal of the Mechanical Behavior of Biomedical Materials,* 62(Supplement C)**,** 384-398.

Medvedev, A. E., Ng, H. P., Lapovok, R., Estrin, Y., Lowe, T. C. & Anumalasetty, V. N. (2016b). Effect of bulk microstructure of commercially pure titanium on surface characteristics and fatigue properties after surface modification by sand blasting and acid-etching. *Journal of the Mechanical Behavior of Biomedical Materials,* 57**,** 55-68.

Mellado-Valero, A., Buitrago-Vera, P., Solá-Ruiz, M. F. & Ferrer-García, J. C. (2013). Decontamination of dental implant surface in peri-implantitis treatment: a literature review. *Medicina Oral, Patologia Oral y Cirugia Bucal,* 18(6)**,** e869-e876.

Menčík, J. (2007). Determination of mechanical properties by instrumented indentation. *Meccanica,* 42(1)**,** 19-29.

Mendonça, G., Mendonca, D., Aragao, F. J. & Cooper, L. F. (2008). Advancing dental implant surface technology–from micron-to nanotopography. *Biomaterials,* 29(28)**,** 3822-3835.

Mendoza-Arnau, A., Vallecillo-Capilla, M.-F., Cabrerizo-Vílchez, M.-Á. & Rosales-Leal, J.-I. (2016). Topographic characterisation of dental implants for commercial use. *Medicina Oral, Patologia Oral y Cirugia Bucal,* 21(5)**,** e631–e636.

Menini, M., Piccardo, P., Baldi, D., Dellepiane, E. & Pera, P. (2015). Morphological and chemical characteristics of different titanium surfaces treated by bicarbonate and glycine powder air abrasive systems. *Implant Dentistry,* 24(1)**,** 47-56.

Milleret, V., Tugulu, S., Schlottig, F. & Hall, H. (2011). Alkali treatment of microrough titanium surfaces affects macrophage/monocyte adhesion, platelet activation and architecture of blood clot formation. *European Cells and Materials*, 21**,** 430-444.

Mills, M. P., Rosen, P. S., Chambrone, L., Greenwell, H., Kao, R. T., Klokkevold, P. R., McAllister, B. S., Reynolds, M. A., Romanos, G. E. & Wang, H. L. (2018). American academy of periodontology best evidence consensus statement on the efficacy of laser therapy used alone or as an adjunct to non-surgical and surgical treatment of periodontitis and peri-implant diseases. *Journal of Periodontology,* 89(7)**,** 737-742.

Mints, D., Elias, C., Funkenbusch, P. & Meirelles, L. (2014). Integrity of implant surface modifications after insertion. *International Journal of Oral & Maxillofacial Implants,* 29(1)**,** 97-104.

Miron, R. J., Oates, C. J., Molenberg, A., Dard, M. & Hamilton, D. W. (2010). The effect of enamel matrix proteins on the spreading, proliferation and differentiation of osteoblasts cultured on titanium surfaces. *Biomaterials,* 31(3)**,** 449-460.

Mishler, O. P. & Shiau, H. J. (2014). Management of peri-implant disease: a current appraisal. *Journal of Evidence Based Dental Practice,* 14(Supplement)**,** 53-59.

Mo, S.-D. & Ching, W. (1995). Electronic and optical properties of three phases of titanium dioxide: rutile, anatase, and brookite. *Physical Review B,* 51(19)**,** 13023.

Moëne, R., Décaillet, F., Andersen, E. & Mombelli, A. (2010). Subgingival plaque removal using a new air-polishing device. *Journal of Periodontology,* 81(1)**,** 79-88.

Mohedano, M., Matykina, E., Arrabal, R., Pardo, A. & Merino, M. (2014). Metal release from ceramic coatings for dental implants. *Dental Materials,* 30(3)**,** e28-e40.

Möller, B., Terheyden, H., Açil, Y., Purcz, N., Hertrampf, K., Tabakov, A., Behrens, E. & Wiltfang, J. (2012). A comparison of biocompatibility and osseointegration of

ceramic and titanium implants: an in vivo and in vitro study. *International Journal of Oral and Maxillofacial Surgery,* 41(5)**,** 638-645.

Mombelli, A. (2002). Microbiology and antimicrobial therapy of peri-implantitis. *Periodontology 2000,* 28(1)**,** 177-189.

Mombelli, A. & Décaillet, F. (2011). The characteristics of biofilms in peri-implant disease. *Journal of Clinical Periodontology,* 38(s11)**,** 203-213.

Mombelli, A., Müller, N. & Cionca, N. (2012). The epidemiology of peri-implantitis. *Clinical Oral Implants Research,* 23(s6)**,** 67-76.

Mombelli, A., Van Oosten, M., Schürch Jr, E. & Lang, N. (1987). The microbiota associated with successful or failing osseointegrated titanium implants. *Oral Microbiology and Immunology,* 2(4)**,** 145-151.

Montero, J., Bravo, M., Guadilla, Y., Portillo, M., Blanco, L., Rojo, R., Rosales-Leal, J. & López-Valverde, A. (2015). Comparison of clinical and histologic outcomes of zirconia versus titanium implants placed in fresh sockets: a 5-month study in beagles. *International Journal of Oral & Maxillofacial Implants,* 30(4)**,** 773-780.

Montes, C. C., Pereira, F. A., Thome, G., Alves, E. D. M., Acedo, R. V., de Souza, J. R., Melo, A. C. M. & Trevilatto, P. C. (2007). Failing factors associated with osseointegrated dental implant loss. *Implant Dentistry,* 16(4)**,** 404-412.

Moraschini, V., Almeida, D., Calasans-Maia, J. & Calasans-Maia, M. D. (2018). The ability of topical and systemic statins to increase osteogenesis around dental implants: a systematic review of histomorphometric outcomes in animal studies. *International Journal of Oral and Maxillofacial Surgery,* 47(8)**,** 1070-1078.

Moritz, N., Jokinen, M., Peltola, T., Areva, S. & Yli-Urpo, A. (2003). Local induction of calcium phosphate formation on TiO_2 coatings on titanium via surface treatment with a CO_2 laser. *Journal of Biomedical Materials Research Part A,* 65(1)**,** 9-16.

Morra, M. (2006). Biochemical modification of titanium surfaces: peptides and ECM proteins. *European Cells and Materials,* 12(1)**,** 1-15.

Morra, M., Cassinelli, C., Bruzzone, G., Carpi, A., Santi, G. D., Giardino, R. & Fini, M. (2003). Surface chemistry effects of topographic modification of titanium dental implant surfaces: 1. Surface analysis. *International Journal of Oral & Maxillofacial Implants,* 18(1)**,** 40-45.

Morra, M., Cassinelli, C., Cascardo, G., Bollati, D. & Rodriguez y Baena, R. (2010). Multifunctional implant surfaces: Surface characterization and bone response to

acid-etched Ti implants surface-modified by fibrillar collagen I. *Journal of Biomedical Materials Research Part A: An Official Journal of The Society for Biomaterials, The Japanese Society for Biomaterials, and The Australian Society for Biomaterials and the Korean Society for Biomaterials,* 94(1)**,** 271-279.

Morra, M., Cassinelli, C., Cascardo, G., Mazzucco, L., Borzini, P., Fini, M., Giavaresi, G. & Giardino, R. (2006). Collagen I-coated titanium surfaces: Mesenchymal cell adhesion and in vivo evaluation in trabecular bone implants. *Journal of Biomedical Materials Research Part A: An Official Journal of The Society for Biomaterials, The Japanese Society for Biomaterials, and The Australian Society for Biomaterials and the Korean Society for Biomaterials,* 78(3)**,** 449-458.

Morton, D. & Pollini, A. (2017). Evolution of loading protocols in implant dentistry for partially dentate arches. *Periodontology 2000,* 73(1)**,** 152-177.

Mouhyi, J., Sennerby, L., Pireaux, J. j., Dourov, N., Nammour, S. & Van Reck, J. (1998). An XPS and SEM evaluation of six chemical and physical techniques for cleaning of contaminated titanium implants. *Clinical Oral Implants Research,* 9(3)**,** 185-194.

Muddugangadhar, B., Amarnath, G., Tripathi, S., Dikshit, S. & Divya, M. (2011). Biomaterials for Dental Implants: an overview. *International Journal of Oral Implantology and Clinical Research,* 2(1)**,** 13-24.

Mueller, C. K., Thorwarth, M., Schmidt, M., Schlegel, K. A. & Schultze-Mosgau, S. (2011). Comparative analysis of osseointegration of titanium implants with acid-etched surfaces and different biomolecular coatings. *Oral Surgery, Oral Medicine, Oral Pathology, Oral Radiology, and Endodontology,* 112(6)**,** 726-736.

Mundy, G., Garrett, R., Harris, S., Chan, J., Chen, D., Rossini, G., Boyce, B., Zhao, M. & Gutierrez, G. l. (1999). Stimulation of bone formation in vitro and in rodents by statins. *Science,* 286(5446)**,** 1946-1949.

Murphy, M., Walczak, M., Thomas, A., Silikas, N., Berner, S. & Lindsay, R. (2017). Toward optimizing dental implant performance: Surface characterization of Ti and TiZr implant materials. *Dental Materials,* 33(1)**,** 43-53.

Mustafa, K., Wroblewski, J., Lopez, B. S., Wennerberg, A., Hultenby, K. & Arvidson, K. (2001). Determining optimal surface roughness of TiO_2 blasted titanium implant material for attachment, proliferation and differentiation of cells derived from human mandibular alveolar bone. *Clinical Oral Implants Research,* 12(5)**,** 515-525.

Muthukuru, M., Zainvi, A., Esplugues, E. O. & Flemmig, T. F. (2012). Non-surgical therapy for the management of peri-implantitis: a systematic review. *Clinical Oral Implants Research,* 23(s6)**,** 77-83.

Najeeb, S., Zafar, M. S., Khurshid, Z., Zohaib, S., Hasan, S. M. & Khan, R. S. (2017). Bisphosphonate releasing dental implant surface coatings and osseointegration: a systematic review. *Journal of Taibah University Medical Sciences,* 12(5)**,** 369-375.

Nakada, H., Sakae, T., LeGeros, R. Z., LeGeros, J. P., Suwa, T., Numata, Y. & Kobayashi, K. (2007). Early tissue response to modified implant surfaces using back scattered imaging. *Implant Dentistry,* 16(3)**,** 281-289.

Natto, Z. S., Aladmawy, M., Levi Jr, P. A. & Wang, H.-L. (2015). Comparison of the efficacy of different types of lasers for the treatment of peri-implantitis: a systematic review. *International Journal of Oral & Maxillofacial Implants,* 30(2)**,** 338-345.

Ng, E., Byun, R., Spahr, A. & Divnic-Resnik, T. (2018). The efficacy of air polishing devices in supportive periodontal therapy: a systematic review and meta-analysis. *Quintessence International,* 49(6)**,** 453-467.

Niinomi, M. (1998). Mechanical properties of biomedical titanium alloys. *Materials Science and Engineering: A,* 243(1)**,** 231-236.

Niinomi, M. (2002). Recent metallic materials for biomedical applications. *Metallurgical and Materials transactions A,* 33(3)**,** 477-486

Niinomi, M. (2003). Recent research and development in titanium alloys for biomedical applications and healthcare goods. *Science and Technology of Advanced Materials,* 4(5)**,** 445-454.

Niinomi, M. (2008). Mechanical biocompatibilities of titanium alloys for biomedical applications. *Journal of the Mechanical Behavior of Biomedical Materials,* 1(1)**,** 30-42.

Niinomi, M., Hattori, T., Morikawa, K., Kasuga, T., Suzuki, A., Fukui, H. & Niwa, S. (2002). Development of low rigidity beta-type titanium alloy for biomedical applications. *Materials Transactions,* 43(12)**,** 2970-2977.

Niinomi, M. & Nakai, M. (2011). Titanium-based biomaterials for preventing stress shielding between implant devices and bone. *International Journal of Biomaterials*, 2011. Article ID 836587.

Niinomi, M., Nakai, M. & Hieda, J. (2012). Development of new metallic alloys for biomedical applications. *Acta Biomaterialia,* 8(11)**,** 3888-3903.

Nikolidakis, D., Meijer, G. J., Oortgiesen, D. A., Walboomers, X. F. & Jansen, J. A. (2009). The effect of a low dose of transforming growth factor β1 (TGF-β1) on the early bone-healing around oral implants inserted in trabecular bone. *Biomaterials,* 30(1)**,** 94-99.

Nishiguchi, S., Fujibayashi, S., Kim, H. M., Kokubo, T. & Nakamura, T. (2003). Biology of alkali-and heat-treated titanium implants. *Journal of Biomedical Materials Research Part A,* 67(1)**,** 26-35.

Nociti, J. F. H., Machado, M. Â. N., Stefani, C. M. & Sallum, E. A. (2001). Absorbable versus nonabsorbable membranes and bone grafts in the treatment of ligature-induced peri-implantitis defects in dogs: a histometric investigation. *International Journal of Oral & Maxillofacial Implants,* 16(5)**,** 646-652.

Noda, K., Arakawa, H., Kimura-Ono, A., Yamazaki, S., Hara, E. S., Sonoyama, W., Maekawa, K., Okura, K., Shintani, A. & Matsuka, Y. (2015). A longitudinal retrospective study of the analysis of the risk factors of implant failure by the application of generalized estimating equations. *Journal of Prosthodontic Research,* 59(3)**,** 178-184.

Noguerol, B., Muñoz, R., Mesa, F., de Dios Luna, J. & O'valle, F. (2006). Early implant failure. Prognostic capacity of Periotest®: retrospective study of a large sample. *Clinical Oral Implants Research,* 17(4)**,** 459-464.

Noronha Oliveira, M., Schunemann, W., Mathew, M., Henriques, B., Magini, R., Teughels, W. & Souza, J. (2017). Can degradation products released from dental implants affect peri-implant tissues? *Journal of Periodontal Research,* 53(1)**,** 1-11.

Novaes Jr, A. B., de Souza, S., de Barros, R., Pereira, K., Iezzi, G. & Piattelli, A. (2010). Influence of implant surfaces on osseointegration. *Brazilian Dental Journal,* 21(6)**,** 371-8.

O'Donoghue, J. G. & Haverty, D. (2012). *Method of doping surfaces*. US patent application 11/853,764. Feb.21, 2012.US 8,119,183 B2.

O'Neill, L., O'Sullivan, C., O'Hare, P., Sexton, L., Keady, F. & O'Donoghue, J. (2009). Deposition of substituted apatites onto titanium surfaces using a novel blasting process. *Surface and Coatings Technology,* 204(4)**,** 484-488.

O'Sullivan, C., O'Hare, P., O'Leary, N. D., Crean, A. M., Ryan, K., Dobson, A. D. W. & O'Neill, L. (2010). Deposition of substituted apatites with anticolonizing properties onto

titanium surfaces using a novel blasting process. *Journal of Biomedical Materials Research Part B: Applied Biomaterials,* 95B(1)**,** 141-149.

O'Sullivan, C., O'Hare, P., Byrne, G., O'Neill, L., Ryan, K. B. & Crean, A. M. (2011). A modified surface on titanium deposited by a blasting process. *Coatings,* 1(1)**,** 53-71.

Ogle, O. E. (2015). Implant surface material, design, and osseointegration. *Dental Clinics,* 59(2)**,** 505-520.

Okazaki, Y. & Gotoh, E. (2005). Comparison of metal release from various metallic biomaterials in vitro. *Biomaterials,* 26(1)**,** 11-21.

Okazaki, Y., Ito, Y., Ito, A. & Tateishi, T. (1993). Effect of alloying elements on mechanical properties of titanium alloys for medical implants. *Materials Transactions, Japan Institute of Metals,* 34(12)**,** 1217-1222.

Olate, S., Lyrio, M. C. N., de Moraes, M., Mazzonetto, R. & Moreira, R. W. F. (2010). Influence of diameter and length of implant on early dental implant failure. *Journal of Oral and Maxillofacial Surgery,* 68(2)**,** 414-419.

Oliver, W. C. & Pharr, G. M. (1992). An improved technique for determining hardness and elastic modulus using load and displacement sensing indentation experiments. *Journal of Materials Research,* 7(06)**,** 1564-1583.

Oliver, W. C. & Pharr, G. M. (2004). Measurement of hardness and elastic modulus by instrumented indentation: advances in understanding and refinements to methodology. *Journal of Materials Research,* 19(1)**,** 3-20.

Oliver, W. C. & Pharr, G. M. (2010). Nanoindentation in materials research: past, present, and future. *Materials Research Society Bulletin,* 35(11)**,** 897-907.

Olmedo-Gaya, M. V., Manzano-Moreno, F. J., Cañaveral-Cavero, E., de Dios Luna-del Castillo, J. & Vallecillo-Capilla, M. (2016). Risk factors associated with early implant failure: a 5-year retrospective clinical study. *Journal of Prosthetic Dentistry,* 115(2)**,** 150-155.

Ong, J. L., Carnes, D. L. & Bessho, K. (2004). Evaluation of titanium plasma-sprayed and plasma-sprayed hydroxyapatite implants in vivo. *Biomaterials,* 25(19)**,** 4601-4606

Osman, R. B. & Swain, M. V. (2015). A critical review of dental implant materials with an emphasis on titanium versus zirconia. *Materials,* 8(3)**,** 932-958.

Oyen, M. L. & Cook, R. F. (2009). A practical guide for analysis of nanoindentation data. *Journal of the Mechanical Behavior of Biomedical Materials,* 2(4)**,** 396-407.

Pabst, A. M., Walter, C., Ehbauer, S., Zwiener, I., Ziebart, T., Al-Nawas, B. & Klein, M. O. (2015). Analysis of implant-failure predictors in the posterior maxilla: a retrospective study of 1395 implants. *Journal of Cranio-Maxillofacial Surgery,* 43(3)**,** 414-420.

Palmquist, A., Engqvist, H., Lausmaa, J. & Thomsen, P. (2012). Commercially available dental implants: review of their surface characteristics. *Journal of Biomaterials and Tissue Engineering,* 2(2)**,** 112-124.

Palmquist, A., Omar, O., Esposito, M., Lausmaa, J. & Thomsen, P. (2010). Titanium oral implants: Surface characteristics, interface biology and clinical outcome. *Journal of The Royal Society Interface,* 7 (s5)**,** s515-s527.

Panich, N. & Yong, S. (2005). Improved method to determine the hardness and elastic moduli using nano-indentation. *King Mongkut's Institute of Technology Ladkrabang Science Journal,* 5(2)**,** 483-492.

Parham, J. P., Cobb, C., French, A., Love, J., Drisko, C. & Killoy, W. (1989). Effects of an air-powder abrasive system on plasma-sprayed titanium implant surfaces: an in vitro evaluation. *Journal of Oral Implantology,* 15(2)**,** 78-86.

Park, J.-B., Jang, Y. J., Koh, M., Choi, B.-K., Kim, K.-K. & Ko, Y. (2013). In vitro analysis of the efficacy of ultrasonic scalers and a toothbrush for removing bacteria from resorbable blast material titanium disks. *Journal of Periodontology,* 84(8)**,** 1191-1198.

Park, J.-M., Jai-Young, K., Jun-Hyeog, J., Chong-Hyun, H., Seong-Kyun, K. & Seong-Joo, H. (2006). Osseointegration of anodized titanium implants coated with fibroblast growth factor-fibronectin (FGF-FN) fusion protein. *International Journal of Oral & Maxillofacial Implants,* 21(6)**,** 859-866.

Parlar, A., Bosshardt, D. D., Çetiner, D., Schafroth, D., Ünsal, B., Haytaç, C. & Lang, N. P. (2009). Effects of decontamination and implant surface characteristics on re-osseointegration following treatment of peri-implantitis. *Clinical Oral Implants Research,* 20(4)**,** 391-399.

Passanezi, E., Sant'Ana, A. C. P. & Damante, C. A. (2017). Occlusal trauma and mucositis or peri-implantitis? *Journal of the American Dental Association,* 148(2)**,** 106-112.

Pazos, L., Corengia, P. & Svoboda, H. (2010). Effect of surface treatments on the fatigue life of titanium for biomedical applications. *Journal of the Mechanical Behavior of Biomedical Materials,* 3(6)**,** 416-424.

Pecora, G. E., Ceccarelli, R., Bonelli, M., Alexander, H. & Ricci, J. L. (2009). Clinical evaluation of laser microtexturing for soft tissue and bone attachment to dental implants. *Implant Dentistry,* 18(1)**,** 57-66.

Pérez-Chaparro, P. J., Duarte, P. M., Shibli, J. A., Montenegro, S., Lacerda Heluy, S., Figueiredo, L. C., Faveri, M. & Feres, M. (2016). The current weight of evidence of the microbiologic profile associated with peri-implantitis: a systematic review. *Journal of Periodontology,* 87(11)**,** 1295-1304.

Persson, G. R., Roos-Jansåker, A.-M., Lindahl, C. & Renvert, S. (2011). Microbiologic results after non-surgical erbium-doped:yttrium, aluminum, and garnet laser or air-abrasive treatment of peri-implantitis: a randomized clinical trial. *Journal of Periodontology,* 82(9)**,** 1267-1278.

Persson, G. R., Samuelsson, E., Lindahl, C. & Renvert, S. (2010). Mechanical non-surgical treatment of peri-implantitis: a single-blinded randomized longitudinal clinical study. II. Microbiological results. *Journal of Clinical Periodontology,* 37(6)**,** 563-573.

Persson, L. G., Berglundh, T., Lindhe, J. & Sennerby, L. (2001). Re-osseointegration after treatment of peri-implantitis at different implant surfaces. *Clinical Oral Implants Research,* 12(6)**,** 595-603.

Petrie, T. A., Reyes, C. D., Burns, K. L. & García, A. J. (2009). Simple application of fibronectin–mimetic coating enhances osseointegration of titanium implants. *Journal of Cellular and Molecular Medicine,* 13(8b)**,** 2602-2612.

Piattelli, A., Scarano, A., Piattelli, M. & Calabrese, L. (1996). Direct bone formation on sand-blasted titanium implants: an experimental study. *Biomaterials,* 17(10)**,** 1015-1018.

Piattelli, M., Scarano, A., Paolantonio, M., Iezzi, G., Petrone, G. & Piattelli, A. (2002). Bone response to machined and resorbable blast material titanium implants: an experimental study in rabbits. *Journal of Oral Implantology,* 28(1)**,** 2-8.

Pieralli, S., Kohal, R.-J., Hernandez, E. L., Doerken, S. & Spies, B. C. (2017). Osseointegration of zirconia dental implants in animal investigations: a systematic review and meta-analysis. *Dental Materials,* 34(2)**,** 171-182.

Pjetursson, B., Asgeirsson, A., Zwahlen, M. & Sailer, I. (2014). Improvements in implant dentistry over the last decade: comparison of survival and complication rates in older and newer publications. *International Journal of Oral and Maxillofacial Implants,* 29(Supplement)**,** 308-324.

Porter, A., Hobbs, L., Rosen, V. B. & Spector, M. (2002). The ultrastructure of the plasma-sprayed hydroxyapatite–bone interface predisposing to bone bonding. *Biomaterials,* 23(3)**,** 725-733.

Porter, J. A. & Von Fraunhofer, J. A. (2005). Success or failure of dental implants? A literature review with treatment considerations. *General Dentistry,* 53(6)**,** 423-32; quiz 433, 446.

Prevéy, P. S. (2000). X-ray diffraction characterization of crystallinity and phase composition in plasma-sprayed hydroxyapatite coatings. *Journal of Thermal Spray Technology,* 9(3)**,** 369-376.

Proussaefs, P. & Lozada, J. (2004). Immediate loading of hydroxyapatite-coated implants in the maxillary premolar area: three-year results of a pilot study. *Journal of Prosthetic Dentistry,* 91(3)**,** 228-233.

Puleo, D. A. & Thomas, M. V. (2006). Implant surfaces. *Dental Clinics of North America,* 50(3)**,** 323-338.

Quintero, D. G., Taylor, R. B., Miller, M. B., Merchant, K. R. & Pasieta, S. A. (2017). Air-abrasive disinfection of implant surfaces in a simulated model of periimplantitis. *Implant Dentistry,* 26(3)**,** 423-428.

Quirynen, M., Al-Nawas, B., Meijer, H. J., Razavi, A., Reichert, T. E., Schimmel, M., Storelli, S. & Romeo, E. (2015). Small-diameter titanium Grade IV and titanium–zirconium implants in edentulous mandibles: three-year results from a double-blind, randomized controlled trial. *Clinical Oral Implants Research,* 26(7)**,** 831-840.

Raines, A. L., Olivares-Navarrete, R., Wieland, M., Cochran, D. L., Schwartz, Z. & Boyan, B. D. (2010). Regulation of angiogenesis during osseointegration by titanium surface microstructure and energy. *Biomaterials,* 31(18)**,** 4909-4917.

Rainey, J. T. (2002). Air abrasion: an emerging standard of care in conservative operative dentistry. *Dental Clinics,* 46(2)**,** 185-209.

Ramaglia, L., di Lauro, A. E., Morgese, F. & Squillace, A. (2006). Profilometric and standard error of the mean analysis of rough implant surfaces treated with different instrumentations. *Implant Dentistry,* 15(1)**,** 77-82.

Ramazanoglu, M., Lutz, R., Ergun, C., von Wilmowsky, C., Nkenke, E. & Schlegel, K. A. (2011). The effect of combined delivery of recombinant human bone morphogenetic protein-2 and recombinant human vascular endothelial growth

factor 165 from biomimetic calcium-phosphate-coated implants on osseointegration. *Clinical Oral Implants Research,* 22(12)**,** 1433-1439.

Rasmusson, L., Kahnberg, K. E. & Tan, A. (2001). Effects of implant design and surface on bone regeneration and implant stability: an experimental study in the dog mandible. *Clinical Implant Dentistry and Related Research,* 3(1)**,** 2-8.

Rausch-Fan, X., Qu, Z., Wieland, M., Matejka, M. & Schedle, A. (2008). Differentiation and cytokine synthesis of human alveolar osteoblasts compared to osteoblast-like cells (MG63) in response to titanium surfaces. *Dental Materials,* 24(1)**,** 102-110.

Reddy, E. S., Patil, N. P., Guttal, S. S. & Jagadish, H. (2007). Effect of different finishing and polishing agents on the surface roughness of cast pure titanium. *Journal of Prosthodontics,* 16(4)**,** 263-268.

Reichelt, R. (2007). Scanning electron microscopy, *In:* Hawkes, P. W. & Spence, J. C. H. (eds.) *Science of microscopy.* New York: Springer, 133-273. [Online]. Available: https://doi.org/10.1007/978-0-387-49762-4_3.

Renouard, F. & Nisand, D. (2006). Impact of implant length and diameter on survival rates. *Clinical Oral Implants Research,* 17(s2)**,** 35-51.

Renvert, S., Lessem, J., Dahlén, G., Renvert, H. & Lindahl, C. (2008a). Mechanical and repeated antimicrobial therapy using a local drug delivery system in the treatment of peri-implantitis: a randomized clinical trial. *Journal of Periodontology,* 79(5)**,** 836-844.

Renvert, S., Lindahl, C., Renvert, H. & Persson, G. R. (2008b). Clinical and microbiological analysis of subjects treated with Brånemark or AstraTech implants: a 7-year follow-up study. *Clinical Oral Implants Research,* 19(4)**,** 342-347.

Renvert, S., Lindahl, C., Roos Jansåker, A.-M. & Persson, G. R. (2011). Treatment of peri-implantitis using an Er:YAG laser or an air-abrasive device: a randomized clinical trial. *Journal of Clinical Periodontology,* 38(1)**,** 65-73.

Renvert, S., Persson, G. R., Pirih, F. Q. & Camargo, P. M. (2018). Peri-implant health, peri-implant mucositis, and peri-implantitis: case definitions and diagnostic considerations. *Journal of Clinical Periodontology,* 45(s20)**,** S278-S285.

Renvert, S. & Polyzois, I. (2015a). Risk indicators for peri-implant mucositis: a systematic literature review. *Journal of Clinical Periodontology,* 42(s16)**,** S172-S186.

Renvert, S., Polyzois, I. & Maguire, R. (2009a). Re-osseointegration on previously contaminated surfaces: a systematic review. *Clinical Oral Implants Research,* 20(s4)**,** 216-227.

Renvert, S. & Polyzois, I. N. (2015b). Clinical approaches to treat peri-implant mucositis and peri-implantitis. *Periodontology 2000,* 68(1)**,** 369-404.

Renvert, S., Roos-Jansåker, A. M. & Claffey, N. (2008c). Non-surgical treatment of peri-implant mucositis and peri-implantitis: a literature review. *Journal of Clinical Periodontology,* 35(s8)**,** 305-315.

Renvert, S., Samuelsson, E., Lindahl, C. & Persson, G. R. (2009b). Mechanical non-surgical treatment of peri-implantitis: a double-blind randomized longitudinal clinical study. I: clinical results. *Journal of Clinical Periodontology,* 36(7)**,** 604-609.

Rho, J.-Y., Tsui, T. Y. & Pharr, G. M. (1997). Elastic properties of human cortical and trabecular lamellar bone measured by nanoindentation. *Biomaterials,* 18(20)**,** 1325-1330.

Riben-Grundstrom, C., Norderyd, O., André, U. & Renvert, S. (2015). Treatment of peri-implant mucositis using a glycine powder air-polishing or ultrasonic device: a randomized clinical trial. *Journal of Clinical Periodontology,* 42(5)**,** 462-469.

Ricci, M., Mangano, F., Tercio, T., Tonelli, P., Barone, A., Raspanti, M. & Covani, U. (2012). Nanometrical evaluation of direct laser implant surface. *Surface and Interface Analysis,* 44(13)**,** 1582-1586.

Roach, P., Eglin, D., Rohde, K. & Perry, C. C. (2007). Modern biomaterials: a review—bulk properties and implications of surface modifications. *Journal of Materials Science: Materials in Medicine,* 18(7)**,** 1263-1277.

Roach, P., Farrar, D. & Perry, C. C. (2005). Interpretation of protein adsorption: surface-induced conformational changes. *Journal of the American Chemical Society,* 127(22)**,** 8168-8173.

Roccuzzo, M., Bonino, F., Bonino, L. & Dalmasso, P. (2011). Surgical therapy of peri-implantitis lesions by means of a bovine-derived xenograft: comparative results of a prospective study on two different implant surfaces. *Journal of Clinical Periodontology,* 38(8)**,** 738-745.

Roccuzzo, M., Bunino, M., Prioglio, F. & Bianchi, S. D. (2001). Early loading of sandblasted and acid-etched (SLA) implants: a prospective split-mouth comparative study. *Clinical Oral Implants Research,* 12(6)**,** 572-578.

Romanos, G., Ko, H.-H., Froum, S. & Tarnow, D. (2009). The use of CO_2 laser in the treatment of peri-implantitis. *Photomedicine and Laser Surgery,* 27(3)**,** 381-386.

Romanos, G. E., Javed, F., Delgado-Ruiz, R. A. & Calvo-Guirado, J. L. (2015). Peri-implant diseases: a review of treatment interventions. *Dental Clinics,* 59(1)**,** 157-178.

Romanos, G. E. & Weitz, D. (2012). Therapy of peri-implant diseases. Where is the evidence? *Journal of Evidence Based Dental Practice,* 12(3)**,** 204-208.

Romeo, E., Lops, D., Amorfini, L., Chiapasco, M., Ghisolfi, M. & Vogel, G. (2006). Clinical and radiographic evaluation of small-diameter (3.3-mm) implants followed for 1–7 years: a longitudinal study. *Clinical Oral Implants Research,* 17(2)**,** 139-148.

Rompen, E., Domken, O., Degidi, M., Farias Pontes, A. E. & Piattelli, A. (2006). The effect of material characteristics, of surface topography and of implant components and connections on soft tissue integration: a literature review. *Clinical Oral Implants Research,* 17(s2)**,** 55-67.

Ronay, V., Merlini, A., Attin, T., Schmidlin, P. R. & Sahrmann, P. (2017). In vitro cleaning potential of three implant debridement methods. Simulation of the non-surgical approach. *Clinical Oral Implants Research,* 28(2)**,** 151-155.

Rong, M., Zhou, L., Gou, Z., Zhu, A. & Zhou, D. (2009). The early osseointegration of the laser-treated and acid-etched dental implants surface: an experimental study in rabbits. *Journal of Materials Science: Materials in Medicine,* 20(8)**,** 1721-1728.

Rønold, H., Lyngstadaas, S. & Ellingsen, J. (2003). Analysing the optimal value for titanium implant roughness in bone attachment using a tensile test. *Biomaterials,* 24(25)**,** 4559-4564.

Rønold, H. J. & Ellingsen, J. E. (2002). Effect of micro-roughness produced by TiO_2 blasting—tensile testing of bone attachment by using coin-shaped implants. *Biomaterials,* 23(21)**,** 4211-4219.

Rosales-Leal, J. I., Rodríguez-Valverde, M. A., Mazzaglia, G., Ramón-Torregrosa, P. J., Díaz-Rodríguez, L., García-Martínez, O., Vallecillo-Capilla, M., Ruiz, C. & Cabrerizo-Vílchez, M. A. (2010). Effect of roughness, wettability and morphology of engineered titanium surfaces on osteoblast-like cell adhesion. *Colloids and Surfaces A: Physicochemical and Engineering Aspects,* 365(1)**,** 222-229.

Rupp, F., Gittens, R. A., Scheideler, L., Marmur, A., Boyan, B. D., Schwartz, Z. & Geis-Gerstorfer, J. (2014). A review on the wettability of dental implant surfaces I: theoretical and experimental aspects. *Acta Biomaterialia,* 10(7)**,** 2894-2906.

Rupp, F., Liang, L., Geis-Gerstorfer, J., Scheideler, L. & Hüttig, F. (2017). Surface characteristics of dental implants: a review. *Dental Materials,* 34(1)**,** 40-57.

Rupp, F., Scheideler, L., Olshanska, N., De Wild, M., Wieland, M. & Geis-Gerstorfer, J. (2006). Enhancing surface free energy and hydrophilicity through chemical modification of microstructured titanium implant surfaces. *Journal of Biomedical Materials Research Part A,* 76(2)**,** 323-334.

Rupp, F., Scheideler, L., Rehbein, D., Axmann, D. & Geis-Gerstorfer, J. (2004). Roughness induced dynamic changes of wettability of acid etched titanium implant modifications. *Biomaterials,* 25(7)**,** 1429-1438.

Russell, R. G. G., Xia, Z., Dunford, J. E., Oppermann, U., Kwaasi, A., Hulley, P. A., Kavanagh, K. L., Triffitt, J. T., Lundy, M. W. & Phipps, R. J. (2007). Bisphosphonates: an update on mechanisms of action and how these relate to clinical efficacy. *Annals of the New York Academy of Sciences,* 1117(1)**,** 209-257.

Saber-Samandari, S., Berndt, C. C. & Gross, K. A. (2011). Selection of the implant and coating materials for optimized performance by means of nanoindentation. *Acta Biomaterialia,* 7(2)**,** 874-881.

Sader, M. S., Balduino, A., de Almeida Soares, G. & Borojevic, R. (2005). Effect of three distinct treatments of titanium surface on osteoblast attachment, proliferation, and differentiation. *Clinical Oral Implants Research,* 16(6)**,** 667-675.

Safii, S. H., Palmer, R. M. & Wilson, R. F. (2010). Risk of implant failure and marginal bone loss in subjects with a history of periodontitis: a systematic review and meta-analysis. *Clinical Implant Dentistry and Related Research,* 12(3)**,** 165-174.

Saghiri, M.-A., Asatourian, A., Garcia-Godoy, F. & Sheibani, N. (2016). The role of angiogenesis in implant dentistry part I: Review of titanium alloys, surface characteristics and treatments. *Medicina Oral, Patologia Oral y Cirugia Bucal,* 21(4)**,** e514-e525.

Sahm, N., Becker, J., Santel, T. & Schwarz, F. (2011). Non-surgical treatment of peri-implantitis using an air-abrasive device or mechanical debridement and local application of chlorhexidine: a prospective, randomized, controlled clinical study. *Journal of Clinical Periodontology,* 38(9)**,** 872-878.

Sahrmann, P., Ronay, V., Hofer, D., Attin, T., Jung, R. E. & Schmidlin, P. R. (2015). In vitro cleaning potential of three different implant debridement methods. *Clinical Oral Implants Research,* 26(3)**,** 314-319.

Sahrmann, P., Ronay, V., Sener, B., Jung, R. E., Attin, T. & Schmidlin, P. R. (2013). Cleaning potential of glycine air-flow application in an in vitro peri-implantitis model. *Clinical Oral Implants Research,* 24(6)**,** 666-670.

Saini, M., Singh, Y., Arora, P., Arora, V. & Jain, K. (2015). Implant biomaterials: a comprehensive review. *World Journal of Clinical Cases,* 3(1)**,** 52-57.

Sakka, S., Baroudi, K. & Nassani, M. Z. (2012). Factors associated with early and late failure of dental implants. *Journal of Investigative and Clinical Dentistry,* 3(4)**,** 258-261.

Sakka, S. & Coulthard, P. (2009). Bone quality: a reality for the process of osseointegration. *Implant Dentistry,* 18(6)**,** 480-485.

Sakka, S. & Coulthard, P. (2011). Implant failure: etiology and complications. *Medicina Oral, Patologia Oral y Cirugia Bucal.,* 16(1)**,** e42-44.

Salvi, G. E., Aglietta, M., Eick, S., Sculean, A., Lang, N. P. & Ramseier, C. A. (2012). Reversibility of experimental peri-implant mucositis compared with experimental gingivitis in humans. *Clinical Oral Implants Research,* 23(2)**,** 182-190.

Salvi, G. E., Cosgarea, R. & Sculean, A. (2017). Prevalence and mechanisms of peri-implant diseases. *Journal of Dental Research,* 96(1)**,** 31-37.

Santos, P. & Júlio, E. N. (2013). A state-of-the-art review on roughness quantification methods for concrete surfaces. *Construction and Building Materials,* 38**,** 912-923

Sasani, N., Khaki, J. V. & Zebarjad, S. M. (2014). Characterization and nanomechanical properties of novel dental implant coatings containing copper decorated-carbon nanotubes. *Journal of the Mechanical Behavior of Biomedical Materials,* 37**,** 125-132.

Saulacic, N., Bosshardt, D., Bornstein, M., Berner, S. & Buser, D. (2012). Bone apposition to a titanium-zirconium alloy implant, as compared to two other titanium-containing implants. *European Cells and Materials,* 23(1)**,** 273-286.

Saulacic, N., Erdösi, R., Bosshardt, D. D., Gruber, R. & Buser, D. (2014). Acid and alkaline etching of sandblasted Zirconia implants: a histomorphometric study in miniature pigs. *Clinical Implant Dentistry and Related Research,* 16(3)**,** 313-322.

Sawase, T., Jimbo, R., Baba, K., Shibata, Y., Ikeda, T. & Atsuta, M. (2008). Photo-induced hydrophilicity enhances initial cell behavior and early bone apposition. *Clinical Oral Implants Research,* 19(5)**,** 491-496.

Scarano, A., Di Carlo, F., Quaranta, M. & Piattelli, A. (2003). Bone response to zirconia ceramic implants: an experimental study in rabbits. *Journal of Oral Implantology,* 29(1)**,** 8-12.

Schiegnitz, E. & Al-Nawas, B. (2018). Narrow-diameter implants: a systematic review and meta-analysis. *Clinical Oral Implants Research,* 29(S16)**,** 21-40.

Schimmel, M., Müller, F., Suter, V. & Buser, D. (2017). Implants for elderly patients. *Periodontology 2000,* 73(1)**,** 228-240.

Schliephake, H., Rublack, J., Förster, A., Schwenzer, B., Reichert, J. & Scharnweber, D. (2015). Functionalization of titanium implants using a modular system for binding and release of VEGF enhances bone-implant contact in a rodent model. *Journal of Clinical Periodontology,* 42(3)**,** 302-310.

Schliephake, H., Scharnweber, D., Dard, M., Sewing, A., Aref, A. & Roessler, S. (2005). Functionalization of dental implant surfaces using adhesion molecules. *Journal of Biomedical Materials Research Part B: Applied Biomaterials: An Official Journal of The Society for Biomaterials, The Japanese Society for Biomaterials, and The Australian Society for Biomaterials and the Korean Society for Biomaterials,* 73(1)**,** 88-96.

Schliephake, H., Scharnweber, D., Roesseler, S., Dard, M., Sewing, A. & Aref, A. (2006). Biomimetic calcium phosphate composite coating of dental implants. *International Journal of Oral & Maxillofacial Implants,* 21(5)**,** 738-746.

Schmage, P., Kahili, F., Nergiz, I., Scorziello, T. M., Platzer, U. & Pfeiffer, P. (2014). Cleaning effectiveness of implant prophylaxis instruments. *International Journal of Oral & Maxillofacial Implants,* 29(2)**,** 331-337.

Schmage, P., Thielemann, J., Nergiz, I., Scorziello, T. M. & Pfeiffer, P. (2012). Effects of 10 cleaning instruments on four different implant surfaces. *International Journal of Oral & Maxillofacial Implants,* 27(2)**,** 308-317.

Schmidt, K. E., Auschill, T. M., Heumann, C., Frankenberger, R., Eick, S., Sculean, A. & Arweiler, N. B. (2017). Influence of different instrumentation modalities on the surface characteristics and biofilm formation on dental implant neck, in vitro. *Clinical Oral Implants Research,* 28(4)**,** 483-490.

Schou, S., Holmstrup, P., Jørgensen, T., Skovgaard, L. T., Stoltze, K., Hjørting-Hansen, E. & Wenzel, A. (2003). Implant surface preparation in the surgical treatment of

experimental peri-implantitis with autogenous bone graft and ePTFE membrane in cynomolgus monkeys. *Clinical Oral Implants Research,* 14(4)**,** 412-422.

Schouten, C., Meijer, G., Van den Beucken, J., Spauwen, P. & Jansen, J. (2009). Effects of implant geometry, surface properties, and TGF-β1 on peri-implant bone response: an experimental study in goats. *Clinical Oral Implants Research,* 20(4)**,** 421-429.

Schroeder, A., van der Zypen, E., Stich, H. & Sutter, F. (1981). The reactions of bone, connective tissue, and epithelium to endosteal implants with titanium-sprayed surfaces. *Journal of Maxillofacial Surgery,* 9(0)**,** 15-25.

Schuh, C. A. (2006). Nanoindentation studies of materials. *Materials Today,* 9(5)**,** 32-40.

Schüpbach, P., Glauser, R., Rocci, A., Martignoni, M., Sennerby, L., Lundgren, A. & Gottlow, J. (2005). The human bone–oxidized titanium implant interface: a light microscopic, scanning electron microscopic, back-scatter scanning electron microscopic, and energy-dispersive x-ray study of clinically retrieved dental implants. *Clinical Implant Dentistry and Related Research,* 7(s1)**,** s36-s43.

Schwartz, Z. & Boyan, B. (1994). Underlying mechanisms at the bone–biomaterial interface. *Journal of Cellular Biochemistry,* 56(3)**,** 340-347.

Schwartz, Z., Lohmann, C., Oefinger, J., Bonewald, L., Dean, D. & Boyan, B. (1999). Implant surface characteristics modulate differentiation behavior of cells in the osteoblastic lineage. *Advances in Dental Research,* 13(1)**,** 38-48.

Schwarz, F., Becker, K. & Renvert, S. (2015a). Efficacy of air polishing for the non-surgical treatment of peri-implant diseases: a systematic review. *Journal of Clinical Periodontology,* 42(10)**,** 951-959.

Schwarz, F., Derks, J., Monje, A. & Wang, H. L. (2018). Peri-implantitis. *Journal of Clinical Periodontology,* 45(s20)**,** S246-S266.

Schwarz, F., Ferrari, D., Herten, M., Mihatovic, I., Wieland, M., Sager, M. & Becker, J. (2007). Effects of surface hydrophilicity and microtopography on early stages of soft and hard tissue integration at non-submerged titanium implants: an immunohistochemical study in dogs. *Journal of Periodontology,* 78(11)**,** 2171-2184.

Schwarz, F., Ferrari, D., Popovski, K., Hartig, B. & Becker, J. (2009a). Influence of different air-abrasive powders on cell viability at biologically contaminated titanium dental implants surfaces. *Journal of Biomedical Materials Research. Part B, Applied Biomaterials,* 88(1)**,** 83-91.

Schwarz, F., John, G., Mainusch, S., Sahm, N. & Becker, J. (2012). Combined surgical therapy of peri-implantitis evaluating two methods of surface debridement and decontamination. A two-year clinical follow up report. *Journal of Clinical Periodontology,* 39(8)**,** 789-797.

Schwarz, F., Sahm, N., Bieling, K. & Becker, J. (2009b). Surgical regenerative treatment of peri-implantitis lesions using a nanocrystalline hydroxyapatite or a natural bone mineral in combination with a collagen membrane: a four-year clinical follow-up report. *Journal of Clinical Periodontology,* 36(9)**,** 807-814.

Schwarz, F., Sahm, N., Schwarz, K. & Becker, J. (2010). Impact of defect configuration on the clinical outcome following surgical regenerative therapy of peri-implantitis. *Journal of Clinical Periodontology,* 37(5)**,** 449-455.

Schwarz, F., Schmucker, A. & Becker, J. (2015b). Efficacy of alternative or adjunctive measures to conventional treatment of peri-implant mucositis and peri-implantitis: a systematic review and meta-analysis. *International Journal of Implant Dentistry,* 1(1)**,** 22.

Schwarz, F., Sculean, A., Bieling, K., Ferrari, D., Rothamel, D. & Becker, J. (2008). Two-year clinical results following treatment of peri-implantitis lesions using a nanocrystalline hydroxyapatite or a natural bone mineral in combination with a collagen membrane. *Journal of Clinical Periodontology,* 35(1)**,** 80-87.

Schwarz, F., Sculean, A., Rothamel, D., Schwenzer, K., Georg, T. & Becker, J. (2005). Clinical evaluation of an Er:YAG laser for nonsurgical treatment of peri-implantitis: a pilot study. *Clinical Oral Implants Research,* 16(1)**,** 44-52.

Schwarz, F., Wieland, M., Schwartz, Z., Zhao, G., Rupp, F., Geis-Gerstorfer, J., Schedle, A., Broggini, N., Bornstein, M. M. & Buser, D. (2009c). Potential of chemically modified hydrophilic surface characteristics to support tissue integration of titanium dental implants. *Journal of Biomedical Materials Research Part B: Applied Biomaterials: An Official Journal of The Society for Biomaterials, The Japanese Society for Biomaterials, and The Australian Society for Biomaterials and the Korean Society for Biomaterials,* 88(2)**,** 544-557.

Sevilla, P., Sandino, C., Arciniegas, M., Martínez-Gomis, J., Peraire, M. & Gil, F. J. (2010). Evaluating mechanical properties and degradation of YTZP dental implants. *Materials Science and Engineering: C,* 30(1)**,** 14-19.

Shi, L., Shi, L., Wang, L., Duan, Y., Lei, W., Wang, Z., Li, J., Fan, X., Li, X., Li, S. & Guo, Z. (2013). The improved biological performance of a novel low elastic modulus implant. *Public Library of Science,* 8(2)**,** e55015.

Shibata, N. & Okuno, O. (1987). Bone and fibrous tissue ingrowth into the porous Zr-Ti implants. *Dental Materials Journal,* 6(2)**,** 185-200.

Shibata, Y. & Tanimoto, Y. (2015). A review of improved fixation methods for dental implants. Part I: Surface optimization for rapid osseointegration. *Journal of Prosthodontic Research,* 59(1)**,** 20-33.

Shibata, Y., Tanimoto, Y., Maruyama, N. & Nagakura, M. (2015). A review of improved fixation methods for dental implants. Part II: Biomechanical integrity at bone–implant interface. *Journal of Prosthodontic Research,* 59(2)**,** 84-95.

Shibli, J. A., Mangano, C., Mangano, F., Rodrigues, J. A., Cassoni, A., Bechara, K., Ferreia, J. D. B., Dottore, A. M., Iezzi, G. & Piattelli, A. (2013). Bone-to-implant contact around immediately loaded direct laser metal-forming transitional implants in human posterior maxilla. *Journal of Periodontology,* 84(6)**,** 732-737.

Shibli, J. A., Martins, M. C., Ribeiro, F. S., Garcia, V. G., Nociti, F. H. & Marcantonio, E. (2006). Lethal photosensitization and guided bone regeneration in treatment of peri-implantitis: an experimental study in dogs. *Clinical Oral Implants Research,* 17(3)**,** 273-281.

Shrestha, S. & Joshi, S. (2014). Current concepts in biomaterials in dental implant. *Science Research,* 2(1)**,** 7-12.

Siddiqi, A., Payne, A. G., De Silva, R. K. & Duncan, W. J. (2011). Titanium allergy: could it affect dental implant integration? *Clinical Oral Implants Research,* 22(7)**,** 673-680.

Sierra-Sánchez, J. L., Martínez-González, A., Bonmatí, F. G.-S., Mañes-Ferrer, J. F. & Brotons-Oliver, A. (2014). Narrow-diameter implants: are they a predictable treatment option? A literature review. *Medicina Oral, Patologia Oral y Cirugia Bucal,* 19(1)**,** e74-e81.

Simka, W., Mosiałek, M., Nawrat, G., Nowak, P., Żak, J., Szade, J., Winiarski, A., Maciej, A. & Szyk-Warszyńska, L. (2012). Electrochemical polishing of Ti-13Nb-13Zr alloy. *Surface and Coatings Technology,* 213**,** 239-246.

Simon, Z. & Watson, P. A. (2002). Biomimetic dental implants-new ways to enhance osseointegration. *Journal-Canadian Dental Association,* 68(5)**,** 286-289.

Sista, S., Wen, C. e., Hodgson, P. D. & Pande, G. (2011). The influence of surface energy of titanium-zirconium alloy on osteoblast cell functions in vitro. *Journal of Biomedical Materials Research Part A,* 97(1)**,** 27-36.

Smeets, R., Henningsen, A., Jung, O., Heiland, M., Hammächer, C. & Stein, J. M. (2014). Definition, etiology, prevention and treatment of peri-implantitis–a review. *Head and Face Medicine,* 10(1)**,** 1-13.

Srinivasan, M., Meyer, S., Mombelli, A. & Müller, F. (2017). Dental implants in the elderly population: a systematic review and meta-analysis. *Clinical Oral Implants Research,* 28(8)**,** 920-930.

Stadlinger, B., Hennig, M., Eckelt, U., Kuhlisch, E. & Mai, R. (2010). Comparison of zirconia and titanium implants after a short healing period. A pilot study in minipigs. *International Journal of Oral and Maxillofacial Surgery,* 39(6)**,** 585-592.

Stadlinger, B., Korn, P., Tödtmann, N., Eckelt, U., Range, U., Bürki, A., Ferguson, S., Kramer, I., Kautz, A. & Schnabelrauch, M. (2013). Osseointegration of biochemically modified implants in an osteoporosis rodent model. *European Cells & Materials,* 25**,** 326-340.

Stanford, C. M. & Keller, J. C. (1991). The concept of osseointegration and bone matrix expression. *Critical Reviews in Oral Biology & Medicine,* 2(1)**,** 83-101.

Steinberg, D., Klinger, A., Kohavi, D. & Sela, M. N. (1995). Adsorption of human salivary proteins to titanium powder. I. Adsorption of human salivary albumin. *Biomaterials,* 16(17)**,** 1339-1343.

Steinemann, S. (2012). *Binary titanium-zirconium alloy for surgical implants and a suitable manufacturing process*. US patent application 12/367,978. May. 1,2012.US 8,168,012 B2.

Steinemann, S. G. & Perren, S. M. (1977). *Surgical implant and alloy for use in making an implant*. US patent application 552,216. Aug. 9,1977.US 4,040,129 A.

Stout, K. J. & Blunt, L. (2000). Instruments and measurement techniques of three dimensional surface topography, *Three dimensional surface topography.* Second ed. London: Penton Press, 21-70. [Online]. Available: http://www.sciencedirect.com/science/article/pii/B978185718026850117X.

Strnad, Z., Strnad, J., Povysil, C. & Urban, K. (2000). Effect of plasma-sprayed hydroxyapatite coating on the osteoconductivity of commercially pure titanium implants. *International Journal of Oral and Maxillofacial Implants,* 15(4)**,** 483-490.

Suárez-López Del Amo, F., Yu, S.-H. & Wang, H.-L. (2016). Non-surgical therapy for peri-implant diseases: a systematic review. *Journal of Oral & Maxillofacial Research,* 7(3)**,** e13-e13.

Suarez, F., Monje, A., Galindo-Moreno, P. & Wang, H.-L. (2013). Implant surface detoxification: a comprehensive review. *Implant Dentistry,* 22(5)**,** 465-473.

Subramani, K., Jung, R. E., Molenberg, A. & Hämmerle, C. H. (2009). Biofilm on dental implants: a review of the literature. *International Journal of Oral & Maxillofacial Implants,* 24(4)**,** 616-626.

Subramani, K., Lavenus, S., Rozé, J., Louarn, G. & Layrolle, P. (2018). Impact of nanotechnology on dental implants. *In:* Subramani, K. & Ahmed, W. (eds.) *Emerging nanotechnologies in dentistry.* Second ed. Amsterdam: William Andrew Publishing, 83-93.

Subramani, K. & Wismeijer, D. (2012). Decontamination of titanium implant surface and re-osseointegration to treat peri-implantitis: a literature review. *International Journal of Oral & Maxillofacial Implants,* 27(5)**,** 1043-1054.

Sul, Y.-T. (2010). Electrochemical growth behavior, surface properties, and enhanced in vivo bone response of TiO_2 nanotubes on microstructured surfaces of blasted, screw-shaped titanium implants. *International Journal of Nanomedicine,* 5**,** 87-100.

Sul, Y.-T., Johansson, C., Wennerberg, A., Cho, L.-R., Chang, B.-S. & Albrektsson, T. (2005). Optimum surface properties of oxidized implants for reinforcement of osseointegration: surface chemistry, oxide thickness, porosity, roughness, and crystal structure. *International Journal of Oral and Maxillofacial Implants,* 20(3)**,** 349-359.

Sul, Y. T., Jeong, Y., Johansson, C. & Albrektsson, T. (2006). Oxidized, bioactive implants are rapidly and strongly integrated in bone. Part 1–experimental implants. *Clinical Oral Implants Research,* 17(5)**,** 521-526.

Sul, Y. T., Kang, B. S., Johansson, C., Um, H. S., Park, C. J. & Albrektsson, T. (2009). The roles of surface chemistry and topography in the strength and rate of osseointegration of titanium implants in bone. *Journal of Biomedical Materials Research Part A,* 89(4)**,** 942-950.

Sullivan, R. M. (2001). Implant dentistry and the concept of osseointegration: a historical perspective. *Journal of California Dental Association,* 29(11)**,** 737-45.

Sun, H. L., Wu, Y. R., Huang, C. & Shi, B. (2011). Failure rates of short (≤ 10 mm) dental implants and factors influencing their failure: a systematic review. *International Journal of Oral & Maxillofacial Implants,* 26(4)**,** 816-825.

Sun, L., Berndt, C. C., Gross, K. A. & Kucuk, A. (2001). Material fundamentals and clinical performance of plasma-sprayed hydroxyapatite coatings: a review. *Journal of Biomedical Materials Research,* 58(5)**,** 570-592.

Surmenev, R. A., Surmeneva, M. A. & Ivanova, A. A. (2014). Significance of calcium phosphate coatings for the enhancement of new bone osteogenesis – A review. *Acta Biomaterialia,* 10(2)**,** 557-579.

Sutter, F., Schroeder, A. & Buser, D. A. (1988). The new concept of ITI hollow-cylinder and hollow-screw implants: Part 1. Engineering and design. *International Journal of Oral Maxillofacial Implants,* 3(3)**,** 161-172.

Svanborg, L. M., Andersson, M. & Wennerberg, A. (2010). Surface characterization of commercial oral implants on the nanometer level. *Journal of Biomedical Materials Research Part B: Applied Biomaterials,* 92B(2)**,** 462-469.

Sygkounas, E., Louropoulou, A., Schoenmaker, T., de Vries, T. J. & Van der Weijden, F. A. (2017). Influence of various air-abrasive powders on the viability and density of periodontal cells: an in vitro study. *Journal of Biomedical Materials Research Part B: Applied Biomaterials,* 106(5)**,** 1955-1963.

Tahriri, M., Rasoulianboroujeni, M., Bader, R., Vashaee, D. & Tayebi, L. (2017). Growth factors for oral and maxillofacial regeneration applications. *In:* Tayebi, L. & Moharamzadeh, K. (eds.) *Biomaterials for oral and dental tissue engineering.* Cambridge, MA: Woodhead Publishing, 205-219.

Takasaki, A. A., Aoki, A., Mizutani, K., Kikuchi, S., Oda, S. & Ishikawa, I. (2007). Er: YAG laser therapy for peri-implant infection: a histological study. *Lasers in Medical Science,* 22(3)**,** 143-157.

Takasaki, A. A., Aoki, A., Mizutani, K., Schwarz, F., Sculean, A., Wang, C.-Y., Koshy, G., Romanos, G., Ishikawa, I. & Izumi, Y. (2009). Application of antimicrobial photodynamic therapy in periodontal and peri-implant diseases. *Periodontology 2000,* 51(1)**,** 109-140.

Takebe, J., Champagne, C. M., Offenbacher, S., Ishibashi, K. & Cooper, L. F. (2003). Titanium surface topography alters cell shape and modulates bone morphogenetic

protein 2 expression in the J774A.1 macrophage cell line. *Journal of Biomedical Materials Research Part A,* 64A(2)**,** 207-216.

Takeuchi, K., Saruwatari, L., Nakamura, H. K., Yang, J. M. & Ogawa, T. (2005). Enhanced intrinsic biomechanical properties of osteoblastic mineralized tissue on roughened titanium surface. *Journal of Biomedical Materials Research Part A,* 72(3)**,** 296-305.

Takeuchi, M., Abe, Y., Yoshida, Y., Nakayama, Y., Okazaki, M. & Akagawa, Y. (2003). Acid pretreatment of titanium implants. *Biomaterials,* 24(10)**,** 1821-1827.

Tan, F., Naciri, M., Dowling, D. & Al-Rubeai, M. (2012). In vitro and in vivo bioactivity of CoBlast hydroxyapatite coating and the effect of impaction on its osteoconductivity. *Biotechnology Advances,* 30(1)**,** 352-362.

Tanaka, Y. & Yamashita, K. (2008). Fabrication processes for bioceramics. *In:* Kokubo, T. (ed.) *Bioceramics and Their Clinical Applications.* Cambridge: Woodhead Publishing and Maney Publishing on behalf of The Institute of Materials, Minerals & Mining.

Taschieri, S., Weinstein, R., Del Fabbro, M. & Corbella, S. (2015). Erythritol-Enriched air-polishing powder for The surgical treatment of peri-implantitis. *The Scientific World Journal,* 2015**,** 9. Article ID 802310.

Tastepe, C. S., Lin, X., Donnet, M., Doulabi, B. Z., Wismeijer, D. & Liu, Y. (2018a). Re-establishment of biocompatibility of the in vitro contaminated titanium surface using osteoconductive powders with air-abrasive treatment. *Journal of Oral Implantology,* 44(2)**,** 94-101.

Tastepe, C. S., Lin, X., Werner, A., Donnet, M., Wismeijer, D. & Liu, Y. (2018b). Cleaning effect of osteoconductive powder abrasive treatment on explanted human implants and biofilm-coated titanium discs. *Clinical and Experimental Dental Research,* 4(1)**,** 25-34.

Tastepe, C. S., Liu, Y., Visscher, C. M. & Wismeijer, D. (2013). Cleaning and modification of intraorally contaminated titanium discs with calcium phosphate powder abrasive treatment. *Clinical Oral Implants Research,* 24(11)**,** 1238-1246.

Tastepe, C. S., van Waas, R., Liu, Y. & Wismeijer, D. (2012). Air powder abrasive treatment as an implant surface cleaning method: a literature review. *International Journal of Oral & Maxillofacial Implants,* 27(6)**,** 1461-1473.

Terheyden, H., Lang, N. P., Bierbaum, S. & Stadlinger, B. (2012). Osseointegration–communication of cells. *Clinical Oral Implants Research,* 23(10)**,** 1127-1135.

Teughels, W., Van Assche, N., Sliepen, I. & Quirynen, M. (2006). Effect of material characteristics and/or surface topography on biofilm development. *Clinical Oral Implants Research,* 17(s2)**,** 68-81.

Tey, V. H. S., Phillips, R. & Tan, K. (2017). Five-year retrospective study on success, survival and incidence of complications of single crowns supported by dental implants. *Clinical Oral Implants Research,* 28(5)**,** 620-625.

Thoma, D. S., Jones, A. A., Dard, M., Grize, L., Obrecht, M. & Cochran, D. L. (2011). Tissue integration of a new titanium-zirconium dental implant: a comparative histologic and radiographic study in the canine. *Journal of Periodontology,* 82(10)**,** 1453-1461.

Thomason, J. M., Feine, J., Exley, C., Moynihan, P., Müller, F., Naert, I., Ellis, J. S., Barclay, C., Butterworth, C. & Scott, B. (2009). Mandibular two implant-supported overdentures as the first choice standard of care for edentulous patients-the York Consensus Statement. *British Dental Journal,* 207(4)**,** 185-186.

Tinsley, D., Watson, C. J. & Russell, J. L. (2001). A comparison of hydroxylapatite coated implant retained fixed and removable mandibular prostheses over 4 to 6 years. *Clinical Oral Implants Research,* 12(2)**,** 159-166.

Tolentino, L., Sukekava, F., Seabra, M., Lima, L., Garcez-Filho, J. & Araújo, M. (2014). Success and survival rates of narrow diameter implants made of titanium–zirconium alloy in the posterior region of the jaws–results from a 1-year follow-up. *Clinical Oral Implants Research,* 25(2)**,** 137-141.

Toma, S., Lasserre, J. F., Taïeb, J. & Brecx, M. C. (2014). Evaluation of an air-abrasive device with amino acid glycine-powder during surgical treatment of peri-implantitis. *Quintessence International,* 45(3)**,** 209-219.

Tonetti, M. S. & Schmid, J. (1994). Pathogenesis of implant failures. *Periodontology 2000,* 4(1)**,** 127-138.

Traini, T., Mangano, C., Sammons, R., Mangano, F., Macchi, A. & Piattelli, A. (2008). Direct laser metal sintering as a new approach to fabrication of an isoelastic functionally graded material for manufacture of porous titanium dental implants. *Dental Materials,* 24(11)**,** 1525-1533.

Trenkle, J. C., Packard, C. E. & Schuh, C. A. (2010). Hot nanoindentation in inert environments. *Review of Scientific Instruments,* 81(7)**,** 073901.

Trisi, P., Lazzara, R., Rebaudi, A., Rao, W., Testori, T. & Porter, S. S. (2003). Bone-implant contact on machined and dual acid-etched surfaces after 2 months of healing in the human maxilla. *Journal of Periodontology,* 74(7)**,** 945-956.

Tsui, Y. C., Doyle, C. & Clyne, T. W. (1998). Plasma sprayed hydroxyapatite coatings on titanium substrates Part 1: Mechanical properties and residual stress levels. *Biomaterials,* 19(22)**,** 2015-2029.

Tugulu, S., Löwe, K., Scharnweber, D. & Schlottig, F. (2010). Preparation of superhydrophilic microrough titanium implant surfaces by alkali treatment. *Journal of Materials Science: Materials in Medicine,* 21(10)**,** 2751-2763.

Turkyilmaz, I. & McGlumphy, E. A. (2008). Influence of bone density on implant stability parameters and implant success: a retrospective clinical study. *Bio Medical Central Oral Health*, 8(1)**,** 32. [Online]. Available: https://www.ncbi.nlm.nih.gov/pmc/articles/PMC2614413/.

Umeda, H., Mano, T., Harada, K., Tarannum, F. & Ueyama, Y. (2017). Appearance of cell-adhesion factor in osteoblast proliferation and differentiation of apatite coating titanium by blast coating method. *Journal of Materials Science: Materials in Medicine*, 28(8)**,** 112. [Online]. Available: https://doi.org/10.1007/s10856-017-5913-8.

Urist, M. R. (1965). Bone: formation by autoinduction. *Science,* 150(3698)**,** 893-899.

Valverde, G. B., Jimbo, R., Teixeira, H. S., Bonfante, E. A., Janal, M. N. & Coelho, P. G. (2013). Evaluation of surface roughness as a function of multiple blasting processing variables. *Clinical Oral Implants Research,* 24(2)**,** 238-242.

Van Velzen, F. J. J., Ofec, R., Schulten, E. A. J. M. & ten Bruggenkate, C. M. (2015). 10-year survival rate and the incidence of peri-implant disease of 374 titanium dental implants with a SLA surface: a prospective cohort study in 177 fully and partially edentulous patients. *Clinical Oral Implants Research,* 26(10)**,** 1121-1128.

Vandamme, K., Naert, I., Vander Sloten, J., Puers, R. & Duyck, J. (2007). Effect of implant surface roughness and loading on peri-implant bone formation. *Journal of Periodontology,* 79(1)**,** 150-157.

Vercaigne, S., Wolke, J. G., Naert, I. & Jansen, J. A. (1998). Bone healing capacity of titanium plasma-sprayed and hydroxylapatite-coated oral implants. *Clinical Oral Implants Research,* 9(4)**,** 261-271.

Vigolo, P., Givani, A., Majzoub, Z. & Oordioli, G. (2004). Clinical evaluation of small-diameter implants in single-tooth and multiple-implant restorations: a 7-year retrospective study. *International Journal of Oral and Maxillofacial Implants,* 19(5)**,** 703-709.

Viornery, C., Chevolot, Y., Léonard, D., Aronsson, B.-O., Péchy, P., Mathieu, H. J., Descouts, P. & Grätzel, M. (2002). Surface modification of titanium with phosphonic acid to improve bone bonding: characterization by XPS and ToF-SIMS. *American Chemical Society,* 18(7)**,** 2582-2589.

Wall, I., Donos, N., Carlqvist, K., Jones, F. & Brett, P. (2009). Modified titanium surfaces promote accelerated osteogenic differentiation of mesenchymal stromal cells in vitro. *Bone,* 45(1)**,** 17-26.

Wang, H., Eliaz, N., Xiang, Z., Hsu, H.-P., Spector, M. & Hobbs, L. W. (2006). Early bone apposition in vivo on plasma-sprayed and electrochemically deposited hydroxyapatite coatings on titanium alloy. *Biomaterials,* 27(23)**,** 4192-4203.

Weber, H. P., Weber, M. D. & Papaspyridakos, P. (2015). Complications associated with implant planning: etiology, prevention, and treatment, *In:* Froum, S. J. (ed.) *Dental implant complications.* Second ed. John Wiley & Sons, Inc, 68-101. [Online]. Available: https://doi.org/10.1002/9781119140474.ch4.

Welsch, G., Boyer, R. & Collings, E. (eds.) (1993). *Materials properties handbook: titanium alloys,* Ohio, USA: ASM International.

Wen, B., Chen, J., Dard, M. & Cai, Z. (2016). The performance of titanium-zirconium implants in the elderly: a biomechanical comparative study in the minipig. *Clinical Implant Dentistry and Related Research,* 18(6)**,** 1200-1209.

Wennerberg, A. (1998). The importance of surface roughness for implant incorporation. *International Journal of Machine Tools and Manufacture,* 38(5)**,** 657-662.

Wennerberg, A. & Albrektsson, T. (1999). Suggested guidelines for the topographic evaluation of implant surfaces. *The International Journal of Oral and Maxillofacial Implants,* 15(3)**,** 331-344.

Wennerberg, A. & Albrektsson, T. (2009). Effects of titanium surface topography on bone integration: a systematic review. *Clinical Oral Implants Research,* 20(s4)**,** 172-184.

Wennerberg, A. & Albrektsson, T. (2010). On implant surfaces: a review of current knowledge and opinions. *International Journal of Oral and Maxillofacial Implants,* 25(1)**,** 63-74.

Wennerberg, A., Albrektsson, T. & Andersson, B. (1996a). Bone tissue response to commercially pure titanium implants blasted with fine and coarse particles of aluminum oxide. *International Journal of Oral and Maxillofacial Implants,* 11(1)**,** 38-45.

Wennerberg, A., Albrektsson, T. & Jimbo, R. (2015). Overview of Surface Evaluation Techniques, *In:* Wennerberg, A., Albrektsson, T. & Jimbo, R. (eds.) *Implant surfaces and their biological and clinical impact.* First ed. Berlin: Springer, 1-5. [Online]. Available: https://www.springer.com/gp/book/9783662453780.

Wennerberg, A., Ohlsson, R., Rosén, B.-G. & Andersson, B. (1996b). Characterizing three-dimensional topography of engineering and biomaterial surfaces by confocal laser scanning and stylus techniques. *Medical Engineering and Physics,* 18(7)**,** 548-556.

Wennerberg, A., Svanborg, L. M., Berner, S. & Andersson, M. (2013). Spontaneously formed nanostructures on titanium surfaces. *Clinical Oral Implants Research,* 24(2)**,** 203-209.

Wetzel, A. C., Vlassis, J., Caffesse, R. G., Hämmerle, C. H. F. & Lang, N. P. (1999). Attempts to obtain re-osseointegration following experimental peri-implantitis in dogs. *Clinical Oral Implants Research,* 10(2)**,** 111-119.

Whitefield, R. (1975). Noncontact optical profilometer. *Applied Optics,* 14(10)**,** 2480-2485.

Wiltfang, J., Zernial, O., Behrens, E., Schlegel, A., Warnke, P. H. & Becker, S. T. (2012). Regenerative treatment of peri-implantitis bone defects with a combination of autologous bone and a demineralized xenogenic bone graft: a series of 36 defects. *Clinical Implant Dentistry and Related Research,* 14(3)**,** 421-427.

Wirth, J., Tahriri, M., Khoshroo, K., Rasoulianboroujeni, M., Dentino, A. R. & Tayebi, L. (2017). Surface modification of dental implants, *In:* Tayebi, L. & Mohammadreza, K. (eds.) *Biomaterials for oral and dental tissue engineering.* First ed. Elsevier, 85-94. [Online]. Available: https://doi.org/10.1016/B978-0-08-100961-1.00006-2.

Wohlfahrt, J. C., Lyngstadaas, S. P., Rønold, H. J., Saxegaard, E., Ellingsen, J. E., Karlsson, S. & Aass, A. M. (2012). Porous titanium granules in the surgical treatment of peri-implant osseous defects: a randomized clinical trial. *International Journal of Oral & Maxillofacial Implants,* 27(2)**,** 401-410.

Xiao, M., Biao, M., Chen, Y., Xie, M. & Yang, B. (2016). Regulating the osteogenic function of rhBMP 2 by different titanium surface properties. *Journal of Biomedical Materials Research Part A,* 104(8)**,** 1882-1893.

Xu, L.-C. & Siedlecki, C. A. (2007). Effects of surface wettability and contact time on protein adhesion to biomaterial surfaces. *Biomaterials,* 28(22)**,** 3273-3283.

Xue, W., Tao, S., Liu, X., Zheng, X. & Ding, C. (2004). In vivo evaluation of plasma sprayed hydroxyapatite coatings having different crystallinity. *Biomaterials,* 25(3)**,** 415-421.

Xuereb, M., Camilleri, J. & Attard, N. J. (2015). Systematic review of current dental implant coating materials and novel coating techniques. *International Journal of Prosthodontics,* 28(1)**,** 51-59.

Yamagami, A., Yoshihara, Y. & Suwa, F. (2004). Mechanical and histologic examination of titanium alloy material treated by sandblasting and anodic oxidization. *International Journal of Oral and Maxillofacial Implants,* 20(1)**,** 48-53.

Yang, D., Liu, H., Zheng, Z., Yuan, Y., Zhao, J.-c., Waclawik, E. R., Ke, X. & Zhu, H. (2009). An efficient photocatalyst structure: TiO_2 (B) nanofibers with a shell of anatase nanocrystals. *Journal of the American Chemical Society,* 131(49)**,** 17885-17893.

Yang, F., Zhao, S.-f., Zhang, F., He, F.-m. & Yang, G.-l. (2011). Simvastatin-loaded porous implant surfaces stimulate preosteoblasts differentiation: an in vitro study. *Oral Surgery, Oral Medicine, Oral Pathology, Oral Radiology, and Endodontology,* 111(5)**,** 551-556.

Yang, W.-E. & Huang, H.-H. (2010). Improving the biocompatibility of titanium surface through formation of a TiO_2 nano-mesh layer. *Thin Solid Films,* 518(24)**,** 7545-7550.

Yang, Y. C. & Chang, E. (2001). Influence of residual stress on bonding strength and fracture of plasma-sprayed hydroxyapatite coatings on Ti–6Al–4V substrate. *Biomaterials,* 22(13)**,** 1827-1836.

Yarramaneni, V., Narayan, A., Sachdeva, A., Balakrishnan, D. & Prabhu, N. (2016). Emerging antibacterial coated dental implants: a preventive measure for peri-implantitis. *World Journal of Dentistry,* 7(4)**,** 195-198.

Yeo, I.-S. (2014). Reality of dental implant surface modification: a short literature review. *The Open Biomedical Engineering Journal,* 8**,**114-119. [Online]. Available: http://www.ncbi.nlm.nih.gov/pmc/articles/PMC4231373/.

Yoo, D., Tovar, N., Jimbo, R., Marin, C., Anchieta, R. B., Machado, L. S., Montclare, J., Guastaldi, F. P., Janal, M. N. & Coelho, P. G. (2014). Increased osseointegration effect of bone morphogenetic protein 2 on dental implants: an in vivo study. *Journal of Biomedical Materials Research Part A,* 102(6)**,** 1921-1927.

Yoshinari, M., Oda, Y., Inoue, T., Matsuzaka, K. & Shimono, M. (2002). Bone response to calcium phosphate-coated and bisphosphonate-immobilized titanium implants. *Biomaterials,* 23(14)**,** 2879-2885.

Zabtotsky, M. H., Diedrich, D. L. & Meffert, R. M. (1992). Detoxification of endotoxin-contaminated titanium and hydroxyapatite-coated surfaces utilizing various chemotherapeutic and mechanical modalities. *Implant Dentistry,* 1(2)**,** 154-158.

Zahran, R., Leal, J. R., Valverde, M. R. & Vílchez, M. C. (2016). Effect of hydrofluoric acid etching time on titanium topography, chemistry, wettability, and cell adhesion. *Public Library of Science*, 11(11)**,** e0165296. [Online]. Available: https://doi.org/10.1371/journal.pone.0165296.

Zareidoost, A., Yousefpour, M., Ghaseme, B. & Amanzadeh, A. (2012). The relationship of surface roughness and cell response of chemical surface modification of titanium. *Journal of Materials Science: Materials in Medicine,* 23(6)**,** 1479-1488.

Zhang, L., Yan, J., Yin, Z., Tang, C., Guo, Y., Li, D., Wei, B., Xu, Y., Gu, Q. & Wang, L. (2014). Electrospun vancomycin-loaded coating on titanium implants for the prevention of implant-associated infections. *International Journal of Nanomedicine*, 9**,** 3027-3036. [Online]. Available: https://doi.org/10.2147/IJN.S63991.

Zhang, Y., Andrukhov, O., Berner, S., Matejka, M., Wieland, M., Rausch-Fan, X. & Schedle, A. (2010). Osteogenic properties of hydrophilic and hydrophobic titanium surfaces evaluated with osteoblast-like cells (MG63) in coculture with human umbilical vein endothelial cells (HUVEC). *Dental Materials,* 26(11)**,** 1043-1051.

Zhang, Y., Wang, J., Wang, P., Fan, X., Li, X., Fu, J., Li, S., Fan, H. & Guo, Z. (2013). Low elastic modulus contributes to the osteointegration of titanium alloy plug. *Journal of Biomedical Materials Research Part B: Applied Biomaterials,* 101B(4)**,** 584-590.

Zhao, B., Van Der Mei, H. C., Subbiahdoss, G., de Vries, J., Rustema-Abbing, M., Kuijer, R., Busscher, H. J. & Ren, Y. (2014a). Soft tissue integration versus early biofilm formation on different dental implant materials. *Dental Materials,* 30(7)**,** 716-727.

Zhao, G., Raines, A. L., Wieland, M., Schwartz, Z. & Boyan, B. D. (2007). Requirement for both micron- and submicron scale structure for synergistic responses of

osteoblasts to substrate surface energy and topography. *Biomaterials,* 28(18)**,** 2821-2829.

Zhao, G., Schwartz, Z., Wieland, M., Rupp, F., Geis-Gerstorfer, J., Cochran, D. & Boyan, B. (2005). High surface energy enhances cell response to titanium substrate microstructure. *Journal of Biomedical Materials Research Part A,* 74(1)**,** 49-58.

Zhao, S., Wen, F., He, F., Liu, L. & Yang, G. (2014b). In vitro and in vivo evaluation of the osteogenic ability of implant surfaces with a local delivery of simvastatin. *International Journal of Oral & Maxillofacial Implants,* 29(1)**,** 211-220.

Zhou, W., Apkarian, R., Wang, Z. L. & Joy, D. (2006). Fundamentals of scanning electron microscopy (SEM). *In:* Zhou, W. & Wang, Z. L. (eds.) *Scanning microscopy for nanotechnology.* New York: Springer, 1-40. [Online]. Avialable: https://doi.org/10.1007/978-0-387-39620-0_1.

Zhou, W., Liu, Z., Xu, S., Hao, P., Xu, F. & Sun, A. (2011). Long-term survivability of hydroxyapatite-coated implants: a meta-analysis. *Oral Surgery,* 4(1)**,** 2-7.

Zhou, Y., Gao, J., Luo, L. & Wang, Y. (2016). Does bruxism contribute to dental implant failure? A systematic review and meta-analysis. *Clinical Implant Dentistry and Related Research,* 18(2)**,** 410-420.

Zinelis, S., Akhtar, R., Tsakiridis, P., Watts, D. & Silikas, N. (2008). In-depth hardness profiles of stainless steel and Ni-Ti endodontic instrument cross-sections by nano-indentation. *International Endodontic Journal,* 41(9)**,** 747-754.

Zinelis, S., Al Jabbari, Y. S., Thomas, A., Silikas, N. & Eliades, G. (2014). Multitechnique characterization of CPTi surfaces after electro discharge machining (EDM). *Clinical Oral Investigations,* 18(1)**,** 67-75.

Zinger, O., Zhao, G., Schwartz, Z., Simpson, J., Wieland, M., Landolt, D. & Boyan, B. (2005). Differential regulation of osteoblasts by substrate microstructural features. *Biomaterials,* 26(14)**,** 1837-1847.

Zinsli, B., Sägesser, T., Mericske, E. & Mericske-Stern, R. (2004). Clinical evaluation of small-diameter ITI implants: a prospective study. *International Journal of Oral and Maxillofacial Implants,* 19(1)**,** 92-99.

Zitzmann, N., Berglundh, T., Marinello, C. & Lindhe, J. (2001). Experimental peri-implant mucositis in man. *Journal of Clinical Periodontology,* 28(6)**,** 517-523.

Zitzmann, N. U. & Berglundh, T. (2008). Definition and prevalence of peri-implant diseases. *Journal of Clinical Periodontology,* 35(s8)**,** 286-291.

Zukalova, M., Kalbac, M., Kavan, L., Exnar, I. & Graetzel, M. (2005). Pseudocapacitive lithium storage in TiO_2 (B). *Chemistry of Materials,* 17(5)**,** 1248-1255.

Zysset, P. K., Edward Guo, X., Edward Hoffler, C., Moore, K. E. & Goldstein, S. A. (1999). Elastic modulus and hardness of cortical and trabecular bone lamellae measured by nanoindentation in the human femur. *Journal of Biomechanics,* 32(10)**,** 1005-1012.

Appendix I

3D Profiling of Titanium and Titanium–Zirconia Alloys with Various Surfaces

Pilot study

Materials and methods

A pilot study was conducted to test the methodology, scanning parameters, and the number of readings per sample. Different resolutions (501 and 1001 points/mm), spacing between readings (1 and 2 µm), lengths or area to be measured (0.5 x 0.5 mm and 1 x 1 mm), and 1–3 readings per sample were assessed. Previous research indicated that 3 discs enable the assessment of the surface roughness of implant material with different surface treatments (Rupp *et al.*, 2006; Elias *et al.*, 2008; Dos Santos *et al.*, 2011; Sista *et al.*, 2011; Zhao *et al.*, 2014a). Based on these studies, the sample size was decided to be 3 samples per group. The most consistent data were achieved with 3 readings per sample over 1 x 1 mm at a resolution of 1001 points/mm and spacing of 1 µm. One sample from the CpTi2 group with a sandblasted and acid-etched surface (TiSLA) previously detailed in Chapter 3 using the latter settings was tested and the results are presented below.

Results

Table A-1 Representation of the means of roughness parameters of the TiSLA at 3 different positions

Position	R_a (µm)	S_a (µm)	S_p (µm)	R_p (µm)	S_v (µm)	R_v (µm)
1	2.40	2.94	17.50	6.11	17.20	6.81
2	2.69	2.94	21.20	8.25	18.30	7.67
3	2.53	3.80	19.60	6.79	20.40	6.38
Mean	2.54	3.22	19.43	7.05	18.63	6.95

Nanomechancial and Micro-Nanomechancial Properties of Surface-Modified Dental Implants

Pilot study

Materials and methods

Nanoindentation

A pilot study was conducted to confirm the methodology. The samples were initially tested without any grinding or polishing. However, due to the sensitivity of the nanoindentation testing to surface roughness, no accurate or consistent results were obtained. Consequently, sample preparation was performed with different grinding and polishing protocols until a smooth surface for testing was achieved. Three samples and 30 indents were chosen based on prior research (Takeuchi *et al.*, 2005; Cattani-Lorente *et al.*, 2014; Grubova *et al.*, 2016) and the results of the pilot study. After testing, each sample and indent graph were analysed using the NanoSuite 6.2 Agilent software to ensure the accuracy of the measurement. One commercially pure control sample (CpC) was tested, and the results are presented below.

Micro-nanoindentation

In order to compare the two methods, the same sample size was decided for micro-nanoindentation. Similarly, the micro-nanoindentation testing required a smooth surface preparation, and therefore the same surface preparation for nanoindentation was performed. However, the number of indents per sample was different due to the different magnitude of force applied that would result in a deeper indent. Thus, the space between indents would need to be greater. After considering the different diameters of

the discs and leaving sufficient spaces between the indents, as well as previous research (Takeuchi *et al.*, 2005; Sasani *et al.*, 2014; Cordeiro *et al.*, 2018), 5 indents per sample were carried out. Different loads (50, 100, 200, 400 g) and pauses (10, 20 seconds) were tested. The most consistent results were obtained with a load of 100 g for 20 seconds. After testing, each sample and indent graph were analysed using the Nanovea Nano Hardness software (Ver.1.6.2) to ensure the accuracy of the measurement. One commercially pure control sample (CpC) was tested, and the results are presented below.

Results

Micro-nanoindentation

Table A-2 Representation of the hardness and elastic modulus means of 5 indents on CpC using micro-nanoindentation

Test number	Hardness (GPa)	Elastic modulus (GPa)
Test 1	0.87	25.75
Test 2	1.20	32.59
Test 3	1.27	34.20
Test 4	1.34	34.64
Test 5	1.32	35.05
Mean	1.20	32.44
Standard deviation	0.17	3.45

Nanoindentation

Table A-3 Representation of the hardness and elastic modulus means of 30 indents on CpC sample using nanoindentation

Indent number	Hardness (GPa)	Elastic modulus (GPa)
1	2.86	98.14
2	3.42	108.93
3	3.41	110.32
4	3.37	109.89
5	3.95	120.31
6	3.28	107.39
7	3.39	109.28
8	3.38	108.86
9	3.30	109.43
10	3.30	105.41
11	3.44	107.05
12	3.68	110.85
13	3.40	113.03
14	3.38	109.02
15	2.91	101.04
16	3.29	107.79
17	3.48	111.74
18	3.26	106.01
19	3.16	107.32
20	3.34	111.97
21	3.11	103.63
22	2.77	98.35
23	2.83	100.50
24	3.07	104.75
25	3.35	109.92
26	3.56	117.80
27	3.15	106.08
28	3.16	106.77
29	3.08	107.94
30	3.59	112.93
Mean	3.29	108.08
Standard deviation	0.25	4.9

Surface Characterisation of Bioceramic-Treated Implant Surfaces

Pilot study

Materials and methods

A pilot study was conducted to evaluate the validity of the methodology. Three samples were used in the study based on reports using 3 samples for the surface characterisation of implant surfaces (Elias *et al.*, 2008; Coelho and Lemons, 2009; Coelho *et al.*, 2011; Tastepe *et al.*, 2013; Hakki *et al.*, 2017; Kulkarni Aranya *et al.*, 2017). The discs were treated with bioceramic powders and air abrasion. The air abrasion unit was used at 0.41 MPa pressure setting, as recommended by the manufacturer for clinical use. Air abrasion was first applied freely to test the powder flow. However, in order to standardise the air abrasion protocol, the distance between the sample and the tip of the instrument, and the angle, the air abrasion unit was fixed at two positions. The same approach was used in other air abrasion studies (Tastepe *et al.*, 2018b). The distance between the sample and the tip of the nozzle was chosen after several tests, in order to simulate the clinical situation that is applied freely and close to the implant surface. After assessing the powder flow and distribution, a 1–2 mm distance was chosen in accordance with other research (Schwarz *et al.*, 2009a; Tastepe *et al.*, 2013; John *et al.*, 2016). During the treatment, the nozzle was perpendicular to the samples, as in previous research (Duarte *et al.*, 2009b; Schwarz *et al.*, 2009a; Bennani *et al.*, 2015; John *et al.*, 2016), while the surface and the sample were moved to ensure a uniform distribution of the powders. The treatment time was continued until the entire surface was covered by the powders. After several tests of the time required to treat the samples, the time was standardised to be 2 minutes.

Surface characterisation

In order to compare the surface roughness profiles of the samples before and after applying the bioceramic abrasives, the same settings for surface roughness measurements in Chapter 3 before the treatment were applied.

The EDS analysis was performed on different areas of the samples, in accordance with previous studies (Koller *et al.*, 2007; Coelho and Lemons, 2009; Tan *et al.*, 2012; Hakki *et al.*, 2017). Four areas were examined to assess the distribution of the powder on the treated surfaces. One sample was used for pilot testing to test the methodology.

Results

Surface roughness

Table A-4 Representation of the means of surface roughness parameters of the RSLACT treated with 95 % HA/5 % CaO at 3 positions

Position	R_a (µm)	S_a (µm)	S_p (µm)	R_p (µm)	S_v (µm)	R_v (µm)
1	1.21	3.11	15.20	2.70	18.51	3.53
2	1.55	2.35	12.00	5.00	10.31	2.22
3	1.00	4.20	21.11	3.90	20.20	2.44
Mean	1.25	3.22	16.10	3.86	16.34	2.73

SEM-EDS analysis

SEM images are provided in Chapter 5. The EDS analysis of the CpC sample is presented below for the before and after air abrasion treatment.

Table A-5 Representation of the elemental wt % analysis of the CpC sample before treatment

Position	Ti wt %	P wt %	Ca wt %	Al wt %	Mg wt %	V wt %	O wt %	C wt %	Si wt %
1	98.24	0.02	0.00	0.09	0.00	0.00	0.94	0.63	0.08
2	98.39	0.01	0.04	0.05	0.00	0.00	0.86	0.56	0.09
3	98.30	0.00	0.00	0.09	0.02	0.20	0.88	0.44	0.07
4	97.76	0.00	0.05	0.14	0.05	0.04	1.02	0.85	0.09
Mean	98.17	0.01	0.02	0.09	0.02	0.06	0.93	0.62	0.08

Table A-6 Representation of the elemental wt % analysis of the CpC sample treated with 90 % HA/10 % CaO

Position	Ti wt %	P wt %	Ca wt %	Al wt %	Mg wt %	V wt %	O wt %	C wt %	Si wt %
1	82.35	2.52	8.03	0.12	0.18	0.20	5.16	0.99	0.00
2	84.93	2.47	7.23	0.04	0.16	0.13	4.17	0.77	0.09
3	72.76	6.01	13.89	0.06	0.20	0.41	5.98	0.69	0.01
4	85.36	2.72	7.93	0.03	0.08	0.42	2.97	0.47	0.00
Mean	81.35	3.43	9.27	0.06	0.15	0.29	4.68	0.73	0.02

Table A-7 Representation of the medians of the S_p parameter for all groups before and after treatment with the bioceramic powders

Group	Median S_p (µm)	Median S_p (µm)	Median S_p (µm)
	Before treatment	After treatment with 95 % HA/5 % CaO	After treatment with 90 % HA/10 % CaO
CpC	9.65	58.03	20.83
SB	24.70	17.97	28.60
SBE	15.93	16.90	35.80
TiSLACT	19.00	32.30	20.80
RSLACT	13.60	16.53	28.23

Table A-8 Representation of the medians of the S_v parameter for all groups before and after treatment with the bioceramic powders

Group	Median S_v (µm)	Median S_v (µm)	Median S_v (µm)
	Before treatment	After treatment with 95 % HA/5 % CaO	After treatment with 90 % HA/10 % CaO
CpC	8.63	9.97	14.63
SB	29.33	14.83	17.13
SBE	27.33	14.14	31.06
TiSLACT	19.70	22.23	16.13
RSLACT	19.30	15.16	19.56